Regulatory T cells in skin homeostasis and inflammation

Krista Adelmann

University of Oxford

St. Edmund Hall

A Thesis Submitted for the Degree of Doctor of Philosophy

Trinity Term, 2015

Abstract

Regulatory T cells (Tregs) are crucial controllers of inflammation. Patients with a genetic defect in the lineage defining transcription factor Foxp3 suffer from a broad spectrum of autoimmune diseases, including early manifestation of various types of skin inflammation. However, our knowledge about the properties of skin resident regulatory T cells under homeostatic and pathologic conditions and in particular in inflammatory diseases of the skin such as psoriasis is limited.

In order to address this open question, phenotypic characterization and transcriptomic analyses of murine skin Tregs were performed. The majority of $CD4^+$ T cells in homeostatic skin express the transcription factor Foxp3. These Tregs show a unique profile, are mainly thymic derived nTregs and are enriched in markers associated with a highly suppressive phenotype such as CD25, CD103, IL-10, ST2, and GATA-3. To delineate the role of Tregs in psoriasis-like inflammation, the imiquimod model of psoriasiform inflammation was used. Tregs are significantly increased during skin inflammation and retain their suppressive phenotype and trancriptome. Treg depletion before and during imiquimod treatment led to exacerbated inflammation and dense leukocytic infiltrate in the dermis and epidermis. Furthermore, the exacerbated inflammation was characterized by a significant increase in IL-12 and infiltration of IFN-γ and TNF-α producing, T-bet^+ $CD8^+$ and $CD4^+$ T cells. IL-23 and IL-17 secreting dermal γδ T cells are pathogenic in the imiquimod model, but their cell numbers decreased in the absence of Tregs. Functional experiments demonstrated that myeloid-derived type I Interferon drove the exacerbated inflammation, which was dependent on $CD4^+$ and $CD8^+$ T cells.

In conclusion, skin Tregs have a protective role in psoriasis-like inflammation and depletion of Tregs causes disease exacerbation and triggers an altered cytokine profile and cellular infiltrate. These findings assist in our understanding of tissue resident Tregs and how they maintain homeostasis and prevent inflammation in the skin.

Acknowledgments

First of all, I would like to express my sincere gratitude to both my supervisors Prof. Fiona Powrie and Prof. Graham Ogg for their continuous guidance and support throughout my DPhil. They granted me the opportunity to undertake this exciting and eventful journey. Without their time, dedication and encouragement I wouldn't have been able to follow my passion and commence on the challenge of this project. I will forever be grateful to the Wellcome Trust for funding me and in particular Prof. Keith Gull and Fiona for allowing me to be part of this great programme.

It is with great appreciation that I would like to thank and express my gratitude to all my colleagues and friends in the Powrie lab, whom I have worked with over the years. I would like to express my special thanks to Dr Ahmed Hegazy, who always made time in his busy schedule to assist with my experiments, give invaluable advice on data interpretation and experimental plans, and being a good friend. I am thankful to Dr. Isabelle Arnold, not only for help in the lab, but also because she was always there for a word of advice and guidance whenever I felt stuck. Further, I would like to thank Dr. Nathan West for taking the time to proofread this thesis and his kind help and generous advice throughout the years. I am very thankful to Dr. Chris Schiering who introduced me to the joy of very early experiments and late FACS nights, taught me many techniques and sparked my enthusiasm for Tregs. I am grateful to Dr. Emily Thornton for her assistance with imaging experiments and Dr. Nicholas Ilott for help with data analysis. Further, I want to thank Dr. Ben Owens, Dr. Julie Schulthess, Dr. Hannah Chen, Dr. Thibault Griseri and my fellow students Ms. Anna-Lena Schaupp and Ms. Fanny Franchini for companionship in the office. I also want to thank Dr. Claire Pearson, Dr. Sam Bullers and Mr. Sebastian Rogatti for their tireless assistance with practically everything I needed for my experiments.
I thank all the members of the Ogg lab, in particular Dr. Danuta Gutowska-Owsiak, for their support and encouragement. I would also like to thank Prof. Herman Waldmann for generously sharing his knowledge and providing reagents for my work. I am thankful to Prof. Paul Klenerman for his guidance throughout my first rotation and Dr. Cormac Cosgrove for teaching me more than I could have hoped for in my first rotation. I also want to express my thankfulness to the entire staff from Biomedical Services for their immense support in the past three years.

I owe much gratitude to my family. Sabine, Klaus, Dieter, and Verena, they have supported me in so many ways throughout my life and academic endeavours, celebrated the successes and helped me through the hard times. I will be ever grateful to my grandparents who were always there for me and believed I could do anything. They will always be in my heart.
Finally, and above all, I must acknowledge with deep thanks and love my fiancé Alexander. Words cannot describe how lucky I am to have you in my life. I would not have done this without your patience and encouragement and I can't wait to find out what future journeys lie ahead.

Table of Contents

Abbreviations

AD	atopic dermatitis
AMP	anti-microbial peptides
AP1	activator protein 1
APC	antigen presenting cells
AREG	amphiregulin
BCL	B-cell lymphoma encoded protein
BFA	Brefeldin A
BSA	bovine serum albumin
CARD	caspase activation and recruitment domain
CCL	chemokine ligand
CCR	chemokine (CC-motif) receptor
CD	cluster of differentiation
cDC	classical DC
CHS	contact hypersensitivity
CLA	cutaneous lymphocyte-associated antigen
CREB	cAMP response element-binding protein
CREM	cAMP response element modulator
CTLA	cytotoxic T-lymphocyte-associated protein
CTSH	cathepsin H
CXCR	chemokine (CXC-motif) receptor
DC	dendritic cells
DETC	dendritic epidermal T cells
DETC	dendritic epidermal T cells
DGAT	diacylglycerol O-acyltransferase
DNA	deoxyribonucleic acid
DTR	diphtheria toxin receptor
DTx	diphtheria toxin
EAE	experimental autoimmune encephalitis
EDTA	Ethylenediaminetetraacetic acid
Eomes	eomesodermin
et al	and others

FACS	fluorescence activated cell sorting
FCS	foetal calf serum
FMO	fluorescence minus one
Foxp3	forkhead box P3
FP	fusion protein
GFP	green fluorescent protein
GITR	glucocorticoid-induced TNFR-related protein
GM-CSF	granulocyte macrophage colony-stimulating factor
GO	Gene Ontology
GPR	G-protein coupled receptor
GzmB	granzyme B
GWAS	genome-wide association studies
H&E	Haematoxylin & Eosin
HLA	human leukocyte antigen
HSP	heat shock protein
i.p.	intraperitoneal
i.v.	intravenous
IBD	inflammatory bowel disease
ICOS	inducible T-cell costimulator
IFN	interferon
IFNAR1	interferon-alpha/beta receptor alpha chain
Ig	immunoglobulin
IL-2RG	common γ chain
IL	interleukin
ILC	innate lymphoid cells
IMDM	Iscove's modified Dulbecco's medium
iNOS	inducible nitric oxide synthase
IPEX	Immunodysregulation, polyendocrinopathy, enteropathy, X-linked
IPS1	IFN-β promoter stimulator 1
IRAK	IL-1 receptor associated protein kinases
IRES	internal ribosome entry site
IRF	interferon regulatory factor
KC	keratinocytes
KLRG	killer cell lectin-like receptor subfamily G

KO	knockout
LC	Langerhans cells
LCMV	lymphocytic choriomeningitis virus
LFA	lymphocyte-function associated antigen
LPS	lipopolysaccharide
mAb	monoclonal antibody
MAPK	mitogen-activated protein kinases
MFI	mean fluorescence intensity
MHC	major histocompatibility complex
MNP	mononuclear phagocytes
moDC	monocyte-derived DC
mRNA	messenger RNA
MyD88	myeloid differentiation primary response protein 88
NA	nucleic acid
NF-κB	nuclear factor kappa B
NFAT	nuclear factor of activated T cells
NK	natural killer
nTregs	natural Tregs
OCT	optimal cutting temperature compound
OVA	ovalbumin
PBMC	peripheral blood mononuclear cells
PBS	phosphate-buffered saline
pDC	plasmacytoid DC
PDCA	plasmacytoid dendritic cell antigen
PGD2	prostaglandin D2
PMA	phorbol 12-myristate 13-acetate
PPR	pattern-recognition receptor
PSORS	psoriasis susceptibility locus
iTregs	peripheral Treg
RAG	recombination-activation gene
RANKL	receptor activator of NF-κB
RIG-I	retinoic acid-inducible gene I
RIN	RNA integrity number
RLR	RIG-I-like receptors

RNA	ribonucleic acid
RORγt	retinoic acid-related orphan receptor C
RPMI	Roswell Park Memorial Institute medium
RT-qPCR	quantitative reverse transcription polymerase chain reaction
SALT	skin-associated lymphoid tissue
SATB1	special AT-rich sequence binding protein 1
sdLN	skin draining lymph nodes
SEM	standard error of the mean
SHG	second harmonic generation
SLE	systemic lupus erythematosus
SLEC	short-lived effector cells
STAT	signal transducer and activator of transcription
STING	stimulator of interferon genes
T-bet	T-box transcription factor
IFN-I	type I interferon
TBK	tank binding kinase
Tc	cytotoxic T cell
Tcm	central memory T cell
TCR	T-cell receptor
TF	transcription factor
Tfh	T follicular helper
TGF	transforming growth factor
Th	T helper cell
TIP-DC	TNFα/iNOS-producing DC
TLR	Toll-like receptor
TNF	Tumor necrosis factor
Tregs	regulatory T cells
Trif	TIR-containing-domain adaptor-inducing interferon-β
Trm	resident memory T cells
TSLP	thymic stromal lymphopoietin
VAT	visceral adipose tissue
WT	wild type

Chapter 1. Introduction

The skin is the body's largest organ. It forms the interface between our body and its environment and fulfils several vital roles. As a barrier surface the skin prevents entry of noxious organisms and chemicals while also allowing perspiration and preventing excessive water loss. It is an important sensory organ and plays a central role in controlling our body temperature but also provides us with vital vitamin D. The skin is fundamental for the protection of our internal organs and is often faced with external insults. However, the skin has great adaptive capacity and usually returns to a homeostatic state after facing physical or biological challenges such as injury or infection. Nonetheless, when it is unable to do so, skin diseases can arise. (Goldsmith et al., 2012)

Skin diseases are multi-factorial and can involve external factors such as UV-radiation, infections and trauma as well as internal factors such as genetic predisposition, internal diseases and psychological factors (Figure 1.1) (Weller et al., 2015).

The immune system of the skin is vital for maintaining its physiological function and contributes to the restoration of homeostasis after injury and inflammation. The skin contains many immune cells of different ontogeny and distinct function that together comprise the skin-associated lymphoid tissue (SALT). Impairment of components of our skin's immune system can contribute to prolonged inflammation and chronic diseases of the skin (Pasparakis et al., 2014).

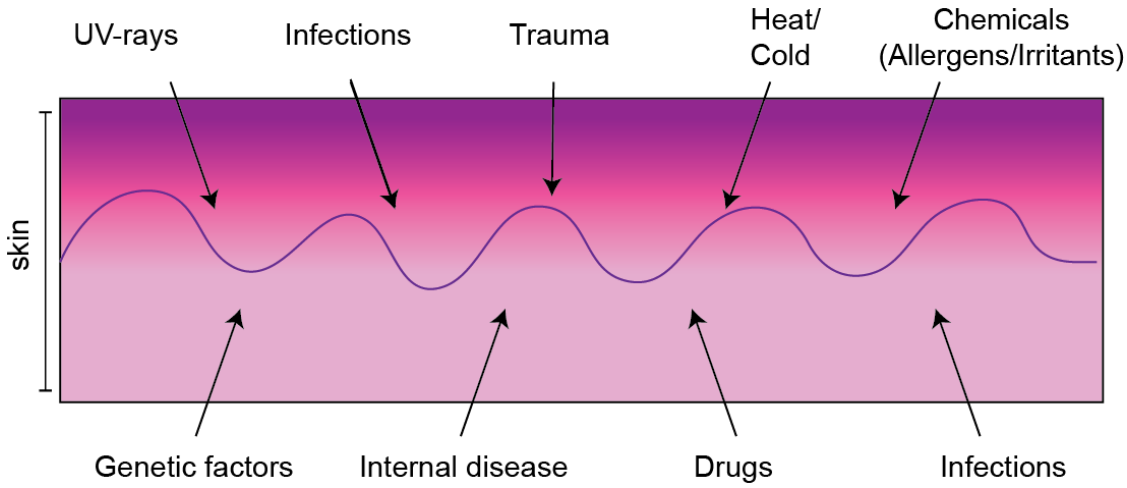

Figure 1.1. Internal and external factors underlying skin disease

External noxious influences and internal factors can lead to the development of skin diseases
Adapted from Weller et al, 2015.

1.1. The Immune System of the Skin

1.1.1. The anatomic distribution of the skin immune system

The epithelium and connective tissue make up the majority of the cellular mass in the skin. Although most cell types are shared between mouse and human skin, there are considerable differences that should be considered when research findings are translated between the two species (Pasparakis et al., 2014) (Figure 1.2).

The epithelium of the skin can be divided into the follicular and interfollicular epidermis and is largely composed of keratinocytes (KC). While these two components constitute similar fractions of the skin in rodents, due to the drastically reduced body hair of humans, the interfollicular epidermis makes up the majority of the outer layer of human skin. The functional differences between these two areas are the subject of ongoing investigations and will help us interpret species-specific disparities that are observed. In the mouse the epidermis consists of only 3-4 layers of KC that sit on a basement membrane, whereas it is made up of 6-10 layers in humans. The main component of the outermost layer of the epidermis is keratin. Together with antimicrobial peptides and lipids it forms an efficient physical barrier to the environment. The differentiation process of KC is accompanied by structural and functional changes that give the epidermis a stratified appearance, which is more prominent in humans than mice (Wikramanayake et al., 2014). At hair follicles, the epidermis protrudes deeply into the dermis.

At steady state, immune cells in the epidermis are present in slightly different proportions in humans vs. mice. The most prevalent immune cells in humans are Langerhans cells (LC) and $CD8^+$ T cells. In mice however, a distinct population of γδ T cells with a Vγ5 chain and a dendritic appearance that gives them the name dendritic epidermal T cells (DETC) is abundant (Pasparakis et al., 2014).

The dermis is largely composed of extracellular matrix. Fibroblasts, fibrocytes and immune cells make up the majority of cells in the dermis with blood and lymphatic vessels connecting it to the circulation. Both, lymphatic and blood vessels are absent in the epithelium at steady state. In humans and mice a variety of myeloid cells are present in the dermis at steady state and disease. Dendritic cells (DC) can be largely divided into two groups: $CD103^+$ DC in mouse, the equivalent of human $CD8^+$ migratory DC in lymph nodes, and $CD11b^+$ DC (Merad et al., 2013). The macrophage population at steady state has recently been described as more diverse than previously recognized, with a pool of macrophages established independent of blood precursors and a short-lived blood derived population (Tamoutounour et al., 2013).

T cells in the dermis are mainly $CD4^+$ T cells with a memory phenotype (Clark, 2015). In the mouse about half of this population are $Foxp3^+$ regulatory T cells (Tregs). In humans, Tregs make up about 15-25% of $CD4^+$ T cells, reaching a very high proportion compared to other organs. Mast cells are found in the dermis in steady state conditions and contain granules with preformed immune mediators such as histamine that allows immediate reaction to insults and infection (Harvima & Nilsson, 2011). More recently, a small proportion of innate

lymphoid cells (ILC)s, mainly ILC2 and ILC3 have been described at steady state in human and mouse dermis (Kim, 2014; Salimi et al., 2013).

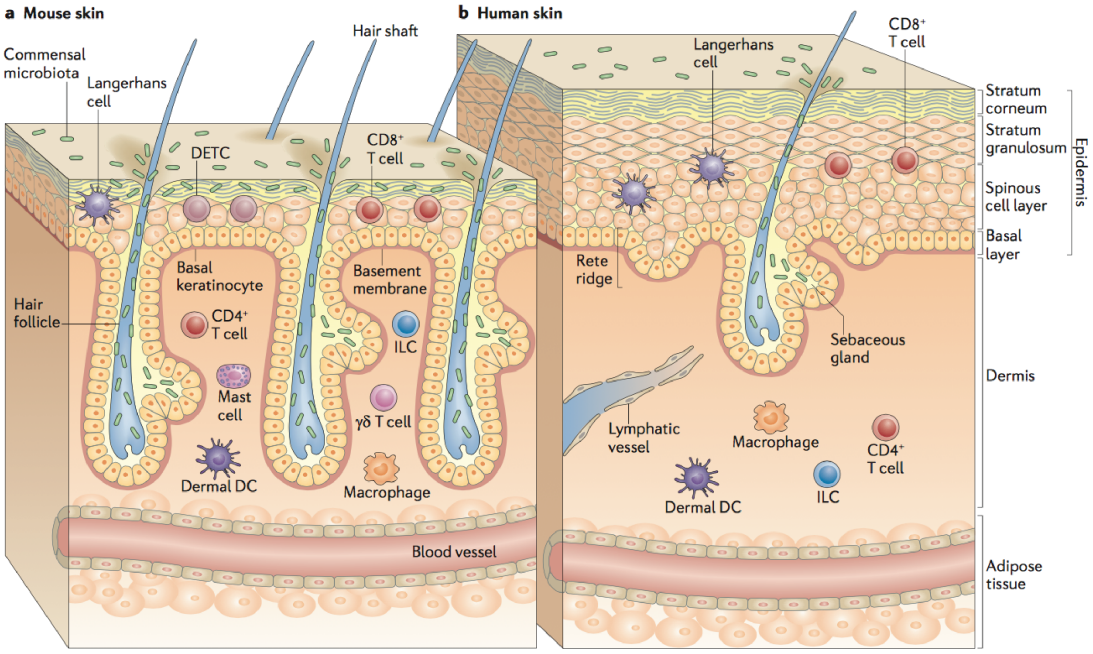

Figure 1.2. The immune system of the skin

Schematic overview of the key components of the skin immune system in mouse and human skin

Image reprinted with permission from Pasparakis et al, 2014; *Nature Reviews Immunology*

1.2. Innate immune system

1.2.1. Cellular components

Epithelium

The epidermis is a stratified squamous epithelium and forms the outermost layer of the human body. It consists predominantly of epidermal keratinocytes that form several distinct layers. The stratum basale contains proliferating KC, which undergo constant low-level cell division and differentiation as they migrate upwards through the stratum spinosum and stratum granulosum towards the stratum corneum (Figure 1.2). The cells of the basal layer are linked to the underlying basement membrane that forms the dermo-epidermal junction separating the two sheets of the skin. KC are tightly connected to each other facilitating the formation of a physical barrier. The pH of the outermost epidermal layer, the stratum corneum is acidic (pH ca. 5) and contains little water. This composition makes it a hostile environment for many pathogens. However, the skin is colonized by commensal microbiota that prevents infections by competition with pathogens and can contribute to epithelial and immune-cell homeostasis (Grice & Segre, 2011) (Belkaid & Segre, 2014).

Three distinct additional cell types are also present in the epidermis. Melanocytes synthesize melanin that is crucial for protection against damaging UV radiation. Merkel cells are highly adapted sensory cells and are transducers for fine touch. Langerhans cells (LC) are antigen presenting mononuclear phagocytic cells that originate from embryonic macrophages and are key contributors to many immune responses.

Mononuclear phagocytes: macrophages / monocytes and dendritic cells

Macrophages, monocytes and DC are members of the mononuclear phagocyte (MNP) system. However, the origin and development of these cells and their distribution in the tissues is complex and has not been fully elucidated to date. Based on recent studies of the ontogeny of MNP three groups have been proposed: embryonically-derived macrophages, common DC precursor-derived classical DC (cDC) and monocyte-derived cells that include monocytes, tissue macrophages, and a population of monocyte-derived DC (Guilliams et al., 2014).

Macrophages

Macrophages are professional phagocytes that scavenge the tissues for intruding microbes and take up any encountered invading pathogens or damaged cells. This process involves acidification of the phagocytosed compounds and production of antimicrobial peptides such as defensins and enzymes such as lysozymes and hydrolases (Murray, 1979).

Traditionally, blood monocytes were thought to be precursors of all tissue macrophages at steady state (van Furth & Cohn, 1968). However, specific subsets of tissue resident macrophages such as microglia of the brain and Kupfer cells in the liver have been described as self-sufficient populations derived from the yolk sac before birth and are independent of haematopoiesis in later life (Ginhoux & Jung, 2014; Merad et al., 2013). Similarly, the macrophage pool in the skin has been shown to be in part established prenatally and in part replenished continuously throughout life by blood-derived monocytes that express the CC-chemokine receptor 2 (CCR2) and Ly6C

(Geissmann et al., 2010; Jakubzick et al., 2013; Tamoutounour et al., 2013). Once extravasated $CCR2^{+}Ly6C^{high}$ monocytes enter the dermis, CCR2 signaling is dispensable for their maintenance in the tissue (Tamoutounour et al., 2013). It appears that a subset of these cells matures into monocyte derived DC. Even though the progeny of these cells are $CCR2^{+}$ blood derived monocytes, phenotypically and transcriptionally they more closely resemble cDC in the skin than the related dermal macrophage population and are termed monocyte derived DC (moDC) (Tamoutounour et al., 2013). In healthy murine skin, macrophages are replaced at a much slower rate than the short-lived cDC or monocyte derived DC (Malissen et al., 2014). A recent study identified MNP as being positioned near dermal capillaries where they actively recruit neutrophils from the blood to the infected tissue (Abtin et al., 2013). Further research suggests that the relative percentage of dermal MNP derived from extravasated $Ly6C^{high}$ monocytes increases with repeated infections of the skin (Abtin et al., 2013).

Dendritic cells

DC are professional antigen presenting cells (APC) that arise from common DC precursors in an Flt3L-dependent manner (Liu et al., 2009). They bridge the gap between the innate and adaptive immune system by migrating to the lymph node where they present captured and processed antigens to T cells via major histocompatibility complex (MHC) class I and II molecules. DC comprise diverse subtypes including cDC, plasmacytoid DC (pDC) and moDC.

cDC in the skin can undergo ‘homeostatic maturation’, a process that is independent of microbial signaling and in which morphological and phenotypic

changes prompt cell migration to the draining lymph nodes. Here they present self-antigens of the skin which may trigger abortive programs in autoreactive T cells or keep naïve T cells alert for antigen encounter (Wilson et al., 2008). Upon activation by foreign antigen, cDC are subject to terminal differentiation. Under these circumstances they upregulate co-stimulatory molecules and transport antigens to the lymph node where they activate naïve T cells and promote their clonal expansion. However, this interaction is reciprocal and T cells can instruct cDC by altering their cytokine profile or level of co-stimulatory molecules expression (Chorro et al., 2009; Muth et al., 2012).

$CD11b^+$ and $CD11b^-$ DC in the skin originate from blood derived pre-cDC progenitors. $CD11b^-$ DC express langerin (CD207), and have similar ontogeny to the $CD8\alpha^+$ DC in lymph nodes (Crozat et al., 2011; Poulin et al., 2007). $CD11b^+$ dermal DC are the most abundant DC population in the dermis.

Langerhans cells were traditionally regarded as classical tissue DC. However, it has become evident that LCs are seeded during embryonic development and are self-replenishing without the input of blood precursors. These cells are radio-resistant and depend on CSF1R signaling and express MHC II, langerin and CD11c. They are confined to the epidermis where they are capable of extending their dendrites through the stratum corneum and thus probe the environment for antigens (Ouchi et al., 2011). They are in constant contact with KC through E-cadherin but upon maturation, LCs are capable of migrating to the dermis and subsequently to lymph nodes in a similar manner to cDC (Kissenpfennig et al., 2005). Several distinct and sometimes contrasting functions have been reported for LC ranging from immunosuppressive functions in contact hypersensitivity (CHS) models and induction of Tregs in

allergic contact dermatitis to promoting T helper 17 (Th17) cells in response to cutaneous *Candida albicans* infection (Bobr et al., 2010; Gomez de Agüero et al., 2012; Igyártó et al., 2011). Langerhans cells sit at the very forefront of our body's barrier and are equipped with various capabilities to react to external and internal signals. It therefore seems plausible that they retain a certain degree of functional plasticity to react to and integrate the diverse signals to which they are continuously exposed.

pDC are a rare and unique subset of DC that are mainly found in the blood and lymphoid tissues. They are capable sensing foreign nucleic acids through endoplasmatic Toll-like receptors (TLR) and produce large amounts of type I interferon (IFN-I) upon activation (Merad et al., 2013). pDC are absent from the skin at steady state conditions.

Innate lymphoid cells

Innate lymphoid cells (ILC) are more recently discovered members of the innate immune cell family and are increasingly recognized as important players of innate immunity at tissue sites. They have a lymphoid appearance, express CD45, and function independent of rearranged antigen specific surface receptors. They are mostly dependent on the common cytokine receptor γ-chain (IL-2RG) for development as well as maintenance (Spits et al., 2013). On the basis of their transcription factor profile, developmental pathways, and cytokine profile, they are divided into three distinct groups termed Group 1, Group 2, and Group 3 ILC (Spits et al., 2013).

Similar to T helper 1 (Th1) cells, Group 1 ILCs produce the hallmark cytokine IFN-γ and express the transcription factors T-bet, NFil3 and Eomes (Gordon et al., 2012). They comprise natural killer (NK) cells and the distinct non-cytotoxic ILC1s. There is some degree of plasticity between ILC1 and Group 3 ILC, the later giving rise to the former in certain conditions under the influence of IL-15 and IL-12 (Bernink et al., 2013). ILC1 contribute to intestinal inflammation in patients suffering with Crohn's disease and in mouse models of colitis (Bernink et al., 2013). These cells have also been identified in the skin, however their function in skin disease and homeostasis remains to be elucidated (Kim, 2014).

Group 2 ILC express the transcription factor GATA-3 and secrete the Th2-associated cytokines IL-5 and IL-13 when stimulated with PGD2, IL-25, IL-33 and/or TSLP (Fort et al., 2001; Hurst et al., 2002; Xue et al., 2014). They have been well characterized in the gut and the lung and contribute to parasite

expulsion (Fallon et al., 2006), epithelial regeneration (Monticelli et al., 2011) and airway hyper reactivity (Chang et al., 2011).

ILC2 have been identified in mouse and human skin biopsies and are present in altered numbers in patients with atopic dermatitis (AD) and animal models of the disease, supporting a contribution of ILC2 towards the pathogenesis of AD (Roediger et al. 2013; Kim et al. 2013; Salimi et al. 2013). Interestingly, recent findings in human skin have highlighted that resident ILC2 can respond rapidly to cytokines such as IL-33, IL-25 and TSLP as well as lipid mediators such as PGD2; these agents also contribute to ILC2 recruitment. Activated ILC2 amplify adaptive T cell responses by presentation of antigens via MHCII (Oliphant et al. 2014 and unpublished observations Salimi et al.) These data suggest a complex and context dependent function of ILC2 in orchestrating a response to infection and regulating tissue homeostasis.

Group 3 ILC comprise the distinct lymphoid tissue inducer cells, NCR^+ ILC3 and NCR^- ILC3. These are similar to Th17 cells as they depend on the transcription factor RORγt and are capable of producing IL-17A as well as IL-22 either singly or in combination, depending on the cell subset and model studied (Spits et al., 2013). ILC3 mediate pathology in murine colitis models and accumulate in human IBD (Buonocore et al., 2010; Geremia et al., 2011). ILC3 have been described to promote pathology in a mouse model of psoriasiform skin inflammation, where they contribute to disease by producing IL-17 and IL-22 (Pantelyushin et al., 2012). Further research undertaken in ILC-deficient mice lacking RAG and IL-2RG, showed marked reduction in symptom severity (Pantelyushin et al., 2012). Subsequently, it has been revealed that they are enriched in blood and skin biopsies taken from psoriasis

patients, suggesting a potential direct contribution to disease pathogenesis (Teunissen et al., 2014; Villanova et al., 2014).

1.2.2. Immune sensing in the skin

The innate immune system of the skin provides an effective first line of defence against invading pathogens. The expression of germ-line encoded pattern recognition receptors (PRRs) allows pathogen detection and subsequent initiation of an inflammatory response. Epithelial cells, fibroblasts and resident innate and adaptive immune cells in the skin express PRRs (Demaria et al., 2014; Lai & Gallo, 2008). The expression of PPRs varies among immune cells and reflects their specialized responses. PRRs recognize pathogen-associated molecular patterns (PAMPS) that can be of lipid, protein or nucleic acid origin. Engagement of PRRs leads to cell activation, maturation and cytokine secretion.

Toll-like receptors (TLRs) are a well-described family of PRRs and are expressed in many cell types found in the skin where they respond to distinct fungal, bacterial, protozoan and viral ligands (Janeway & Medzhitov, 2002; Miller, 2008). TLRs can be categorized by their cellular location. TLR1, TLR2, TLR4, TLR5 and TLR6 are located on the cell surface whereas TLR3, TLR7, TLR8 and TLR9 are located in the cytosol or intracellular compartments (Lai & Gallo, 2008). All TLRs initiate a signalling cascade via myeloid differentiation primary response protein 88 (MyD88) or TIR-containing-domain adaptor-inducing interferon-β (Trif, only TLR3) that ultimately leads to secretion of cytokines, chemokines, AMPs and co-stimulatory molecules (Gay et al., 2014). MyD88 or Trif activation leads to proinflammatory responses via IκB kinase (IKK) complex/nuclear factor-κB (NF- κB) activation and induction of mitogen-activated kinases (MAPKs)/activator protein 1 (AP1) pathways. It further

induces interferon regulatory factor (IRF) 7 and IRF3 that promote IFN-I production (Gay et al., 2014) (Figure 1.3).

TLR2 can form homodimers with TLR1 or TLR6 and recognizes bacterial lipopeptides. Engagement of TLR2/1 in skin resident MNP triggers events that lead to production of AMPs by increase of vitamin D synthesis and upregulation of the vitamin D receptor (Liu et al., 2006). Similarly skin injury leads to TLR2 activation in KC that triggers production of AMPs via a vitamin D dependent pathway (Schauber et al., 2007). TLR2 as well as TLR4 upregulation in wounds has been associated with impaired healing in diabetic skin and burn injury (Breslin et al., 2008; Dasu et al., 2010). Genes involved in the TLR4 pathway are upregulated in skin of patients with systemic sclerosis (SSc), an autoimmune disease with progressive fibrosis of several organs including the skin (Stifano et al., 2014). Chronic skin exposure to the TLR4 ligand LPS mediates early as well as late inflammatory responses that lead to prolonged inflammation and induce pro-fibrotic pathways via TGF-β (Stifano et al., 2014). These results suggest a potential connection of microbe sensing and fibrosis in the skin. TLR2/6 ligands from *S. aureus* as well as the synthetic ligand Pam2Cys initiated an IL-6 mediated immunosuppression through induction of myeloid-derived suppressor cells. This interaction prevented elicitation of cutaneous hypersensitivity, revealing a microbe driven TLR dependent protective effect (Skabytska et al., 2014). However, a previous study using a different hypersensitivity model revealed conflicting results as TLR2 ligation by *S. aureus* products exacerbated skin inflammation by suppression of IL-10 (Kaesler et al., 2014).

This suggests a highly selective and dynamic regulation of inflammation and immunosuppression mediated by bacterial sensing. This could be a mechanism by which the immune system discriminates between pathogenic and non-pathogenic organisms at barrier surfaces such as the skin. The TLR pathway might also present an opportunity for potential therapeutic intervention at early stages of diseases that involve skin fibrosis and scar formation.

Most intracellular sensors are nucleic acid (NA) receptors that sense intracellular single- (ss) or double-stranded (ds) viral DNA and RNA and are divided by their cytosolic and endosomal distribution. TLR3, TLR7, TLR8 and TLR9 are located in endosomes and sense viral nucleic acids after uptake through scavenger receptors or Fc receptors (Demaria et al., 2014). The endosome is further connected to the cytoplasm via autophagy, which facilitates a crosstalk between the compartments. TLR9 senses microbial DNA via CpG-containing DNA motifs whereas single stranded RNA is sensed by TLR7 and TLR8 (Gay et al., 2014). TLR3 recognizes viral dsRNA and leads to secretion of IFN-I via TIR-domain containing adaptor protein inducing IFN-β (TRIF) and activation of the tank binding kinase 1 (TBK1)-IRF3 pathway (Tanaka et al. 2012).

Cytosolic NA sensors include several distinct proteins including IFI16, DAI, cGAS and RNA polymerase III. They all signal via the endoplasmatic reticulum transmembrane protein stimulator of interferon gene (STING) and TBK-IRF3 to activate IFN-I production (Ishikawa et al., 2009). STING itself is capable of interacting with nucleic acids without upstream activation and absence of STING leads to altered IFN-I production after challenge with bacterial, viral and

mammalian nucleic acids (Burdette et al., 2011). A further group of cytosolic NA sensors are retinoic acid-inducible gene I (RIG-I)-like receptors (RLRs) that are involved in inflammasome formation (Yoneyama et al., 2004). RLRs, including RIG-I and melanoma differentiation-associated gene 5 (MDA5) signal through caspase activation and recruitment domain (CARD) and bind to the IFN-β promoter stimulator 1 (IPS1) that can activate IRFs and NF-κB and subsequently lead to IFN-I and proinflammatory cytokine production (Demaria et al., 2014).

Host-derived RNA and –DNA are released during host cell necrosis and several important mechanisms exist to prevent activation of NA sensors in these situations. As mentioned above, these molecules are localized inside cells and thus prevent activation via extracellular NA. Forced surface expression of TLR9 leads to uncontrolled activation of NA sensing pathways and consequently autoinflammation (Barton et al., 2006). Extracellular NAs are rapidly degraded via tissue nucleases, preventing them from activating NA sensors. Deficiency of such exonucleases leads to uncontrolled STING activation and subsequently to autoinflammation (Ahn et al., 2012; Stetson et al., 2008). Despite these safety measures, self-NA are capable of triggering immune responses under certain conditions promoting inappropriate activation of innate immunity. This can contribute to skin inflammation and the development of autoimmune diseases of the skin such as systemic lupus erythematosus (SLE) and psoriasis (Ahn et al., 2012). UVB-radiation of the skin, for instance, triggers generation of altered noncoding self-RNA that triggers TNF-α and IL-6 production in a TLR3-dependent manner but also mediates immunosuppressive pathways associated with UVB exposure. This

highlights a complex role of TLR3 in UV-mediated photosensitivity as well as UV-induced immunosuppression, which is regularly utilized during phototherapy of inflammatory skin disorders (Bernard et al., 2012).

Antimicrobial peptides (AMPs) are an important line of the skin's defence against invading pathogens, but have been implicated in the pathogenesis of autoimmune disorders of the skin (Zasloff, 2002). AMPs bind to negatively charged phospholipids and disrupt pathogen membranes. However this generally protective feature also allows the formation of AMPs-self-NA complexes which consequently hinders NA degradation by exonucleases (Lande et al., 2007; Zasloff, 2002). Furthermore, these complexes can trigger endocytosis and thus can lead to activation of intracellular NA sensors. The intranuclear DNA binding protein HMGB1 (high mobility group box 1 protein) can be released into the extracellular space during necrosis and has been shown to trigger TLR9 mediated IFN-I production in pDC (Lande et al., 2007). Autoantibodies against DNA or RNA are present in certain autoimmune diseases (Lövgren et al., 2006; Means et al., 2005). These autoantibodies form complexes with self-NA, triggering endocytosis and thereby leading to IFN-I production via activation of endosomal TLR7/8 or TLR9 activation in pDC and moDC (Boulé et al., 2004; Lande et al., 2011). AMPs such as LL-37 can associate with such complexes and further enhance the immunogenicity of these self-NAs, as described by Lande et al in psoriatic skin (Lande et al., 2014; Lande et al., 2007).

As mentioned above, pDC are absent from steady state skin but are able to promote wound healing upon injury. pDC specifically express TLR7 and TLR9 and produce large quantities of IFN-I upon activation. While the precise

mechanism remains elusive, pDC and IFN-I plays a crucial role in promoting re-epithelialization (Gregorio et al., 2010).

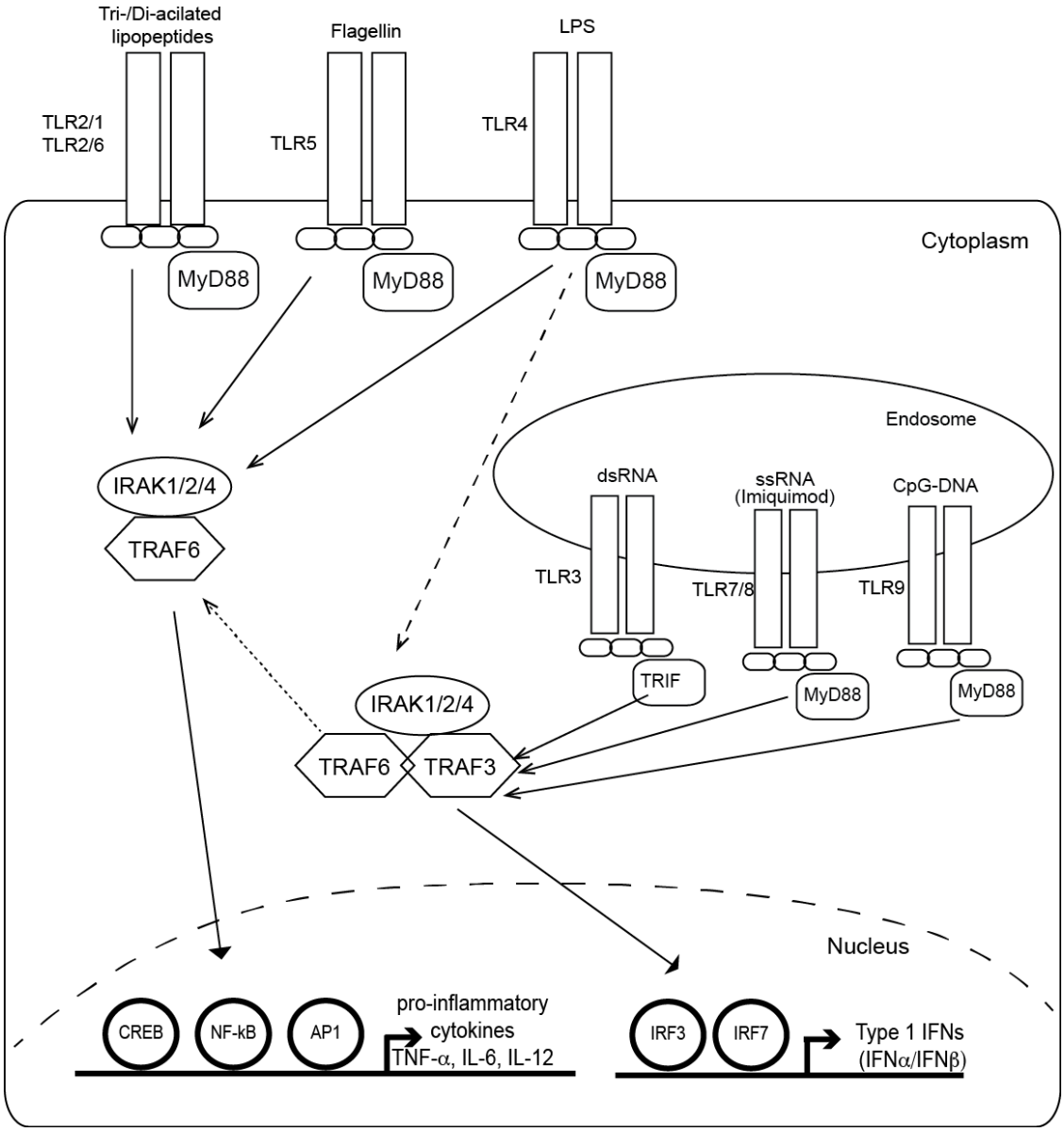

Figure 1.3. TLR signalling pathways

Microbial components are recognized by extracellular and intracellular TLRs. TLR2 can form heterodimers with TLR1 and TLR6 and sense tri- or di-acylated lipopeptides, respectively. TLR4 recognizes LPS and TLR5 flagellin. The intracellular TLRs recognize viral NA. TLR3 recognizes dsRNA, TLR7 and 8 recognize ssRNA and are activated by imiquimod. TLR 9 binds to bacterial and viral CpG DNA motifs.
TLRs activate a signaling cascade that involves IRAK and TRAF those in turn initiate TFs that promote the transcription of proinflammatory and anti-viral proteins.

1.3. Adaptive Immune System

T cells

T cells are lymphocytes that express a T-cell receptor (TCR) complex usually composed of an α and β chain or γ and δ chains in association with CD3 molecules. T cells expressing the TCR α and β chain typically express the co-receptor CD4 or CD8 and consequently are termed $CD4^+$ and $CD8^+$ T cells. Professional APC such as DC, macrophages and B cells are capable of taking up antigen and presenting the processed epitopes to $CD4^+$ T cells in the context of MHC class II molecules. Depending on the additional stimuli from the environment and other immune cell populations, $CD4^+$ T cells can then differentiate into T helper subsets with distinct capabilities, which are discussed later. Most nucleated cells are capable of presenting antigen to $CD8^+$ T cells via MHCI molecules through which they recognize their specific antigen. Once $CD8^+$ T cells are activated, they can exert cytotoxicity and eliminate infected cells.

T cells positive for the invariant or semi-invariant γ and δ chains are termed γδ T cells. Their restricted TCR variability makes them non-conventional, innate-like T cells. How γδ T cells recognize their antigens is subject of ongoing investigation, however it is clear they recognize MHC and MHC-like molecules and can do so in the presence and absence of antigens.

1.3.1. γδ T cells

Invariant γδ T cells are found at barrier surfaces of most mammals (Allison &

Havran, 1991). γδ T cells are capable of recognizing peptide as well as lipid antigens via MHC and MHC-like and CD1 molecules and are developmentally pre-programmed to produce IL-17 or IFN-γ. (Schmolka et al., 2015; Uldrich et al., 2013). This enables them to contribute to the early phase of the immune response.

The epidermis of mice harbors a distinct population of γδ T cells, which are characterized by the expression of two conserved TCR chains: Vγ5 (also called Vγ3 depending on nomenclature used) and Vδ1. Their dendritic appearance and unique anatomical location in the tightly packed stratum basale has earned them the name dendritic epidermal T cells (DETC) (Ramirez et al., 2015). Similar to LC in the epidermis, DETC are seeded early in embryonic development and are radio resistant. They are in constant contact with KC and appear to monitor the epithelium for “stress” signals and have been shown to promote wound-healing responses by recruiting macrophages, secreting proinflammatory cytokines and chemokines and providing growth factors for KC (Hayday, 2009). Although there are γδ T cells in the human epidermis that can also contribute to wound healing in the skin, an equivalent of murine DETC have not been described (Toulon et al. 2009).

In addition to the DETC, the murine and human dermis has a $V\gamma4^+$ population of γδ T cells that do not have a dendritic like appearance, but are closer to typical lymphocytes in their phenotype. These dermal cells enhance $CD4^+$ T cell responses, can express the transcription factor RORγt, and are capable of producing high amounts of proinflammatory cytokines such as IL-17A and IL-22 in mouse models of psoriasis (Pantelyushin et al., 2012). Dermal γδ T cells in human skin also produce these cytokines in psoriatic skin, but the

significance of their contribution to the pathogenesis is not known (Cai et al., 2011).

1.3.2. αβ T cell subsets

The skin harbours large quantities of αβ T cells, which are estimated to outnumber the circulating blood T cell pool in humans by two to one (Clark, et al. 2006). Under homeostatic conditions both $CD4^+$ and $CD8^+$ T cells are present in the skin and almost universally express the cutaneous lymphocyte antigen (CLA) on their surface (Clark, et al. 2006). Skin T cells in human and mouse are all $CD45RO^+$ or $CD44^+$, respectively, suggestive of an effector / memory phenotype (Clark, et al. 2006; Clark, Chong, et al. 2006). Furthermore, T cells present in skin biopsies of non-lesional skin of psoriatic patients are sufficient to initiate disease when transplanted onto immunodeficient mice and highlight the importance of T cells already present in the engrafted tissue (Boyman et al., 2004).

Recently, two distinct populations of resident memory T cells (Trm) and a further two distinct populations of recirculating skin T cells have been described (Watanabe et al., 2015). These had differential sensitivity to antibody depletion in cutaneous lymphoma and were capable of eliciting distinct inflammatory skin lesions. This indicates that the skin T cell pool is made up of functionally heterogeneous skin resident T cell populations. Recently, different types of skin immunization models showed that immunizing via this route not only gives rise to Trm cell clones in the skin, but also central memory T cell (Tcm) clones in the draining lymph node that bear the same TCR (Gaide et al. 2015). Trm and Tcm have different effector functions and

this common TCR repertoire facilitates quick responses upon antigen reencounter in the same organ as well as different tissues.

Both, $CD4^+$ and $CD8^+$ Trm cells have been characterized in the skin of humans and mice with $CD8^+$ Trm mainly locating to the epidermis following viral infection where they are highly efficient in protecting from re-infections. In contrast, $CD4^+$ Trm are found in the dermis, where they co-exist with a re-circulating counterpart (Boyman et al., 2004; Gebhardt et al., 2011; Mackay et al., 2013). Both $CD4^+$ and $CD8^+$ Trm populations increase with age and rates of skin infection. Together with similar findings in other barrier organs such as the lung and the gut, these discoveries have led to a shift in the original paradigm that circulating T cells need to be recruited to the tissues during infection and exit these tissues after the inflammation has been resolved.

1.3.2.1. $CD4^+$ T cells

Naïve $CD4^+$ T cells migrate from the thymus to the periphery where they recirculate through the lymphatic system to the lymph nodes. They constantly scan the peptide:MHCII complexes on the surfaces of professional antigen presenting cells. Mature DC migrate to lymph nodes where they present the captured antigen to T cells. Upon functional recognition of antigen, $CD4^+$ T cells undergo an activation process and clonal expansion that can result in a Teff clone. During this vital process the naïve cells receive a variety of signals from their TCR, co-stimulatory molecules on the APCs, and cytokines in the environment that shape their differentiation process. In particular, co-stimulation from APCs via CD80/CD86 and CD28 on the T cells mediates this second signal, which enhances the secretion of IL-2 and expression of its

recetor IL-2Rα. This IL-2 feedback is important for T cell activation, proliferation and survival (Boyman & Sprent, 2012). Several other co-stimulatory molecules have inhibitory and activating properties and are involved in the activation process and include CTLA-4, CD40-L, OX-40, GITR and RANKL on the T cell and CD40, OX-40L, GITRL, RANK on the APC. In the absence of co-stimulation T cells undergo anergy that renders them inactive. The cytokine milieu further dictates the subsets of T helper (Th) cells that will emerge from these interactions. Collectively, this information determines the fate of the T cell and shapes them into several effector subsets. Almost three decades ago Mosmann and Coffman described two distinct T helper subsets on the basis of their secreted signature cytokines: Th1 cells that produced IFN-γ and Th2 cells that produced IL-4 (Cherwinski et al., 1987; Mosmann et al., 1986). In the past ten years this view has been further expanded since Th17 cells have been discovered and it has been suggested that Th22 and Th9 cells further extend the T helper cell family. In addition to signature cytokines, lineage defining transcription factors have been assigned to the specific subsets of T helper cells. However, this is a fast moving field of active investigation and the *in vivo* reality suggests more complexity with varying degrees of plasticity existing within and between the different lineages.

T helper 1 cells

Th1 responses protect from invasive bacterial infections and are important in protecting the host from viral and protozoan infection. They have further been implicated in the pathogenesis of immune mediated diseases such as diabetes

and IBD. In skin diseases, Th1 cells play a role in contact dermatitis and psoriasis.

Th1 cells are important players of the adaptive immune response and are characterized by production of their signature cytokine IFN-γ and expression of the transcription factor T-box-containing protein expressed in T cells (T-bet) (Mullen et al., 2001; Szabo et al., 2000). T-bet is the master regulator of the Th1 differentiation program and indispensible for effective immune defence against intracellular pathogens (Szabo et al., 2000).

Activation of TCR and CD28 initiates IL-2 secretion and sensitivity in naïve T cells through signal transducer and activator of transcription 5 (STAT5) to drive T cell proliferation. IFN-γ secretion from NK cells and APCs leads to activation of STAT1 and expression of T-bet and upregulation of IL-12R as a consequence (Afkarian et al., 2002).

IL-12 is a proinflammatory heterodimeric cytokine made up of a p40 subunit shared with IL-23 and the unique p35 (Trinchieri, 2003). It is produced by DC and phagocytes and is a strong promoter of Th1 immunity (Trinchieri, 2003). IL-12, IL-18 and IFN-I can synergistically induce Th1 differentiation. These can activate STAT3 and STAT4 that further promote the differentiation process (Mullen et al., 2001; Szabo et al., 2000). T-bet sets the scene for increased expression of IFN-γ by epigenetic remodelling of the *Ifng* gene locus and promotes expression of IL-12R subunit β2 which synergistically further promote an amplification loop for Th1 development (Mullen et al., 2001).

In cutaneous immunity, Th1 cells are crucial for effective immunity against intracellular pathogens like *Mycobacterium spp.* and *Leishmania spp.* (Belkaid et al., 2000). Furthermore, Th1 cells in orchestration with $CD8^+$ T cells that

express type 1 cytokines (Tc1 cells) contribute to contact dermatitis in humans and murine contact hypersensitivity (CHS) (Honda et al., 2012; Ishizaki et al., 2007). These diseases are mediated by hapten-specific T cells and are caused by delayed-type hypersensitivity reactions of the skin (Ishizaki et al., 2007). Th1 cells are also implicated in the pathogenesis of psoriasis, which will be discussed in further detail later in this chapter.

T helper 2 cells

Th2 cells are crucial for protecting our bodies from diseases caused by extracellular pathogens such as helminth infections. However, these cells are also responsible for adverse reactions to food allergens and contribute substantially to atopic disease and asthma. Th2 cells play an important role in the pathogenesis and exacerbation of skin disease such as atopic dermatitis. It has been suggested that they substantially contribute to pruritus, a common symptom of skin diseases such as eczema that contributes to the vicious cycle of scratching and barrier dysfunction in patients (Cowden et al., 2010; Sonkoly et al., 2006).

IL-4, the hallmark cytokine of the Th2 lineage, activates STAT6 which in turn induces transcription of their master transcription factor GATA binding protein 3 (GATA-3) and enhances secretion of IL-4, IL-5 and IL-13 (Le Gros, 1990; Swain et al., 1990; Zheng & Flavell, 1997). At barrier sites such as the gut and the skin, non-hematopoietic and epithelial cells can contribute substantially to induction and differentiation of Th2 cells by secretion of thymic stromal lymphopoietin (TSLP), IL-33 and IL-25 (IL-17E) (Fort et al., 2001; Leyva-Castillo et al., 2013; Schmitz et al., 2005; Soumelis et al., 2002).

In allergic reactions, Th2 cells regulate both the acute- and late-phases. The Th2 cytokines and cell-contact dependent CD40/CD40L interactions mediate a strong signal in B-cells leading to IgE class-switch, crucial for activating mast cells and eosinophils.

T helper 17 cells

Th17 cells were described after Th1 and Th2 cells. They are characterized by expression of the cell surface receptors CCR6 and IL-23R and secrete the hallmark cytokine IL-17A along with IL-17F, IL-21, IL-22 and granulocyte-macrophage colony-stimulating factor (GM-CSF) (Hirota et al., 2007; Langrish et al., 2005; Liang et al., 2006; Weaver et al., 2013). Since their discovery some degree of plasticity between the T cell subsets has been described and further T helper subsets have been identified (Muranski & Restifo, 2013). The precise requirements and *in vivo* counterparts of experimentally described cell types is an ongoing and exciting field of immunological research.

Th17 cells are key players in the immunological response towards extracellular pathogens such as bacteria and fungi, with exceptional importance at barrier sites such as the skin, the gut and the lung. Here they induce inflammatory and chemotactic molecules as well as antibacterial agents that contribute to the physiological immune defence of our body. The importance of Th17 cells in barrier function is highlighted in patients with genetic deficiency in the IL-17 pathway. These patients suffer from a variety of symptoms many of them skin manifestations such as cutaneous candidiasis (Huppler et al., 2012).

A transcriptional programme that is co-ordinated by RORγt drives Th17 differentiation. Th17 cells are absent in mice deficient in *Rorc,* the gene that encodes RORγt (Ivanov et al., 2006). The differentiation of Th17 cells is driven by TGF-β, IL-6, IL-21 and IL-1β (Bettelli et al., 2006; Mangan et al., 2006; Zhou et al., 2007). However, IL-6 and TGF-β induce Th17 cells that also co-express IL-10 and are incapable in inducing autoimmunity *in vivo,* whereas the addition of IL-23 promoted Th17 cells with pathogenic capacity (McGeachy et al., 2007, 2009). The importance of TGF-β in Th17 differentiation has been challenged by findings that IL-1β, IL-6 and IL-23 are sufficient to elicit Th17 cells in both mice and men. These cells have high disease inducing potential and have been suggested to be the "pathogenic Th17 cells" in contrast to the TGF-β induced "non-pathogenic Th17 cells" (Acosta-Rodriguez et al., 2007; Lee et al., 2012; Zielinski et al., 2012). The lineage specific transcription factor RORγt is indispensible for Th17 cell generation and drives expression of key genes required for their differentiation and activation (Ciofani et al., 2012). However, several other transcription factors such as T-bet and RUNX can be co-expressed and might be contributing to the pathogenic vs. non-pathogenic phenotype setting the scene for the context-dependent function and cytokine secretion of Th17 cells (Duhen et al., 2013; Wang et al., 2014). Delineating this delicate balance of host protection and autoimmune potential of Th17 cells is of high interest and the subject of ongoing research in the field.

Th17 cells have been implicated in many autoimmune diseases such as psoriasis and atopic dermatitis, but also rheumatoid arthritis, psoriatic arthritis, ankylosing spondylitis, systemic lupus erythematosus and EAE.

In skin immunity, Th17 cells have undoubtedly a protective role that becomes evident in cases of fungal infections with C*. albicans* infection in patients with genetic deficiencies in this pathway (Huang et al., 2004; Puel et al., 2012). However, they can also be pathogenic in auto-inflammatory diseases of the skin. This is particularly highlighted by the unprecedented success of biological therapies that target the IL-23/IL-17 pathway in psoriasis (Kopp et al., 2015; Langley et al., 2014; Lebwohl et al., 2015; Leonardi et al., 2012; Papp et al., 2008; Papp, Leonardi, et al., 2012). To date, this condition, which will be discussed in further detail below, is the only disease routinely treated with monoclonal antibodies against the shared subunit of IL-12 and IL-23 (ustekinumab) or antibodies targeting IL-17A directly.

1.3.2.2. Regulatory T cells

One very important duty of the adaptive immune system is to prohibit dangerous responses against self and environmental antigens such as food and the microbiota. The negative selection of self-reactive T cells in the thymus, induction of anergy through chronic TCR engagement and lack of co-stimulatory molecules in the periphery are powerful mechanisms to promote tolerance. However, these mechanisms alone are insufficient to prevent the threat of immune-mediated pathology.

Early studies identified the thymus and spleen as a source of a population that was capable of preventing inflammation arising after neonatal thymectomy (Nishizuka & Sakakura, 1969; Sakaguchi et al., 1982). Antigen-experienced $CD4^+$ T cells capable of suppressing colitis were described and these studies highlighted the capacity of a $CD4^+$ T cell population to induce tolerance not only to self-antigens but potentially also to food and microbiota derived antigens in the gut (Morrissey et al., 1993; Powrie et al., 1993; Powrie & Mason, 1990)

Later, the discovery of a highly suppressive subset of $CD4^+$ T cells expressing high amounts of the IL-2Rα (CD25) facilitated the identification of these regulatory T cells (Tregs) (Sakaguchi et al., 1995). Foxp3 was identified as the essential transcription factor for Treg development and maintenance (Fontenot et al., 2003; Hori, 2003). The devastating and ultimately fatal disease caused by genetic mutations of Foxp3 highlights the unique and crucial importance of $Foxp3^+$ Tregs. The resulting disease, termed Immune dysregulation polyendocrinopathy enteropathy X-linked syndrome (IPEX), manifests with

multi-organ autoimmune diseases. It only affects hemizygous males but not heterozygous females due to the random inactivation of the X-chromosome (Gambineri et al., 2003). Foxp3 mutations in mice result in the “scurfy” phenotype and recapitulate many of the human features of the disease that include very early onset of intestinal inflammation, skin inflammation and type 1 diabetes (Brunkow et al., 2001). Targeted genetic deletion of Foxp3 in $CD4^+$ T cells precisely phenocopies the germ line mutated scurfy mouse and underpinned the non-redundant role of Tregs in promoting tissue homeostasis and tolerance (Fontenot et al., 2003).

Treg development

$Foxp3^+$ Tregs can arise in distinct locations. In the thymus, $Foxp3^+$ Tregs develop from $CD4^+$ precursors and are promoted by interactions of self-peptide MHC:TCR and CD28 co-stimulation (Itoh et al., 1999). IL-2 signalling is vital for the development of these cells that exit the thymus as natural Tregs (nTreg) (Zorn et al., 2006). The amount of self-antigen presented in the thymus correlates with nTreg development and the affinity of the TCR for self-peptide (Weissler & Caton 2014; Lee et al. 2012).

In the periphery, naïve $CD4^+$ T cells can up-regulate Foxp3 and differentiate into induced Tregs (iTregs) in the presence of IL-2 and TGFβ signalling (Chen et al., 2003; Kretschmer et al., 2005) (Coombes et al., 2007). Even though the transcriptional processes underlying the development of iTregs and nTregs have been delineated (Bilate & Lafaille, 2012), it is difficult to distinguish them once generated. Helios, a member of the Ikaros family of transcription factors, has been highlighted as a marker for nTregs (Thornton et al., 2010). Neuropilin

1 (Nrp-1), is a surface protein and potential marker of nTregs (Weiss et al. 2012; Yadav et al. 2012). However, the use of Helios and Nrp-1 to distinguish nTregs from iTregs has been questioned (Gottschalk et al., 2012; Himmel et al., 2013; Ross et al., 2014; Singh et al., 2015).

Transcriptional and epigenetic requirements for Tregs

In nTreg development, MHC:TCR interactions and co-stimulation lead to the upregulation of CD25. These stimuli lead to activation of several factors such as TAK1, IKK, BCL-10, CARMA1, and LAT, which are all upstream of NF-κB activation interaction (Koonpaew et al., 2006; Medoff et al., 2009; Schmidt-Supprian et al., 2003, 2004; Wan et al., 2006). NF-κB signalling enhances Foxp3 expression by triggering c-rel binding to the conserved non-coding sequence 3 (CNS3) in the Foxp3 locus (Long et al., 2009). Several transcription factors such as cyclic-AMP response element binding protein (CREB), ATF1 and ATF2 interact with the *Foxp3* promoter region and enhance Foxp3 expression (Kim & Leonard, 2007). TCR engagement leads to binding of nuclear factor of activated T cells (NFAT) and Smad3, a TGFβ signalling component, to the Foxp3 enhancer to stabilize Foxp3 expression (Marson et al., 2007; Tone et al., 2008). Foxo1 and Foxo3 are thought to contribute further to increase Foxp3 expression (Ouyang et al., 2012).

STAT5 phosphorylation in Tregs, which leads to expression of Foxp3 is mediated by the common γ-chain cytokines, mainly IL-2 but also IL-7 and IL-15 expression (Marson et al., 2007). Lack of IL-2 or IL-2R leads to development of autoimmune pathologies that can be rescued by IL-2 sufficient Tregs, highlighting its fundamental importance in Treg homeostasis (Zorn et al.,

2006). IL-2 is not produced by Tregs themselves, but their suppressive capacity depends on IL-2 signalling (Oldenhove et al., 2009).

Expression of Foxp3 in Tregs is fundamental for their function, but transient Foxp3 upregulation is also observed during activation of T cells (Miyao et al., 2012). However, this does not lead to a suppressive phenotype showing that Foxp3 alone is insufficient for stable Treg formation (Komatsu et al., 2009; Miyao et al., 2012). Two simultaneously published studies used a proteomic and a computational approach that led to the identification of several factors that contribute to Treg function and make up the 'Foxp3 interactome' (Fu et al., 2012; Rudra et al., 2012). The proteomic approach analysed proteins that associated with Foxp3 and identified several hundred proteins, many of them transcriptional targets of Foxp3 such as GATA-3 (Rudra et al., 2012). GATA-3 had previously been shown to be crucial for the maintenance and function of Tregs *in vivo* (Wohlfert et al., 2011). The computational approach identified five transcription factors (Eos, IRF4, Satb1, Lef1 and GATA-1) that lead to a regulatory phenotype in T cells. They have partly redundant functions and act in synergy with Foxp3 to a stable and 'locked' Treg phenotype (Fu et al., 2012).

Mechanisms of suppression

Tregs exercise their suppressive and immune regulatory capacity through an array of cell-contact dependent and independent mechanisms. They can regulate the priming and differentiation process of naïve T cells in lymphoid organs as well as the effector functions at the site of inflammation in the tissues (Dudda et al., 2008; Sather et al., 2007; Suffia et al., 2005).

IL-10 and TGFβ are secreted by various immune cell types and have immunosuppressive functions. Deficiency of IL-10 in Treg cells leads to multiorgan inflammation and autoimmunity (Rubtsov et al., 2008). TGFβ as well as IL-10 can act in a feedback loop to maintain Foxp3 expression and regulatory T cell function (Chen et al., 2003; Murai et al., 2009). This highlights that these cytokines act on other cells in a suppressive manner but amplify the immunoregulatory functions of Tregs themselves.

CTLA-4 is expressed on most Tregs and promotes anergy in self-reactive T cells. CTLA-4 deficiency in Tregs and blockade of this molecule leads to impaired suppressive functions and disease development (Wing & Sakaguchi, 2012). DC can induce and promote Treg function in part via MHCII dependent mechanisms and depletion of DC leads to a decrease in Treg frequency (Darrasse-Jèze et al., 2009). However, this regulation has a reciprocal dynamic as Tregs are capable of suppressing the capacity of DC to induce $CD4^+$ Teff differentiation (Onishi et al., 2008). They downregulate co-stimulatory molecules such as CD80/86 even in the presence of high levels of proinflammatory cytokines making this a likely process of dynamic regulation in an inflamed environment. Other molecules on Tregs are capable of exerting suppression and include the ectonucleotidases CD39 and CD73, glucocorticoid-induced tumor necrosis factor-related receptor (GITR), and OX-40 (Ephrem et al., 2013; Griseri et al., 2010; Howie et al., 2014).

Environmental adaptation of Tregs

Recently, several studies have highlighted the function and adaptation of Tregs in peripheral tissues. The environmental stimuli such as oxygen, nutrients, cytokines, and chemokines that Tregs are exposed to vary widely between tissues but fluctuate even more in different inflammatory settings in the periphery. Distinct subpopulations of Tregs have been described in many organs such as the skin, colon, lung, liver and adipose tissues (Burzyn et al. 2013).

Colonic Tregs have a distinct transcriptional profile. They are enriched for ST2, the receptor for the IL-1 family member IL-33 which is typically associated with induction of Th2 immunity (Schmitz et al., 2005). The importance of IL-33 signalling or control of intestinal inflammation has recently been demonstrated. IL-23 limits the responsiveness of Tregs to IL-33, highlighting the sensitivity of peripheral Tregs to different environmental cues (Schiering et al., 2014).

In the visceral adipose tissue (VAT) Tregs express the TF PPAR-γ which is required for their accumulation and suppressive function *in vivo* (Cipolletta et al., 2012). Differentiation of VAT Tregs also depends on the TFs IRF4 and Batf that directly regulate PPAR-γ and ST2. Similar to the gut, IL-33 signalling promoted Treg function in the VAT (Vasanthakumar et al., 2015).

Tregs have been shown to contribute to tissue repair in several organs. Amphiregulin (AREG) is highly expressed by muscle Tregs and contributes to muscle repair injuries by stimulating satellite cell growth (Burzyn, et al. 2013). AREG is further highly expressed by colonic T cells (Schiering et al., 2014). Recently, Treg specific deficiency in AREG was shown to promote lung injury *in vivo* and AREG secretion was mediated by IL-18 and IL-33 (Arpaia et al.,

2015). Responsiveness to IL-1 family members such as IL-18 and IL-33 and their capacity to initiate tissue repair is likely to be a general feature of tissue resident Tregs and aid in restoring homeostasis after inflammation.

In order to exert their suppressive function in a multitude of inflammatory settings and tissues, Tregs are capable of co-expressing lineage defining transcription factors that are important for regulation of immune responses. The transcription factor GATA-3 in Tregs is found at high levels at barrier sites such as the skin and the gut (Wohlfert et al., 2011). IL-33 can promote GATA-3 phosphorylation in Tregs, specifically at tissue sites (Arpaia et al., 2015; Schiering et al., 2014). IRF4 is another transcription factor important in Th2 function and as previously mentioned is a TF that 'locks' the Treg phenotype (Fu et al., 2012). *Irf4* deficiency in Tregs impairs their capacity to suppress Th2 cells and results in Th2 skewed inflammation *in vivo* (Zheng et al., 2009).

T-bet expression by Tregs upon IFN-γ stimulation is important for restraint of Th1 driven inflammation in the tissue (Koch et al., 2009). Regulatory T cell responses to *Toxoplasma gondii* depend in part on their capacity to upregulate CXCR3 in response to IFN-γ and IL-27 signalling (Hall et al., 2012). Tregs can also secrete IFN-γ themselves, contributing to graft survival in graft versus host disease (GVHD) and suppression of intestinal inflammation (Feng et al., 2011; Koenecke et al., 2012). The conversion of Tregs to secrete IFN-γ was driven by IL-12 but not IL-23 (Feng et al., 2011). As discussed above, IL-23 inhibited the IL-33 mediated suppressive capacity of Tregs in colitis and suggests an opposing impact of Th1 and Th17 inducing cytokines on Tregs.

As discussed earlier the transcription factor RORγt is important for Th17 differentiation. iTregs and Th17 cells share certain requirements for

differentiation and RORγt acts as an antagonist of Treg generation. STAT3 is a vital initiating factor for Th17 responses, but is also activated in Tregs. *Stat3* deficiency in Tregs renders them ineffective to suppress Th17 mediated inflammation (Chaudhry et al., 2009). Recent publications utilizing different models of colitis have demonstrated that RORγt^{+}Foxp3^{+} tissue resident Tregs are capable of restraining Teff responses *in vivo* (Ohnmacht et al., 2015; Sefik et al., 2015). These studies also highlighted the context dependent specialization of Tregs within the tissue, as RORγt^{+} Foxp3^{+} controlled different CD4^{+} Teff subsets in different models. This plasticity allows Tregs to adapt to their specific niche. The precise requirements and functions for Treg subsets in the tissue are only starting to be elucidated.

Another outstanding issue is the specificity of Tregs. A large fraction of Tregs is thought to be self-antigen-specific. Tregs express activation markers such as ICOS, CD69, CD38 and other markers that indicate that these cells are consistently encountering their antigen (Fisson et al., 2003). However, it is not yet understood what these antigens precisely are, if they differ between tissues, and if self-specific Tregs are widely shared between different organs.

Tregs in the skin

As one of our largest barrier organs, the skin harbours an enormous quantity of Tregs in both mouse and man, even under homeostatic conditions. Many circulating Tregs express markers associated with skin homing such as CCR4, CD103 and CLA (Hirahara et al., 2006). Genetic impairment of some of these molecules prevents Treg mediated suppression of skin inflammation (Dudda et al., 2008; Sather et al., 2007; Suffia et al., 2005). Virtually all Tregs in the skin

display an antigen-experienced phenotype and are referred to as effector-memory Tregs. Langerhans cells in the skin have the capacity to activate resident Tregs and induce their proliferation without presenting foreign antigen (Seneschal et al., 2012). This proliferation was mediated in part by IL-15 and interaction of Tregs with dermal fibroblasts (Clark et al. 2007).

A model using inducible keratinocyte driven expression of ovalbumin (OVA), a protein that is not expressed in the host under normal condition, has demonstrated that Tregs are activated upon encounter of the model antigen and reside in the skin where they are able to control inflammation resulting from subsequent antigen expression (Rosenblum et al., 2011). The maintenance of these tissue resident memory Tregs was dependent on IL-7 as blockade of IL-7R led to loss of these cells in the tissue but not the draining lymph nodes (Gratz et al., 2013).

*A*n *in vivo* microscopy study shows that the migratory potential is limited over short periods of time, i.e. under 1 hour (Chow et al., 2013). Another study conducted with the Kaede mouse strain, which allows permanent fluorescent marking of cells via UV exposure and thus tracking of cells over a long period of time, demonstrated that skin resident Tregs migrate to lymph nodes and recirculate to a high degree over an extended period of time (Tomura et al., 2010). The paramount importance of Tregs in skin homeostasis is revealed in patients with IPEX or IPEX-like diseases, where the skin is often one of the earliest and most severely affected organs (Halabi-Tawil et al. 2009; Goudy et al. 2013).

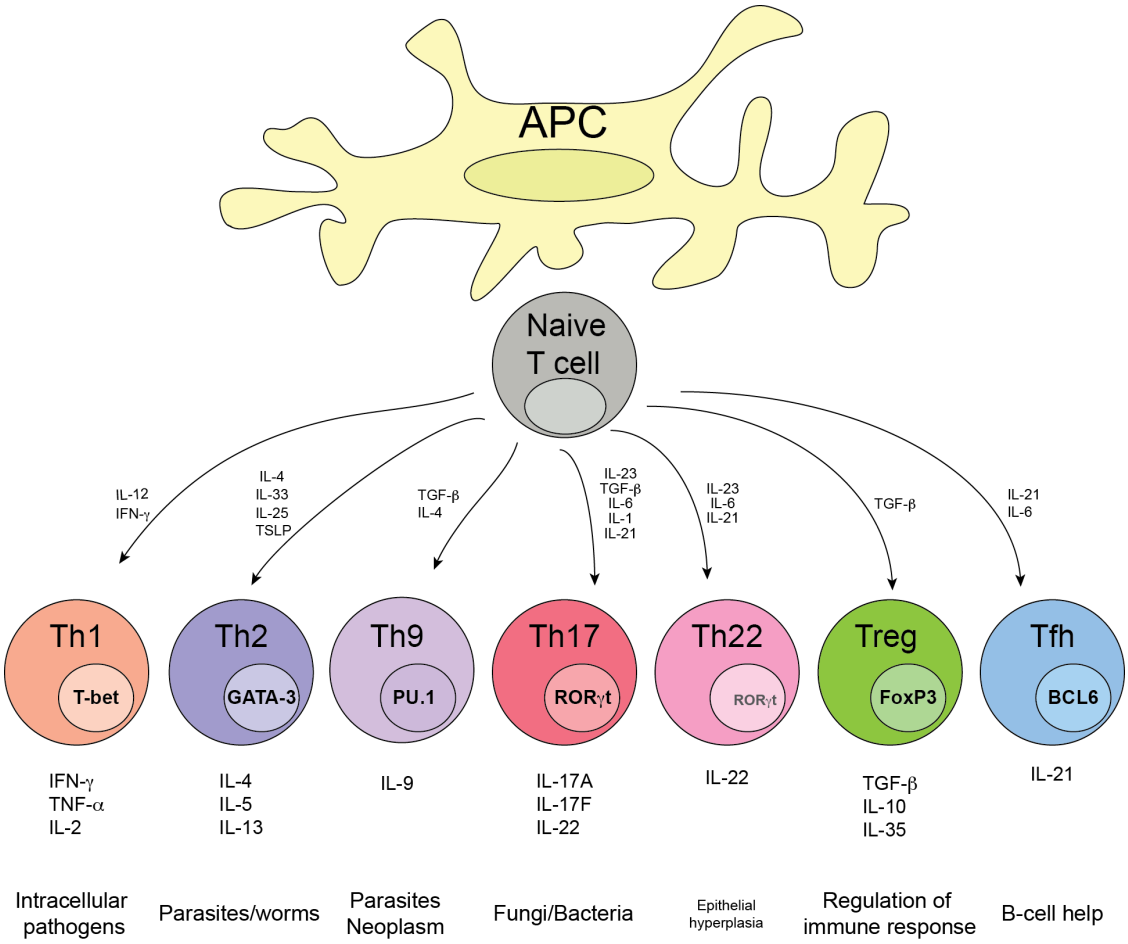

Figure 1.4. Differentiation of $CD4^+$ T helper cell subsets

Naïve T cells differentiate into the illustrated T helper subset in the presence of the indicated polarizing cytokines. These promote the differentiation and expression of lineage defining transcription factors. Each subset is characterized by the potential to secrete signature cytokines that mediate unique effector functions

1.3.2.3. $CD8^+$ T cells

$CD8^+$ T cells undergo a well-characterized selection process. Following pre-selection based on their ability to recognize and respond to MHC class I molecules presenting foreign antigens they leave the thymus as naïve cells. In secondary lymphoid organs like the spleen and lymph nodes these naïve $CD8^+$ T cells can be activated by interactions with APCs. DC have been shown to secrete the chemokines CCL3, CCL4 and CCL17 thereby attracting naïve $CCR5^+$ and $CCR4^+$ $CD8^+$ T cells during the priming process (Castellino et al., 2006). This interaction leads to a rapid expansion of $CD8^+$ T cells, which are capable of entering tissues and recognizing antigen on all nucleated cells via MHCI interactions. For example, in the context of LCMV infection, successful priming leads to a rapid expansion of mainly antigen-specific $CD8^+$ T cells, undergoing mitosis up to every 2 hours (Murali-Krishna et al., 1998; Yoon et al., 2010).

This wave of antigen-specific cytotoxic T cells is largely composed of short-lived effector cells (SLEC) and rapidly contracts after clearance of infection (Zhang & Bevan, 2011). This contraction leads to the formation of $CD8^+$ memory T cells that provide the potential for rapid re-expansion upon antigen re-encounter. For optimal expansion, $CD8^+$ T cells need to receive and integrate three signals. TCR stimulation and co-stimulatory signals such as CD80/86 are crucial for optimal expansion. IL-12 and IFN-I provide the third necessary signal and further shape the expansion and differentiation of $CD8^+$ T cells (Curtsinger et al., 2005; Gately et al., 1992). IL-12 contributes to the balance of effector and memory phenotype. While IL-12 signalling induces T-

bet and thereby promotes effector cell generation, it depresses expression of the TF Eomes, important for memory formation (Takemoto et al., 2006). It has been demonstrated that this balance is regulated in an mTOR-dependent manner (Rao et al., 2010).

IL-2 further shapes the memory and effector differentiation. High levels of IL-2 increase the effector and cytotoxic capacity of $CD8^+$ T cells and *IL-2ra*$^{-/-}$ cells have decreased expression of granzyme B and perforin, which are crucial for cytotoxic effects (Pipkin et al., 2010). Low levels of IL-2 signalling promote memory formation and highlight the role of IL-2 as a differentiation factor of $CD8^+$ T cells.

In addition to APCs, $CD4^+$ T (helper) cells are important for eliciting sufficient $CD8^+$ T cell responses. This requirement for $CD4^+$ T cell help depends on pathologic cause and tissue type. In influenza, LCMV, and *Listeria* infections, $CD4^+$ T cell help is dispensable but generation of adequate $CD8^+$ T cell responses to non-inflammatory antigens requires $CD4^+$ T cells (Bevan, 2004). In a model of vaginal herpes simplex infection, $CD4^+$ T cells enter the tissue before $CD8^+$ Teff and mediate their recruitment by up-regulation of chemokines such as CXCL9 and CXCL10 from the epithelium through IFN-γ secretion (Nakanishi et al., 2009).

$CD8^+$ T cell proliferation in the tissue is driven by antigen-specific interactions and contribute largely to the magnitude of the response to infection (McGill & Legge, 2009). The amplitude of such an expansion is connected to an increase in moDC in the tissue. While these APCs are dispensable for $CD8^+$ Teff degranulation per se, they increase their cytokine producing capacity via CD80/86 co-stimulation (Hufford et al., 2011).

Following the contraction of the initial effector phase, $CD8^+$ memory T cells arise. A subset of these, $CD8^+$ resident memory T cells (Trm) locate to the epithelium of body surfaces where they can persist in previously uninfected areas and pose a first line of defence. Upon antigen encounter they secrete cytokines such as IL-2, IFN-γ and TNF-α and rapidly initiate an immune response and initiate a tissue-wide alert state (Ariotti et al., 2014; Schenkel et al., 2014). These findings identify Trm as crucial initiators of the immune response and show that adaptive immunity is a key contributor to immune sensing in barrier tissues.

1.2. Psoriasis

Psoriasis is a chronic inflammatory disease of the skin with a relapsing and remitting pattern and frequently requires a life-long treatment for patients. The most common form plaque psoriasis, also termed psoriasis vulgaris, becomes clinically apparent by widespread erythematous plaques with adherent scales. It affects 2-3% of the general population worldwide, with higher incidence among Caucasians (Nestle et al., 2009). The prevalence of psoriasis increases with distance from the equator and has a very low incidence in children that rises with age (Parisi et al., 2012). Two distinct age groups associated with increased incidence have been observed, with one in childhood and early adulthood and a further incidence peak later in life. Evidence suggests different genetic predispositions, as the later incidence peak has been associated with HLA-C alleles.

Psoriasis is associated with increased mortality and many patients suffer from co-morbidities such as cardiovascular disease, metabolic syndrome and psychological disorders like depression. However, the most prevalent co-morbidity in patients with skin manifestations is psoriatic arthritis with approximately 1/3 of patients affected during their lifetime (Gladman et al., 2005; Nestle et al., 2009). In a population study, patients had an up to 5 year lower life-expectancy than controls (Gelfand et al., 2007). Together, this implicates a strong socio-economic burden of psoriasis due to a lifetime of medical interventions paired with decreased productivity due to associated diseases and decreased life expectancy. Interestingly, the difference in incidence of psoriasis between women or men varies between studies and a

strong gender bias that can be found in other autoimmune pathologies is not clear in patients with psoriasis (Parisi et al., 2012).

Even though psoriasis has certain features of an autoimmune pathology, the existing data do not support its classification as a bona fide autoimmune disease. To date, antigenic drivers of psoriasis have not been identified and even though the contribution of infectious agents has been suggested, this is certainly not the case in all individuals affected (Valdimarsson et al., 2009). Based on these findings, psoriasis might be best regarded as a chronic inflammatory disorder with certain aspects of an autoimmune disease.

1.2.1. Clinical and histological features of psoriasis

The hallmark feature of psoriasis is plaques with a typical raised, well-demarcated, erythematous appearance with adhering silvery-white scales. Elbows, knees, the lower lumbar region and the scalp are predilection sites where plaques typically appear. This typical presentation makes the diagnosis fairly easy. Besides the most common form, plaque psoriasis, patients can suffer from an array of clinical phenotypes such as guttate, inverse, pustular, erythrodermic, palmo-plantar, and the acute and life threatening generalized pustular psoriasis von Zumbush (Lowes et al., 2014). It will remain to be seen if these different presentations might be associated with a distinct immunogenetic profile.

The histological analysis of a psoriatic plaque reveals a greatly thickened epidermis (acanthosis) that is due to a highly accelerated keratinocyte proliferation. As a result, the normal KC differentiation process is disturbed and as a consequence, the stratification of the epidermis changes. The normal granular layer is lost, the stratum corneum is thickened (hyperkeratosis) and the nuclei of KC are not expulsed (parakeratosis). Immune cells accumulate at an abnormal rate, leading to neutrophil abscesses (Munro's abscess) in the epidermis (Lowes et al., 2014). The red appearance of the skin is caused by an increase and dilation of dermal blood vessels that reach up to the dermo-epidermal junction and cause pinpoint bleeding when the thick scales are removed from the skin (Auspitz sign). Immune infiltrates are also found in the usually oligocellular dermis, with abundant mononuclear cells and T cells present.

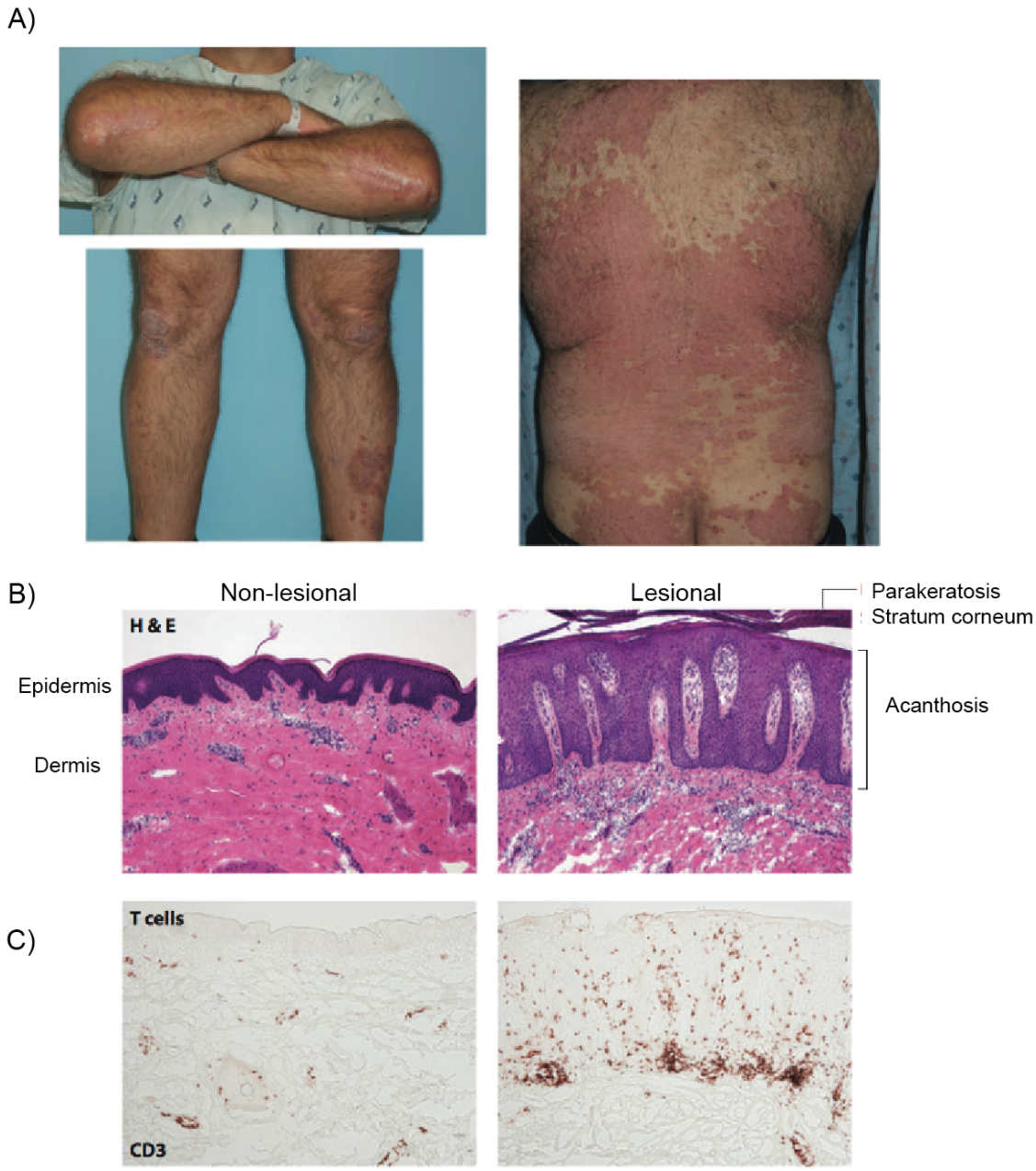

Figure 1.5. Clinical and histological manifestation of psoriasis

(A) Macroscopic appearance of psoriatic plaques with demarcated, erythematous plaques.

(B) H&E staining of lesional and non-lesional skin.

(C) Staining for T cells (CD3) in lesional and non-lesional skin.

Figure adapted with permission from Lowes et al, 2014; Ann Rev. Immunology

1.2.2. Immune cell axis in psoriasis

T cells

It was long disputed if KC or T cells are the disease driving cells in psoriasis, with the other components perpetuating the inflammation by a secondary response. This question was elucidated to some degree by studies using drugs to target T cells in patients. The first study used a fusion protein that induced apoptosis in activated T cells expressing the IL-2 receptor. This finding demonstrated that depleting activated T cells in patients could lead to clinical and histological clearance of the disease and proved that T cells were indeed non-redundant in the disease pathogenesis (Gottlieb et al., 1995). Further studies showed that a complete depletion of T cells was not necessary, but preventing migration of T cells into the tissue or blocking activation of T cells by inhibiting integrin interactions or co-stimulatory molecules was sufficient, (Abrams et al., 1999; Chamian et al., 2005).

Activated memory T cells are increased in lesional psoriatic skin. $CD4^+$ T cells are mainly confined to the diseased dermis, whereas high numbers of $CD8^+$ T cells are found in the epidermis. Studies have revealed that some T cells found in affected skin of individuals with psoriasis are of oligoclonal origin (Chang et al., 1994; Lin et al., 2001). This might be in part explained by evidence suggesting that psoriasis has an association with streptococcal throat infection, and that by molecular mimicry, bacteria-reactive T cells are cross-reacting to components found in the skin (Valdimarsson et al., 2009).

T cells in psoriatic skin produce large amounts of cytokines compared to those from healthy skin. $CD4^+$ Th1 cells that produce increased amounts of production of IFN-γ and TNF-α is a prominent feature of skin-resident T cells extracted from diseased biopsies (Austin et al., 1999). KC and myeloid cells secrete chemokines such as CXCL9, CXCL10 and CXCL11, which aids migration of these cells into the tissue.

IL-23 levels are high in affected skin and drive a prominent Th17 infiltrate in the dermis. Patients under successful treatment with TNF-neutralizing antibodies rapidly down-regulate genes associated with Th17 polarization (Zaba et al., 2007; Zaba, Krueger, et al., 2009). Studies show that the IL-17 is mainly coming from Th17 cells, but additionally $CD8^+$ T cells expressing IL-17 (Tc17) and also dermal γδ T cells can be the source of this cytokine (Lowes et al., 2014).

Tregs play a crucial role in controlling inflammation and defects in regulatory pathways can lead to the development of autoimmune diseases and chronic inflammation, as discussed above. Some studies suggest that the function of Tregs in affected psoriatic skin is impaired and facilitate pathogenic Teff function (Sugiyama et al., 2005). However, the role of Tregs has not been fully elucidated and further investigation can provide valuable insight in the local dynamic of inflammatory cells in the skin of patients suffering with psoriasis.

$CD8^+$ T cells accumulate in the psoriatic skin and are located in the dermis as well as the epidermis, but make up the main T cell population in the latter (Baker et al., 1984). IL-17A-producing $CD8^+$ T cells have been identified in

psoriatic plaques. (Kryczek et al., 2008; Ortega et al., 2009) $CD8^+$ T cells from psoriatic skin have an increased capacity to secrete IL-22 or IL-17 in response to stimulation compared to those derived from healthy control skin. In contrast, $CD4^+$ T cells from both populations secreted equal amounts (Res et al., 2010). IL-17A and IFN-γ production by $CD8^+$ T cells in the epidermis drove inflammation in a mouse model of psoriasis, in which IFN-γ or CD8 depletion attenuated inflammation (Gunderson et al., 2013). $CD8^+$ T cells are likely involved in the pathogenesis of psoriasis. Their location in the epidermis suggests that they have a non-redundant pathogenic function that needs to be further investigated.

Myeloid derived cells: Monocytes/Macrophages and DC

Different types of DC and macrophages are increased in the psoriatic plaque. Plasmacytoid DC are absent from healthy skin under homeostatic conditions. However, psoriatic individuals harbour pDC in their uninvolved skin (Nestle et al., 2005). pDC are also termed professional interferon producing cells due to their capacity to secrete large amounts of IFN-I (Swiecki & Colonna, 2015). The importance of IFN-I and thus potentially of pDC was highlighted by observations that IFNα was increased in lesional skin more than 20 years ago (Schmid et al., 1994; van der Fits et al., 2004). Through the use of a xenotransplant model utilizing immunocompromised mice and transplanting uninvolved skin of psoriatic patients, it was demonstrated that pDC contribute substantially to the early phases of plaque formation mainly by supplying IFN-I (Nestle et al., 2005). DC can sense viral infections via detection of viral RNA and DNA through endosomal toll-like receptors that leads to cytokine induction and an immune response (Brencicova & Diebold, 2013). Interestingly, LL-37, an antimicrobial peptide increased in psoriatic skin can form complexes with self-DNA to activate his pathway via TLR7 in the endosomal compartments of pDC and induce increased IFN-I production (Ganguly et al., 2009). In the presence of self-LL-37 complexes, pDC can facilitate KC- immune cell crosstalk and contribute to the maturation of mDC and T cells, which contributes to plaque formation. LC in individuals affected by early- vs. late-onset psoriasis demonstrate different behaviour and impaired LC mobility was observed in psoriatic patients that was restored with successful therapy (Shaw et al., 2010, 2013). However, the importance of these observations remains to be clarified.

Myeloid DC have been observed in greater numbers in the psoriatic skin with a 30-fold increase of $CD11c^+$ mDC (Lowes et al., 2005). Drugs inhibiting the co-stimulatory interaction of DC and T cells such as alefacept and efalizumab have proven to be effective in the therapy of psoriasis (Chamian et al., 2005; Lowes et al., 2005). This strongly suggests a contribution to disease pathogenesis. Isolated from psoriatic skin, mDC can induce Th1 and Tc1 as well as Th17 cells and thus increase the levels of IL-17 and IFN-γ, two cytokines that are increased in affected skin of patients (Zaba, Fuentes-Duculan, et al., 2009; Zaba, Krueger, et al., 2009). Similar to pDC mentioned above, mDC can be activated by LL-37 that forms complexes with self-nucleotides. Here, self-RNA-LL-37 complexes activate the endosomal TLR7/8 pathway and induce an inflammatory DC phenotype (Ganguly et al., 2009). TNFα and inducible nitric oxide synthase (iNOS) are elevated in psoriatic skin and are potent in inducing tissue inflammation. $CD11c^+$ DC are a dominant source of TNFα and iNOS in the inflamed psoriatic skin and are reduced with anti-TNFα targeting therapies (Leonardi et al., 2003; Serbina et al., 2003). Pre-clinical evidence of the importance of $CD11c^+$ cells, was generated from the imiquimod model of psoriasiform skin inflammation. Disease induction in this model is MyD88 dependent (discussed in more detail below). However, cell type specific expression of MyD88 in $CD11c^+$ cells is sufficient to induce skin inflammation to the same level as in WT mice (Wohn et al., 2013). DC are a major source of IL-23 and IL-12 and both cytokines have been strongly implicated in the pathogenesis psoriasis. Ustekinumab, an antibody targeting the shared p40 subunit is extremely efficacious in the treatment of moderate to severe psoriasis (Papp et al., 2008). As previously discussed, IL-23 and IL-12

drive the differentiation of Th17 and Th1 cells, respectively. Drugs targeting the IL-23/Th17 axis have had unparalleled success in the treatment of psoriasis.

As previously mentioned, pDC are not found under homeostatic conditions and have been proposed to promote a wound-healing effect (Gregorio et al., 2010). In a xenotransplant model of human psoriasis pDC were involved in the early initial phase of the disease and contributed to the pathogenesis by production of IFN-I (Nestle et al., 2005). Further supporting a deregulated immune sensing component in psoriasis are reports that some patients receiving topical treatment with the TLR7 agonist imiquimod develop psoriatic plaques (Gilliet et al., 2004). Furthermore, this phenomenon has led to the development of a mouse model of psoriasis by topical imquimod treatment, which closely recapitulates the human disease and will be discussed later (van der Fits et al., 2009).

1.2.3. Genetic elements of psoriasis

Psoriasis is a multi-factorial disease in which genetic as well as environmental factors contribute to disease pathogenesis. (Capon et al., 2012; Di Meglio et al., 2011). Genetic predisposition to psoriasis has been demonstrated in family studies that revealed significant higher concordance rates for monozygotic twins (65-72%) than dizygotic twins (15-30%). On this basis several studies have led to the identification of psoriasis susceptibility genes that can be divided into three broad categories: tissue-specific, immunologically innate, and immunologically adaptive. (Perera et al., 2012).

The segment psoriasis susceptibility 1 (PSORS1) locus on chromosome 6 was identified over 40 years ago and accounts for 35-50% of the heritability of psoriasis (Russel et al., 1972). The MHC class I molecule HLA-C with its allele *HLA-Cw*060* is the most likely gene responsible for the association (Fan et al., 2008; Ying Liu et al., 2008; Nair et al., 2006). Several genome-wide association studies (GWAS) and gene specific studies have led to the identification of susceptibility loci. A GWAS performed in a Chinese population confirmed HLA-Cw6 as a risk allele in early onset psoriasis (<40years), but not in older patients (Zhang et al., 2009). As $CD8^+$ T cells are activated via MHCI, this further supports a role for this cell type in disease pathogenesis.

The epidermal differentiation complex (EDC) located on chromosome 1 contains approximately 20 genes that are crucial for the differentiation of keratinocytes and forming of the cornified envelope of the skin. GWAS have led to the identification of several genes in this area, highlighting the importance of KC and their differentiation as well as pathologic wound-healing

responses in the pathogenesis of psoriasis (de Cid et al., 2009; Zhang et al., 2009). This association could explain the still elusive “Köbner phenomenon” where skin injury leads to plaque formation in patients.

A GWAS performed in a European population identified several susceptibility loci located in NF-κB, IL-23, and Th2 mediated pathways (Nair et al., 2009). The NF-κB pathway is crucial in cell-cycle control and essential in the inflammatory response (Hayden & Ghosh, 2012). It is activated by a plethora of proinflammatory stimuli such as different cytokines and bacterial products and can initiate activating signalling cascades in the adaptive and innate arms of the immune system (Hayden & Ghosh, 2012). An increase of NF-κB in skin biopsies of both involved and uninvolved skin of patients suffering with psoriasis further supports the suggestion that the negative regulation of the proinflammatory activity of NF-κB is compromised (Lizzul et al., 2005).

As discussed above, IL-23 has been implicated as a crucial cytokine in several inflammatory autoimmune responses including psoriasis and inflammatory bowel disease (IBD). Genetic studies have begun to clarify the clinical and pre-clinical observations that human psoriatic skin contains high amounts of IL-23 and Th17 cells and that local injection of IL-23 in mouse skin leads to psoriasiform inflammation (Zheng et al., 2007). In psoriasis, SNPs in the *IL-23R* gene have been confirmed independently by several studies (Capon et al., 2007; Cargill et al., 2007). Patients carrying the protective *IL-23R Arg381Gln* variant had impaired Th17 effector function as they had decreased STAT3 activation and IL-17A cytokine production when stimulated with IL-23 compared to controls (Di Meglio et al., 2011). This variant has also been

shown to be protective for ankylosing spondylitis and Crohn's disease (Di Meglio et al., 2011).

1.2.4. Cytokine axis in psoriasis

Over the last decade, the complex cytokine network involved in psoriasis has been acknowledged as the most important driver of inflammation and simultaneously poses a powerful angle for therapeutic intervention. Below are some, but by no means all, important cytokines discussed in brief.

IL-1 was the first cytokine detected in the skin and various of its many family members are elevated and involved in psoriasis (Johnston et al., 2011; Luger et al., 1982). IL-1α and IL-1β are present in normal skin and act in an autocrine and paracrine fashion on keratinocytes as well as on stromal cells, lymphocytes and APCs (Murphy et al., 2000). In inflammation, IL-1α appears to be critical for formation of T-cell/APC clusters in the skin and synergizes with IL-23 in the induction of Th17 responses (Kryczek et al. 2008; Natsuaki et al. 2014). However, use of anakinra, an IL-1R antagonist has failed to show efficacy in psoriasis patients (Jung et al., 2010). IL-36 is a sub-family in the IL-1 family and includes three receptor agonists and one receptor antagonist. All IL-36 cytokines are up-regulated in psoriasis and have a role in neutrophil and T cell attraction as well as enhancement of APC function in the skin (Foster et al., 2014). In the rare but severe generalized pustular psoriasis, families with loss-of-function mutations in the IL-36 receptor antagonist gene have been identified and support the proinflammatory role of IL-36 cytokines (Tortola et al., 2012). Taken together, IL-36 might be an attractive therapeutic target for psoriasis.

As for many auto-inflammatory diseases, IL-17 plays a key role in the pathogenesis of psoriasis. IL-17A, IL-17F and IL-17C are all increased in

psoriatic skin (Johnston et al., 2013; Kryczek et al., 2008; Lowes et al., 2008). IL-17A and IL-17F are mainly derived from immune cells whereas keratinocytes appear to be the main source for IL-17C (Johnston et al. 2013). An array of biological therapies and small molecule inhibitors targeting either IL-17 family members, their inducing cytokines, their receptors or critical transcription factors have been developed. One such drug, the IL-17A neutralizing antibody secukinumab has had outstanding success and was recently approved for routine use (Langley et al., 2014; Sanford & McKeage, 2015).

As introduced and discussed in detail previously, IL-12 and IL-23 have distinct and intimate roles in differentiation of Th1 and Th17 cells, respectively. They both belong to the same family and each consists of two subunits, of which the p40 subunit is shared. All three subunits are overexpressed in psoriatic lesions (Lee et al., 2004; Yawalkar et al., 1998). A blocking antibody targeting p40, ustekinumab, has had an immense impact for the treatment of psoriatic patients (Kauffman et al., 2004; Yeilding et al., 2007). Originally, psoriasis was regarded as a mixed Th1/Th17 disease. IL-12 is a major inducer of Th1 cells and IFN-γ interestingly can induce skin-homing markers such as CLA on memory T cells (Sigmundsdóttir et al., 2004). Genetic variations in IL-12 lead to enhanced Th1 polarization in patients with psoriasis (Johnston, et al. 2013).

The importance of IL-23 in the pathogenesis of psoriasis is underscored by genetic polymorphisms in the *Il23R* that are associated with psoriasis, but also Crohn's disease and psoriatic arthritis (Capon et al. 2007; Nair et al. 2008; Di Meglio, et al. 2011). IL-23 amplifies and sustains Th17 cell function and successful pharmacological intervention by cytokine or receptor blockade of IL-

23 emphasizes the role of IL-17 as a major culprit in psoriasis (Kopp et al., 2015).

TNFα has been a hallmark cytokine of successful therapeutic intervention in several autoimmune diseases. In the skin it appears to act in synergy with IL-17A and IL-17C by stabilization of mRNA, and reciprocal receptor induction (Hartupee et al., 2007; Johnston et al., 2014). Not all psoriasis patients show responses to anti-TNF treatment alone, highlighting the heterogeneous nature of this disease and indicating that perhaps a combined approach would be beneficial to some (Papp et al. 2012).

IFN-I were first associated with psoriatic skin almost four decades ago (Kariniemi, 1977). However, to date their precise role still remains elusive. IFN-I are known to be involved in early phases of psoriatic plaque initiation as demonstrated in an engrafted mouse model (Nestle et al., 2005). Supportive of their importance in disease pathogenesis are various reports of patients developing psoriasis while undergoing interferon alpha therapy (Afshar et al., 2013). However, a blocking antibody of IFNα has failed to show efficacy in a phase I clinical trial (Bissonnette et al., 2010). A potential reason for these ambiguous findings could be that IFN-I are key players of the psoriatic cytokine networks in either a subset of patients only or act at a very precise time in disease development.

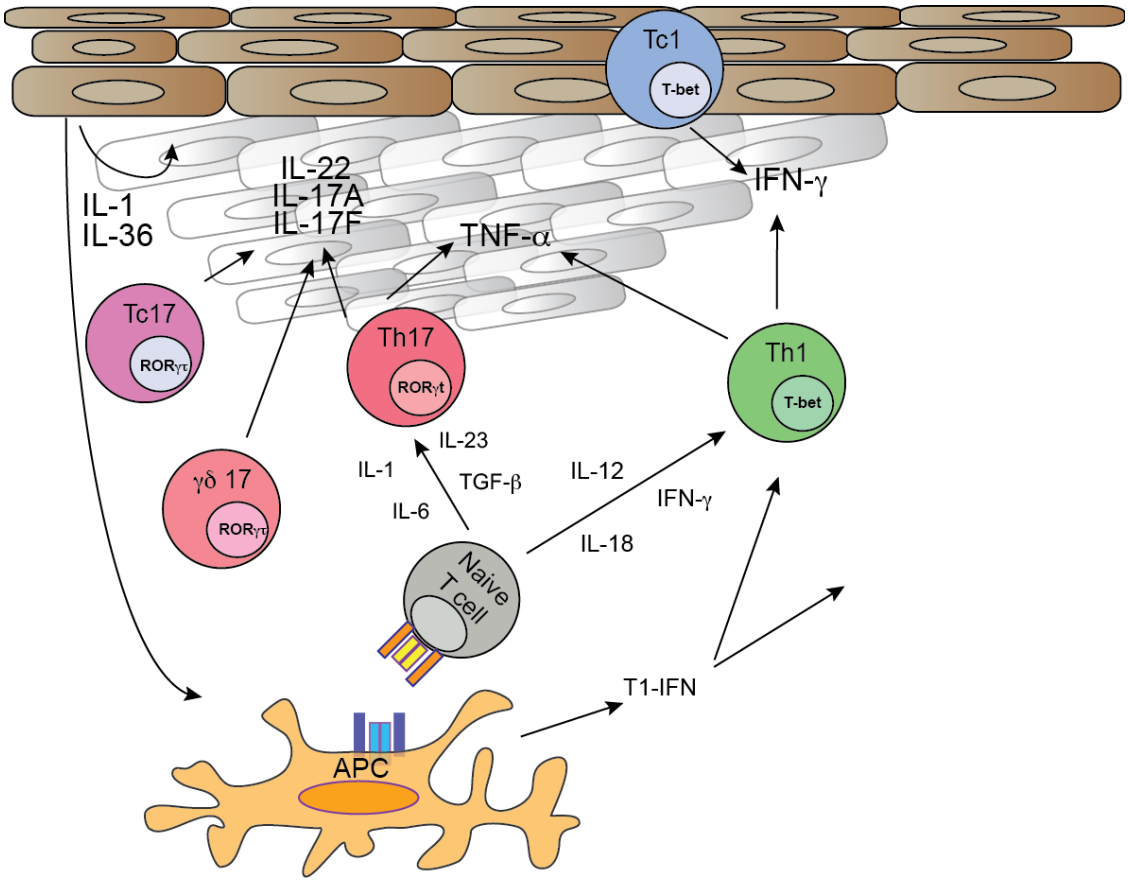

Figure 1.6. Cytokine axis involved in psoriasis

Psoriasis is regarded as a disease with mixed Th1/Th17 involvement. Further, γδ T cells and $CD8^+$ T cells contribute to the pathogenesis the cytokines involved in T helper cell development and pathogenic functions are strongly unregulated in affected skin.

1.2.5. Therapeutic options for psoriasis

For clinical and treatment purposes, patients are often grouped into mild-to-moderate (5-10% of body surface affected) and moderate-to-severe (>5-10 % or face, palm/sole involvement) disease categories. For the former, treatment is often attempted with topical agents only, whereas the later group usually requires systemic therapy that is also largely guided by accompanying symptoms such as psoriatic arthritis (Feldman, 2015).

The medical management for mild-to-moderate affected patients includes UV-light therapy, topical corticosteroids, tar, anthralin, topical Vitamin-D analog, and topical immunosuppressants. A combination of topical and systemic medication benefits patients suffering with more severe disease. Traditionally, methotrexate and cyclosporine as well as retinoids are routinely used in systemic therapy. In the last decade, biologicals including anti-TNF and anti-IL-23 antibodies have demonstrated superior efficacy over traditional therapies, but are reserved for most severely affected patients due to their high economic cost. To date, the TNF alpha targeting drugs etanercept, infliximab, adalimumab and the IL-23/IL-17 targeting drugs ustekinumab and secukinumab are approved for routine clinical use. Further biological therapies targeting the IL-23/IL-17 axis are in clinical trials and it remains to be determined if their long-term safety and efficacy profile will allow their wide clinical use. Nevertheless, the development, successful trials and clinical use of these biologicals have immensely aided not only the patients suffering from severe disease, but also our understanding of the underlying immunological aetiologies of this skin disease.

The agent denileukin diftitox triggers apoptosis via the IL-2R in activated T cells and was the first drug used for the treatment of psoriasis that proved that directly supported a causative role for T cells in this disease (Gottlieb et al., 1995). CTLA-4-IgG (abatacept) proved that depletion of T cells was not essential as it showed consistent improvements at high doses correlated with decreased immune infiltrates in the skin (Abrams et al., 1999). Later, agents targeting the activation of T cells such as the LFA-3-Ig fusion protein alefacept that inhibited the CD2-dependent activation and led to a strong decrease in skin T cells but also circulating memory T cells, proved efficient (Chamian et al. 2005; Chamian et al. 2007). Efalizumab, a monoclonal antibody targeting the integrin CD11a (which facilitates T cell migration to the tissue as well as co-stimulation and leads to a decrease in inflammatory TIP DC) was also successful but is no longer used due to increased risk for development of progressive multifocal leukoencephalopathy (Kothary et al., 2011; Lowes et al., 2005).

As discussed above, targeted blockade of cytokines is highly efficient in psoriasis and further agents are currently in clinical trials and development (Table 1.1).

Target	Agent	Drug	Trade name
IL-2R	DAB389IL-2 FP	Denileukin diftidox	Ontak
B7 (CD80/CD86)	CTLA-4-Ig FP	Abatacept	Orencia
CD2	LFA-3-Ig FP	Alefacept	Amevive
CD11a	Anti-CD11a	Efalizumab	Raptiva
TNF	mAb Anti-TNF	Infliximab, Adalimumab	Remicade, Humira
TNF	mAb TNFR-Ig FP	Etanercept	Enbrel
IL-12/IL-23	Anti-IL-12/-23p40 mAb	Ustekinumab, Briakinumab	Stelara, Ozespa
IL-23	Anti-IL-23p19 mAb	LY2525623, SCH 900222, CNTO 1959, AMG 139	
IL-17A	Anti-IL-17A mAb	Secukinumab, Ixekizumab	
IL-17R	Anti-IL-17RA mAb	Brodalumab	

Table 1.1. Biologic treatments for psoriasis

These agents have been tested or are in current trials and clinical use for moderate-to severe psoriasis. (Adapted from Lowes et al, 2014; Ann Rev. Immunology)

1.3. Murine Models of Psoriasiform Skin Inflammation

As previously mentioned, mouse skin differs from human skin in various aspects. Even though the stratification of the skin is similar, mouse skin is much thinner than human skin. Mice also exhibit a synchronized hair cycle, lack sweat glands and evidently have more dense hair follicles than humans (Wagner et al., 2010). Further differences in immune cell populations were discussed above and have to be taken into consideration when interpreting conclusions and results of animal based research. Swindell et al. compared transcriptomic analysis of five mouse models to human psoriatic skin and highlighted similarities and discrepancies between the models and also in comparison with the clinical samples (Swindell et al., 2011). Nevertheless, using mice as pre-clinical experimental models for human disease is of great value and importance for developing new drug targets and for the identification of novel pathways involved in disease pathogenesis.

Broadly, most mouse models can be divided into transplantation models with xenografts or allografts, transgenics, targeted mutations, spontaneous models and cytokine or TLR challenge models (Wagner et al., 2010).

A new mouse model of psoriasiform skin inflammation was introduced in 2009 by van der Fits and colleagues (van der Fits et al., 2009). For this model, the drug Aldara™, a cream containing 5% of the active compound imiquimod is applied daily to the skin of mice for at least 5 consecutive days (van der Fits et al., 2009). In its original description the model was mainly attributed to the TLR7 agonistic properties of the imidazoquinoline imiquimod and later publications highlighted the importance of $CD11c^+$ DC for this model (Tortola et

al., 2012; van der Fits et al., 2009; Walter et al., 2013). Treatment with Aldara™ is routinely used in the clinic for virus-associated skin abnormalities like genital warts as well as pre-cancerous skin lesions such as actinic keratosis and basal cell carcinomas (Geisse et al., 2002; Szeimies et al., 2004). The model was developed on the basis of case reports demonstrating that topical imiquimod therapy can induce psoriasis-like plaques in patients using this topical therapy, but do not suffer from psoriasis (Gilliet et al., 2004). It was further reported that Aldara™ has the potential of provoking and exacerbating disease even in well-controlled patients suffering with psoriasis on previously unaffected skin and even at sites the cream was not applied to (Fanti et al., 2006; Rajan & Langtry, 2006).

In the first study using the imiquimod model of psoriasiform skin inflammation, the authors demonstrated that this is mediated through the IL-23/Th17 axis as blockade of the receptor for IL-23 and IL-17 abrogated the disease (van der Fits et al., 2009). IL-22 is also required for the formation of the lesions, further underlining the similarities with human disease where the levels of IL-22 positively correlate with disease severity (Caproni et al., 2009; Van Belle et al., 2012). An IL-22 blocking antibody has been in clinical trials, however the trials were discontinued and to date no results have been published (Gudjonsson et al., 2012; Hao, 2014).

One study has highlighted the impact of isostearic acid, another compound found in Aldara™ (Walter et al., 2013). It is suggested to act via inflammasome activation and IL-1β release in KC. This further supports the use of the imiquimod model of psoriasiform skin disease as it jointly activates the innate as well as the adaptive arm of the immune system; this is important as their

cooperative involvement has been proposed in human psoriasis (Tsoi et al., 2012). In contrast to human psoriasis, the main sources of IL-17 and IL-22 in the imiquimod model are not $CD4^+$ αβ T cells, but γδ T cells that infiltrate the dermis. These cells are responsive to IL-23 and are positive for the transcription factor RORγt. However, in mice lacking γδ T cells, αβ T cells act as the primary source of these disease-driving cytokines. Furthermore, ILCs have the capacity to secrete IL-17 and are sufficient to induce disease in the absence of RAG and consequently all T and B cell populations (Cai et al., 2011; Pantelyushin et al., 2012). These observations in the imiquimod model have led to the findings of cytokine producing ILC3 in psoriatic skin of patients. (Teunissen et al., 2014; Villanova et al., 2014).

While the evidence for a pathogenic role for IL-23 and its downstream cytokines like IL-17 is strong in this model, little is known about possible regulatory mechanisms, such as Tregs and IL-10, which may control and resolve the inflammatory response. Research of these and further regulatory mechanisms will aide the identification and assessment of their importance in human disease.

1.4. Hypothesis and Aims of this Investigation

Tregs make up a large proportion of $CD4^+$ T cells found in the skin of humans and even more so in mice. Studies conducted over a decade ago revealed that Tregs could be impaired in the skin of psoriatic patients (Sugiyama et al., 2005). However, little additional data has been published since.

Tregs are crucial regulators of the immune systems and are key cells in the immune response. Indeed, dysfunctional Tregs have been implicated in many inflammatory diseases on the autoimmune spectrum such as type 1 diabetes and inflammatory bowel disease. Imaging studies demonstrated that Tregs are dispersed throughout the dermis at steady state with limited short term but significant long-term migratory capacity (Chow et al., 2013; Tomura et al., 2010). Notably, Tregs in the skin are largely of a memory phenotype and can convey “regulatory memory” crucial for challenges with previously encountered pathogens (Rosenblum et al., 2011). Tregs with a memory phenotype are found in murine and human skin (Rodriguez et al., 2014).

Genetic mutations in the *Foxp3* gene lead to a severe disease phenotype called the IPEX syndrome. These patients suffer from an array of symptoms, which include early manifestation of skin inflammation, usually of atopic dermatitis or psoriatic appearance and require a bone marrow transplant within the first decade of life (Halabi-Tawil et al., 2009).

The clear evidence that Tregs are prevalent in the skin and are indispensible for homeostasis warrants further investigations into their functions at this barrier organ. The hypothesis to be tested in this thesis is whether $Foxp3^+$ Tregs have a protective role in psoriasiform skin inflammation. The imiquimod

model of psoriasiform skin inflammation is used as the main tool to investigate this hypothesis.

The aims of this thesis are:

1. To perform phenotypic and transcriptomic analysis of skin resident Tregs in homeostasis and inflammation (discussed in Chapter 3)

2. To evaluate if Tregs can restrain skin inflammation (discussed in Chapter 4)

3. To investigate the mechanisms used by skin resident Tregs to control tissue inflammation (discussed in Chapter 5)

Chapter 2. Materials and Methods

2.1. Mice

C57BL/6 (B6) WT, B6 IL-23R$^{GFP/+}$ (generated in our facility by crossing B6 IL-23R$^{GFP/GFP}$ (Mohamed Oukka, Harvard Medical School) with B6 WT mice), B6 Foxp3^{GFP}, B6 ST2$^{-/-}$ (Padraic Fallon, Trinity College Dublin) B6 Foxp3^{hCD2}, B6 Foxp3^{hCD2}IL-10$^{GFP/+}$ (generated in our facility by crossing B6 Foxp3^{hCD2} mice with B6 Foxp3^{hCD2}IL-10$^{GFP/GFP}$ mice, the latter were previously generated by crossing B6 IL-10$^{GFP/GFP}$ (Kamanaka et al., 2006) with B6Foxp3^{hCD2} (Kendal et al., 2011), B6 CD45.1, B6 CD45.1 OTI were bred and maintained under specific pathogen-free conditions in accredited animal facilities at the University of Oxford, UK.

All experiments were conducted in accordance with the UK Scientific Procedures Act of 1986 and were carried out by persons holding a Personal License (PIL) under a Project License (PPL) authorized by the UK Home office. Mice were held under SPF conditions and were at least 6 weeks of age or older when used for any experiments described.

2.2. Imiquimod model of Skin inflammation

2.2.1. Skin treatment

The imiquimod model of psoriasiform skin inflammation was adapted after the method of van der Fits et al (van der Fits et al., 2009). Cream containing 5% imiquimod, Aldara (3M Pharmaceuticals) was topically applied to the dorsal and ventral sides of both ears or the shaved back. Treatment was repeated with 20.8mg cream per ear or 41.6mg on the back every 24 hours for 7 consecutive days, or otherwise as indicated in the specific experiment. 24 hours after last application mice were sacrificed. Ear thickness was measured prior to first application and daily before treatment with a dial thickness gauge (Mitutoyo UK). The mean of two measurements was determined. Mice were weighed daily.

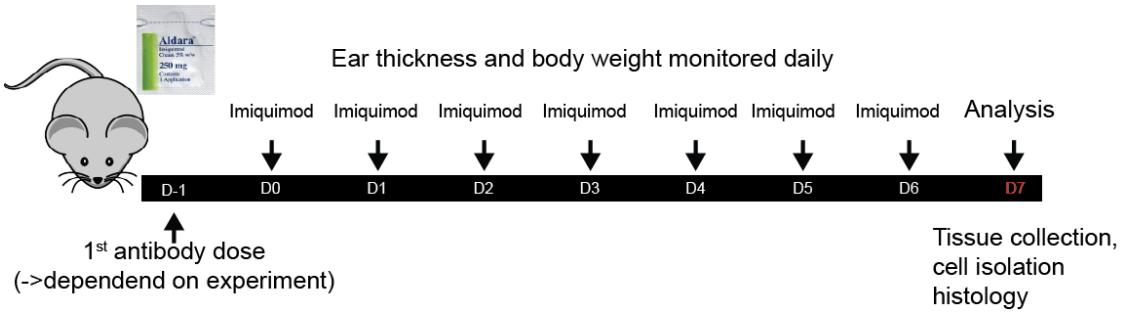

Figure 2.1. Time line of the imiquimod model of psoriasiform skin inflammation

Ears of mice were treated with imiquimod containing cream (Aldara) every 24 hours. Body weight and ear thickness were monitored daily before cream application. In experiments using depleting or blocking antibodies, the first dose was administered 24 hours before first cream application. Unless indicated, mice were sacrificed on day 7 and tissue collected for further analysis.

2.2.2. *In vivo* antibody treatment

The following unconjugated anti-mouse monoclonal antibodies were administered *in vivo* as described in detail in every section:

Specificity	**Clone**	**Isotype**
anti-CD4	YTS 191	Rat IgG2b
anti-CD8	53-6.72	Rat IgG2a
anti-human CD2	YTH 655	Rat IgG2b
anti-IL-10Rα	1B1.2	Mouse IgG 1
anti-IFNAR1 (blocking)	MAR1-5A3	Mouse IgG 1
anti-IFN-γ (blocking)	XMG1.2	Rat IgG 1
anti-mPDCA1	JF05-1C2.4.1	Rat IgG2b

Antibodies YTS 191 and YTH 655 as well as hybridoma line for YTH 655 were generous donations from Professor Herman Waldmann, Sir William Dunn School of Pathology, University of Oxford. Matched isotype controls were used with all *in vivo* antibodies.

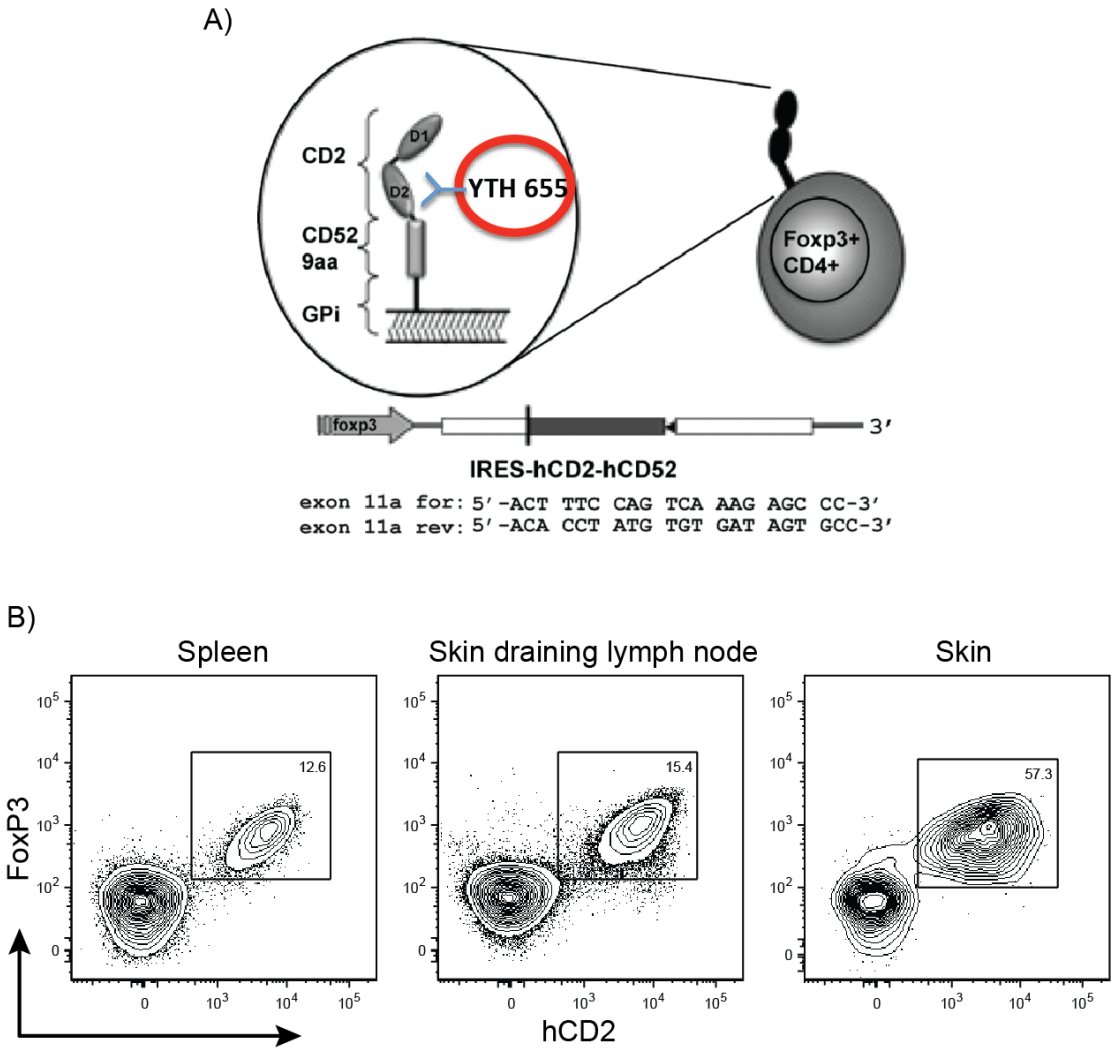

Figure 2.2. B6 Foxp3^{hCD2} reporter mouse

Illustration of B6 Foxp3^{hCD2} reporter mouse and tissue specific reporting quality

(A) B6 Foxp3^{hCD2} reporter mouse construct. Strain provided by Herman Waldmann, University of Oxford. The depleting anti-hCD2 antibody-binding site is illustrated. Adapted from Kendal et al 2011

(B) Quality of Foxp3 reporting in spleen, lymph nodes and skin in the B6 Foxp3^{hCD2} reporter mouse

2.3. Cell isolation

2.3.1. Isolation of skin leukocytes

The protocol for isolation of leukocytes from the skin was continuously improved over the research period for this thesis. Main differences included type of base media used for digestion buffers Roswell Park Memorial Institute (RPMI) 1640 medium; Iscove's Modified Dulbecco's Medium (IMDM)); use of digestion enzymes: type and concentration of collagenase (type VIII, type IV, type P, type D); addition and concentration of Liberase (TM or TL) and addition of dispase. Including density gradient centrifugations and changing size of cell strainers achieved further improvement of purity and full removal of hair.

Ears were harvested at the base after sacrifice and stored on ice in PBS containing 0.1%BSA after collection of tissue for histological assessment and RNA extraction (both described in detail in this chapter).

Ears were split into two halves by mechanical separation using forceps and finely minced using surgical scissors. Ears were digested in a 50ml conical tube containing 3.5ml of RPMI with 0.1% BSA and 3mg/ml collagenase D (Roche), 400ug/ml Liberase^{TM} TL (Roche) at 37°C in a shaking incubator for 80 minutes.

Cell suspension was aspirated several times into a syringe and pressed through a 18G needle before pushing the cell suspension through a 50um cell strainer. Digestion was stopped by adding 4°C cold PBS containing 5mM ethylenediaminetetraacetic acid (EDTA; 1L 0.5M stock made in-house by dissolving 186.12g of $Na_2EDTA.2H_2O$ adjusted to pH8 with NaOH) prior to centrifugation (500G 7 minutes at 4°C).

Supernatant was aspirated and pellet re-suspended in 6ml RPMI/0.1% BSA/5mM EDTA. In a 15ml falcon tube the cell suspension was underlaid with 4ml Lymphoprep^{TM} (Stemcell Technologies) and centrifuged for 15 min at 10°C and 900G without brake. The interface was recovered and washed thoroughly in cold PBS/0.1%BSA/5mM EDTA and cells re-suspended in appropriate buffer at 4°C for further enrichment, staining for flow cytometry, or snap frozen in RLT (Qiagen)+ 1% 2-Mercaptoethanol (β-ME) for isolation of mRNA.

2.3.2. Isolation of colonic lamina propria leukocytes

For isolation of lamina propria leukocytes (LPL), colon was collected after the sacrafice and opened longitudinally and washed in PBS/0.1% BSA. Colon was cut into pieces and stored on ice in 50ml conical tubes containing RPMI-1640 supplemented with 10% FCS (Sigma-Aldrich). To remove epithelial cells, pieces were washed twice in 20ml pre-warmed RPMI/10%FCS/5mM EDTA. To remove residual EDTA, tissue pieces were incubated in RPMI/10%FCS/15mM Hepes for 10 minutes and then transferred to a fresh tube. 10ml Digestion media (RPMI/10%FCS/15mM Hepes + 100U/ml collagenase VIII (Sigma-Aldrich)) was added and tubes incubated horizontally at 37°C in a shaking incubator (200RPM) for 60 minutes. Cell suspension was filtered through a 70um cell strainer and digestion stopped by addition of one volume ice cold RPMI/10%FCS/5mM EDTA and centrifugation (500G for 7 minutes at 4°C). Using a three-layer Percoll (GE Healthcare) (30%/40%/70%) density-gradient centrifugation at 900G for 15min without brake lymphocytes were further enriched. The 40%-70% interface was recovered and washed thoroughly in

cold PBS/0.1%BSA/5mM EDTA and cells re-suspended in appropriate buffer at 4°C until further analysis.

2.3.3. Isolation of leukocytes from liver, lung and kidney

Following sacrifice liver was flushed *in situ* via the portal vein with 10ml PBS/0.1% BSA. Respective organs were collected and stored in a 50 ml conical tube containing RPMI-1640 supplemented with 10% FCS. 10ml Digestion media (RPMI/10%FCS/15mM Hepes + 100U/ml collagenase VIII (Sigma-Aldrich)) was added and tubes incubated horizontally at 37°C in a shaking incubator (200RPM) for 30 minutes (liver and lung) or 60 minutes (kidney). Cell suspension was filtered through a 70um cell strainer and digestion stopped by addition of one volume ice cold RPMI/10%FCS/5mM EDTA and centrifugation (500G for 7 minutes at 4°C). In a 15ml falcon tube the cell suspension was underlaid with 4ml Lymphoprep^{TM} (Stemcell Technologies) and centrifuged for 15 min at 10°C and 900G without brake. The interface was recovered and washed thoroughly in cold PBS/0.1%BSA/5mM EDTA and cells re-suspended in appropriate buffer at 4°C for further staining for flow cytometry.

2.3.4. Isolation of splenic, lymph node and thymic leukocytes

Spleens were harvested following sacrafice and stored in a microcentrifuge containing 1ml of PBS/0.1% BSA/5mM EDTA and stored on ice. Spleens were weighed, pushed through a 70um mesh into a 50ml conical tube and washed in PBS/0.1% BSA/5mM EDTA. For spleens the cell pellet was re-suspended in

2ml ACK (ammonium chloride potassium) lysis buffer (150mM NH_4Cl), 10mM $KHCO_3$, 0.1mM Na_2EDTA, pH 7.2-7.4) for 2 minutes at room temperature, followed by washing with 30ml PBS/0.1% BSA/5mM EDTA and centrifuged at 450G for 5 min. The lymph node cells were pushed through a 70um mesh and washed with fresh buffer and centrifuged at 450G for 5 min. The cells were re-suspended in buffer and stored on ice until further analysis.

2.3.5. Isolation of blood leukocytes

Blood was collected by cardiac puncture post-mortem with a 1ml 29G fixed needle insulin syringe (Terumo UK LTd.) or by tail bleeding. In this case a scalpel (no.24 blade; Swann-Morton Ltd.) was used to incise the tail vein and blood was collected using a glass capillary and transferred into a microcentrifuge tube (Eppendorf) containing 250ul PBS/5mM EDTA. Tubes were centrifuged and cell pellets re-suspended in 300ul ACK lysis buffer for 2 minutes at room temperature, followed by washing in PBS/0.1% BSA/5mM EDTA and re-suspended in fresh buffer and stored on ice until further analysis.

2.4. Flow cytometry and cell sorting

Cells were extracted from tissues as described in detail in Chapter 2.2. Cells in buffer suspensions were plated into a V bottom 96-well plate (Corning), centrifuged at 450G for 5 min at 4°C and the supernatant flicked off. 50ul of PBS/0.1% BSA/5mM EDTA mixture containing appropriate antibody concentrations was added to each individual well and re-suspended.

2.4.1. Surface staining

For surface staining, cells were incubated in appropriate antibody mixtures for 30 minutes at 4°C in the dark. The antibody mix always contained a viability dye, Fc block to minimize non-specific antibody binding, and the appropriate surface antibodies described in detail in this chapter. Brilliant^{TM} stain buffer (BD biosciences) was added when Brilliant Violet (BV) reagents were included in the FACS panel.

For surface only staining panels, the cells were then washed twice with PBS/0.1% BSA/5mM EDTA and analysed.

2.4.2. Intracellular staining

For intracellular staining, the surface staining protocol detailed above in Chapter 2.3.1 was followed. Cells were then fixed gently using red cell lysis buffer (BD biosciences) and consequently either stored in PBS/0.1% BSA/5mM EDTA over night before proceeding or permeabilized with PBS/0.1%BSA/0.05% saponin. 50ul of the intracellular antibody mix was made

up at appropriate concentrations using PBS/0.1%BSA/0.05% saponin and incubated for 30 minutes at 4°C in the dark. Cells were washed as well as re-suspended in PBS/0.1% BSA/5mM EDTA and analysed promptly.

When cells were stained for the transcription factor FOXP3, surface staining was followed by Foxp3 staining buffer set (eBioscience). Cells were washed as well as re-suspended in PBS/0.1% BSA/5mM EDTA and analysed promptly.

2.4.3. Re-stimulation of cells for intracellular cytokine staining

For intracellular cytokine staining, isolated cells were plated in round-bottom 96-well plates (Corning). Cells were centrifuged and re-suspended in 250ul RPMI-1640/10%FCS containing 0.1uM phorbol 12-myristate 13-acetate (PMA) and 1um Ionomycin (both Sigma-Aldrich) and incubated in the dark at 37°C. After 30 minutes 10ug/ml Brefeldin A (Sigma-Aldrich) was added and cells further incubated for a total time of 4 h. Cells were washed twice with PBS/0.1% BSA/5mM EDTA before continuing with surface and viability staining followed by intracellular staining as described in detail in 2.3.1 and 2.3.2.

2.4.4. Flow cytometry antibodies

Specificity	Fluorochrome	Clone
CD103	PE/BV421	M290/ 2E7
CD11b	V500	M1/70
CD11c	PercP Cy5.5	N418
CD19 (B220)	AF488/BV570	RA3-6B2
CD207 (Langerin)	PE	eBioL31
CD25	PE-Cy7	PC61
CD3	BV650/BV605/PE-Cy5	145-2C11
CD4	BV711/BV605	GK1.5/GK1.5
CD44	V500	IM7
CD45	BV500/BV650	30-F11
CD45.1	PerCPCy5.5	A20
CD45.2	PerCP Cy5.5/PE-Cy7	104
CD62L	PE	MEL-14
CD64	APC	XA54-5/7.1
CD8	BV570/BV605/eF450	53-6.7
GR1	BV711	RB6-8C5
GR1	BV570	RB6-8C5
CD2 (human)	APC/PB/PE-Cy5	RPA-2.10
KLRG1	PE-Cy7	2F1
Ly6C	PE-Cy7/APC	HK1.4
Ly6G	PE-CF594	1A8
MHC II	AF700	M5/114.15.2
PDCA1	PB	eBio927
PDCA1	Biotin	JF05-1C2.4.1
Siglec F	BV421/PE	E50-2440
Siglec H	PE-Cy7/FITC	eBio440c
ST2	Biotin	DJ8
TCR Vβ5.1,5.2	PE	MR9-4
TCRβ	APC/PE-Cy7/PerCP-Cy5.5/PE-Cy5	H57-597
TCRγδ	PE-Cy5/APC/Biotin	GL3
Viability Dye (fixable)	eF780	--

Specificity	Fluorochrome	Clone
Eomes	FITC	Dan11mag
Foxp3	eF450/FITC/PE-Cy5	FJK-16S
GATA-3	AF660	TWAJ
Helios	BV488	22F6
IFNα	FITC	RMMA-1
IFN-γ	FITC/eF450	XMG1.2
IL-13	AF647	ebio13A
IL-17A	AF647	TC11-18H10
IL-17A	FITC	ebio17b7
IL-17F	AF647	9D3.1C8
IL-22	PE	MP1-229E/Poly5164
IL-4	BV421	11B11
Ki-67	PB/PE-CF594	SolA15
RORγt	Pe	Q31-378
T-bet	BV711/BV421	4B10
TNFα	BV421	MP6-XT22

2.4.5. Acquisition and analysis via flow cytometry

Cells were acquired on a SORP LSRII or Fortessa using FACSDiva software (BD Biosciences). Single fluorochrome stained sample for machine set-up and compensation were made using CompBeads (BD Biosciences). Prior to analysis and acquisition compensation was checked and adjusted with the help of fluorescence minus one (FMO) control sample.

Cell numbers were estimated by adding $1x10^4$ count bright beads (life technology) into each well prior to acquisition that included a predefined percentage of the whole tissue sample. This allows a comparable and reliable cell number calculation when acquired bead count, % of whole sample and acquired cell count are taken into consideration.

Post acquisition analysis was performed using FlowJo software (Tree Star, Inc.).

2.4.6. Fluorescence activated cell sorting (FACS)

Cells were stained with appropriate surface and viability marker antibody mixes in PBS/0.1% BSA/5mM EDTA as described in section 2.3.1. Cells were re-suspended in PBS/0.1% BSA/5mM EDTA and strained through a 30um filter (BD Biosciences) into 5ml tubes suitable for sorting.

Cells were sorted on a FACSAriaIII (BD Biosciences) by Drs Ahmed Hegazy, Helen Ferry or Parisa Amjadi. Cells were collected in a microcentrifuge tube (Eppendorf) containing 300ul Trizol (Life technologies) or 400ul RLT + β-ME.

Sorting of Foxp3$^+$ regulatory T cell populations

For microarray analysis (Chapter 3), Foxp3$^+$ Tregs from the skin and skin draining lymph nodes of B6 Foxp3^{GFP} mice were sorted. Mice were treated as described above or left untreated and ears and draining lymph nodes were harvested. Cell suspension from the lymph nodes were enriched for CD4$^+$ T cells using a magnetic enrichment kit (Stem cells) and incubated with a viability dye and antibodies against CD45, TCRβ and CD4. Live, CD45$^+$, TCRβ$^+$ CD4$^+$ GFP$^+$ cells were sorted into Trizol and immediately frozen on dry ice and stored at -80°C until extraction of mRNA.

2.4.7. Magnetic sorting of naïve $CD8^+$ T cells

For $CD8^+$ T cell transfer experiments described and discussed in Chapter 5, spleens and lymph nodes of CD45.1 WT, CD45.1 OTI and/or B6 dsRed CD2 mice were harvested and processed as described in 2.2.3. Cells were magnetically separated using a naïve $CD8^+$ T cell selection kit (Stem Cell Technologies). Cells were checked for purity by staining an aliquot with surface antibodies as described in 2.3.1 and then analysed on a BD Fortessa as described in 2.3.5. Sorted cells were >95% pure and injected into the tail vain of recipient mice.

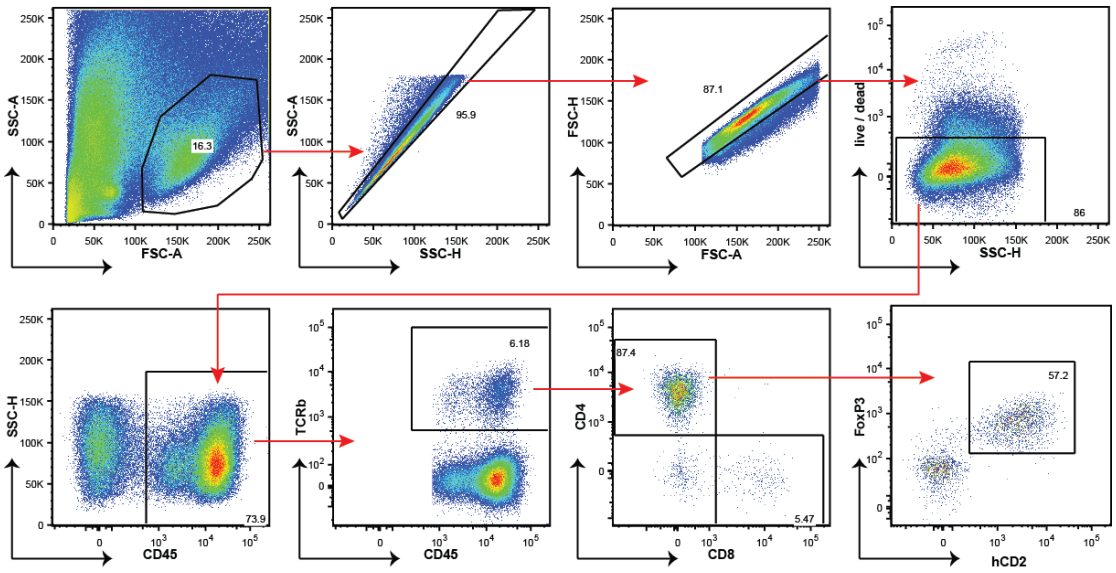

Figure 2.3. FACS gating strategy for CD45$^+$ cells and T cells from digested skin tissue

Gating strategy and numbers of CD45$^+$ cells, CD4$^+$T cells, CD8$^+$ T cells and Foxp3$^+$Tregs extracted from the skin. Intracellular Foxp3 staining as well as the highly efficient co-expressed surface marker hCD2 in the B6 Foxp3hCD2 reporter mouse is used to identify Tregs.
Example plot from a representative B6 Foxp3hCD2 mouse treated with imiquimod for 7 days.

2.6. Analysis of gene expression

2.6.1. Preparation of whole skin tissue for gene expression analysis

At the experimental endpoint mice were sacrificed and ears were harvested. A 1.5mm thick ear section was placed in 2ml cryotubes (Starstedt) snap frozen in liquid nitrogen and stored at -80°C until further processing.

Ear tissues were thawed and 400ul of cold RLT + β-ME was pipetted into the cryotubes. Tissue was disrupted and cells lysed using a Polytron^{TM} PT 1200 E manual disperser with 7mm dispersing aggregate (Kinematica) for 20 seconds and centrifuged at 18000rpm for 3 min. Supernatant was transferred into a new nuclease free microcentrifuge tube (Eppendorf) and placed on ice for immediate RNA extraction.

2.6.2. Preparation of RNA and cDNA

RNA was isolated using the RNeasy Mini kit (Qiagen) according to manufacturers instructions, including the optional DNase I (Qiagen) digestion step. RNA was quantified using a Nanodrop spectrophotometer (Thermo Scientific) and normalized across samples. RNA was stored at -80°C. cDNA was performed in a total volume of 20ul. cDNA synthesis was performed with and following the protocol of the High Capacity cDNA Reverse Transcription Kit (Applied Biosystems). Synthesis was done using a G-storm GS2 thermal cycler (Gene Technologies Ltd.). cDNA was stored at -20°C.

2.6.3. Quantitative reverse transcription PCR (RT-qPCR)

RT-qPCR was performed with TaqMan Gene Expression Assays for mouse (Life Technologies) (see table below) in 96-well skirted PCR plates (Star Lab) using a CFX96 real-time PCR detection system (Bio-Rad Laboratories). Alternatively reactions were performed using 384-well skirted PCR plates in the ViiA^{TM} 7 Real-Time PCR System (Applied Biosystems). All reactions were performed in duplicates. Expression levels of genes of interest were normalized to the housekeeping gene *Hprt* using the $2^{-\Delta Ct}$ method.

Gene	TaqMan Probe
Ccl5	Mm01302427_m1
Ccr5	Mm01963251_s1
Cxcl10	Mm00445235_m1
Cxcl9	Mm00434946_m1
Dgat1	Mm00515643_m1
Dgat2	Mm00499536_m1
Gzmb	Mm00442834_m1
Hprt	Mm01545399_m1
Hspa1a	Mm01159846_s1
Ier3	Mm00519290_g1
Ifit2	Mm00492606_m1
Ifng	Mm01168134_m1
Il10	Mm00439614_m1
Il12a	Mm00434165_m1
Il17a	Mm00439618_m1
Il17c	Mm00521397_m2
Il17f	Mm00521423_m1
Il22	Mm01226722_m1
Il23	Mm00518984_m1
Irf7	Mm00516793_g1
Isg15	Mm01705338_s1
Lmna	Mm00497783_m1
Nfil3	Mm00600292_s1
Prf1	Mm00812512_m1
Stat1	Mm00439531_m1
Tbx21	Mm00450960_m1
Tnf	Mm00443258_m1

2.6.4. Microarray sample preparation and analysis

For the regulatory T cell microarray (Chapter 3), cells were directly sorted into microcentrifuge tubes containing Trizol and stored at -80°C until RNA was extracted. At time of RNA extraction samples were thawed at room temperature and 0.2 parts of chloroform was added, tube vigorously shaken and incubated at room temperature for 2 minutes. Samples were centrifuged at 12.000G for 15 min at 4°C. The upper aqueous phase was coved to a new nuclease free tube. RNA was precipitated with the addition of GlycoBlue (life technologies) for easier detection. 0.5 parts of pure isopropanol (Sigma-Aldrich) was added to the tube and incubated at room temperature for 10 min. Tubes were centrifuged at 12.000g at 4°C and the supernatant discarded. The visibly blue RNA pellet was washed with 1ml of 75% ethanol. Pellet was allowed to air dry and was re-suspended in RNase-free water (Qiagen) and dissolving aided by brief incubation at 55°C.

Samples with adequate RNA integrity number (RIN) as assessed by the Agilent 2100 Bioanalyser using the Agilent RNA 6000 Pico Kit (both Agilent Technologies) were further used for array analysis. RNA was amplified using the TargetAmpT 2-Round Biotin-aRNA Amplification Kit 3.0 (Epicentre, Illumina) and following the provided optimized protocol. All reactions were performed on a G-storm GS2 thermal cycler (Gene Technologies Ltd.). Amplified biotin labelled cRNA samples were assessed by Nanodrop and normalized quantities used for array analysis. Samples were stored at -80°C until further processing.

For the whole tissue microarray (Chapter 4) RNA was extracted using the RNeasy Mini kit (Qiagen) as described in section 2.6.2. Samples with adequate RNA integrity number (RIN) as assessed by the Agilent 2100 Bioanalyser using the Agilent RNA 6000 Nano Kit (both Agilent Technologies) were further used for array analysis. RNA samples were assessed by Nanodrop and normalized quantities used for array analysis. Samples were stored at -80°C until further processing.

After quality assessment of samples as per above, Dr Dilair Baban (Microarray core facility, Wellcome Trust Centre for Human Genetics, University of Oxford) hybridized the samples to Illumina Wg6 v2.0 Expression Bead Chips (Illumina), which were washed and scanned using a HiScan scanner (Illumina) to generate expression profiles for each condition.

Probe signal intensities were extracted using GenomeStudio software (version 1.9.0 Illumina Inc.) and further analysed by Dr. Nicholas Ilott. Probes were used for downstream processing if they were expressed significantly above background (detection p-value < 0.05). This resulted in the analysis of 13847/45281 and 23314/45281 probes in the regulatory T cell microarray (Chapter 3) and whole tissue experiments (Chapter 4), respectively. Array signal intensities were background adjusted, transformed using the variance stabilizing transformation (VST) and quantile normalized using Lumi (PMID:18467348) from R/Bioconductor. Differential expression analysis was performed for each contrast using the empirical bayes method implemented in LIMMA. Significance was defined as a Benjamini-Hochberg adjusted p-value < 0.05 and fold change > 2 (log2 fold change >1).

Enriched Gene ontology (GO) biological processes were assessed in differentially abundant gene sets using a hypergeometric test implemented in the runGO.py script from the CGAT code collection (PMID:24395753) and terms were considered significant at a false discovery rate (FDR) < 0.05.

2.7. Histology

2.7.1. Sample preparation

At sacrifice 2-3mm pieces of ear tissue were harvested and immediately submerged in PBS containing 10% formaldehyde for up to 2 weeks before embedding and preparing 5um thick sections using a microtome and stained with haematoxylin and eosin (H&E) at the histology facility of the Kennedy Institute of Rheumatology, University of Oxford.

Images of ear sections were taken using a CoolScope microscope (Nikon).

2.7.3. Immunofluorescence

Ear tissue was snap frozen in optimal cutting temperature (OCT) (VWR) compound, using liquid nitrogen-cooled isopentane, sectioned into 7µm thick sections and mounted on glass slides.

Immunofluorescence staining against Foxp3 was conducted according to the following protocol. Frozen sections were removed from storage at -20°C and immediately fixed, either in -20°C acetone for 10 minutes. The slides were then washed in PBS and mounted onto Shandon cover plates (Thermo scientific). Blocking solution (PBS plus 5% goat serum) was added onto the slide and left on for one hour. Primary antibody solution (PBS plus 1% BSA, containing the primary antibody in a dilution of 1:100) was then added directly and left on at 4°C over night. Following over night incubation, the slides were washed three times for five minutes with PBS. Consecutively, secondary antibody staining solution (PBS plus 1% BSA, containing fluorescently labelled secondary

antibodies in a dilution of 1:400, and HOECHST nuclear stain in a dilution of 1:1000) was added on the slides for one hour. The slides were then washed and mounted with glass coverslips over night, using ProLong Gold mounting medium. The resulting slides were imaged with a Zeiss 510 MetaHead confocal microscope.

2.8. *In vivo* imaging studies

Mice were anesthetized for the duration of imaging using isoflurane. Images were collected by Dr. Emily Thornton in the Wolfson Imaging Centre (Weatherall Institute of Molecular Medicine, University of Oxford) using a Zeiss 780 upright microscope with a 20x water dipping objective and Zeiss spectral detector array. Images were spectrally unmixed using Zeiss Zen software. Timelapses and 3-dimensional data sets were analysed using Imaris 8.1.2 software (Bitplane).

2.9. Statistics

Statistical analyses of experiments were performed in Prism 6 (GraphPad Software, SD, USA).

Mann-Whitney U test, student's T test, Kruskal-Wallis test, one-way ANOVA or two way ANOVA in combination with adequate post tests were performed.

Microarray analysis and statistical evaluation is described in section 2.6.4.

Differences were considered statistically significant when $p<0.05$. Significance will be indicated as * $p<0.05$; ** $p<0.01$, ***$p<0.001$, ****$p<0.0001$.

Chapter 3. Characterization of Tregs in skin homeostasis and inflammation

3.1. Introduction

Tregs are a subset of $CD4^+$ T cells that are indispensible for controlling inflammation and maintaining self-tolerance. Tregs are found in most peripheral tissues at homeostatic conditions and are crucial for maintaining an adequately balanced immune response.

However, little is known about the functions of Tregs in peripheral tissues such as the skin. The skin is the body's largest organ and constantly exposed to unfiltered environmental factors. It harbours more T cells than are present in the circulation (Clark, et al. 2006). At steady state, $CD4^+$ T cells are mainly confined to the dermis and have a diverse TCR repertoire (Clark 2015). Like most T cells in the skin of humans and mice, these $CD4^+$ T cells display a memory phenotype (Watanabe et al. 2015). Memory T cells have previously encountered and responded to antigen and at such an abundance in the skin allow a directed immune response upon pathogen re-exposure. A prominent proportion of cutaneous $CD4^+$ T cells in human (15-25%) and even more so in mouse (up to 60%) are $Foxp3^+$ Tregs (Rodriguez et al., 2014; Rosenblum et al., 2011). This enrichment of Tregs in the skin suggests a specific role for this population at our largest barrier organ.

Patients who carry a mutation in the Foxp3 gene, IPEX patients, suffer from an array of auto-inflammatory symptoms (Gambineri et al., 2003). The skin is one of the first manifestation sites of inflammation in IPEX patients and also a prominent feature in genetic mouse models of the disease (Godfrey et al., 1991; Halabi-Tawil et al., 2009).

An imbalance of Teff and Tregs has been suggested in many autoimmune diseases (Sakaguchi et al., 2008). Recent evidence emerged suggesting that a potentially “unstable” phenotype in Tregs can contribute to inflammation and autoimmunity in vivo, especially under an inflammatory cytokine milieu (Komatsu et al., 2014; Oldenhove et al., 2009; X. Zhou et al., 2009). Tregs share certain developmental criteria with Th17 cells, which are highly implicated in autoimmune disease, and evidence shows that Tregs can in part convert to RORγt^{+} IL-17 secreting cells. Such converted “ex”-Tregs are not only unable to suppress inflammation, but can support it (Koenen et al., 2008; Komatsu et al., 2014; Xu et al., 2007). On the other hand, it was recently demonstrated that RORγt expressing Tregs actually represent a specialized subset of T cells operating at barrier sites such as the gut where they are required for adequate control of inflammation (Ohnmacht et al., 2015; Sefik et al., 2015). Further supporting and extending our understanding of Th17 and regulatory T cell plasticity, Th17 cells have recently been reported to convert to IL-10 secreting regulatory Tr1 cells (Gagliani et al., 2015).

In psoriasis, patients have similar frequencies of Tregs in the blood compared to healthy donors and also express equal levels of the skin homing marker CLA (Sugiyama et al., 2005). However, Tregs obtained from PBMCs of psoriatic patients demonstrated a lower inhibitory capacity than those obtained

from healthy donors which could not be fully overcome with increased Treg ratios (Sugiyama et al., 2005). In addition, $Foxp3^+$ cells isolated from PBMCs of psoriatic patients showed the propensity to produce IL-17A(Bovenschen et al., 2011). However, it remains unclear if these features observed in PBMCs after *in vitro* re-stimulation also reflect the *in situ* reality in skin resident Tregs and if so, what their contribution to the inflammatory process really is.

The aim of this chapter is to characterize the phenotype and analyse the transcriptome of skin resident Tregs at steady state. The imiquimod model of psoriasiform skin inflammation will be introduced. Utilizing this model, changes of skin resident Tregs during psoriasiform inflammation will be further assessed.

3.2. Results

3.2.1. The skin harbours the highest proportion of Tregs

Initially, the isolation of leukocytes from the skin used throughout this thesis had to be established in our lab to allow further investigation of skin resident cells. The data presented throughout this thesis was obtained using an optimized protocol for skin digestion and cell extraction and is described in detail in Chapter 2. The gating strategy used to identify T cells in this thesis is depicted in Chapter 2 (Figure 2.3). In brief, leukocytes were gated on by size and doublets excluded by forward and side scatter height and area. Live cells were further selected by expression of CD45 and TCRβ, followed by CD4 and subsequently gating on cells positive for Foxp3 or hCD2 expressed under the Foxp3 promoter in B6 Foxp3^{hCD2} reporter mice. As described by Waldmann and colleagues (Kendal et al., 2011), these mice reliably express human CD2 on the surface of Foxp3 expressing cells. Figure 2.2 shows the construct used to generate this mouse and the reliable reporting of the B6 Foxp3^{hCD2} mouse.

First, we set out to investigate the frequency of Tregs in the skin. In order to understand the significance of these results in a wider context frequencies of Tregs in the skin were compared with other organs. We evaluated barrier organs such as the colon and lung as well as internal organs such as the kidney and the liver, in addition to lymphoid tissues including the lymph nodes, spleen and thymus. CD4$^+$ T cells make up the majority of the CD45$^+$ TCRβ$^+$

cells in the skin and a mean of 54.06% of these cells expressed Foxp3 (Figure 3.1), making Tregs the most abundant TCRβ$^+$ cells in the steady state skin. Further, the skin is the organ with the highest proportion of Foxp3 expressing CD4$^+$ T cells (Figure 3.1A and B). Interestingly, even though the skin and the gut (mean 33.62%) are the two organs with the highest percentage of Foxp3$^+$ cells, the lung as the third major barrier organ had a significantly reduced proportion (11.21%) of Foxp3$^+$ Treg cells.

Our data, in accordance with previously published data (Rosenblum et al., 2011) demonstrates that the skin harbours a significant proportion of Foxp3$^+$ Treg cells and this proportion is higher than in other organs investigated.

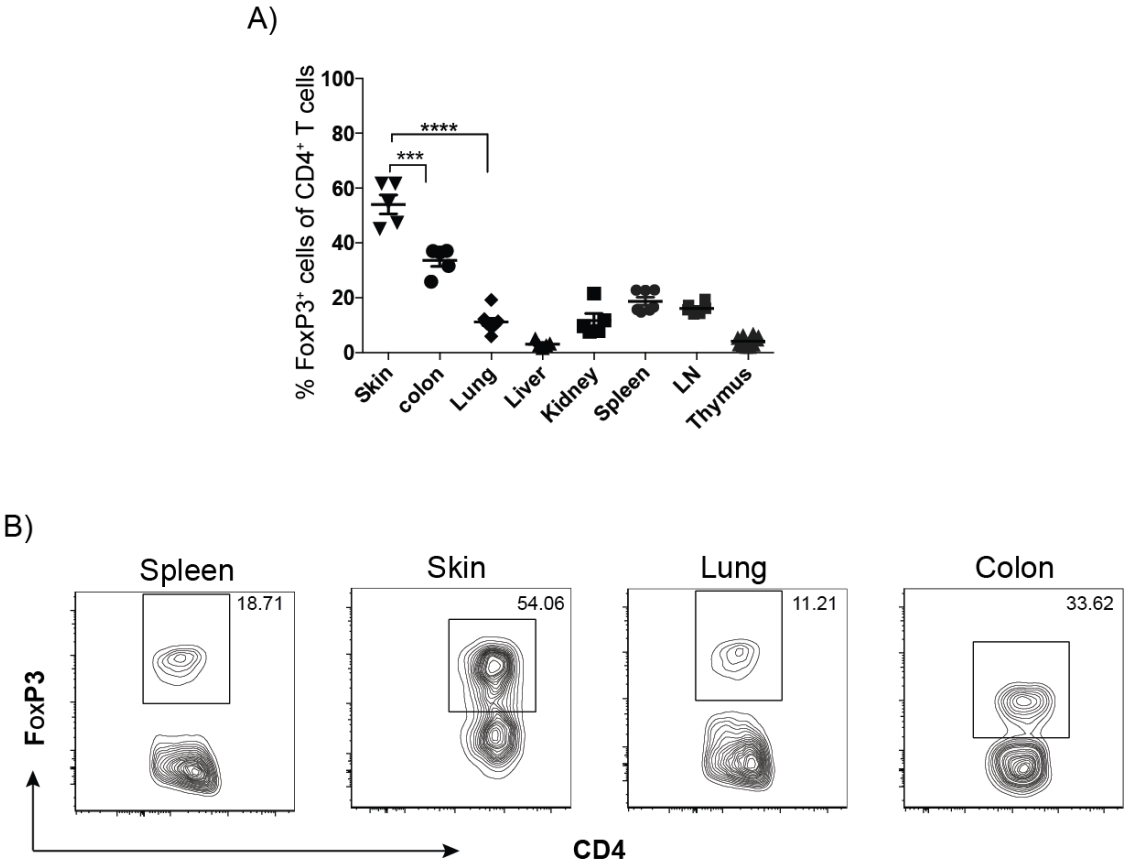

Figure 3.1. Frequency of Foxp3$^+$ Tregs in various lymphoid and non-lymphoid organs

Various organs as indicated were harvested from untreated B6 WT mice. Organs were mechanically disrupted (spleen, lymph nodes and thymus) or enzymatically digested (all other organs) and cells isolated. Cells were stained for surface markers and Foxp3 expression was determined by flow cytometry.

(A) Frequency of Foxp3 expressing cells of CD4$^+$ T cells in various organs.

(B) Representative FACS plots showing Foxp3 frequency of CD4$^+$TCRβ$^+$ cells in spleen, skin, lung and colon, values represent mean frequencies.

Bars represent the mean ± SEM. Each symbol represents one individual animal. Statistical significance between skin, lung and colon was performed using One-way Anova with Bonferroni's post-test for correction of multiple comparisons. Data are representative of 1 of 2 (kidney, thymus, lung, liver, colon) or >5 independently performed experiments (skin, spleen, lymph nodes) with n≥4 each.

3.2.2. Treg cells in the skin display a highly suppressive phenotype

To further phenotype skin resident Tregs surface markers, transcription factors and cytokine expression were investigated. $CD4^+Foxp3^+$ cells were compared with the $CD4^+Foxp3^-$ population in the skin under homeostatic conditions.

Nearly all $CD4^+$ T cells, i.e. Tregs and Teff, extracted from the skin were $CD44^+CD62L^-$, consistent with an effector memory phenotype (Figure 3.2 A). A significant proportion of skin Tregs compared to $CD4^+$ Teff expressed IL-10 in the absence of restimulation as assessed by GFP expression under the control of the *Il10* promoter (Figure 3.2B).

Surface expression of the IL-2 receptor (CD25), the E-cadherin receptor (KLRG-1) and the integrin alpha E chain (CD103) has been associated with functionally suppressive activity of Tregs (Josefowicz et al., 2012). All these markers were highly expressed in skin Tregs (Figure 3.2C).

Further, these cells expressed high amounts of the transcription factors Helios and GATA-3. However, Tregs at steady state conditions did not express the TF T-bet or RORγt above background level. Helios has been associated with thymic-derived natural nTregs as opposed to peripherally induced iTregs (Thornton et al., 2010). GATA-3 expression in Tregs has been associated with an activated and highly suppressive Treg phenotype and was previously reported as expressed at highest amounts in dermal Tregs (Wohlfert et al., 2011).

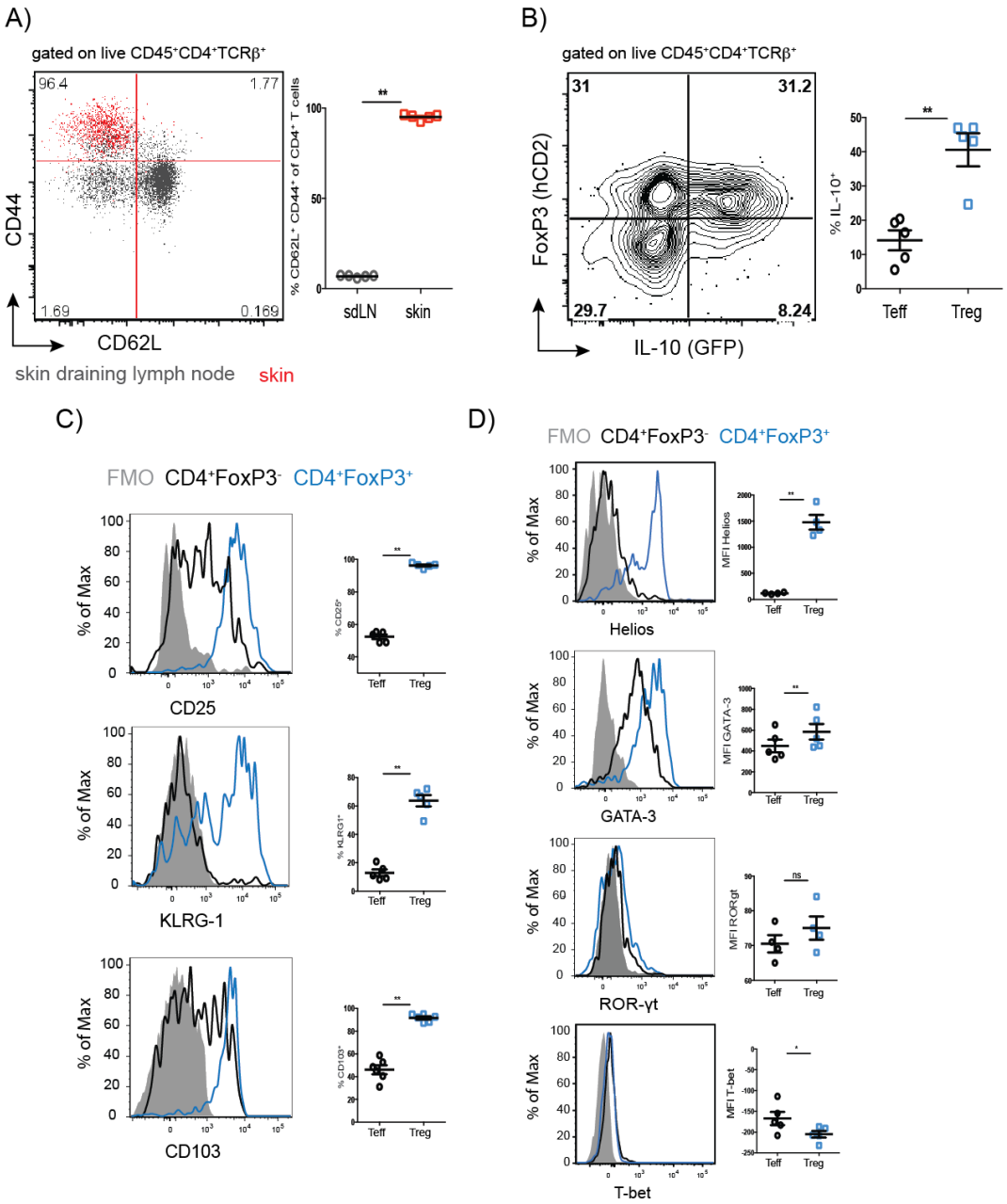

Figure 3.2. Frequency, surface marker and transcription factor expression of Tregs in the steady state skin

Skin and draining lymph nodes from B6 Foxp3^{hCD2}IL-10$^{GFP/+}$ mice were harvested and digested. Single cell suspension was stained for surface antibodies (A,B,C) or additionally stained with intracellular antibodies before analysis by flow cytometry (D)

(A) Representative FACS plot and frequency of naïve and Teff in the lymph node and the skin.
(B) Representative FACS plot and frequency of IL-10 secreting skin Tregs and effector CD4$^+$ T cells in the homeostatic skin.
(C) Representative histograms of cell surface marker expression (gray area: FMO control, black line: Foxp3$^-$CD4$^+$ T cells, blue line: Foxp3$^+$CD4$^+$ Tregs).
(D) Representative histograms of transcription factor expression (gray: FMO control, black: Foxp3$^-$CD4$^+$ T cells, blue: Tregs)

Bars represent the mean ± SEM. Each symbol represents one individual animal. Mann Whitney U test was performed to assess statistical significance. Data are representative of 1 of ≥3 experiments (n≥4 each) (A,C) or ≥2 experiments.(B,D) (n≥4 each) .

The IL-1 family member IL-33 is associated with induction of Th2 immunity (Schmitz et al., 2005). However, recent data highlights the importance of the IL-33 receptor (ST2) on Tregs in inflammation and infection (Schiering et al. 2014; Arpaia et al. 2015). Therefore ST2 expression on $CD4^+$ T cells from various organs was assessed.

Of all organs investigated, the skin displayed the highest percentage of $ST2^+$ Tregs (64.3%) (Figure 3.3A). In the skin and the colon the expression of ST2 was exclusively confined to the $CD4^+Foxp3^+$ population. (Figure 3.3B).

IL-23 inhibits the generation of Tregs and mice lacking the IL-23R express higher proportions of ST2 (Izcue et al., 2008; Schiering et al., 2014). We therefore investigated the IL-23R expression in the skin at homeostatic conditions using a B6 IL-$23R^{GFP/+}$ reporter mouse (Figure 3.4). IL-23R expression was nearly absent on $Foxp3^+$ cells and very low on $CD4^+$ T cells (mean 3.4%). The main population expressing IL-23R were dermal γδ T cells with an average of 59.75%, followed by 38.4% on non-T cells, most likely representing cells of myeloid origin or ILCs (Figure 3.3A and B).

Together, these data demonstrate that the majority of Tregs in the skin are $CD25^+KLRG1^+CD103^+ST2^+Helios^+GATA\text{-}3^+$ Tregs, which is suggestive of a thymic origin and a highly suppressive and responsive phenotype.

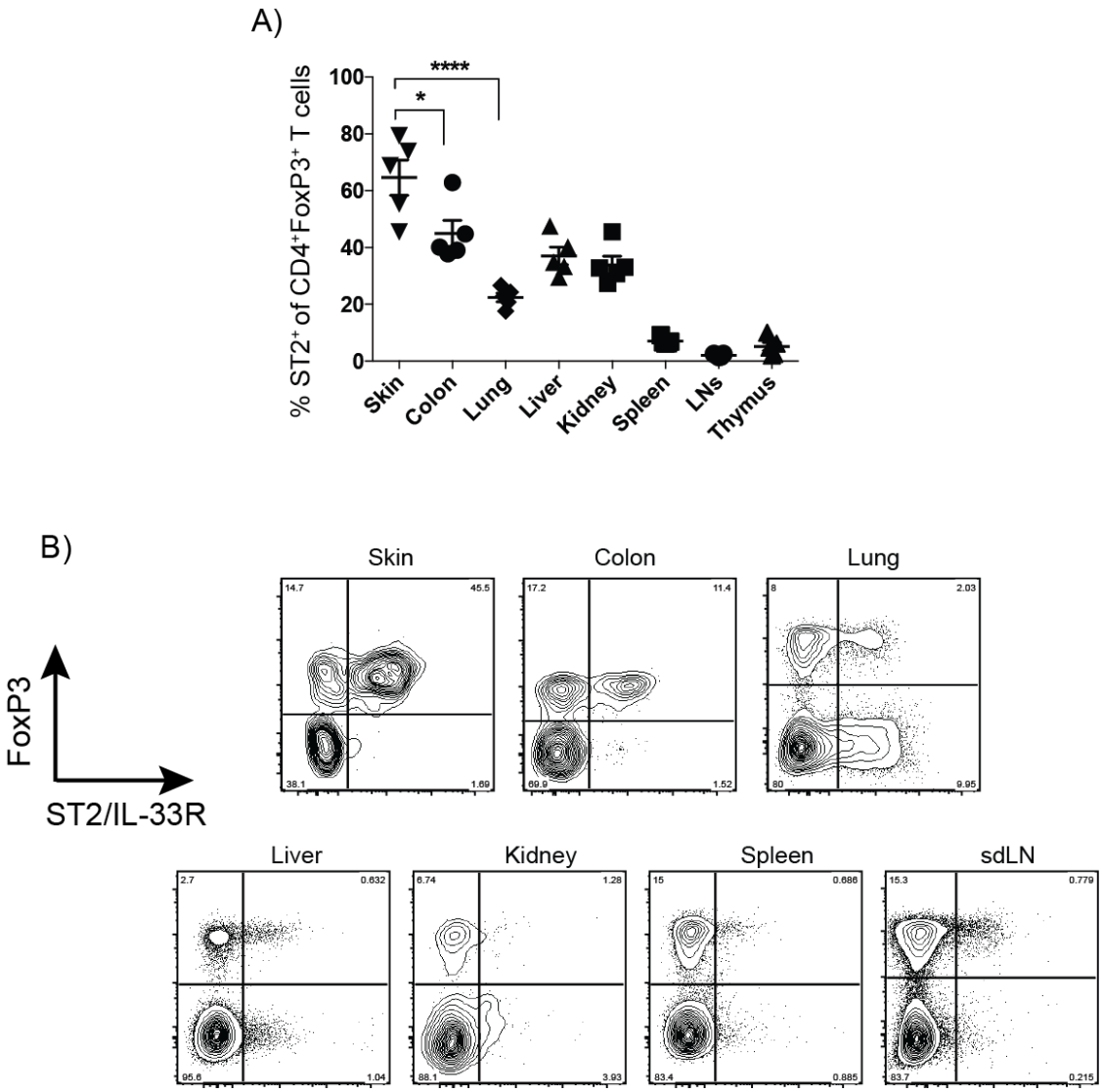

Figure 3.3. ST2 (IL-33R) expression on CD4$^+$ T cells is confined to Foxp3$^+$ Tregs in the skin and the colon at steady state

Various organs as indicated were harvested from untreated B6 WT mice. Organs were mechanically disrupted (spleen, lymph nodes and thymus) or enzymatically digested (all other organs) and cells isolated. Cells were stained for surface markers and Foxp3 expression was determined by flow cytometry.

(A) Frequency of Foxp3 expressing cells of CD4$^+$ T cells.

(B) Representative FACS plots showing ST2 frequency in spleen, skin, lung and colon.

Bars represent the mean ± SEM. Each symbol represents one individual animal. Statistical significance between skin, lung and colon was assessed using One-way Anova with Bonferroni's post-test for correction of multiple comparisons. Data are representative of 1 of 2 (kidney, thymus, lung, liver, colon) or >5 independently performed experiments (skin, spleen, lymph nodes) with n≥4 each.

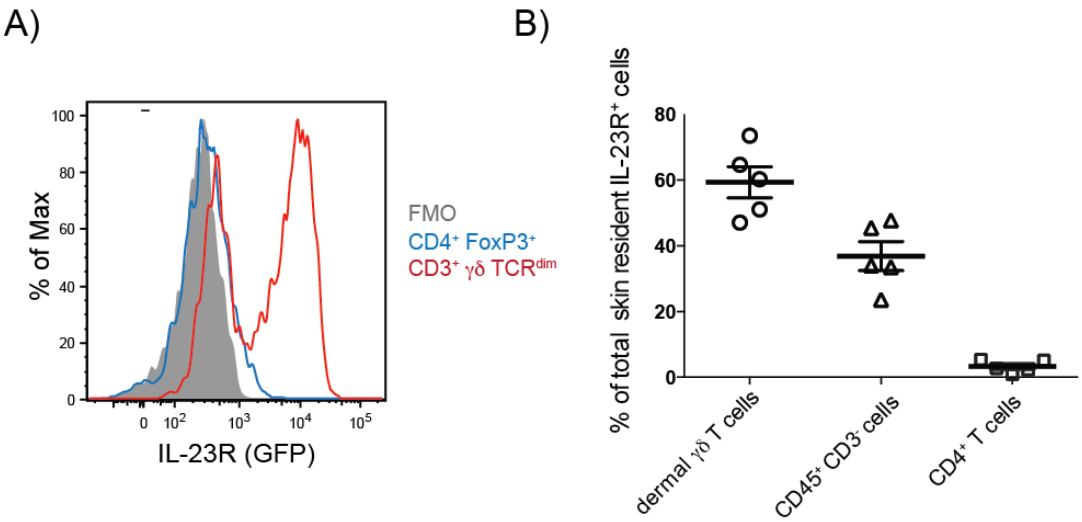

Figure 3.4. γδ T cells but not Tregs express high levels of IL-23R in the skin

Skin from B6 IL-23R$^{GFP/+}$ mice were harvested and enzymatically digested, stained for surface antibodies and analysed by flow cytometry

(A) Representative histogram of Tregs (blue) dermal γδ T cells (red) and control FMO (solid grey).

(B) IL-23R expression in various cell types in the skin

Bars represent the mean ± SEM. Each symbol represents one individual animal. Data are representative of 1 of 2 independent experiments (n=5 each)

3.2.3. Skin resident Tregs have a distinct gene expression profile

Tregs at tissue sites have a transcriptional profile that is very different from lymphoid organs such as the spleen or lymph nodes (Schiering et al. 2014; Yang et al. 2015; Burzyn, Kuswanto, et al. 2013; Burzyn, Benoist, et al. 2013). To our knowledge, no in depth evaluation of the skin resident Treg transcriptome has been published.

To investigate the whole genome transcriptome of skin resident Tregs a microarray approach was used. $CD45^+$ $CD4^+$ $TCR\beta^+$ GFP^+ cells were sorted from lymph nodes and ears of B6 $Foxp3^{GFP}$ mice as described in Chapter 2. 4-6 mice were pooled for each experimental sample and normalized amounts of RNA amplified before analysis on Illumina bead arrays. Tregs from steady state ear tissue (n=4) and steady state skin draining lymph nodes (n=4) were compared. Due to insufficient quality, one sample of skin draining lymph nodes was excluded from further analysis. Detailed analysis and statistical methods are described in Chapter 2. In brief, array signal intensities were background adjusted, transformed quantile normalized and differential expression analysis was performed.

Hierarchical clustering analysis was implemented to assess similarities between the samples. All three samples from the draining lymph nodes grouped together and were clearly separated in the dendrogram from skin Treg samples (Figure 3.5).

This highlights that skin resident Tregs have a transcription profile that is distinct from $Foxp3^+$ cells extracted from the skin draining lymph nodes.

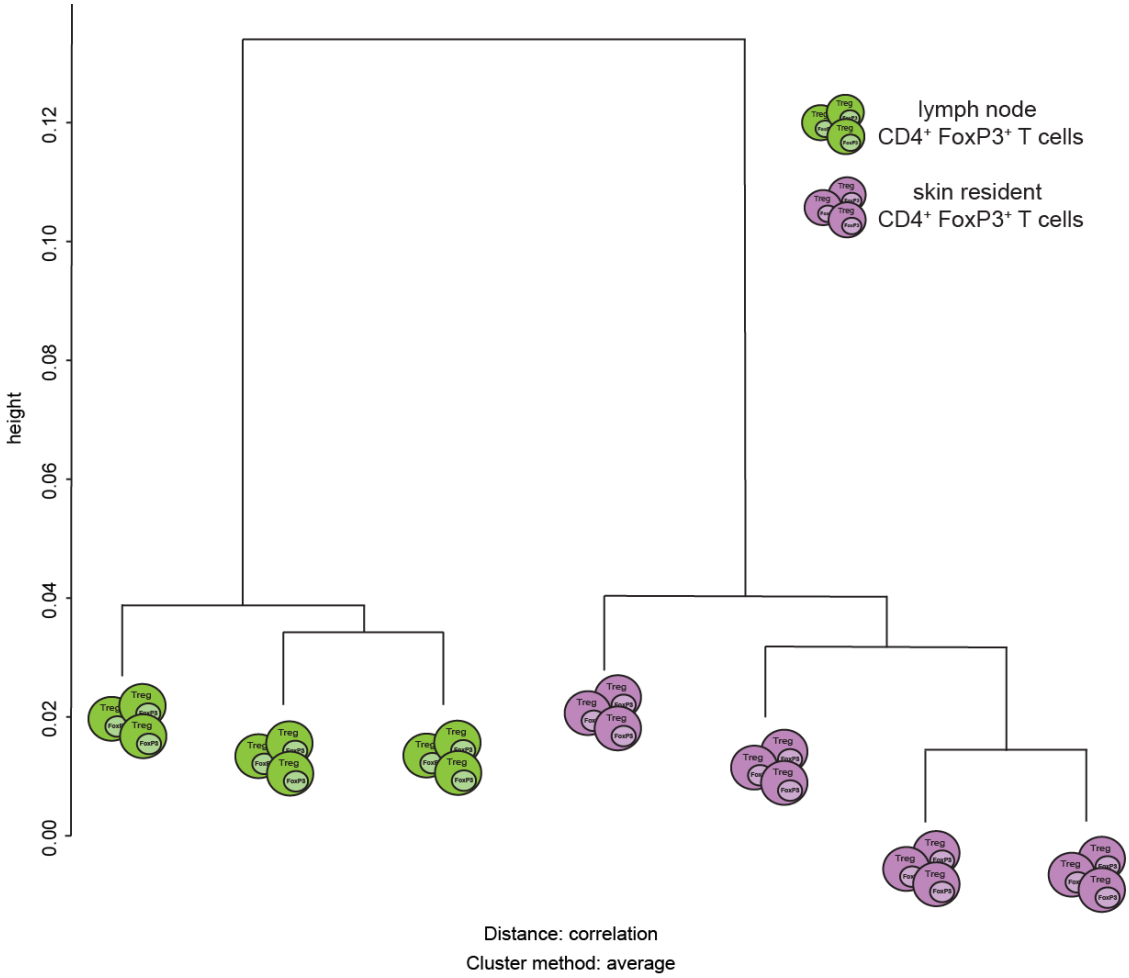

Figure 3.5. Dendrogram of Treg microarray

Steady state B6 Foxp3^{GFP} mice or mice treated with imiquimod for 7 consecutive days were sacrificed at 8-10 weeks of age. Lymph nodes and ears were harvested. Single cell suspensions were obtained, lymph node Tregs magnetically enriched for CD4$^+$ T cells and stained with surface antibodies followed by cell sorting. Viable, CD45$^+$CD4$^+$TCRβ$^+$GFP$^+$ cells were sorted directly into Trizol. RNA was extracted, amplified and gene expression assessed as described in Chapter 2.

Illumina microarray and data normalization and analysis in R were performed. Data represent results from a single experiment (n=3 for LN; n=4 untreated skin)

3.2.4. Foxp3$^+$ T cells from the skin exhibit a tissue specific transcriptome

In order to understand the differences in the gene expression profiles between the two regulatory T cell populations from the lymph node and the skin, the differentially expressed genes were visualized in a volcano plot (Figure 3.6A). Changes that were more than 1 log2-fold different (dashed line, Figure 3.6A) with a p-value <0.05 (blue circles) were judged as potentially important. Using this approach 760 probes were differentially expressed, of which 409 were up and 351 were downregulated (full list in Supplementary Table 1). The accuracy of the microarray data was confirmed by performing a separate skin and lymph node sorting experiment followed by RT-qPCR validation of different genes (Figure 3.7).

The highest upregulated gene was *Lmna* (Lamin A/C). It encodes A-type lamins that are highly expressed following antigen encounter and foster activation of T cells by promoting the formation of the immunological synapse. (González-Granado et al., 2014). *Il10* was the most induced cytokine transcript in skin Tregs, which confirms the findings obtained by flow cytometry (Figure 3.2). Interestingly, *Fosl2* was the highest upregulated transcription factor in tissue Foxp3$^+$ T cells. *Fosl2* belongs to the AP-1 family and has considerable impact on the plasticity of T helper subsets (Ciofani et al., 2012). *Crem* (cAMP response modulator) is a direct target of Foxp3 and mediates cell-contact dependent and independent suppression in Tregs (Bodor et al., 2012; Bopp et al., 2007). *Gadd45b* (growth arrest and DNA damage−inducible, β) is induced by TCR engagement. *Gadd45b* as well as the upregulated *Cdkn1a* (cyclin

dependent kinase inhibitor), are also involved in cell cycle regulation. *Hspa1a* (Hsp70) is important for cellular homeostasis and increases rapidly in response to a variety of stresses. It has potent immunomodulatory functions and promotes suppressive capacity in Tregs (Wachstein et al., 2012). *Ier3* (Immediate early response 3) is an important anti-apoptotic protein protecting cells from FAS or TNF induced apoptosis. *Nfil3* encoding the transcription factor nuclear factor, interleukin 3 regulated has recently been identified as a crucial part of IL-27 mediated anti-inflammatory effects and leads to increased IL-10 production in $CD4^+$ T cells while also dampening Teff functions (Zhu et al., 2015). *IL27Ra* was also upregulated in skin Tregs, supporting the importance of this pathway in skin Tregs. *Dgat1* and *Dgat2* encode diacylglycerol O-acyltransferase (DGAT), which are isoenzymes crucially involved in lipid metabolism (Cases et al., 1998).

The skin Treg markers we identified on protein level via flow cytometry (Figure 3.2 and Figure 3.3) were all found significantly upregulated on mRNA level (i.e. *Gata3, Itgae* (CD103)*, Klrg1, Il2ra* (CD25)*, Cd44)* in the microarray data (Figure 3.6 and Supplementary Table 1)

Sell (L-Selectin, CD62L) was the most downregulated gene in tissue Tregs, highlighting their effector / memory phenotype in the tissue. *Actn1* (alpha-actinin 1) is an actin binding protein important in immune synapse formation and rearrangement of the cytoskeleton in many immune cells (Kikonomou et al., 2011) *Acas2l* (acyl-CoA synthetase short-chain family member 1) is expressed in many cells and involved in fatty acid synthesis and thus contributes to the metabolic state of the cell (Schug et al., 2015).

Recent publications have highlighted the functional importance of IL-33R, IL-18R and amphiregulin (AREG) in Tregs of the gut, lung and adipose tissue (Arpaia et al., 2015; Burzyn, Kuswanto, et al., 2013; Schiering et al., 2014). Interestingly, we also found their genes highly expressed in skin resident Tregs. (Figure 3.6B and Supplementary Table 1).

Together, these data demonstrates a distinct phenotype of skin resident Tregs. In particular genes controlling T cell activation and metabolism were differentially regulated.

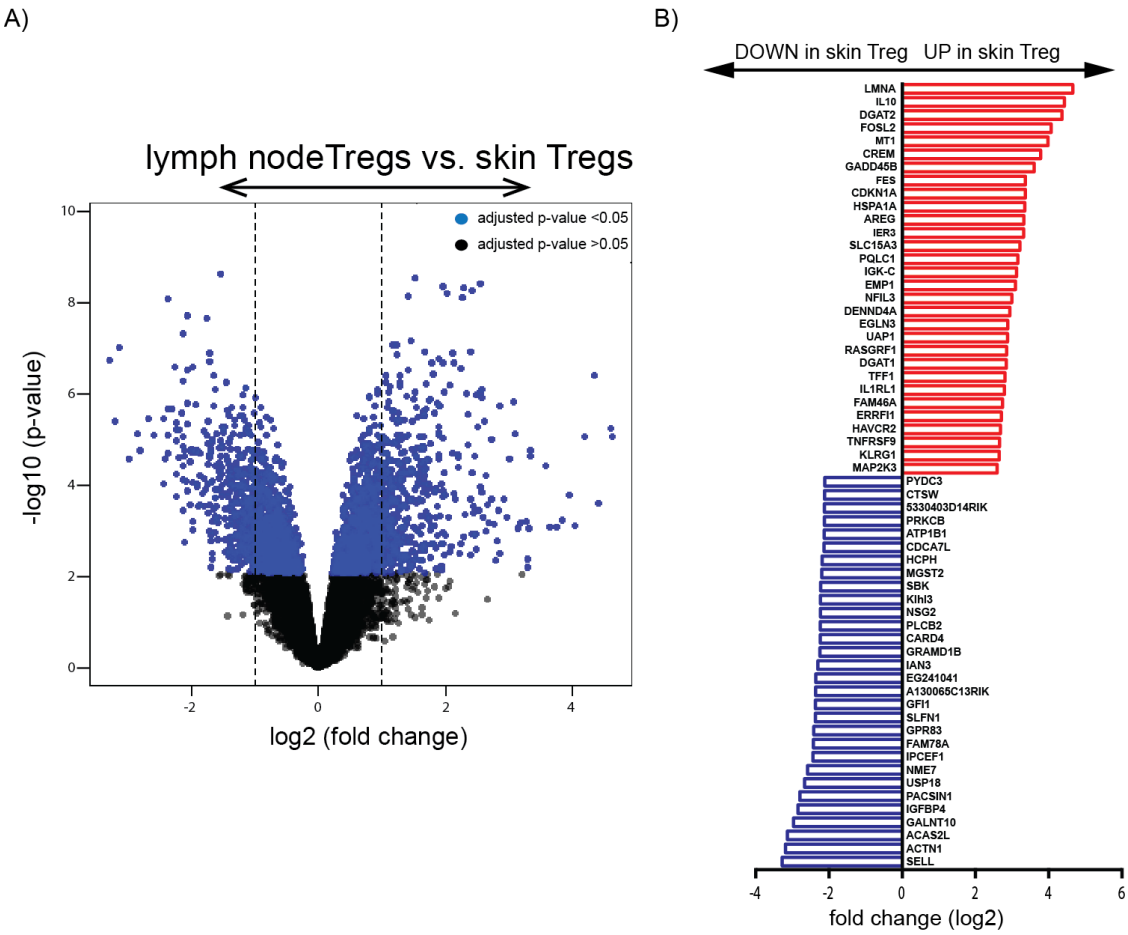

Figure 3.6. Differential gene expression comparing steady state lymph node Tregs and skin resident Tregs

Steady state B6 Foxp3^{GFP} mice were sacrificed at 8-10 weeks of age. Lymph nodes and ears were harvested. Single cell suspensions were obtained, lymph node Tregs magnetically enriched for CD4^{+} T cells and stained with surface antibodies followed by cell sorting. Viable, CD45^{+}CD4^{+}TCRβ^{+} GFP^{+} cells were sorted directly into Trizol. RNA was extracted, amplified and gene expression assessed as described in Chapter 2.

(A) Microarray results from Tregs extracted from untreated lymph nodes and tissue were compared. After normalization, genes were illustrated in a volcano plot. X-axis shows log2 fold changes. Positive values: upregulated in skin Tregs. Y-axis depicts p-value (–log10). genes with adjusted p-value <0.05 (blue), >0.05 (black)

(B) Graph depicts 30 most up (red) and down (blue) regulated genes between lymph node and skin Tregs ranked according to fold change. All genes p>0.05.

Data represents results form a single experiment (n=3 for lymph node Tregs, n=4 for skin resident Tregs) Array signal intensities were background adjusted, transformed using the variance stabilizing transformation (VST) and quantile normalized using Lumi (PMID:18467348) from R/Bioconductor. Differential expression analysis was performed for each comparison using the empirical bayes method implemented in LIMMA. Significance was defined as a Benjamini-Hochberg adjusted p-value < 0.05 and fold change > 2.

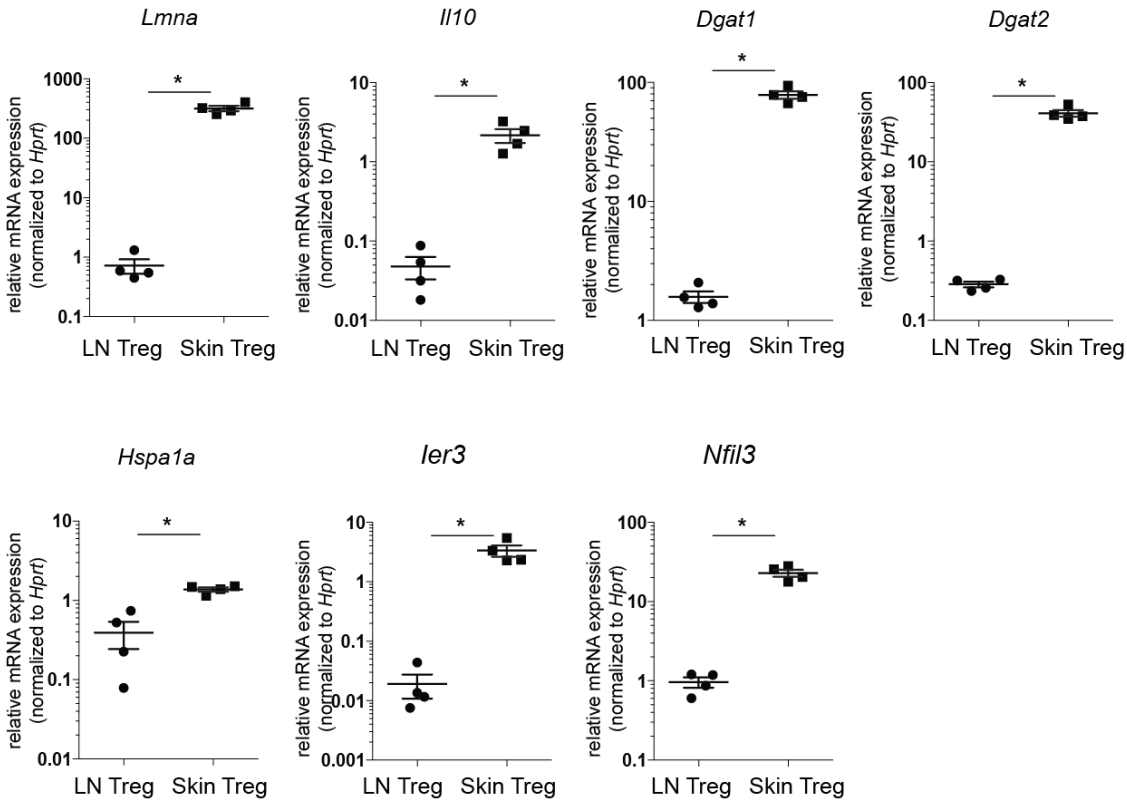

Figure 3.7. RT-qPCR validation of selected genes upregulated in skin resident Tregs

Steady state B6 Foxp3^{GFP} mice were sacrificed at 8-10 weeks of age. Lymph nodes and ears were harvested. Single cell suspensions were obtained, lymph node Tregs magnetically enriched for CD4^{+} T cells and stained with surface antibodies followed by cell sorting. Viable, CD45^{+}CD4^{+}TCRβ^{+} GFP^{+} cells were sorted directly into Trizol. RNA was extracted. Expression levels were normalized to *Hprt*. Bars represent mean; error bars represent SEM.

Bars represent the mean ± SEM. Statistical significance was determined using a Mann-Whitney U Test. Samples were obtained in an independent experiment (n=4 in each group) to the samples used for microarray.

3.2.5. Pathways associated with anti-apoptotic programmes and pathogen encounter are upregulated in skin Tregs

To further investigate the distinctiveness of skin resident Tregs, the microarray data were used to perform enrichment analysis via Gene Ontology (GO) "Biological process" pathway analysis. Using this unbiased approach we found 6 major processes significantly enriched in our data set (Figure 3.8A and B) and (Supplementary Table 2).

"Response to molecule of bacterial origin" was the highest enriched pathway and contained 6 genes: *Il10, Malt1, Cxcl2, Tnfaip3, Cd14 and Bcl10*. As mentioned above, *Il10* was the highest enriched cytokine and is essential for suppression in the tissue. *Malt1* (Mucosa-associated lymphoid tissue lymphoma translocation protein 1) encodes paracaspase and is important for T cell activation (Ruland et al., 2003). It regulates activation of NF-κB signaling as well as IL-2 production (Ruefli-Brasse et al., 2003). *Bcl10* acts upstream of paracaspase in the induction of NF-κB and promotes lymphocyte proliferation (Ruefli-Brasse et al., 2003). *Tnfaip3* (Tumor Necrosis Factor, Alpha-Induced Protein 3) encodes A20, an inducible protein involved in the termination of TLR- and TNF-induced NF-κB activity.

The upregulated genes assigned to the "response to lipopolysaccharide" pathway contained genes involved in TLR signaling such as *Myd88, Cd14, and Irak3* (Supplementary Table 2). As mentioned in the introduction, MyD88 is induced via activation of various TLRs and acts upstream of IL-1 receptor associated protein kinases (IRAK). CD14 functions as a co-receptor for TLR4

(Zanoni et al., 2011). We further found the genes for TLR1, TLR6 and TLR7 selectively upregulated in skin Tregs (Figure 3.6 and Supplementary Table 1).

The process “negative regulation of the inflammatory response” contained genes such as *Il10, Ier3, Il2Ra,* and *Gata3* discussed earlier. Further *Tnfrsf1b*, encoding the TNF receptor 2 was enriched; highlighting that skin Tregs have an increased sensitivity to TNF. *Apoe* encoding apolipoprotein-E is important in lipid transport and cholesterol metabolism (Meir, 2004).

The term “inflammatory response” contained 38 upregulated genes. Among these were genes discussed earlier such as *Il10, Klrg1, Cd14 and MyD88.* However, it further highlighted the upregulation of several chemokines and their receptor such as *Cxcl1, Cxcr4, Ccrl2, Ccr5, Ccl5, Il1b and Il-18rap* (Supplementary Table 2).

“Negative regulation of apoptotic processes” highlighted 78 upregulated genes in skin Tregs. Among them were the previously discussed *Hspa1a, Cd44 and Cdkn1a*. Further regulators of transcription such as *Crebbp* (CREB binding protein) (Gartel & Radhakrishnan, 2005). Cathepsin H (*CTSH*) assists in lysosome formation and degradation and also promotes granzyme B (GzmB) formation (D’Angelo et al., 2010). *Bcl3* is a transcriptional regulator promoting survival in many cancer types. The enriched transcriptional repressor *Bcl6* is essential for differentiation of follicular helper T cells by antagonizing Th1, Th2 and Th17 Teff differentiation (Nurieva et al., 2009).

The pathway “response to organic cyclic compound” contained genes discussed previously such as *Il10 and Cdkn1a.* Further the gene encoding the TFs, *Stat3* and *Pparg* and the adhesion molecule *Icam1* as well as *Tgfb1* were among the enriched genes grouped in this pathway. *Ctgf,* encoding connective

tissue growth factor is a growth factor with unknown function in T cells (Shi-Wen et al., 2008).

Taken together, the GO enrichment analysis highlights that Tregs in the skin have undergone changes in various pathways and are distinct from Tregs in lymphoid organs.

A)

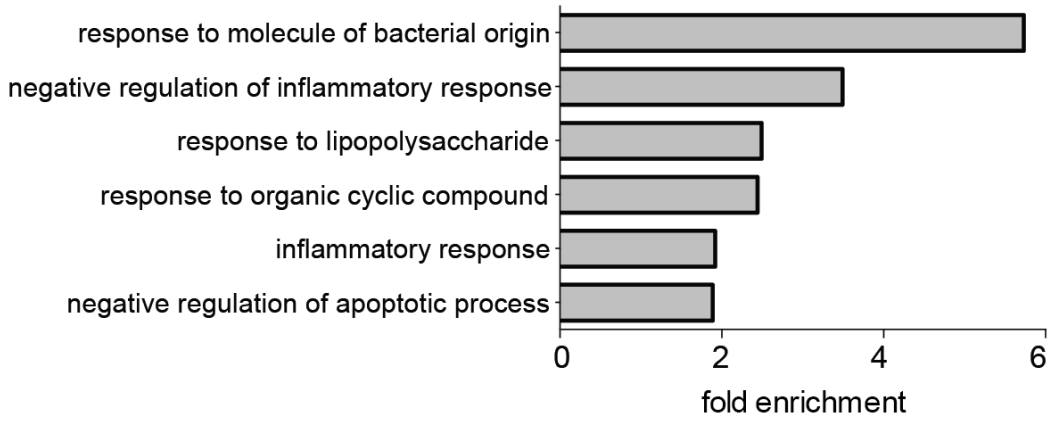

B)

GO biological process	Fold enrichment	p-value	FDR (Benjamini-Hochberg)
negative regulation of apoptotic process	1.89	0.00000004	0.000246
inflammatory response	1.92	0.00003930	0.028722
response to organic cyclic compound	2.44	0.00009800	0.049593
response to lipopolysaccharide	2.49	0.00001930	0.018132
negative regulation of inflammatory response	3.49	0.00003190	0.026266
response to molecule of bacterial origin	5.73	0.00006760	0.040421

Figure 3.8. Enriched biological processes (GO) in skin resident Tregs

Steady state B6 Foxp3^{GFP} mice were sacrificed at 8-10 weeks of age. Lymph nodes and ears were harvested. Single cell suspensions were obtained, lymph node Tregs magnetically enriched for CD4^{+} T cells and stained with surface antibodies followed by cell sorting. Viable, CD45^{+}CD4^{+}TCRβ^{+} GFP^{+} cells were sorted directly into Trizol. RNA was extracted, amplified and gene expression assessed as described in Chapter 2.

Microarray results from Tregs extracted from untreated lymph nodes and tissue were compared. Genes that were significantly upregulated in Tregs from the skin were subjected to pathway enrichment analysis (GO biological processes)

A) Pathways (y-axis) significantly upregulated in skin resident Tregs illustrated in fold enrichment (x-axis) above background.

(B) Table of enriched biological processes; fold up regulation, p-values and corrected p-values.

Data represent results form a single experiment (n=3 for lymph node Tregs, n=4 for skin resident Tregs). Enriched Gene ontology (GO) biological processes were assessed in differentially abundant gene sets using a hypergeometric test implemented in the runGO.py script from the CGAT code collection (PMID:24395753) and terms were considered significant at a false discovery rate (FDR) < 0.05.

3.2.6. The imiquimod model of psoriasiform skin inflammation

Tregs in the skin have a distinct phenotype and transcriptome compared to Tregs found in peripheral lymph nodes. Next, we sought to probe their suppressive capacity and identify any changes that occur during an inflammatory response.

The imiquimod model of psoriasiform skin inflammation is used as the main mouse model to delineate and assess pro- and anti-inflammatory pathways throughout this thesis (van der Fits et al., 2009). This involves applying cream containing 5% imiquimod (Aldara) to the ears of mice daily for a period of up to 7 days. Unless otherwise stated, all cell number and percentages originate from tissues harvested from mice sacrificed at day 7 of treatment.

Ear thickness increased after 3 applications and continued to do so until day 5, after which it slightly plateaued (Figure 3.9A). Animals were sacrificed on day 7 of treatment, by which time they showed clear inflammatory changes on histological examination such as acanthosis, parakeratosis and mixed leukocytic infiltrate in the dermis and thickening of the dermis and epidermis (Figure 3.8B). Initially, mice lose body weight, but start re-gaining weight after day three and reach their initial weight towards the end of the treatment course (Figure 3.8C). Imiquimod application also leads to systemic inflammatory reactions as measured by an increase of spleen weight and draining lymph node size (not depicted) over the treatment period (Figure 3.8D).

A time course of the disease model shows that ear thickness reliably reflects influx of $CD45^+$ cells into the skin and increase of epidermal and dermal thickness (Figure 3.9 E).

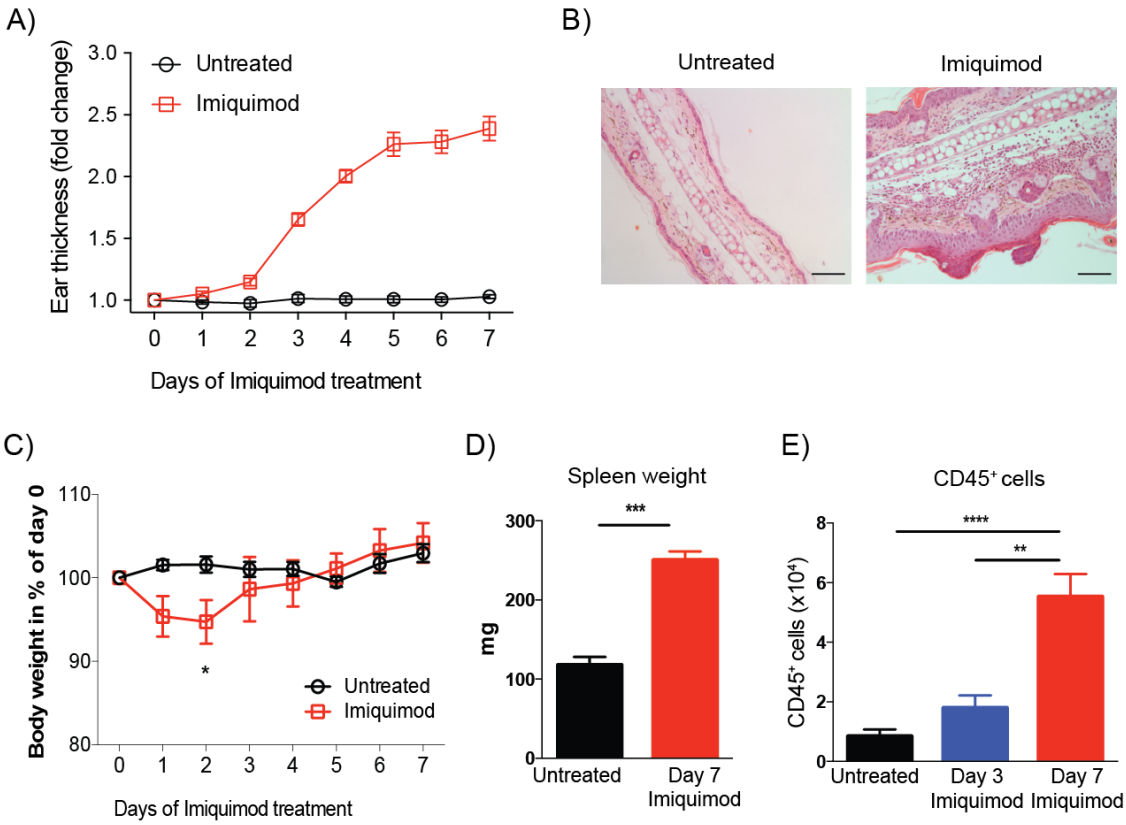

Figure 3.9. The mouse model of imiquimod-induced skin inflammation

20.8mg of Imiqimod (Aldara) was applied to each ear of B6 WT mice for 7 consecutive days. Ear thickness was measured with a thickness gauge and animals checked for weight loss daily. Tissue was harvested for further assessment and histology at sacrifice on day 7.

(A) Ear thickness is represented in fold change over values measured before first cream application. black: untreated group, red: daily imiquimod treatment

(B) Representative histology of ear tissue harvested from an untreated (left) and an imiquimod treated (right) mouse

(C) Body weight measured daily over the course of treatment relative to weight before first cream application

(D) Spleen weight of untreated (black) or treated (red) group

(E) Total cell numbers of $CD45^+$ cells in both ears at indicated time points

Bars represent the mean ± SEM Statistical significance was determined using a two-way Anova followed by Bonferroni post-hoc test (A and C) and Mann Whitney U Test (D). Data are representative of 1 of >5 independent experiments (n≥ 4 each).

3.2.7. The majority of IL-23 responsive cells in inflammation are dermal γδ T cells

IL-23 drives the pathology in this disease and infiltrating IL-17 producing dermal γδ T cells as well as ILC-3 have been described as the pathogenic cell types in the imiquimod model (Cai et al., 2011; Pantelyushin et al., 2012; van der Fits et al., 2009). We can also confirm this observation with $CD3^+$ $TCR\gamma\delta^{dim}$ dermal γδ T cells significantly increasing over the treatment with imiquimod (Figure 3.10A and C). After a 4 hour re-stimulation with PMA and Ionomycin in the presence of BFA, they are the main producers of IL-17A and IL-22 in the inflamed skin (Figure 3.11A). In agreement with published data, $CD4^+$ αβ T cells only produced small amounts of these cytokines in our studies (Figure 3.11A).

As IL-23 is the crucial driver of pathology in this model (van der Fits et al., 2009), we assessed the expression of the IL-23R on the different T cell populations over the course of skin treatment. For this we utilized $IL23R^{GFP/+}$ mice that respond normally to IL-23, but can be reliably used to visualize the receptor expression (Awasthi et al., 2009). Indeed, as we demonstrated under homeostatic conditions, it was mainly the dermal γδ and not the $CD4^+$ αβ T cells that expressed IL-23R in the inflamed skin (Figure 3.4 B). Equally, it was these cells that expressed the highest amount of RORγt under inflammatory conditions (Figure 3.11B). The proportion of γδ T cells among the IL-23R expressing cells increased by day 7, whereas the frequency of $CD3^-$ T cells, most likely ILC3 and myeloid cells, decreased. The frequency of $CD4^+$ T cells

in the skin remained unchanged throughout the course of treatment Figure 3.10B).

The skin harbours two ontogenetically distinct populations of γδ T cells. Epidermal γδ T cells are seeded to the tissue early in embryonic development, express high levels of CD3 and TCRγδ and are present in high numbers under homeostatic conditions in the skin (Jameson & Havran, 2007). Dermal γδ T cells can be identified by lower expression of the TCR and CD3 and use different TCRs than their epidermal counterpart (Sumaria et al., 2011). As previous reports have shown, we also demonstrate that dermal γδ T cells significantly increase in inflammation, whereas the epidermal γδ T cells decrease. The later population also does not express IL-23R or RORγt. (Figure 3.11B)

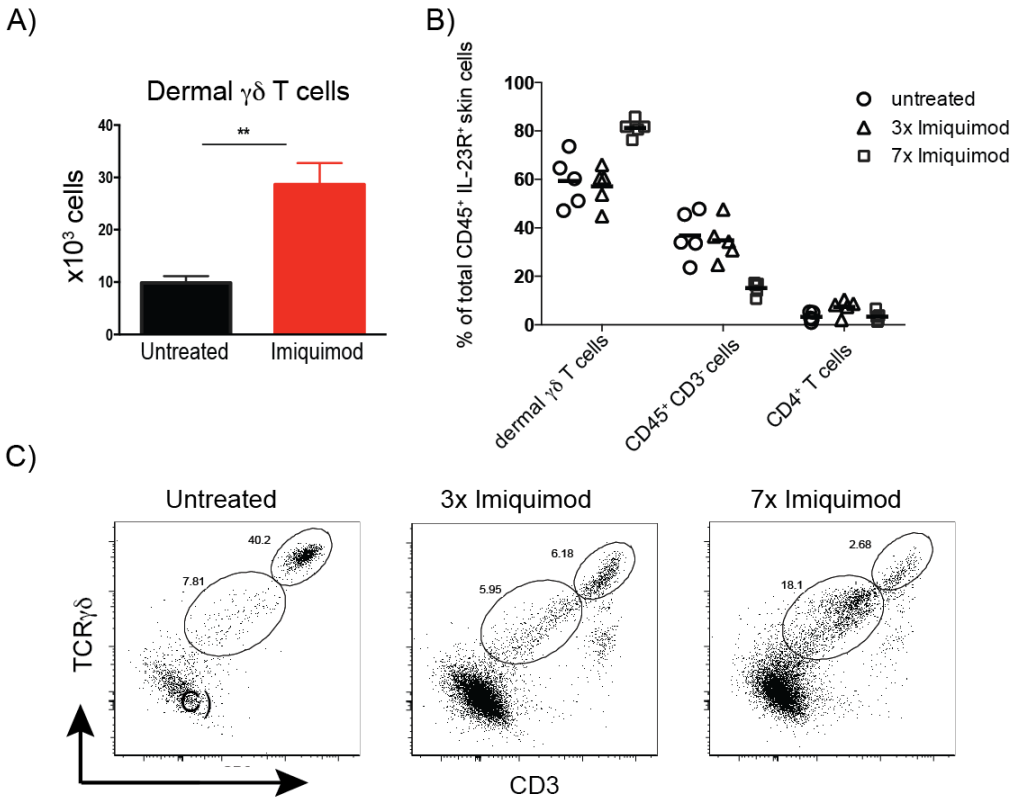

Figure 3.10. Changes in γδ T cell in skin inflammation

B6 WT were treated with imiquimod (Aldara) 1x/day for 3 or 7 days or left untreated. Single cell suspensions were prepared from ear skin and analysed by flow cytometry.

(A) Dermal γδ T cell numbers in the ears

(B) Representative FACS plots and frequency of dermal and epidermal γδ T cells in untreated, 3x and 7x treated mice

Data (A) and bars (B) represent the mean ± SEM. Each symbol represents one individual animal (B). Statistical significance was determined using a Mann-Whitney U Test (D). Data are representative of 1 of ≥4 (A and C) or 2 (B) independent experiments (n≥ 4 each).

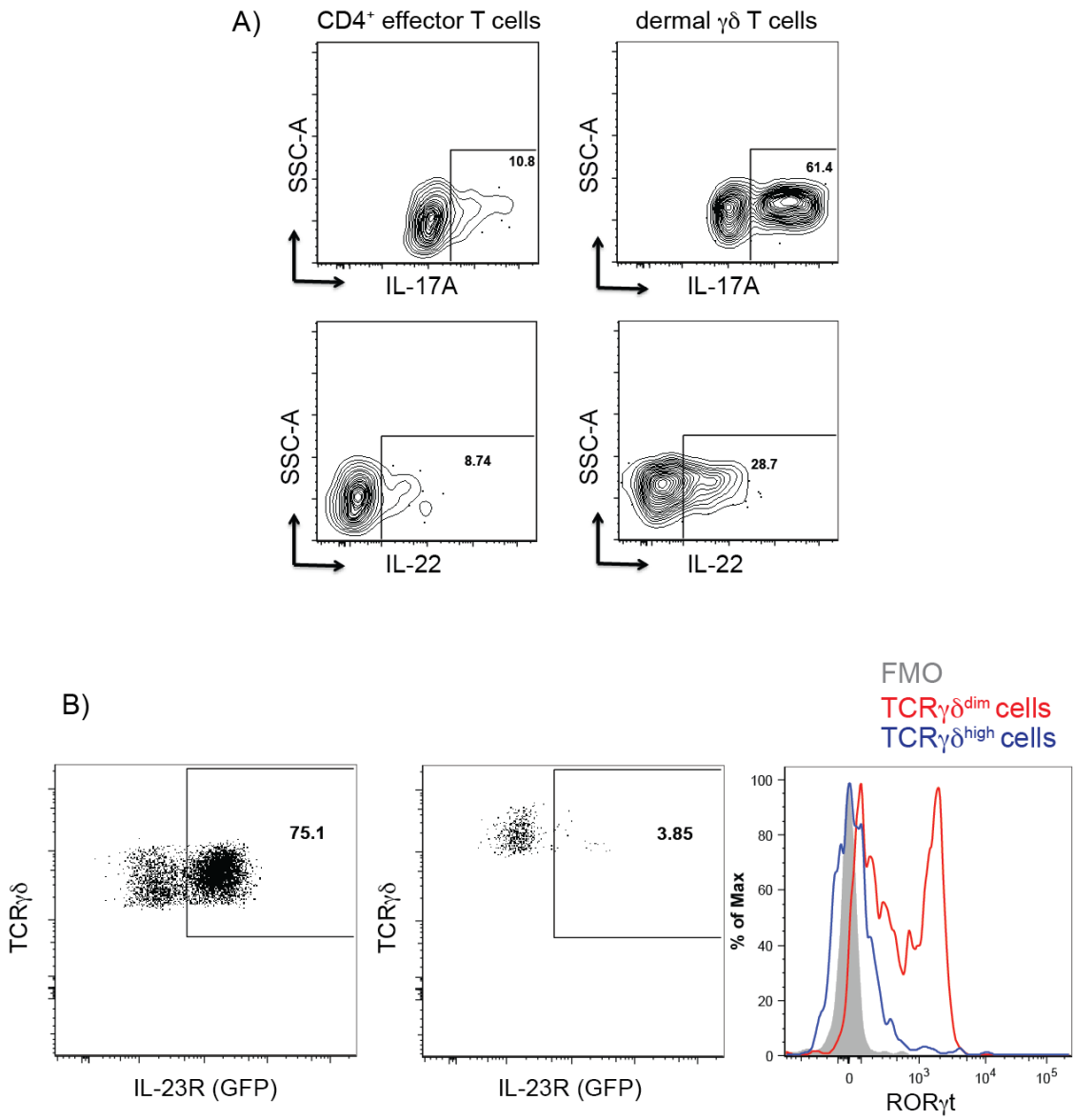

Figure 3.11. Sources of IL-17A and IL-22 in skin inflammation

B6 WT or B6 IL-23R $^{GFP/+\ mice}$ were treated with imiquimod (Aldara) 1x/day for 7 days or left untreated. Single cell suspensions were prepared from ear skin and analysed by flow cytometry or re-stimulated with PMA and ionomycin in the presence of BFA for 4 hours before analysis.

(A) Representative FACS plot of IL-17A and IL-22 production of skin $CD4^+$ αβ T effector cells (left) or dermal γδ T cells (right) at day 7 of treatment

(B) Representative FACS plot of IL-23R (GFP) expression by dermal γδ T cells (left), epidermal γδ T cells (middle). Expression of the transcription factor RORγt by epidermal (blue) or dermal (red) γδ T cells and FMO control (grey)

Data are representative of 1 of 3 (A) or 2 (B) independent experiments (n≥ 4 each).

3.2.8. Tregs are increased in imiquimod-induced skin inflammation

$CD4^+$ αβ T cells are not a crucial source of pathogenic cytokines in this model, however their frequency and absolute numbers increase in correlation with ear thickness (Figure 3.12A). This increase is largely due to a to rising number and percentage of $CD4^+Foxp3^+$ Tregs but also a significant increase in $CD4^+Foxp3^-$ Teff (Figure 3.12A and B).

To investigate if Tregs in the imiquimod model exhibit instability, the mean fluoresce intensity of Foxp3 was analysed. However, no difference in the amount of Foxp3 expression between the two groups was observed (Figure 3.12C).

To further investigate Treg instability, the expression of lineage defining transcription factors as well as IL-17A production of $CD4^+$ $Foxp3^+$ T cells isolated directly from the inflamed skin of treated mice was studied (Figure 3.14). IL-17A production in Tregs was not increased in inflammatory conditions. (Figure 3.13A). Tregs under inflammatory conditions expressed substantial amounts of GATA-3 and did not express T-bet (Figure 3.13B). A significant increase in RORγt MFI was observed, however these changes were minimal and amounts remained very low (Figure 3.13B).

Together these data demonstrated that Tregs in the inflamed skin did not show an unstable Treg phenotype or propensity to convert to Teff cells.

.

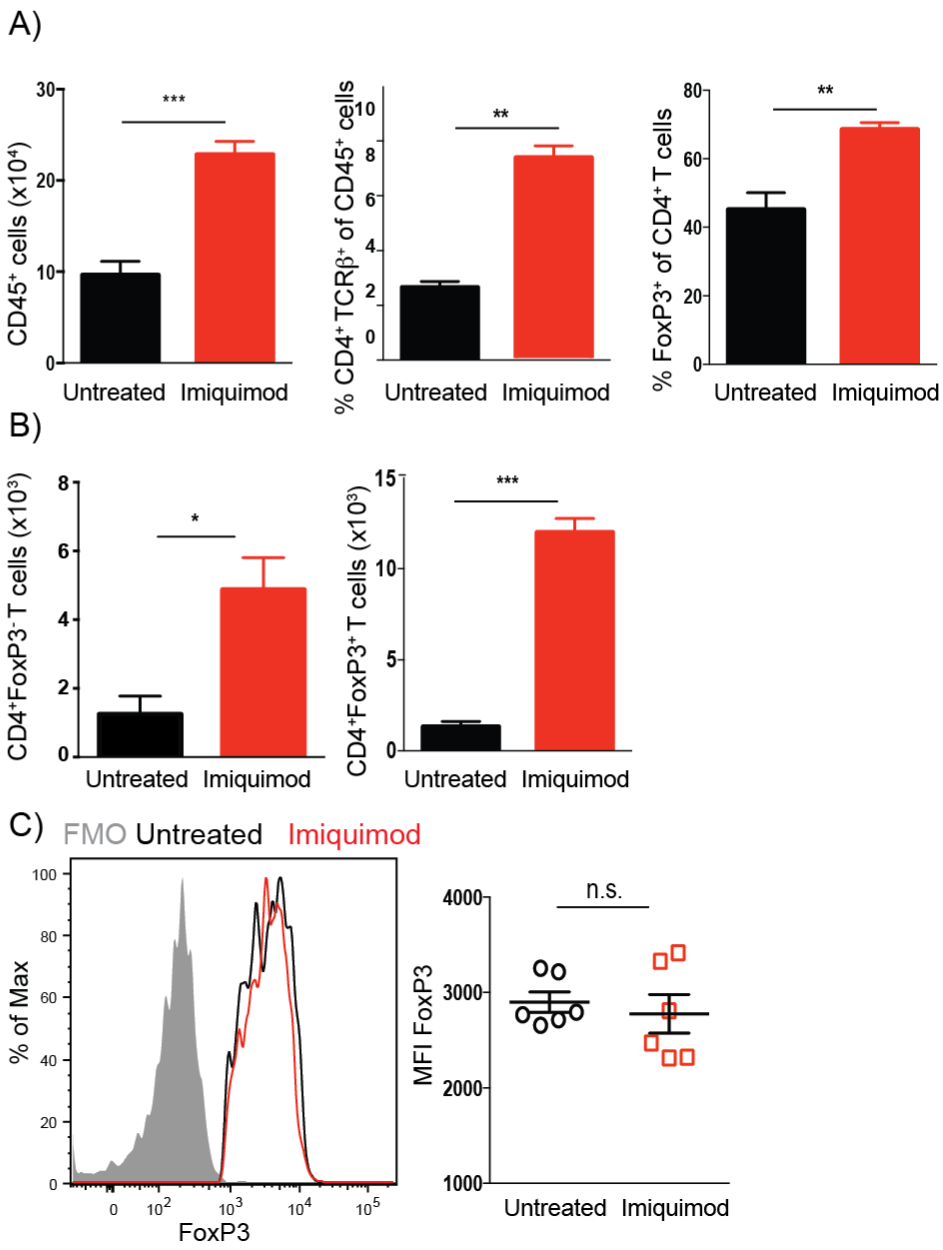

Figure 3.12. Regulatory T cells in skin inflammation

B6 WT were treated with imiquimod (Aldara) 7 days or left untreated. Single cell suspensions were prepared from ear skin and stained with according antibodies before being analysed by flow cytometry or re-stimulated with PMA and ionomycin in the presence of BFA for 4 hours before staining and analysis.

(A) Frequency of $CD45^+$ cells, $CD4^+$ T cells and $Foxp3^+$ Tregs in the skin of steady state (black) and imiquimod (red) treated mice

(B) Absolute numbers of Teff and Treg in the ears of steady state (black) and imiquimod (red) treated mice

(C) Representative FACS plot and Foxp3 MFI of $CD4^+Foxp3^+$ T cells in the ears of steady state (black) and imiquimod (red) treated mice

Data (A and B) and bars (C) represent the mean ± SEM Each symbol represents one individual animal. Statistical significance was determined using a Mann-Whitney U Test (D). Data are representative of 1 of ≥3 independent experiments (n≥ 4 each).

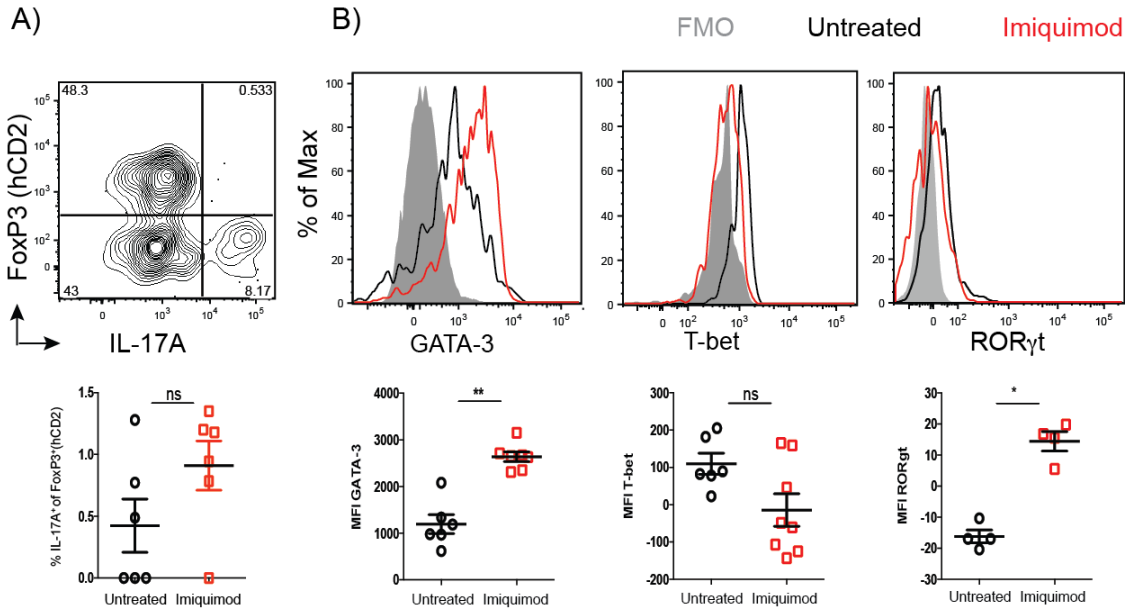

Figure 3.13. Transcription factor and cytokine expression in Tregs during skin inflammation

(A) Representative FACS plot and frequency of IL-17A expression after re-stimulation gated on $CD4^+$ T cells extracted from the skin.

(B) Representative histograms and frequencies of transcription factor expression of skin resident $Foxp3^+CD4^+$ T cells.

Bars represent the mean ± SEM Each symbol represents one individual animal. Statistical significance was determined using a Mann-Whitney U Test (D). Data are representative of 1 of ≥3 (A and C) or 2 (B) independent experiments (n≥ 4 each).

3.2.9. Regulatory T cell positioning in the inflamed skin

Next, we wanted to identify if the physical properties of Tregs changed over the treatment course and set out to investigate where the cells were anatomically located in homeostatic and inflamed conditions. Frozen ear sections harvested at day 7 of treatment or from untreated mice were used for in situ analysis (see detailed description in Chapter 2). Lymph nodes were used as a positive control.

Due to the distinct anatomical arrangement of basal keratinocytes, the dermo-epidermal junction with the basement membrane as its border can be identified easily when nuclei are stained with Hoechst (highlighted by dashed line in Figure 3.14A) In the untreated skin, Tregs are rarely found on the 5um thick sections and are confined to the dermis. In the treated skin, Tregs are found at higher density in the dermis, and intriguingly, they are also found above the dermal-epidermal junction (Figure 3.14A, right).

We set out to confirm these findings and further investigate the behavioural properties of Tregs by *in vivo* microscopy using B6 Foxp3^{GFP} mice (Figure 3.14B and C). Here Tregs were dispersed throughout the dermis in steady state, present in the follicular and inter-follicular regions and at various depths of the dermis (identified by the blue collagen). During inflammation their number increased and they also located to the now thickened epidermis as identified by absence of second harmonic generation (SHG) of collagen. This confirmed the results seen on immunofluorescence staining. At steady state, Tregs were not mobile over the recorded period of up to 35 minutes and this was consistent across three mice imaged. Under inflammatory conditions,

Tregs showed a higher potential to probe their environment. However, during the 40 minutes in which we were able to perform *in vivo* imaging we were not able to image enough events to define the distance moved. For quantitative analysis, more mice would need to be imaged over a longer period of time.

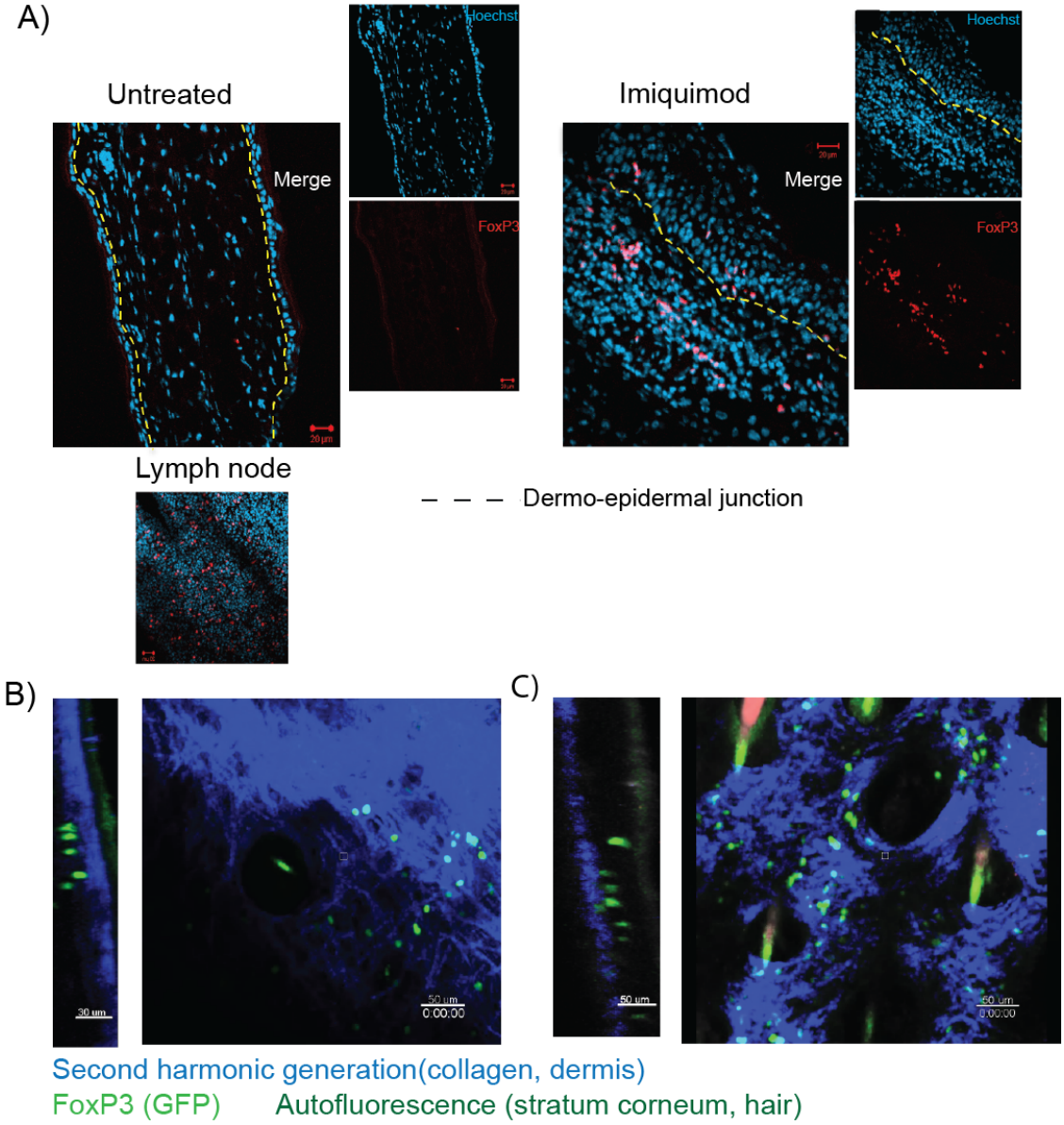

Figure 3.14. Tregs locate to the dermis in steady state and to the dermo-epidermal junction in skin inflammation

B6 WT or B6 Foxp3^{GFP} mice were treated with imiquimod (Aldara) 7 days or left untreated.

(A) Immunofluorescence staining of OCT frozen sections for Foxp3. Tissue was harvested from untreated ears (left) 7x imiquimod treated ears (right) or lymph node as control (bottom)

(B) Representative pictures from *in vivo* imaging of ears of untreated Foxp3^{GFP} mice. Left picture: Sagittal plane of ear (stratum corneum visible by light green autofluorescence on right) with Tregs (green) visible under the dermal collagen (blue) Right picture: Transverse plane of dermis; Tregs (green) hair (autofluorescent green)

(C) Representative pictures from *in vivo* imaging of ear of 7x imiquimod treated Foxp3^{GFP} mice. Left picture: Sagittal plane of ear (stratum corneum visible by light green autofluorescence on right) with Tregs (green) visible above the dermal collagen (blue) Right picture: Transverse plane of dermis; Tregs (green), hair (autofluorescent green)

Images are representative of 2 experiments (each n=3) (A) and 3 mice imaged at two different occasions (B and C)

3.2.10. Identification of genes upregulated in Tregs in skin inflammation

We observed that Tregs in imiquimod-induced inflammation are present at high numbers in the inflamed skin and that they maintained key characteristics associated with high suppressive capacity. In addition, during inflammation Tregs located to additional anatomical locations such as the epidermis.

To investigate the unique properties of skin Tregs and examine potential changes they undergo in an inflammatory setting, we performed a transcriptomic analysis. We compared Tregs from the skin extracted from either untreated or imiquimod treated mice. $CD45^{+}CD4^{+}TCR\beta^{+}GFP^{+}$ cells were sorted from B6 $Foxp3^{GFP}$ mice as described in Chapter 2. 4-6 mice were pooled for each experimental sample and normalized amounts of RNA amplified before analysis on Illumina bead arrays. We compared steady state Tregs extracted from ear tissue (n=4) and Tregs extracted from ears of imiquimod treated mice (n=4).

We performed hierarchical clustering analysis that included the results from lymph node Tregs introduced earlier in this chapter. The Tregs derived from the treated and untreated skin clearly clustered away from the lymph node Tregs, indicating that both tissue populations are more similar to each other than the lymph node. Within the tissue Tregs, a clear sub-branching into the untreated and treated group was apparent, highlighting differences in the transcriptome of skin Tregs under homeostatic vs. inflammatory conditions (Figure 3.15).

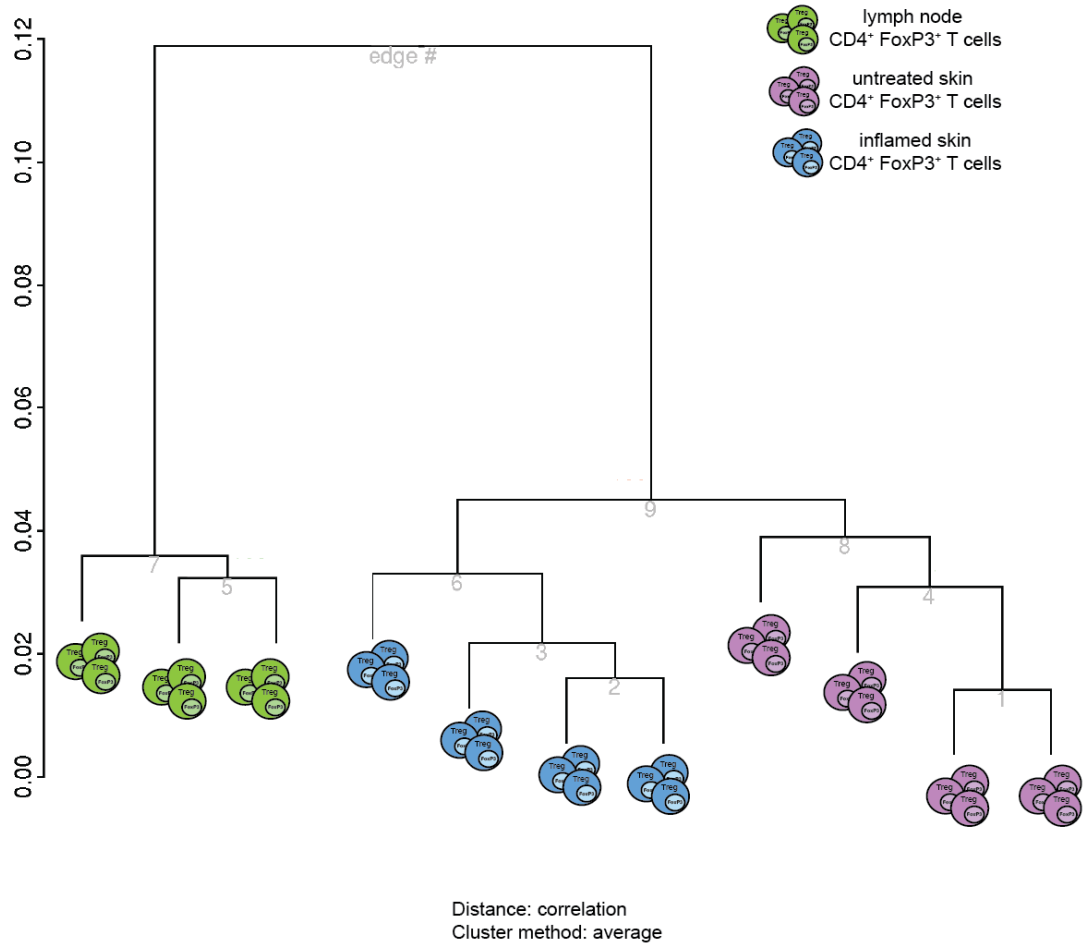

Figure 3.15. Dendrogram of Treg microarray

Steady state B6 Foxp3^{GFP} mice or mice treated with imiquimod for 7 consecutive days were sacrificed at 8-10 weeks of age. Ears were harvested and enzymatically digested. Single cell suspensions were obtained, and stained with surface antibodies followed by cell sorting. Viable, CD45^{+}CD4^{+}TCRβ^{+} GFP^{+} cells were sorted directly into Trizol. RNA was extracted, amplified and gene expression assessed as described in Chapter 2.

Illumina microarray and data normalization and analysis in R were performed.

3.2.11. Tregs in skin inflammation maintain a suppressive phenotype

To further investigate the changes Tregs undergo when they are resident in the skin, data obtained in the microarray was used to performed enrichment analysis using Gene Ontology (GO) biological processes with the up-regulated genes in the skin. However, using this unbiased approach, we did not find any pathways significantly enriched. Nevertheless, we found 29 genes upregulated and 39 genes downregulated ($p<0.05$, log2 fold change≥1). (Figure 3.16 and Supplementary Table 3)

The most upregulated gene in the Tregs from the inflamed skin was *Lag3*. Lymphocyte activation gene 3 is highly associated with effective suppressive capacity of Tregs *in vivo* (Huang et al., 2004). It can be induced via IL-27 and its receptor *Il27Ra* was also significantly upregulated in our data set. *Ccl4*, (CCL4, MIP-1β) was the second highest gene upregulated in inflamed vs. non-inflamed tissue Tregs. *Satb1*, a chromatin organizer in T cells is involved in T cell differentiation and induces expression of GATA-3 in Th2 cells (Burute et al., 2012). *Gpr15* expression on Tregs is important to control T cell mediated colitis by mediating Treg homing to the gut (Kim et al. 2013; Nguyen et al. 2014). *CD5* was significantly upregulated in the Tregs from inflamed skin. The chemokine receptor *CCR8* was expressed at significantly higher levels in the Tregs from inflamed skin and has been implicated in skin homing of T cells (Mccully et al., 2013; McCully et al., 2012).

The skin Treg markers we identified (i.e. *Itgae* (CD103)*, Klrg1, Il10, Ctla4)* on protein and/or mRNA level in steady state skin Tregs (Figure 3.2 and Figure

3.6) were not significantly changed in Tregs under inflammatory condition (Supplementary Table 3). Together, these data suggest that Tregs maintain a suppressive phenotype during psoriasiform skin inflammation and upregulate genes associated with regulation, skin homing and conversion of self-reactive T cells to iTreg. Exploring these data using further experimental approaches will help identify the functional relevance of these genes in skin inflammation.

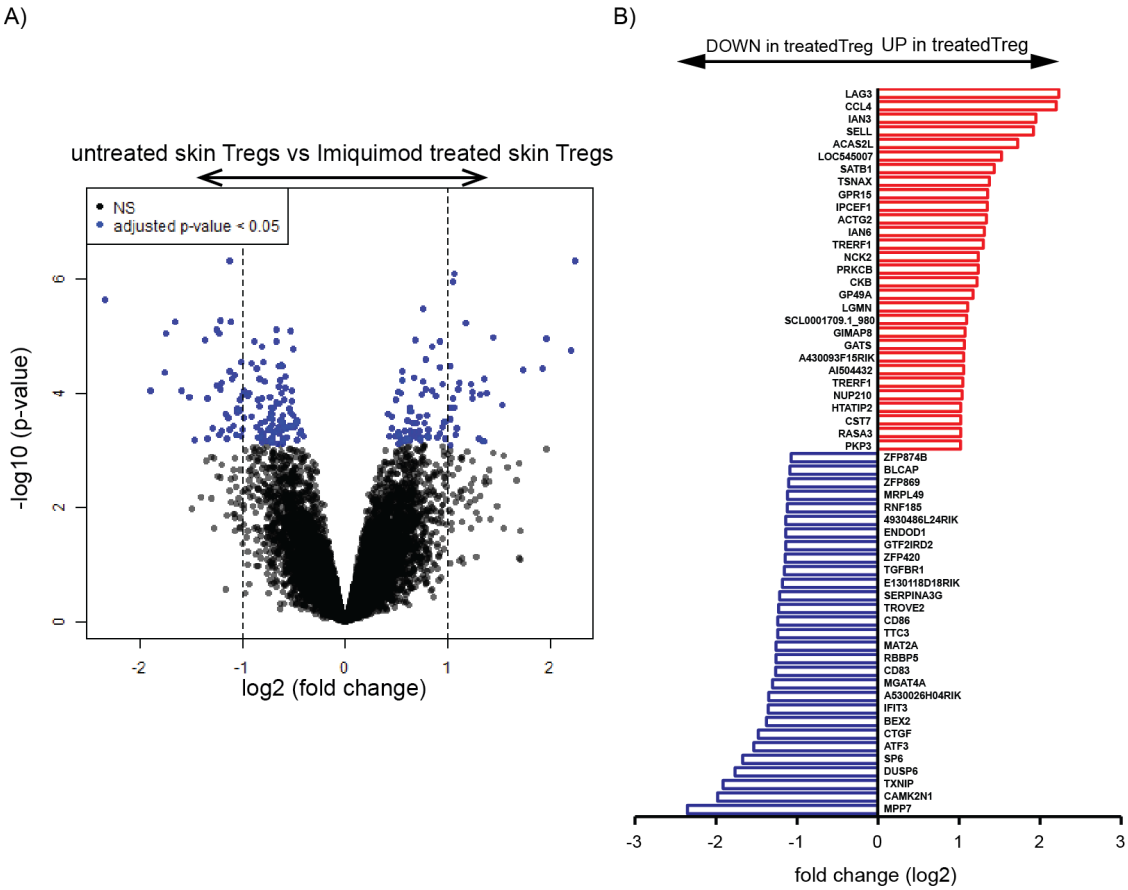

Figure 3.15. Differential gene expression t comparing steady state skin resident Tregs and skin resident Tregs from imiquimod treated animals

Steady state B6 Foxp3^{GFP} mice or mice treated with 7x imiquimod were sacrificed at 8-10 weeks of age. Ears were harvested. Single cell suspensions were obtained, stained with surface antibodies followed by cell sorting. Viable, CD45^{+}CD4^{+}TCRβ^{+} GFP^{+} cells were sorted directly into Trizol. RNA was extracted, amplified and gene expression assessed as described in Chapter 2.

(A) Microarray results from Tregs extracted from untreated and imiquimod treated tissue were compared. After normalization, genes were illustrated in a volcano plot. X-axis shows log2 fold changes. Positive values: upregulated in treated skin Tregs. Y-axis depicts p-value (–log10). genes with adjusted p-value <0.05 (blue), >0.05 (black)

(B) Graph depicts 30 most up (red) and down (blue) regulated genes between Tregs from untreated skin and Tregs from imiquimod treated skin ranked according to fold change.

Data represents results form a single experiment (n=4 Tregs from untreated skin, n=4 Tregs from inflamed skin) Array signal intensities were background adjusted, transformed using the variance stabilizing transformation (VST) and quantile normalized using Lumi (PMID:18467348) from R/Bioconductor. Differential expression analysis was performed for each contrast using the empirical bayes method implemented in LIMMA. Significance was defined as a Benjamini-Hochberg adjusted p-value < 0.05 and log2 fold change > 1.

3.3. Discussion

In this chapter we have shown that Tregs isolated from the skin display a unique phenotype. Like most $CD4^+$ T cells in the skin, Tregs express effector memory phenotype markers such as CD44 and lack CD62L expression. Absence of Treg derived IL-10 leads to spontaneous colitis and increases lung and skin hypersensitivity reactions (Rubtsov et al., 2008). About one third of these tissue Tregs secreted IL-10 under homeostatic conditions without artificial restimulation, highlighting an active suppressive state. They further expressed markers associated with high suppressive capacity such as the IL-2 receptor CD25, KLRG-1 and CD103. In the gut, another major barrier organ, peripherally induced Tregs contribute substantially to the total Treg pool (Bilate & Lafaille, 2012). We therefore investigated the proportions of nTregs and iTregs in the skin.

The majority expressed the transcription factor Helios, suggesting they are of thymic origin. However as mentioned previously, the accuracy of Helios to identify nTregs has been questioned (Gottschalk et al., 2012; Singh et al., 2015). In the gut the constant exposure to microbiota is thought to contribute strongly to the iTreg pool; it was therefore surprising that the Treg pool in the skin, another important barrier organ was largely $Helios^+$. The skin and the gut are both organs that are constantly exposed to pathogens and these interactions are thought to drive iTreg differentiation in the intestine (Belkaid & Segre 2014; Atarashi et al. 2013). It can be speculated that the differences in microbial colonization between these two tissue sites could contribute to the differential Treg pool, however further experiments are needed to identify such

organisms or other factors causal for this difference. Further supporting a difference in Treg populations in the skin and the gut were the results showing that skin Tregs are RORγt$^-$. Recent publications highlighted that RORγt is preferentially expressed in peripherally generated Helios$^-$ Tregs and these cells are highly prevalent in the colon (Ohnmacht et al., 2015; Sefik et al., 2015).

It was previously demonstrated that Tregs at various barrier sites could express the transcription factor GATA-3 (Wohlfert et al., 2011), and we confirmed that most skin Tregs were indeed GATA-3$^+$. GATA-3 is important for inducing the expression of ST2 in Th2 cells and is also associated with ST2 expression in colonic Tregs (Guo et al., 2009; Schiering et al., 2014). ST2 is highly expressed in skin Tregs and IL-33 from stromal and epithelial cells could induce a higher frequency of ST2$^+$ Tregs (Turnquist et al., 2011). ST2 in the skin is thought to contribute to chronic Th2 type diseases such as atopic dermatitis (Savinko et al., 2012). However its role on skin Tregs has not been described and investigated and should be addressed in further experiments.

To assess the changes in skin resident Tregs compared to Tregs from lymph nodes, we performed microarray analysis. This revealed a distinct and unique expression profile of skin Tregs. Many of the upregulated genes have anti-apoptotic and metabolic functions suggesting Tregs in the skin are highly adapted to their unique environment. Furthermore, tissue Tregs upregulated many genes associated with suppression such as *Il10, Itgae* (CD103), *Klrg1, Ctla4* and *Tgfb1.*

The upregulated genes *Nfil3* and *Il27Ra* suggest an increased suppressive capacity. NFIL3 in CD4$^+$ Teff promotes secretion of IL-10 and an anti-

inflammatory phenotype (Zhu et al., 2015). This is in part mediated by IL-27, suggesting Treg cells could use this pathway in the skin to maintain and promote IL-10 secretion. The product of the upregulated gene *Ctsh* (Cathepsin H) is involved in granzyme B (GzmB) secretion, suggesting that skin Tregs might be utilizing GzmB to exert cytotoxicity (Cao et al., 2007). Intracellular staining could easily test Treg secretion of GzmB.

Gadd45b (growth arrest and DNA damage−inducible, β) is induced by TCR engagement and inflammatory signals and deficiency in *Gadd45b* leads to impaired response of $CD4^+$ T cells to these stimuli (Lu et al., 2004). Genes involved in TCR activation, antigen recognition and cell cycle regulation such as *Cdkn1a and Hspa1a* were selectively upregulated and indicate permanent antigen encounter of Tregs in the skin as suggested for tissue resident Tregs in other organs (Gratz & Campbell, 2014)

The GO search approach highlighted the enrichment of genes involved in antigen recognition and immune sensing in skin Tregs. We found TLR1, TLR6 and TLR7 induced in the skin Tregs, suggesting that they have an enhanced capacity to sense bacterial and viral components. The finding that TLR7 was expressed in skin Tregs is of special interest, as the model of skin inflammation used in our studies employs a TLR7 agonist and the contribution of Tregs to this model and also imiquimod treatment in patients remains elusive. *Malt1* was also induced in the skin and has been shown to induce higher levels of TLR2 expression in iTregs and a recent report shows that *Malt1*$^{-/-}$ mice have a defect in nTreg generation (Brüstle et al., 2015). *Cd14,* encoding a co-receptor for TLR4 was also enriched in the skin (Zanoni et al., 2011). TLR4 on Tregs induces their proliferation, promotes upregulation of

suppression markers and anti-apoptotic pathways in response to LPS and highlights the dynamic interaction of microbial products and immune regulation (Caramalho et al., 2003).

Tnfaip3 encoding A20 is involved in termination of TNF and NF-κB induced pathways and *Tnfaip3*$^{-/-}$ mice develop spontaneous inflammation leading to premature death (Lee et al., 2000). DC specific deletion of A20 inhibits Treg generation and leads to autoimmunity (Kool et al., 2011). However, the intrinsic role of A20 in Tregs has not been clarified and could be of importance in tissue resident Tregs, which localize in microbe exposed organs.

A further gene involved in the NF-κB pathway, which can inhibit or promote this pathway is BCL3. *Bcl3* was enriched in skin Tregs. Its T cell specific functions have recently been investigated. *Bcl3*$^{-/-}$ T cells were less pathogenic and produced less cytokines than their WT counterpart in colitis. Cell type specific deletion of *Bcl3* protected mice from EAE whereas full genetic deletion did not show any effect (Tang et al., 2014). However, *Bcl3*$^{-/-}$ T cells did not show a propensity to differentiate into Tregs. A further study investigated the role of *Bcl3* in a CHS model. *Bcl3* deficient mice had higher levels of pathogenic cytokines and chemokines that were mainly associated with an increase in CD8^{+} T cells in the tissue. The inflammation was in part rescued by non-hematopoietic expression of *Bcl3* suggesting keratinocytes might be involved (Tassi et al., 2015). These data suggest that *Bcl3* could be of particular importance in skin Tregs and should be further experimentally addressed.

Several members of the IL-1 family and their receptors were upregulated in skin Tregs. IL-1 family members critically regulate CD4^{+} T cell function (Sims & Smith, 2010). The importance of epithelial derived IL-18 in promoting Treg

function was recently highlighted in the intestine where IL-18 signalling regulated $CD4^+$ Teff cells and was critical for Treg mediated protection in colitis (Harrison et al., 2015). It remains to be tested if IL-18 could also shape the Treg response in skin inflammation.

Fosl2 encodes a member of the AP-1 family of transcription factors. Fosl2 has been identified as a key regulator of naïve T cell differentiation. Absence of Fosl2 in naïve T cells suppresses skewing towards Th1 and Th17 cells and increased Foxp3 expression (Ciofani et al., 2012). These data suggest a role in skin Tregs that are most likely of thymic origin and warrant further investigation of Fosl2 in nTregs.

BCL6 is a transcription factor crucial for development of follicular T helper cells. In Tregs it is important for their immunosuppressive capacity, especially for restraining Th2 driven inflammation. Interestingly, BCL6 represses GATA-3 levels in Tregs (Sawant et al., 2012). However, we observed high levels of GATA-3 despite increased expression of *Bcl6*. This might point to cell heterogeneity within the Treg populations of the skin, however this could also suggest a differential interaction of GATA-3 and BCL6 in the tissues as the cited study compared splenic *ex vivo* activated Tregs.

We further found several genes involved in lipid metabolism upregulated in skin Tregs. *Dgat1* and *Dgat2* are genes encoding isoforms of diacylglycerol O-acyltransferase (DGAT). DGAT is a key metabolic enzyme in triglyceride synthesis and is vital for adipose tissue formation (Cases et al., 1998). *Dgat1* was also highly induced in colonic and VAT Tregs (Cipolletta et al., 2012; Schiering et al., 2014). This highlights DGAT as a potentially important mechanism of metabolic adaptation in several diverse tissues and these

enzymes should be further investigated. The gene for peroxisome proliferator-activated receptor PPAR-γ is crucial in the formation of adipocytes. This nuclear receptor stimulates lipid uptake in cells and is crucial for Treg accumulation and function in the VAT (Cipolletta et al., 2012; Vasanthakumar et al., 2015). A further gene involved in lipid metabolism that is upregulated in skin Tregs is *Apoe*. *Apoe*$^{-/-}$ mice develop severe atherosclerosis and are widely used in atherosclerosis research (Meir, 2004). Transfer of WT Tregs into *Apoe*$^{-/-}$ mice attenuated inflammation and stabilized the atherosclerotic plaques (Feng et al., 2009; Mor et al., 2007). However exactly how this was achieved requires further study.

Together, the data obtained in the transcriptomic analysis of skin Tregs suggests that Tregs extracted from tissue sites share certain common “tissue” genes, but also differ in many aspects depending on the tissue of origin. The distinct transcriptional signature in skin Tregs is likely associated with the change in encountered antigen and environmental challenges. The numerous genes involved in immune suppression, cell cycle and survival, immune sensing and metabolism that were upregulated in skin Tregs support the view that they are highly adapted and specialized to the microenvironment of the skin.

Skin Tregs are further equipped with a number of highly suppressive proteins and transcripts. This underscores that Tregs are constantly engaged with their surrounding and actively maintain a regulated environment, highlighting that our largest organ is under constant influence of environmental factors with potentially damaging consequences for the body.

In the context of the current literature, these data show that skin Tregs display a phenotype of highly effective tissue Tregs. Suppression assays performed with skin Tregs as well as Tregs from different lymphoid and non-lymphoid tissues would reveal differences in the functional suppressive capacity of these cells. However, these experiments were technically not achievable due to the large number of animals needed.

We also investigated Tregs in the skin in a model of psoriasis-like inflammation (van der Fits et al., 2009). Like the human disease, this model is IL-23/IL-17 dependent. Unlike humans, however, dermal γδ T cells are the main IL-17 and IL-22 producers in this model (Pantelyushin et al., 2012; Van Belle et al., 2012). The data presented here show that even under homeostatic conditions these cells make up the majority of the IL-23 responsive cells, and IL-23R is further upregulated during inflammation. However, an increase in $CD4^+$ T cells, which included a highly significant rise in $Foxp3^+$ Tregs in the skin was also observed. Tregs in steady state and inflamed skin constitute more than half of all $CD4^+$ T cells. Treg phenotype and behaviour was assessed in the inflamed setting. Contrary to some data coming from blood of human psoriatic patients (Bovenschen et al., 2011), we did not observe a significant secretion of IL-17A by Tregs. However, a small but significant upregulation of RORγt was seen in these cells. RORγt has recently been described as promoting a special subset of iTregs (Ohnmacht et al., 2015; Sefik et al., 2015) and it could be speculated that a minority of Tregs might display this phenotype in the inflamed skin. However, the genes of RORγt and IL-17A were not increased in our microarray data of Tregs extracted from inflamed skin, calling into question the relevance

of this modest increase. Increased expression of GATA-3 has been observed by several groups and associated with a highly suppressive phenotype (Schiering et al., 2014; Wohlfert et al., 2011) and even though GATA-3 was expressed in most Tregs at steady state, this increased further in inflammation.

To further investigate which changes Tregs undergo during inflammation, microarray analysis on Tregs sorted from inflamed skin was performed. These Tregs displayed a distinct phenotype from the homeostatic skin Tregs. Nevertheless, upon clustering analysis they were still closer to their steady state tissue counterpart than to lymph node Tregs. Previous studies have shown that Tregs from patients suffering with psoriasis do not have a very stable phenotype and under inflammatory conditions adopt a transcription factor and cytokine profile that is associated with lower suppressive capacity (Bovenschen et al., 2011). Under these circumstances they produce IL-17A and as a consequence loose suppressive function and may contribute to inflammation. However, these data were obtained from PBMCs and hence it remains to be elucidated if this malfunction occurs in the psoriasiform skin.

We investigated if Tregs from inflamed skin upregulated genes that could suggest a destabilisation or conversion of Tregs. However, no upregulation of genes associated with effector subsets (*Tbx21* (T-bet) or *Rorc* (RORγt), *Il4, Ifng,* or *Il17a)* that have previously been associated with Treg conversion and instability was observed.

Lag3 was the most upregulated transcript, suggesting these cells are still highly capable of exerting immunosuppression as Lag3 is associated with anti-inflammatory capacity in Tregs (Do et al., 2015; Huang et al., 2004). Lag-3 has

a high affinity for MHCII and functions in part via TGF-β. Lag-3 also regulates self- and tumor-reactive $CD8^+$ T cell accumulation and function and its therapeutic blockade in the treatment of cancer is of high interest (Grosso et al., 2007; Nguyen & Ohashi, 2015). The receptor for IL-27 (*Il27Ra)* was also significantly upregulated in our data set, suggests that pathways upregulated in skin Tregs compared to lymph node Tregs at steady state are further enhanced in inflammation as *Lag3* is in part also induced by IL-27. Further investigation into the importance of the synergy between IL-27 and Lag3 in skin inflammation could be of particular interest.

Gpr15 is a homing receptor particularly for intestinal Tregs and expression on Tregs is important to control T cell mediated colitis by mediating Treg homing to the gut (Kim et al. 2013; Nguyen et al. 2014) The upregulation in the skin could imply a similar function for skin Tregs during inflammation and further experiments should explore this. CCR8 is another homing marker and has been described as a skin specific homing marker for memory T cells (McCully et al., 2012). Epidermal cells such as KC have been shown to induce CCR8 expression in human T cells (Mccully et al., 2013). We have shown earlier in this chapter that Tregs localize to the epidermis in inflammation and CCR8 dependent mechanisms could in part explain how they are recruited.

CD5 was a further surface molecule upregulated in inflammation. Recent publications have highlighted an important role for CD5 in the conversion of self-reactive $CD4^+$ T cells to Tregs (Henderson et al., 2015). Even though the majority of Tregs in the steady state skin are nTregs, such a conversion to iTregs might contribute to their increase in inflammation and this should be explored in further experiments.

The upregulated TF *Satb1* is an important determinant of T cell fate. It has been shown inhibit Treg development in splenocytes. *Satb1* was downregulated in muscle specific Tregs (Burzyn, et al. 2013). Conversely, it was also associated with a Treg signature in conventional $CD4^+$ T cells and can promote a Treg programme in $CD4^+$ T cells (Beyer et al., 2011; Fu et al., 2012). The conflicting data suggest that the function of this transcription factor is highly context dependent and requires further study.

This transcriptomic analysis showed that Tregs further upregulated molecules associated with high suppressive capacity in the inflamed skin and suggests a stable Treg phenotype in the imiquimod model of psoriasiform inflammation.

Using confocal and *in vivo* microscopy, Treg location and behaviour were visualized. In accordance with previous publications (Chow et al., 2013), Treg cells were fairly immobile at steady state. They located throughout the dermis with no apparent clustering or location preference. Considering the high level of anti-inflammatory transcripts and proteins expressed in steady state Tregs, it is likely that these cells are actively policing their surroundings via cell contact dependent and independent mechanisms.

Interestingly, during inflammation Tregs were not only highly increased, but in addition probed their surrounding more actively and also located to the upper layers of the dermis. However, to allow quantification of these minor movements, more animals will need to be imaged over a longer period of time. Tregs further migrated through the basement membrane at the dermo-epidermal junction and were frequently present in the epidermis. The dermis and the epidermis are usually well compartmentalized and, with the exception

of Langerhans cells en route to lymph nodes, migration between the two sites is uncommon. The basement membrane of the skin is a specialized layer of collagen and is a significant barrier for invading pathogens, but also for immune cells and is crucial for maintaining adequate barrier function (Breitkreutz et al., 2013). It can be speculated that $Foxp3^{+}$ regulatory T cells are being recruited towards an unknown antigen encountered in the epidermis during inflammation. LC in the skin have the capacity to promote homeostasis via activation of Tregs and LC could play a role in the Treg increase and relocation observed (Seneschal et al., 2012). However, what antigens could be presented to Tregs and how they are attracted to this location remains to be determined.

The data presented in this chapter showed that skin resident Tregs display a distinct phenotype and transcriptome under homeostatic and inflammatory conditions. We assessed the skin Tregs in the imiquimod model of skin inflammation and could not find evidence supporting a defective or impaired Treg response or instable phenotype that would contribute to inflammatory pathogenesis.

Chapter 4. Manipulation of regulatory mechanisms in skin inflammation

4.1. Introduction

Distinctive populations of Tregs have been described in several non-lymphoid organs of mice and humans. They exercise suppression through an array of mechanisms and are able to do so in lymphoid organs as well as in the target tissues (Burzyn, Benoist, et al., 2013; Campbell & Koch, 2011).

Even though more data about skin Tregs are emerging (Dudda et al., 2008; Gratz et al., 2013; Rodriguez et al., 2014; Rosenblum et al., 2011), their precise function in modulating immune responses in the skin is not yet fully understood. Tregs have been depleted in two different mouse models of allergic contact dermatitis. In both settings absence of Tregs prolonged the inflammatory process in the late stages of the elicitation phase (Lehtimäki et al., 2012; Tomura et al., 2010). This is in line with recent publications that highlight the repair functions of Tregs. In a model of muscle injury, AREG expressing Tregs were identified as key promoters of muscle repair (Burzyn, Kuswanto, et al., 2013). In a model of influenza infection, IL-18 and IL-33 from the epithelium promoted repair via AREG in Tregs. This mechanism was important for the restoration of tissue architecture and function of the lung (Arpaia et al., 2015). In the acute phase of inflammation, IL-10 derived from Tregs appears to be important in restraining skin inflammation as cell specific

deletion of IL-10 in Tregs led to increased inflammation in the acute phase of CHS. In a model of atopic dermatitis, absence of Tregs led to an increase of $CD3^+$ T cells and $CD11b^+$ DC in the lymph nodes and also in the dermis of the mice; however the mechanism was not investigated (Fyhrquist et al., 2012). Contrary to these results, depletion of Tregs in herpes simplex virus infection, a skin tropic virus that triggers acute skin inflammation, led to increased lethal outcomes and heightened viral burden (Fernandez et al. 2013). These studies highlight the importance and context-dependent functions of Tregs in the skin.

However, very little data have emerged to elucidate what mechanisms Tregs use to control skin inflammation. Especially in skin diseases with strong involvement of the IL-23/IL-17 axis such as psoriasis, the role of Tregs has been insufficiently addressed.

Tregs from the blood of psoriatic patients showed that these cells were impaired in their capacity to prevent $CD4^+$ Teff proliferation *in vitro*. The same study highlighted a negative correlation between blood Tregs and $CD4^+$ Teff (Sugiyama et al., 2005). Keijers et al. demonstrated a decrease in the Treg/Teff ratio in lesional skin of psoriatic patients that was not evident in uninvolved skin (Keijsers et al., 2013). A different study identified that Tregs were increased in psoriatic plaques; however in newly formed ‘acute’ plaques Treg numbers were significantly decreased. However, this shift was only evident in the skin as these patients showed similar Treg numbers in circulation (Yun et al., 2010). Furthermore, ex-vivo stimulated Tregs isolated from patient blood showed increased IL-17A production (Bovenschen et al., 2011) and this was confirmed in Tregs isolated from skin of affected patients (Rodriguez et al., 2014).

These studies from patients suffering with psoriasis have revealed that Tregs are functionally impaired and might be contributing to disease pathogenesis. However, these studies have not addressed the functional consequence and biological relevance of these findings.

This chapter addresses the role of Tregs in the IL-23 driven imiquimod model of psoriasiform skin inflammation. To delineate the role of $Foxp3^{+}$ Tregs in inflammation, Tregs were depleted, the $ST2^{-/-}$ strain was used and IL-10 receptor signalling was blocked by antibody administration.

4.2. Results

4.2.1. Blockade of IL-10 signalling enhances imiquimod-induced inflammation

IL-10 is a crucial mechanism by which Tregs control inflammation in many tissues (Campbell & Koch, 2011; Rubtsov et al., 2008). The microarray analysis presented in Chapter 3 revealed that IL-10 is the most upregulated cytokine in Tregs isolated from the steady state skin when compared with Tregs from the draining lymph node (Figure 3.6B). Further, IL-10 is detected in more than 1/3 of skin Tregs at homeostatic conditions (Figure 3.2B). This supports data from other tissue resident Tregs that IL-10 is a crucial mediator of immune regulation in the skin tissue.

We set out to investigate if IL-10 is a vital component of restraining inflammation in the imiquimod model of psoriasiform skin inflammation. For this, anti-IL-10Rα or control antibody (Kullberg et al., 2006) was administered *i.p.* one day prior and on day 4 of imiquimod treatment (Figure 4.1 scheme).

Ear thickness and spleen weight were significantly increased in animals treated with the blocking antibody (Figure 4.1A and C). Interestingly, $CD45^+$ cell number was not different between the two groups and neither were numbers of $CD4^+$ and $CD8^+$ T cells (Figure 4.1E). Similarly, frequency of Tregs was not significantly different between the two treated groups (Figure 4.1E). Ear thickness was increased and on closer examination, an increased thickening of the epidermis was noticed as well as increased polymorphonuclear leukocytes, most likely due to an increase in neutrophil

infiltration (Figure 4.1B). However, we did not see a significant difference between the total $CD45^+$ cell numbers after tissue digestion and FACS analysis (Figure 4.1D). This could be due to increased neutrophil cell death during the enzymatic and mechanical digestion process of the skin.

Together these data suggest that IL-10 controls imiquimod-induced inflammation.

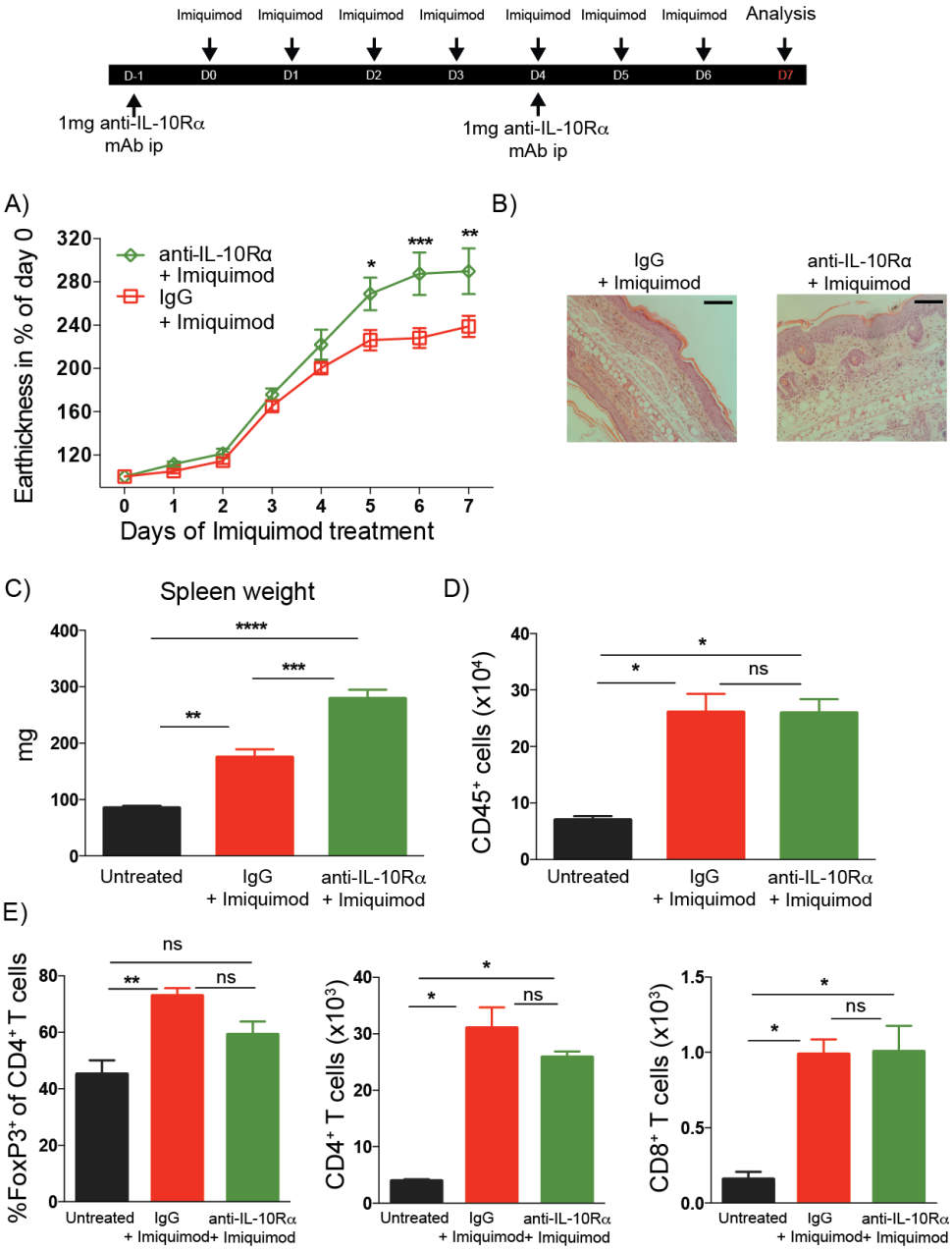

Figure 4.1. The effect of blocking IL-10Rα treatment in the imiquimod model

1mg anti-IL-10Rα blocking antibody was injected i.p. into B6 WT mice one day before and on day 4 of topical treatment. 20.8mg of Imiqimod (Aldara) was applied to each ear for 7 consecutive days. Mice were sacrificed on day 7 and organs harvested for further assessment according to schematic.

(A) Ear thickness relative to values measured on day -1
(B) Representative photomicrographs of H&E stained ear tissue
(C) Spleen weight
(D) Total number of $CD45^+$ cells extracted from the ear tissue
(E) Frequency of Tregs and total numbers of $CD4^+$ and $CD8^+$ T cells

Bars represent means; error bars SEM. Statistical significance was determined using a two-way Anova followed by Bonferroni post-hoc test (A) and Kruskal Wallis two-way analysis and Dunn's post-hoc test. Data are representative of 1 of two independent experiments (n≥ 4 each).

4.2.2. Deficiency of the IL33R ST2 does not aggravate skin inflammation

The IL-33 receptor ST2 is highly expressed in skin resident $CD4^{+}Foxp3^{+}$ T cells (Figure 3.3). Our lab and others have previously demonstrated its importance in restraining inflammation in the gut and the lung (Schiering et al. 2014; Arpaia et al. 2015). Therefore, in order to probe its importance in our model, we used ST2 deficient mice (B6 $ST2^{-/-}$ mice) and treated them with imiquimod.

Ear thickness was not different between the two groups and histologic analysis revealed a similar inflammatory pattern in the treated mice (Figure 4.2B). On flow cytometric analysis $CD45^{+}$ cells were not significantly different between the two treated groups, despite displaying a trend toward decreased numbers in the $ST2^{-/-}$ mice. However, the histological examination did not confirm this trend. $CD4^{+}$ T cells were higher in the WT treated group, though the proportion of $Foxp3^{+}$ cells was unchanged (Figure 4.2 E).

These data suggest that a global defect in IL-33R does not have an obvious impact on imiquimod-induced psoriasiform skin inflammation.

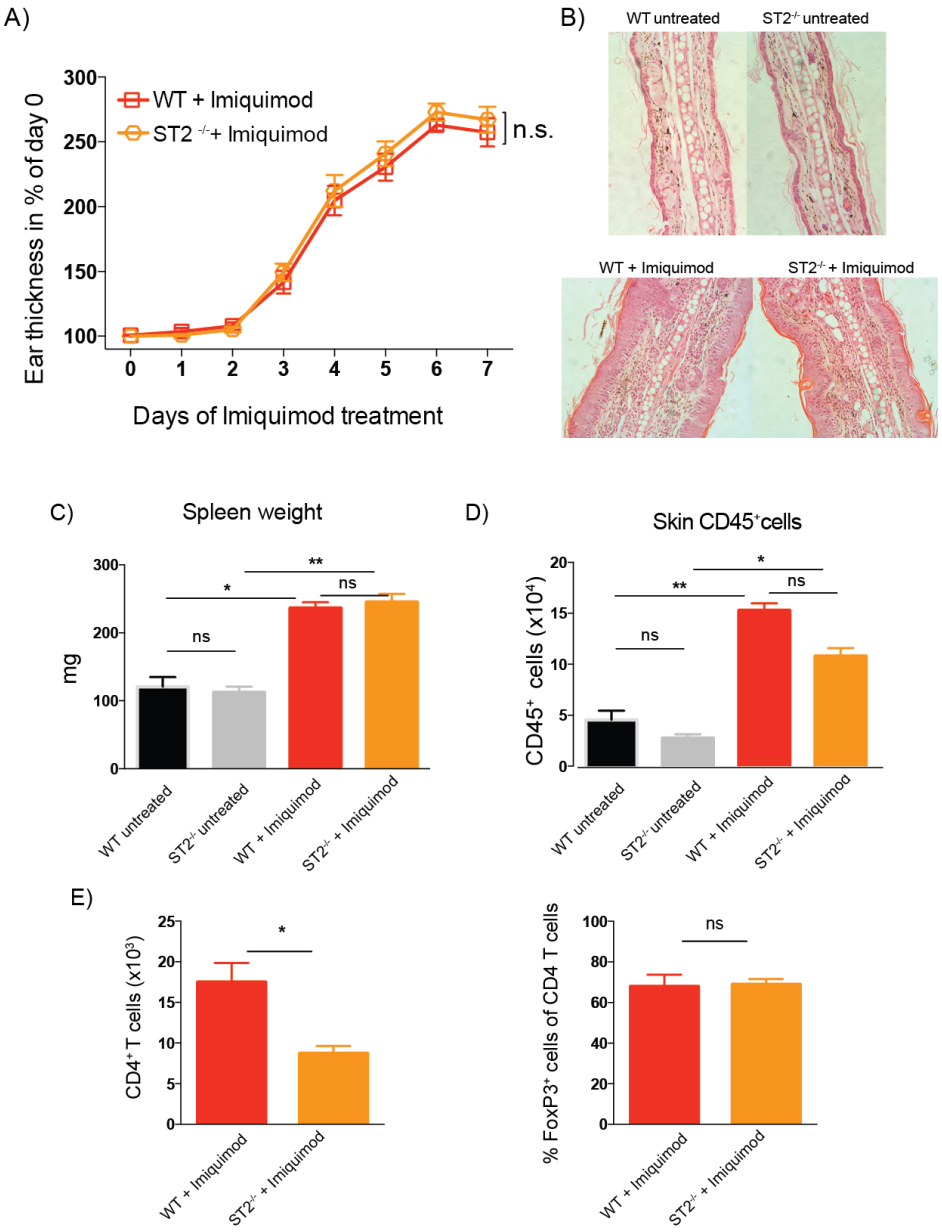

Figure 4.2. The role of IL-33R/ST2 in imiquimod-induced skin inflammation

20.8mg of Imiqimod (Aldara) was applied to each ear of B6 WT or B6 ST2$^{-/-}$ mice for 7 consecutive days. Mice were sacrificed on day 7 and organs harvested and single cell suspension obtained for further assessment.

(A) Ear thickness relative to values measured before first cream application

(B) Representative photomicrographs of H&E stained ear tissue

(C) Spleen weight of untreated and treated groups

(D) Total number of CD45^{+} cells extracted from the ear tissue

(E) Total number of tissue CD4^{+} T cells and frequency of Tregs

Bars represent means; error bars SEM. Statistical significance was determined using a two-way Anova followed by Bonferroni post-hoc test (A), Kruskal Wallis two-way analysis followed by a Dunn's post-hoc test (C,D) and Mann-Whitney U Test (E). Data are representative of 1 of two independent experiments (n≥4 each).

4.2.1. Depletion of Foxp3^{+} cells aggravates skin inflammation

In order to assess the importance of Tregs in the imiquimod model of skin inflammation we depleted these cells systemically and in the tissue. For this we utilized a Foxp3 reporter mouse (B6 Foxp3^{hCD2}), which co-expressed the surface molecule human CD2 under a Foxp3 promoter and was described in detail in Chapter 2 (Kendal et al., 2011; Komatsu et al., 2009) (see Figure 2.2). This mouse provides a reliable reporter system using methods such as flow cytometric analysis. Furthermore, Tregs in the B6 Foxp3^{hCD2} mice are readily depleted using an anti-hCD2 monoclonal antibody (YTH 655) (Figure 2.1).

Tregs were depleted by *i.v.* injection of 250µg anti-human CD2 antibody (clone YTH 655) the day before and on the day of initiation of imiquimod treatment (Figure 4.3). Further doses of anti-hCD2 antibody were administered through the intra-peritoneal (*i.p.*) route on day 2, day 4 and day 6 of imiquimod treatment. Hence, a total amount of 1 mg of antibody was administered. The control group received rat IgG2 at the same doses and via the same routes. Mice were monitored for body weight and ear thickness as well as overall well being throughout treatment. Animals were sacrificed 24 hours after the last treatment with imiquimod. After harvest, ears were digested as described in detail in Chapter 2, stained for Foxp3 and analysed by flow cytometry (Figure 4.3 scheme).

Treg number and percentage was significantly decreased in the group treated with the depleting antibody (Figure 4.3 A and B). However, we did not observe body weight loss above the imiquimod + control IgG treated group. No

difference in ear thickness and body weight in the animals that received the depleting antibody but no imiquimod was detected (Figure 4.4A and 4.5A).

Ear thickness significantly increased in animals treated with anti-hCD2 antibody after 4 days and continued to rise until sacrifice on day 7 (Figure 4.4A). At tissue harvest, it became evident that ear draining lymph node size and spleen weight were increased under topical imiquimod treatment and administration of Treg depleting antibody (Figure 4.5B).

Macroscopically the skin was characterized by increased scaling and increased scale size as well as strong erythema in the Treg depleted group when compared with IgG treated controls (Figure 4.4B). Histological examination revealed increased thickness of the entire skin (Figure 4.4C and D). Microscopically, the dermis was markedly thickened and showed a dense mixed leukocytic infiltrate and increased vascularization (open arrows). Neutrophils and lymphocytes penetrated through the basement membrane at the dermo-epidermal junction into the epidermis and the usually well-demarcated border between the two layers appeared disrupted (#) (Figure 4.4C and D). A dense infiltrate was further visible in the scales (thick arrows). The keratinocyte layers were increased and frequently elongated into the dermis and parakeratosis was observed.

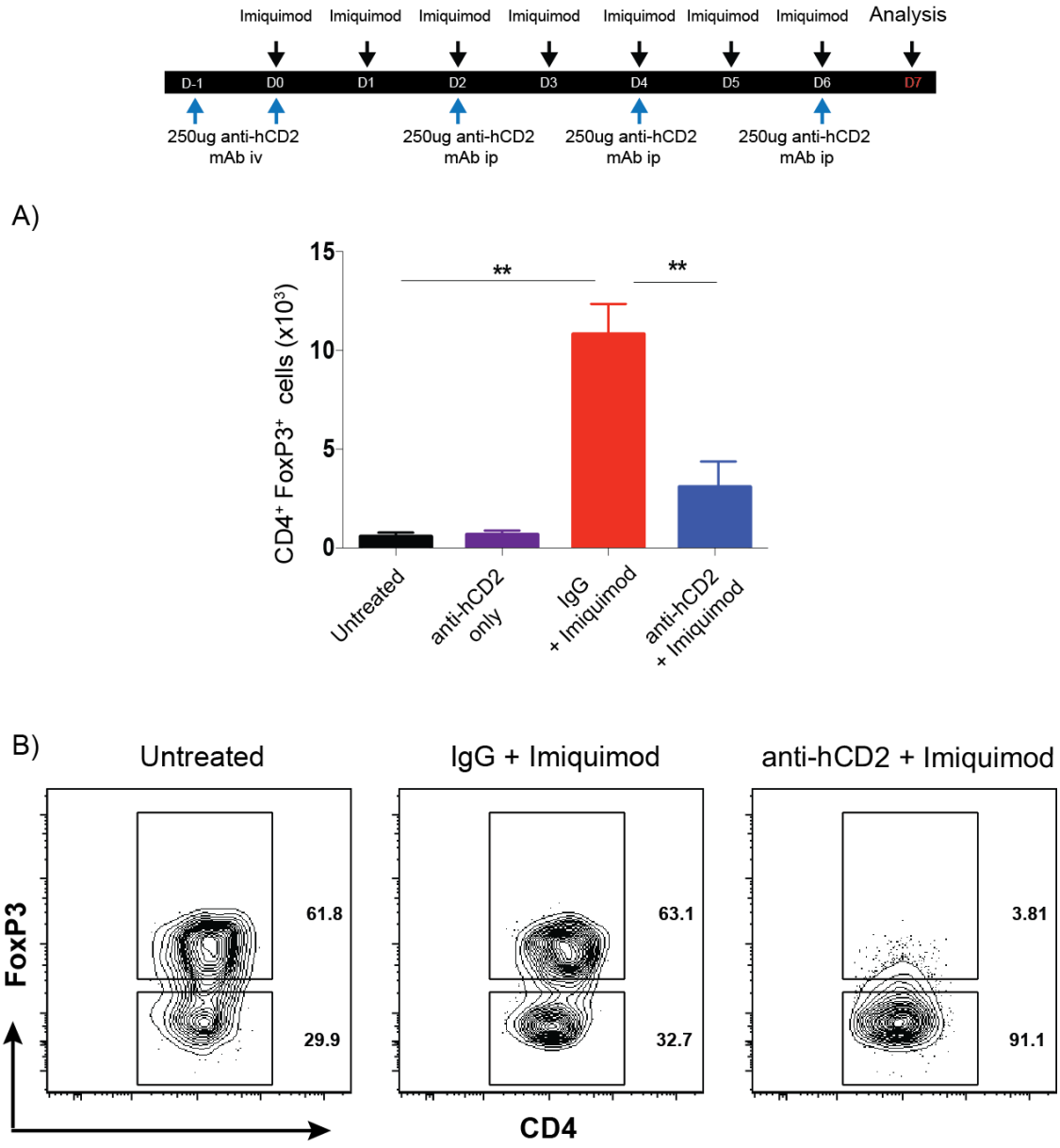

Figure 4.3. Efficient depletion of Tregs in the skin

B6 Foxp3^{hCD2} mice were injected with anti-hCD2 depleting antibody or control IgG according to scheme in figure 4.5. 20.8mg of Imiqimod (Aldara) was applied to each ear for 7 consecutive days or left untreated. Mice were sacrificed on day 7 and single cell suspension from the ear stained for surface and intracellular antibodies prior to analysis by flow cytometry

(A) Total number of Treg cells in ears

(B) Representative FACS plots showing the depletion efficiency of anti-hCD2 antibody.

Bars represent means; error bars SEM. Statistical significance was determined by Kruskal Wallis analysis followed by a Dunn's post-hoc test. Data are representative of 1 of >4 independent experiments (n≥4 each)

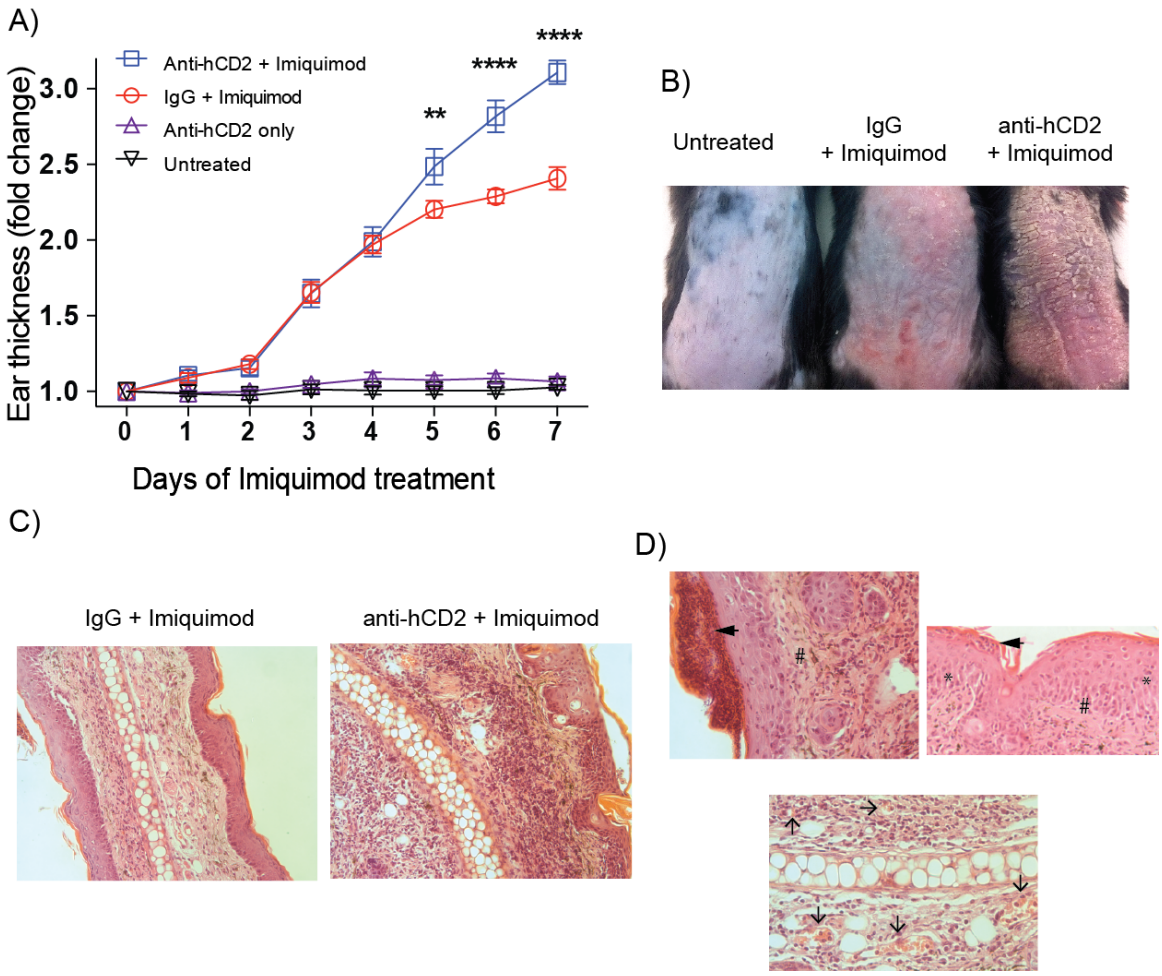

Figure 4.4. Tregs control skin inflammation

B6 Foxp3^{hCD2} mice were injected with anti-hCD2 depleting antibody or control IgG according to scheme. 20.8mg of Imiqimod (Aldara) was applied to each ear or back of mice for 7 consecutive days or left untreated. Mice were sacrificed on day 7 and organs harvested for further assessment.

(A) Ear thickness relative to values measured before first cream application

(B) Macroscopic appearance of back skin

(C) Representative photomicrographs of H&E stained ear tissue

(D) Representative photomicrographs of ears from Treg depleted mice (→ blood vessels; # leucocytes in epidermis, * spongiosis, ➔leucocyte infiltrated scales)

Bars represent means; error bars SEM. Statistical significance was determined using a two-way Anova followed by Bonferroni post-hoc test. Data are representative of 1 of >4 (A,C,D) or two (B) independent experiments (n≥ 4 each).

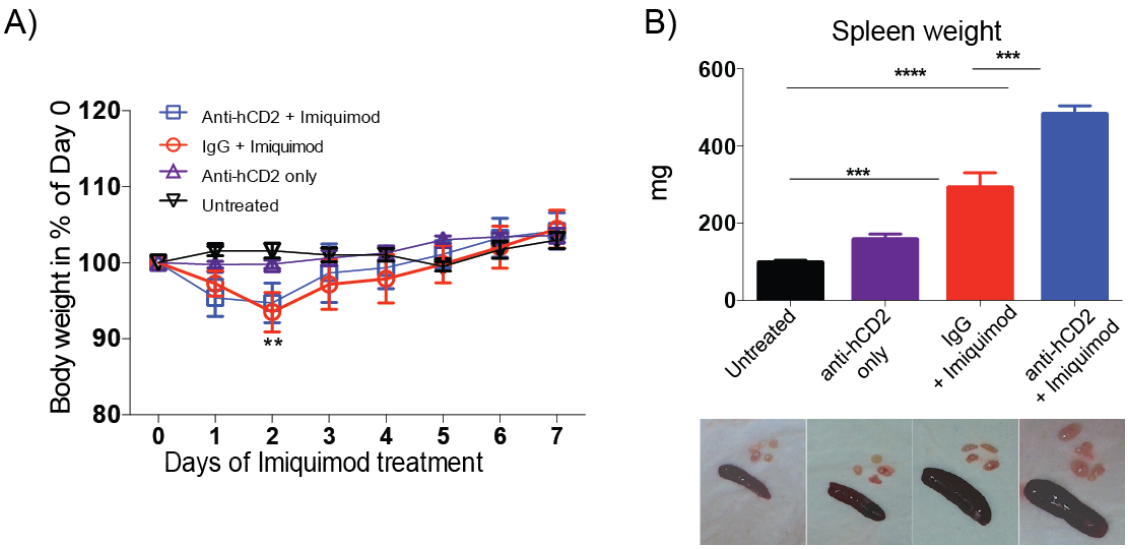

Figure 4.5. Systemic effects of Treg depletion via anti-hCD2 mAb

B6 Foxp3^{hCD2} mice were injected with anti-hCD2 depleting antibody or control IgG according to scheme in previous figure. 20.8mg of Imiqimod (Aldara) was applied to each ear or for 7 consecutive days or left untreated. Mice were sacrificed on day 7 and organs harvested for further assessment.

(A) Body weight changes relative to pre-treatment

(B) Spleen weight and macroscopic changes of spleen and ear draining lymph nodes

Bars represent means; error bars SEM. Statistical significance was determined using a two-way Anova followed by Bonferroni post-hoc test (A) or Kruskal Wallis analysis followed by a Dunn's post-hoc test (B). Data are representative of 1 of >4 independent experiments (n≥4 each).

4.2.2. Tregs control the T cell composition in skin inflammation

The cellular changes in the Treg depleted skin were further investigated by flowcytometric analysis. Reflecting the changes visualized by H&E staining in histology, we observed a significant increase in $CD45^+$ cells in the absence of $Foxp3^+$ cells (Figure 4.6A). The majority of these cells were T cells as defined by expression of CD3 (Figure 4.6B). T cells became the main leukocyte population isolated from the skin when Tregs were absent, whereas $CD11b^+$ myeloid derived cells were predominant in the IgG injected group.

Further characterization of the T cell infiltrate, showed that the majority of $CD3^+$ cells were αβ T cells. This was in contrast to the Treg replete skin, where dermal γδ T cells constitute the majority of skin T cells.

$CD4^+$ T cells and $CD8^+$ T cells made up the highest frequency and cell numbers in the Treg depleted group (Figure 4.6C). $CD4^+$ T cells increased on average 2.5-fold. $CD8^+$ T cells are only found in very low numbers in the steady state skin and do not increase significantly under imiquimod application. However, in the absence of Tregs, $CD8^+$ T cells constituted the majority of $CD3^+$ cells and underwent a more then 60-fold increase (Figure 4.6C).

γδ T cells in the imiquimod model are key drivers of inflammation and are the main source of IL-17 and IL-22 (Cai et al., 2011; Van Belle et al., 2012; van der Fits et al., 2009). As described in Chapter 3, dermal γδ T cells in the skin express RORγt and IL-23R making them efficient producers of IL-23-dependent proinflammatory cytokines (Cai et al., 2011). Interestingly, in the Treg deficient skin, dermal γδ were significantly reduced and at comparable levels to the noninflamed skin (Figure 4.6C).

Together this suggests that Tregs are crucial controllers of skin inflammation in the imiquimod model. Absence of Tregs leads to an increased inflammatory infiltrate in the dermis and epidermis. Tregs have a profound impact on the T cell composition in the tissue and appear to exert particular control over $CD8^+$ T cell accumulation in the skin.

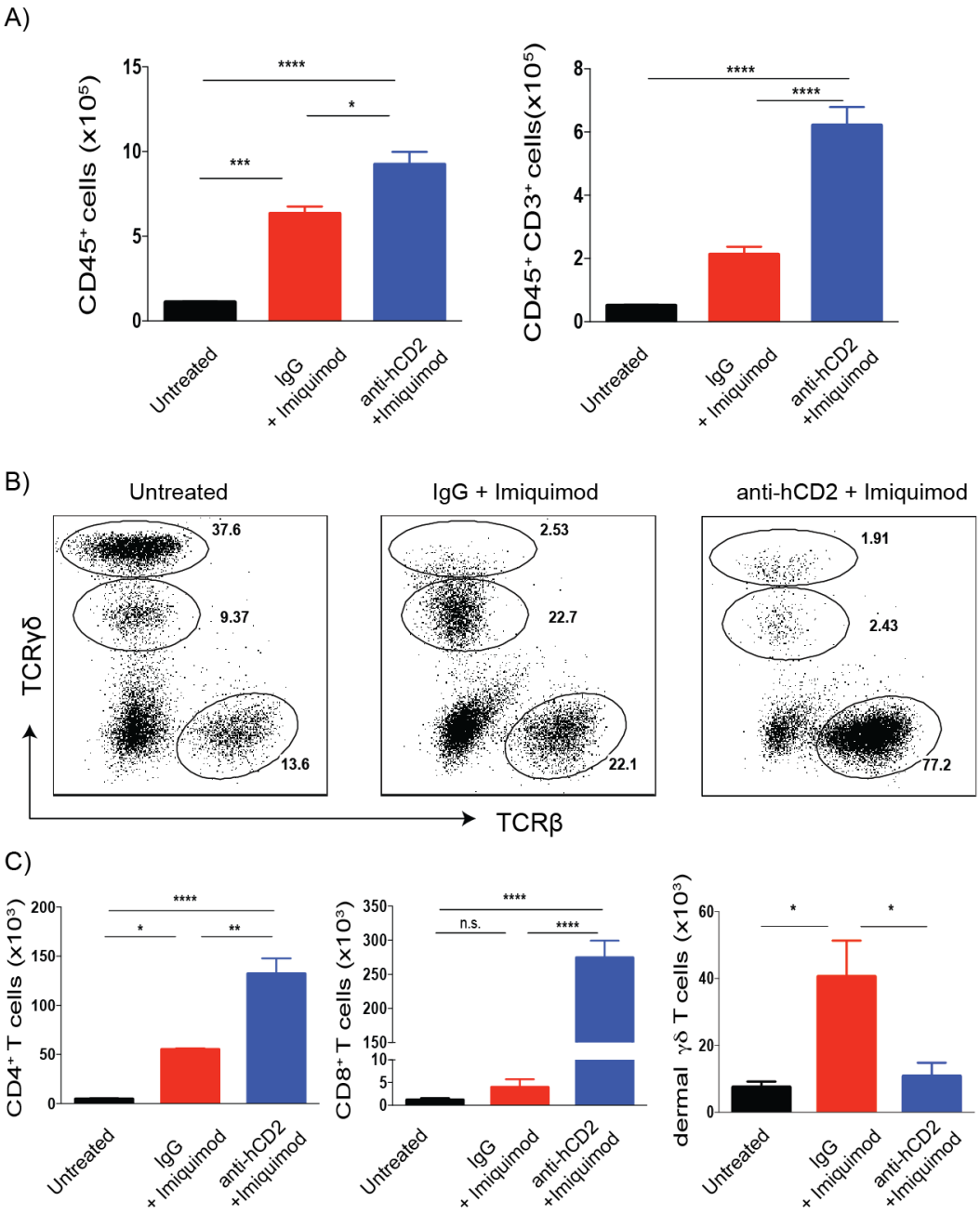

Figure 4.6. Tregs control the T cell composition of the inflamed skin

B6 Foxp3^{hCD2} mice were injected with anti-hCD2 depleting antibody or IgG control according to scheme in figure 4.5. 20.8mg of Imiqimod (Aldara) was applied to each ear for 7 days or left untreated. Mice were sacrificed on day 7 and single cell suspension from the ear stained with surface antibodies prior to analysis by FACS

(A) Total numbers of CD45$^+$ cells (left) and T cells (right) in the ears

(B) Representative plots of changes in T cell populations in Treg sufficient (centre) and deficient (right) inflamed skin

(C) Total numbers of CD4$^+$, CD8$^+$ and dermal γδ T cells in the untreated skin and inflamed skin of Treg sufficient and insufficient mice

Bars represent means; error bars SEM. Statistical significance was determined using One-way Anova with Bonferroni post-hoc test. Data are representative of 1 of ≥3 independent experiments (n≥4 each).

4.2.3. Tregs control T cell polarizing cytokines in the tissue

As shown and discussed in the previous chapter and in agreement with the literature, γδ T cells are highly responsive to IL-23 and produce IL-17 and IL-22. In contrast, $CD4^+$ Teff produce only small quantities of these cytokines in the imiquimod model. We therefore evaluated if the same cytokines were driving the excess disease in absence of Tregs.

The expression of signature genes in whole skin tissue of untreated, imiquimod with IgG treated (Treg sufficient) and imiquimod with anti-hCD2 treated (Treg deficient) animals was compared. Significantly lower *Il23a* expression in Treg deficient skin was observed (Figure 4.7). Whole tissue expression levels of *Il17a, Il17c* and *Il17f* and *Il22* decreased accordingly (Figure 4.7). Considering the possibility that the absence of Tregs might allow for a different T cell lineage to flourish and that human psoriasis is regarded a mixed Th1/Th17 driven disease, we tested for *Il12a* expression. Indeed, *Il12a* levels were significantly higher in Treg depleted skin compared to the untreated and Treg sufficient imiquimod treated group.

These data suggest that Treg cells are able to control the cytokine profile in the skin tissue. Their absence leads to an increase in IL-12 and a decrease in expression of IL-23 and IL-23 regulated cytokines such as IL-17A, IL-17C, IL-17F, and IL-22.

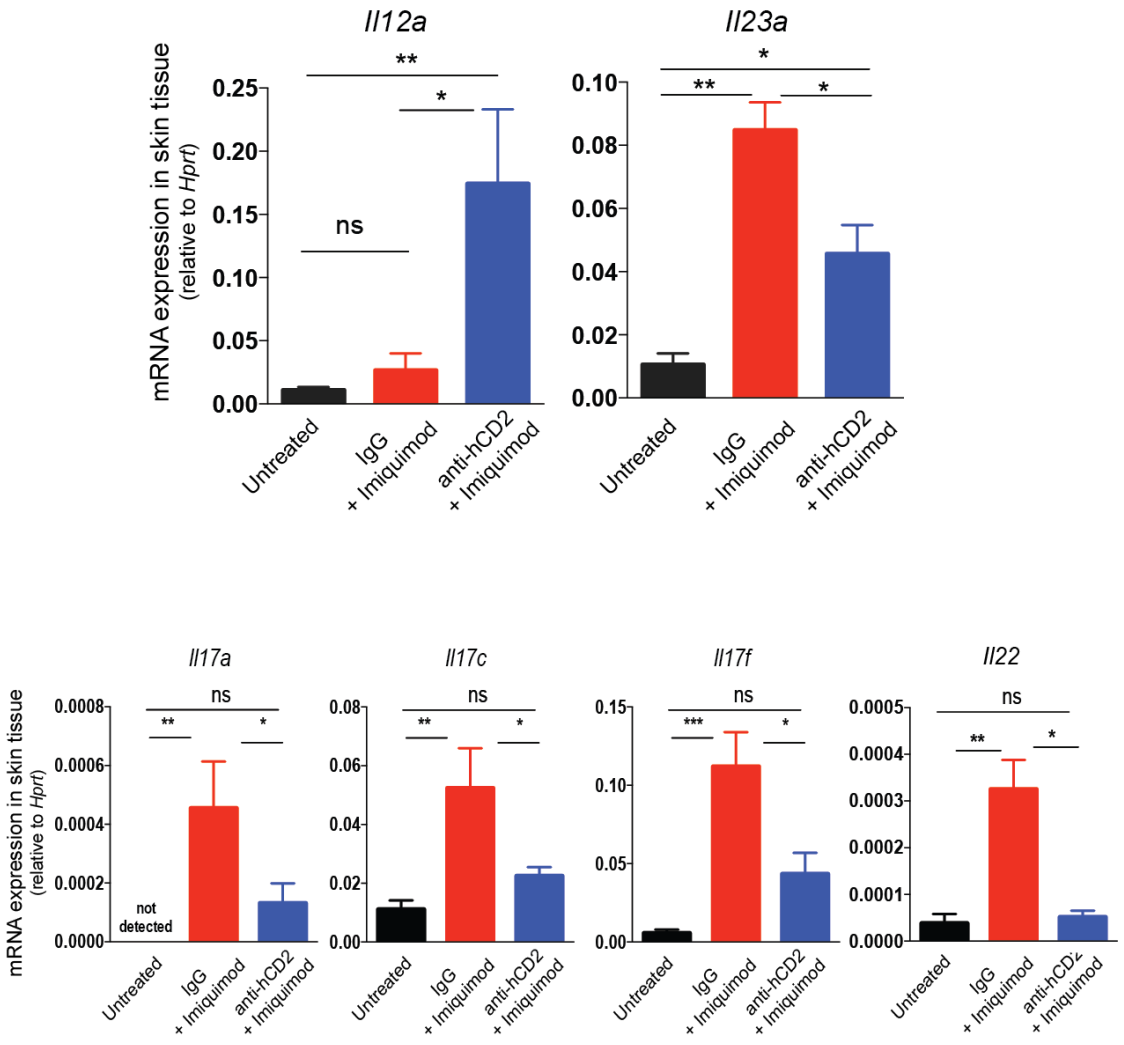

Figure 4.7. Tregs control the balance of IL-23 and IL-12 in the skin

B6 Foxp3^{hCD2} mice were injected with anti-hCD2 depleting antibody or IgG control according to scheme in figure 4.5. 20.8mg of Imiqimod (Aldara) was applied to each ear or for 7 consecutive days or left untreated. Mice were sacrificed on day 7 and RNA was extracted from ear tissue.
mRNA expression relative to *Hprt* in skin tissue of untreated and treated groups

Bars represent means; error bars SEM. Statistical significance was determined using one-way Anova with Bonferroni post-hoc test. Data are representative of 1 of 3 independent experiments (n≥4 each).

4.2.4. T-bet expressing CD8$^+$ T cells are the major source of IFN-γ

To determine the effect of changes in the IL-12 family cytokines IL-12a and IL-23 that we observed in the absence of Tregs, we analysed CD45$^+$CD3$^+$ cells from the skin. Their transcription factor and cytokine profile at the protein level was investigated using flow cytometry.

Intranuclear staining for the Th1-defining transcription factor T-bet revealed a strong positive shift of T cells in inflamed skin in the absence of Tregs, which was absent in untreated and Treg sufficient inflamed skin (Figure 4.8A). Upon closer investigation, CD4$^+$ as well as CD8$^+$ T cells were highly positive for T-bet, supporting the functional impact of increased *Il12a* gene expression observed at the whole tissue level (Figure 4.8A).

As T-bet promotes IFN-γ expression (Araújo-souza et al., 2015; Szabo et al., 2000; Szabo et al., 2002) we next investigated whether the CD4$^+$ and CD8$^+$ T cells in Treg depleted skin produced this cytokine. Indeed, both CD4$^+$ and CD8$^+$ T cells secreted high amounts of IFN-γ in the absence of Tregs (Figure 4.8B). CD4$^+$ and CD8$^+$ T cells further co-expressed TNF-α (Figure 4.8C). However, consistent with their lack of RORγt expression no secretion of IL-17A was observed (Figure 4.8B and C).

Considering the importance of TCR γδ^{dim} cells in the imiquimod model and the decreased transcription of IL-23/IL-17 genes, we examined if these cells also had a changed cytokine and/or transcription factor profile. Although present at much lower levels, TCR γδ^{dim} cells were still the main RORγt expressing T cells (Figure 4.8C). They secreted the highest amounts of IL-17A when compared to CD4$^+$ and CD8$^+$ T cells, but did not produce IL-22 (Figure 4.8B

and C). This suggests they were still able to respond to IL-23. They appear to due so in a different manner as IL-22 production declined, and are less potent in shaping the inflammatory profile (Figure 4.8C and Figure 4.6C).

In summary, these data reveal a shift in the T cell compartment of inflamed Treg depleted skin away from a majority of RORγt^{+} IL-17 and IL-22 producing γδ T cells towards a predominance of T-bet expressing, IFN-γ and TNF- α producing CD8^{+} and CD4^{+} T cells.

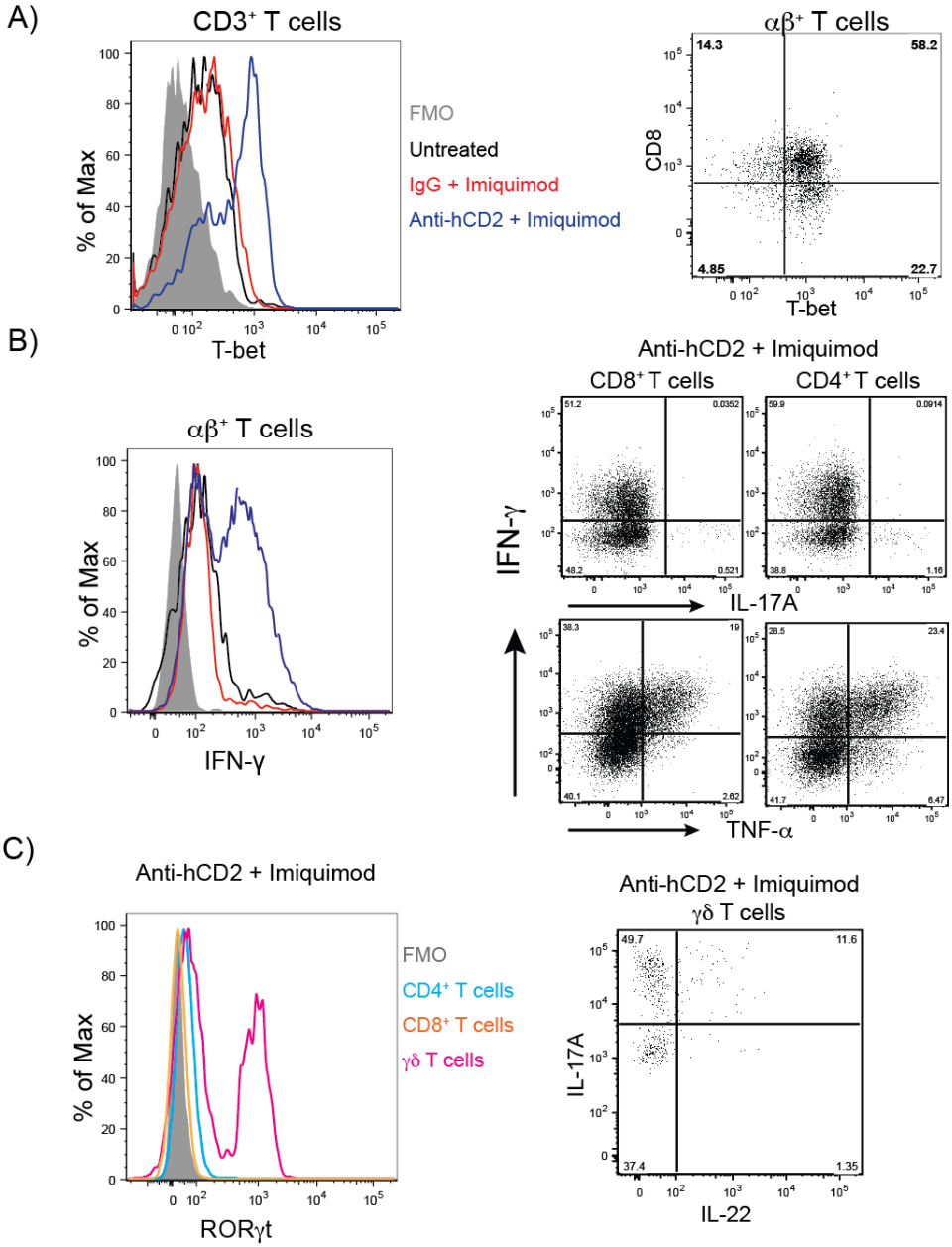

Figure 4.8. Transcription factor and cytokine profile of infiltrating T cells

B6 Foxp3^{hCD2} mice were injected with anti-hCD2 depleting antibody or IgG control according to scheme in figure 4.5. 20.8mg of Imiqimod (Aldara) was applied to each ear for 7 days or left untreated. Ears were harvested on day 7 and single cell suspension was stained with surface and intracellular antibodies prior to analysis by FACS. For cytokine staining, cells were re-stimulated for 4 hours with PMA and Ionomycin in the presence of BFA prior to staining.

(A) Expression of T-bet in total T cells (left) in various treatment groups as indicated and TCRβ$^+$ T cells (right) from the skin of Treg depleted imiquimod treated skin.

(B) Representative histogram of IFN-γ expression in total αβ T cells in various treatment groups as indicated (left) and co-expression of IFN-γ with IL-17A or TNF-α by CD4$^+$ and CD8$^+$ T cells extracted from Treg depleted imiquimod treated skin

(C) Representative histogram of RORγt by CD4$^+$, CD8$^+$ and γδ T cells (left) and FACS plot illustrating expression of IL-17A and IL-22 by dermal γδ T cells (right) from Treg depleted skin

Data are representative of 1 of 3 independent experiments (n≥3 each)

4.2.5. Identification of genes regulated by Treg cells in skin inflammation

As described in detail above, Treg depletion during skin inflammation leads to a significant shift in the Teff population. This was accompanied by a change in cytokines upstream of T cell differentiation, lineage defining transcription factors and effector cytokines (Figure 4.6, 4.7 and 4.8). In order to understand the pathological mechanisms and pathways leading to the exacerbation of tissue inflammation we aimed to further dissect the developments following Treg depletion in skin inflammation.

Therefore we used a gene expression profiling approach and performed microarray analysis on whole tissue of untreated skin and at two time points following imiquimod administration: early (day 3) and peak of inflammation (day 7). Mice were administered either Treg depleting antibody or corresponding isotype control (see scheme in Figure 4.9A).

Upon hierarchical clustering analysis across all array samples, it was apparent that the untreated samples segregated from all groups that received imiquimod treatment (Figure 4.9B). Interestingly, the groups from the early treatment time point branched off to form a separate cluster. No separation between the Treg depleted and control group was evident at day 3. This suggested a similarity in transcription profile at day 3, highlighting that Tregs mainly influence later events. The two groups from the experimental endpoint at day 7 separated into the Foxp3 deficient and sufficient group.

.

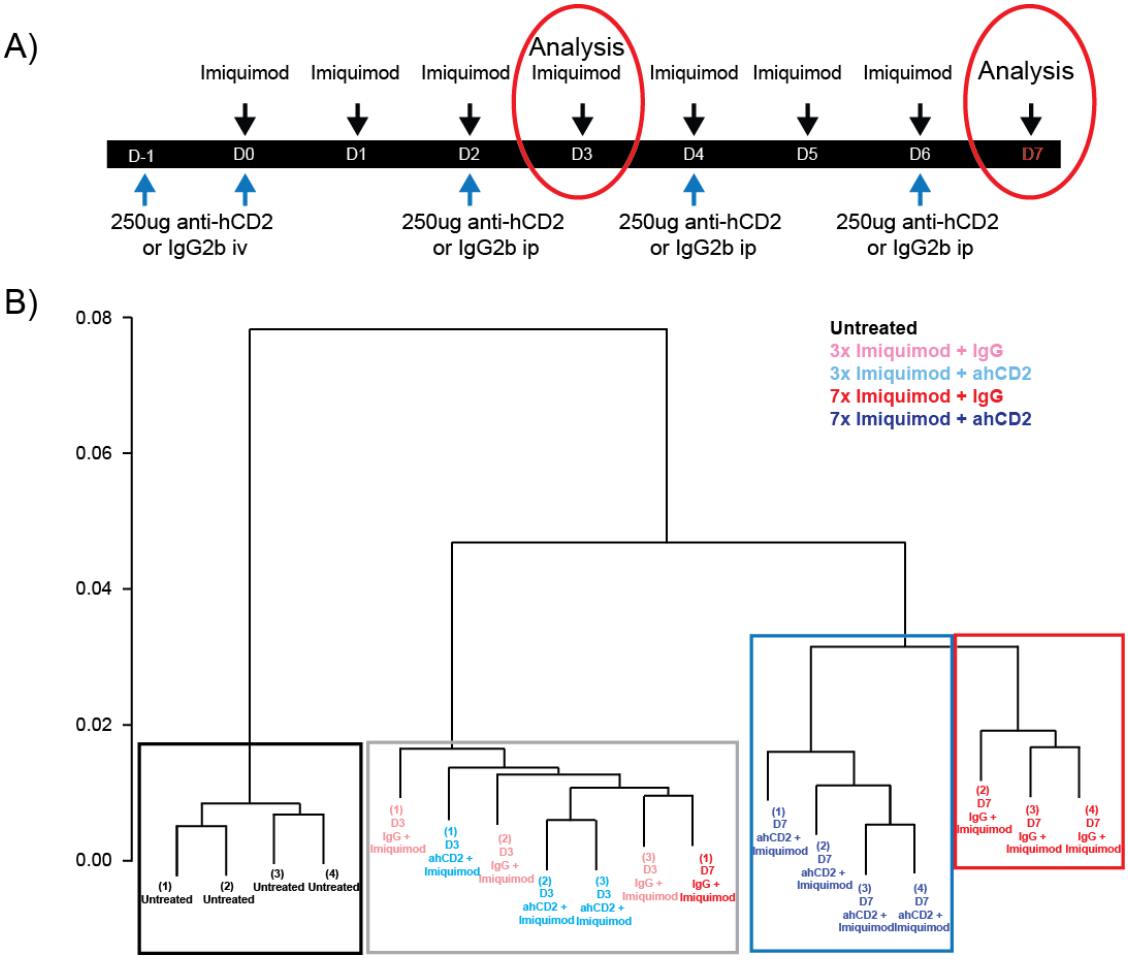

Figure 4.9. Hierarchical clustering analysis of skin tissue underlines diversity in gene expression of Treg depleted inflamed skin

Steady state B6 Foxp3^{hCD2} mice or mice treated with imiquimod for 7 consecutive days were sacrificed at 8-10 weeks of age. Lymph nodes and ears were harvested. RNA was extracted and analysed using Illumina bead arrays (details see Chapter 2)

(A) Scheme of samples analysed. (n=4, untreated and D7 groups, n=3 D3 groups)

(B) Hierarchical clustering with average linkage was performed.

(C) Principal component analysis (PCA) of gene expression from untreated skin (black) and skin harvested on day 7 from Treg depleted (blue) and Treg sufficient (red) animals

Data represents results form a single experiment (n=4, untreated and D7 groups, n=3 D3 groups). Signal intensities were background adjusted, transformed using VST and quantile normalized using Lumi (PMID:18467348) from R/Bioconductor. Differential expression analysis was performed for each contrast using the empirical bayes method in LIMMA. Significance was defined as a Benjamini Hochberg adjusted p-value < 0.05 and fold change > 2.

To identify genes and pathways controlled by Tregs in the skin, we focused on the experimental endpoint at day 7 for further analysis. Consistent with hierarchical clustering, principal component analysis (PCA) demonstrated close proximity of quadruplicates within the untreated and two inflamed groups (Figure 4.10B). However, all three groups were inherently different and located to different areas in the component analysis highlighting their unique transcriptomic signatures.

Homing in further on the differences between the inflamed skin groups, we visualized the differentially regulated genes in a volcano plot (Figure 4.10A). In order to identify relevant genes, we used a cut-off p-value of <0.05 (red circles) and a log (2) fold change of 1 (dotted line). After applying these restrictions we found 285 genes differentially regulated. Of these 272 were up- and 13 downregulated in the Treg depleted skin (Figure 4.10). These results emphasized that Tregs are indeed controlling a plethora of genes in psoriasiform inflammation.

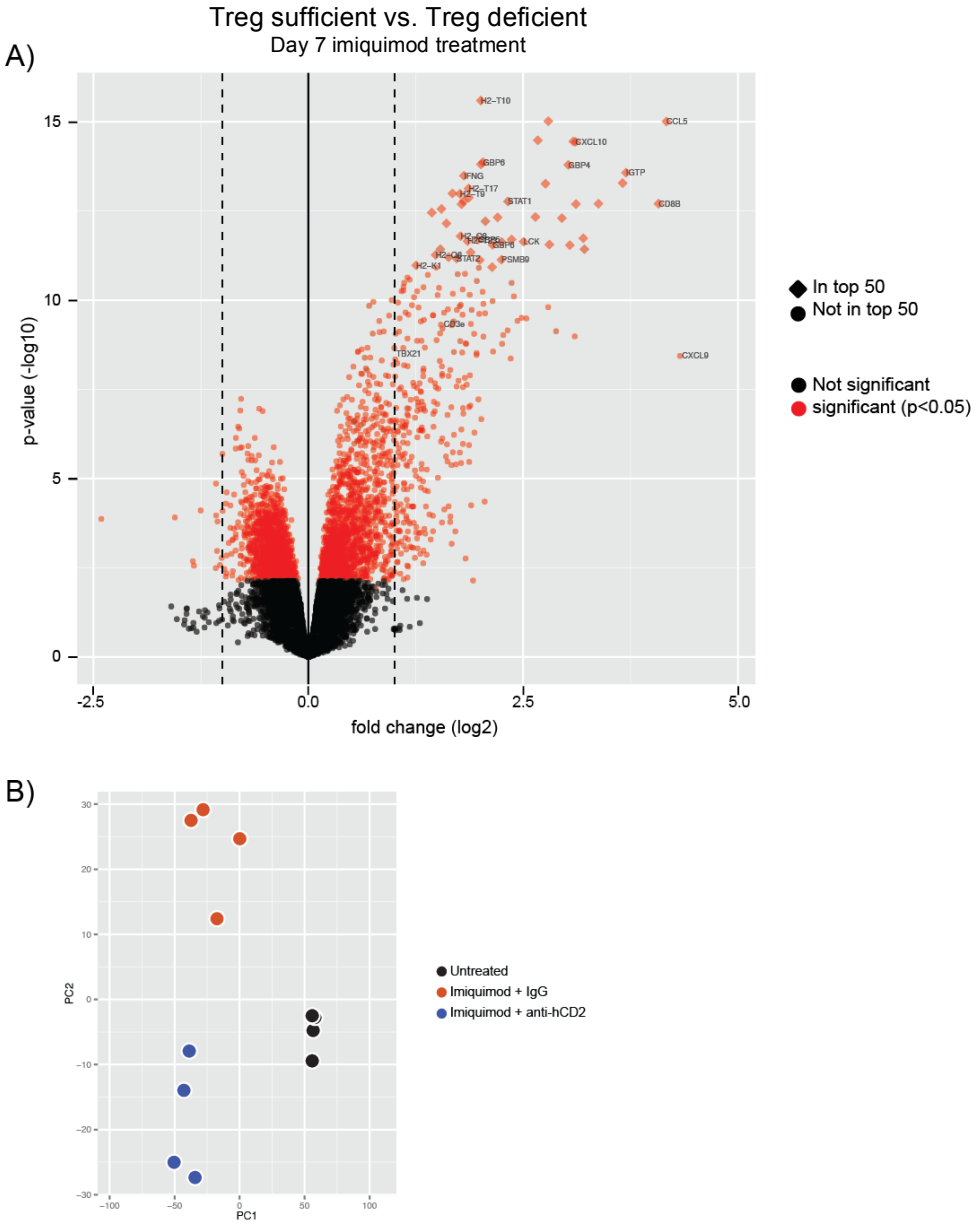

Figure 4.10. Gene expression of Treg deficient vs. Treg sufficient inflamed skin

Steady state B6 Foxp3hCD2 mice or mice treated with imiquimod for 7 consecutive days were sacrificed at 8-10 weeks of age. Ears were harvested, RNA was extracted and analysed using Illumina bead arrays (details see Chapter 2)

(A) Volcano plot illustrating differentially regulated genes at peak of inflammation (day 7) in Treg deficient vs. sufficient skin.

(B) Principal component analysis of untreated (black), day 7 treated Treg deficient (blue) and sufficient (red) groups.

Data represents results form a single experiment (n=4). Array signal intensities were background adjusted, transformed using the variance stabilizing transformation (VST) and quantile normalized using Lumi (PMID:18467348) from R/Bioconductor. Differential expression analysis was performed for each contrast using the empirical bayes method implemented in LIMMA. Significance was defined as a Benjamini Hochberg adjusted p-value < 0.05 and log fold change >1.

4.2.6. Tregs regulate interferon associated pathways in the skin

In order to facilitate interpretation of the differentially regulated genes, Gene Ontology (GO) "biological process" analysis of pathways was used. Using a cut-off of a minimum of 4 genes per search term and a FDR of <0.05 we found 70 search terms upregulated in the Treg depleted skin (Supplementary Table 5).

Strikingly, 6 pathways matched to IFN-I and interferon gamma pathways (Figure 4.11 and 4.9B). 4 of these were IFN-I specific and the most significant "Type I interferon signalling pathway" contained 24 genes (Figure 4.11C). Notably, enrichment in "positive regulation of interferon-alpha production" and "positive regulation of interferon-beta production" highlights pathways that promote the secretion of IFN-I in the skin. In a separate experiment, we confirmed enrichment of the genes *Stat1, Irf7, Isg15, Ifit1* and *Ifit2* via RT-qPCR, which are all indicative of IFN-I signalling in the tissue (Figure 4.12A) (Ivashkiv & Donlin, 2014). *Bst2,* the gene encoding CD317 also known as plasmacytoid dendritic cell antigen 1 (PDCA-1) was also among the significantly highly upregulated genes.

Importantly, the search term "positive regulation of interleukin-12 production" was also significantly induced (Figure 4.9B), underpinning a role for Tregs in the negative regulation of IL-12 in inflammation. This further confirms the data obtained by whole tissue RT-qPCR discussed earlier (Figure 4.7).

Some of the most upregulated genes were the CXCR3 ligands, *Cxcl9* (highest) and *Cxcl10* (9th highest), which are important chemoattractants of CD8^{+} T cells and associate with autoimmune diseases of the skin and clearance of skin

infections (Hickman et al., 2015; Rashighi et al., 2014; Villarroel et al., 2014). Consistent with the increase of $CD8^+$ T cells and the interferon increase, 19 genes (*H2t9, H2t10, H2t17, H2t22, H2t23, H2q2, H2q5, H2q6, H2q7, H2q8, H2m3, H2l, H2k1, H2gs17, H2eb1, H2dmb2, H2dma, H2ab1, H2aa*) of the H2 region encoding MHC class Ib molecules were upregulated, highlighting the increased presentation of self-antigens via MHC class I.

Ccl5 (Rantes) and its receptor *Ccr5* were also among the highest upregulated genes in the skin. CCL5 serves as a chemoattractant for T cells and inflammatory macrophages and highlights the proinflammatory state of the skin in the absence of Tregs (Figure 4.12B).

Further, such as *Gzmb* and *Prf1*, encoding for the $CD8^+$ T effector cell proteins granzyme B and perforin, respectively, were highly enriched. (Figure 4.12C)

The top downregulated cytokine gene was *Il17f,* further validating the results shown in Figure 4.5. To a lower magnitude, but significantly downregulated were the genes for IL-17RC and IL-17RE, both of which dimerise with IL-17RA, and form the receptors for IL-17A / IL-17F and IL-17C, respectively.

In summary, we were identified a set of pathways that are controlled by Tregs. In particular genes involved in the type I and type II interferon pathways were highly upregulated in Treg deficient inflamed mice. Interestingly these pathways have been implicated in early plaque formation of psoriasis, but their exact contribution to disease remains to be further elucidated.

A)

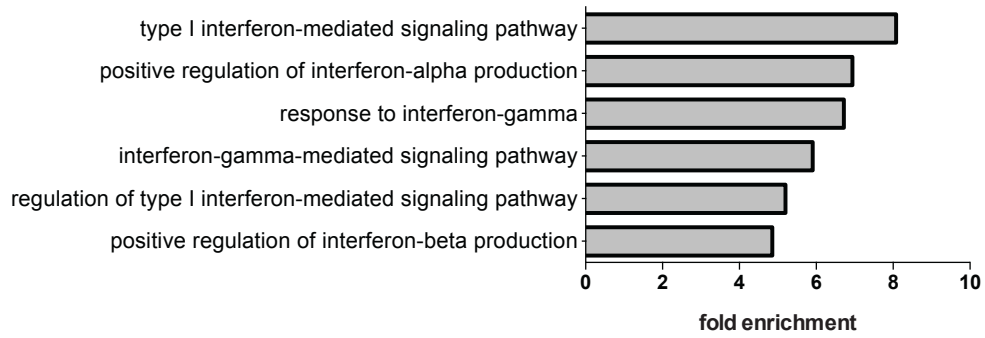

B)

GO biological process	Fold enrichment	p-value	FDR (Benjamini-Hochberg)
type I interferon-mediated signaling pathway	8.08	0.0000000000000001	0.0
positive regulation of interferon-alpha production	6.94	0.0003111700000000	0.010268
response to interferon-gamma	6.72	0.0000228500000000	0.00125
interferon-gamma-mediated signaling pathway	5.91	0.0000000001050700	0.0
positive regulation of interleukin-12 production	5.2	0.0015958000000000	0.036362
regulation of type I interferon-mediated signaling pathway	5.2	0.0015958000000000	0.036362
positive regulation of interferon-beta production	4.86	0.0002968800000000	0.010268

C)

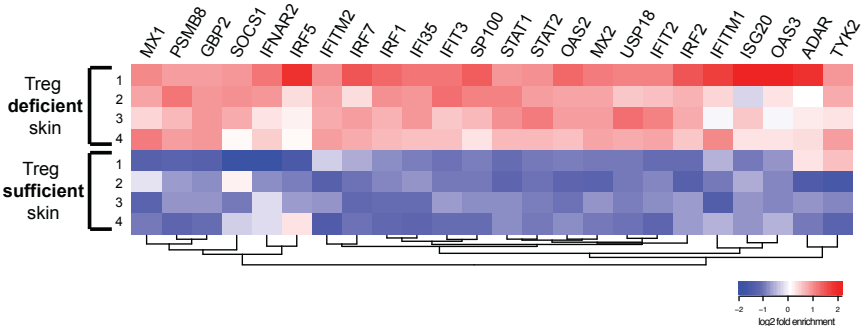

Figure 4.11. Interferon mediated pathways are enriched in Treg depleted skin

B6 Foxp3^{hCD2} mice received anti-hCD2 or isotype antibody and were treated with imiquimod for 7 consecutive days. Ears were harvested; RNA was extracted and analysed using Illumina bead arrays (details see Chapter 2).

(A) Interferon mediated processes enriched in Treg deficient skin. Ranked according to fold-enrichment and FDR

(B) Fold enrichment, adjusted p-value and false discovery rate (FDR) of enriched interferon processes

(C) Heat map of genes upregulated in the individual skin samples of Treg depleted mice that were assigned to the “type I interferon-mediated signaling pathway”

Enriched Gene ontology (GO) biological processes were assessed in differentially abundant gene sets using a hypergeometric test implemented in the runGO.py script from the CGAT code collection (PMID:24395753) and terms were considered significant at a false discovery rate (FDR) < 0.05.

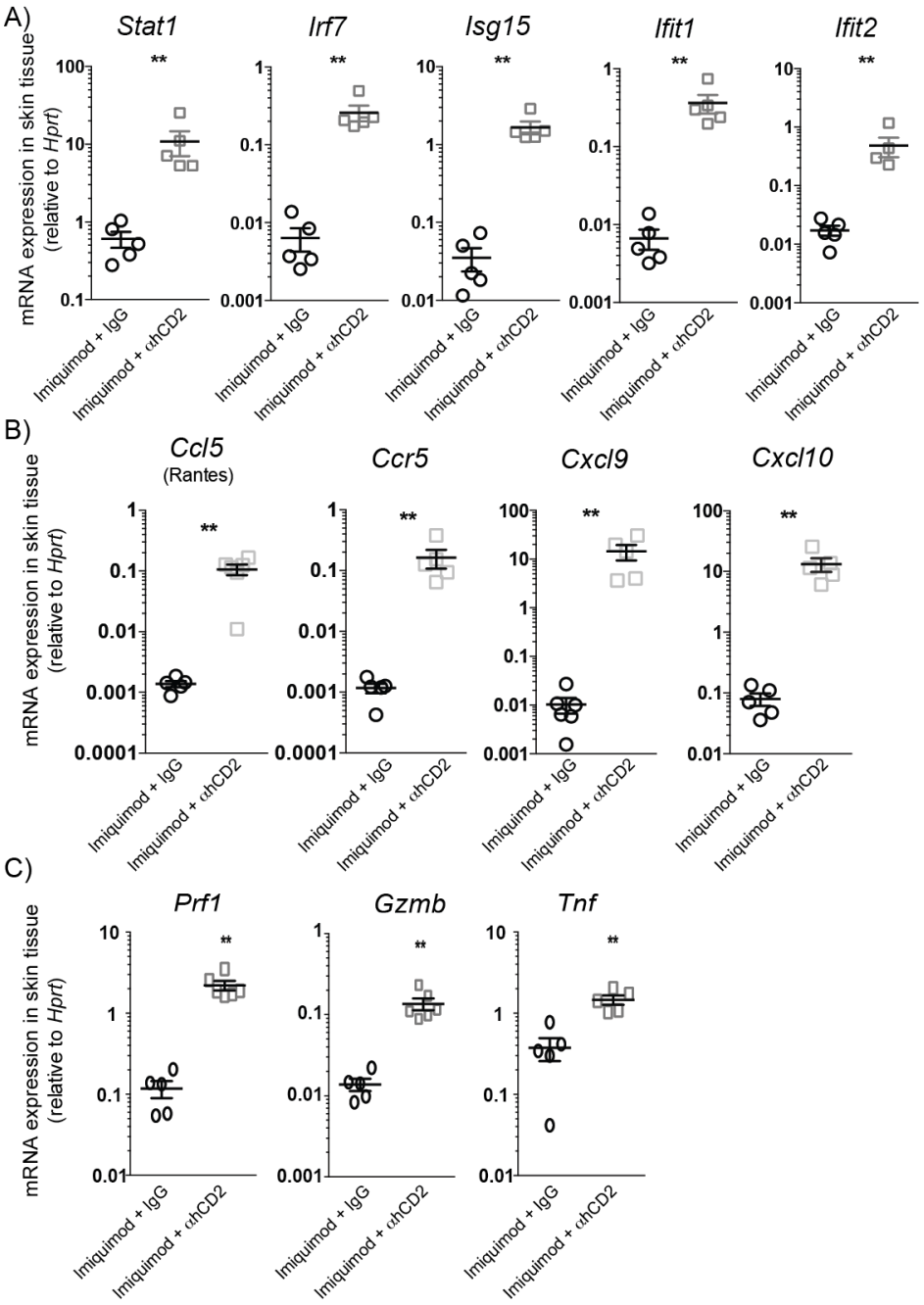

Figure 4.12. RT-qPCR validation of selected genes in Treg depleted inflamed skin

B6 Foxp3^{hCD2} mice received anti-hCD2 or isotype antibody and were treated with imiquimod for 7 consecutive days. Ears were harvested; RNA was extracted and assayed by RT-qPCR.

(A) IFN-I signaling genes in Treg sufficient (black circles) and Treg deficient (grey squares) inflamed skin

(B) Genes of chemokines and receptors in Treg sufficient (black circles) and Treg deficient (grey squares) inflamed skin

(C) Genes encoding Perforin, Granzyme B and TNF-α in Treg sufficient (black circles) and Treg deficient (grey squares) inflamed skin

Bars represent means; error bars SEM. Statistical significance was determined using a Mann-Whitney U Test. Data represents results from ≥2 experiments (n=5 each)

4.2.7. Treg depletion leads to increased IFN alpha secretion

One of the most striking findings of the skin microarray analysis was the upregulation of various pathways involved in IFN-I secretion and action, suggesting that Foxp3$^+$ T cells are involved in their regulation. In order to address how Tregs are impacting this potent proinflammatory pathway, we set out to investigate the source of IFN-I in the skin.

Various cell types are capable of making IFN-I; however plasmacytoid DC (pDC) are capable of producing very large amounts on a per cell basis. pDC have previously been identified as early inducers of inflammation in the skin of psoriasis patients (Nestle et al., 2005). Studies have shown that in the imiquimod model of skin inflammation depletion of pDC does not change any parameters of the disease and that they were not found in the affected areas of murine skin (Wohn et al., 2013). These cells are absent from the skin under homeostatic conditions in mice in humans, but appear to contribute substantially to wound healing responses in the skin (Gregorio et al., 2010). Intriguingly, interferon alpha and pDC play a role in early initiation of psoriasis and their absence prevented plaque development (Nestle et al., 2005).

In our microarray data, the pDC marker (PDCA-1) encoding gene *Bst2* was significantly upregulated in the Treg depleted tissue when compared to IgG treated controls. pDC can directly secrete CCL3 and CCL4 as well as CXCL10 (Swiecki & Colonna 2015), all of which were upregulated in Treg deficient inflamed skin. Considering the changed inflammatory phenotype in the absence of Tregs, we investigated whether pDC have infiltrated the skin and act as a source for IFN-I. As seen in Figure 4.19, we were able to identify pDC

in the skin draining lymph nodes of all three groups (representative IgG + imiquimod group shown in Figure 4.13A) by gating on $CD45^{+}CD19^{-}Ly6G^{-}CD11b^{-}CD11c^{int–high}$ cells and then using PDCA-1 and Siglec H as pDC specific markers (Zhang et al., 2006). However, pDC were not found in the skin of Treg depleted and imiquimod treated animals or in either of the other two groups (Figure 4.13A). Further, we were also unable to identify pDC using antibodies against B220 in place of Siglec H.

In order to identify IFN-I producing cells, we cultured single cell suspensions from the skin draining lymph nodes for 4 hours in the presence of BFA and stained for IFNα. IFNα production was mainly detected in the Treg depleted lymph nodes, but very few cells stained positive in Treg replete skin draining lymph nodes and no positive signal was detected in untreated lymph nodes (Figure 4.13B). All $IFN\alpha^{+}$ cells were $CD45^{+}$ and, interestingly, PDCA-1 as well as Ly6C was preferentially expressed in the $IFN\alpha^{+}$ cells compared with the $IFN\alpha^{-}$ population (Figure 4.13B). The interferon producing cells were also negative for Siglec H, highlighting that pDC are not the source of IFN-I in this model (Figure 4.13C).

Macrophages can secrete significant amounts of IFNα and β in inflammatory settings and can be a substantial contributor of these in virus and parasite infected tissues (Ivashkiv & Donlin, 2014). As described above, the cells secreting IFNα expressed high levels of Ly6C, highlighting a potential contribution of monocytes and monocyte-derived cells to IFN-I.

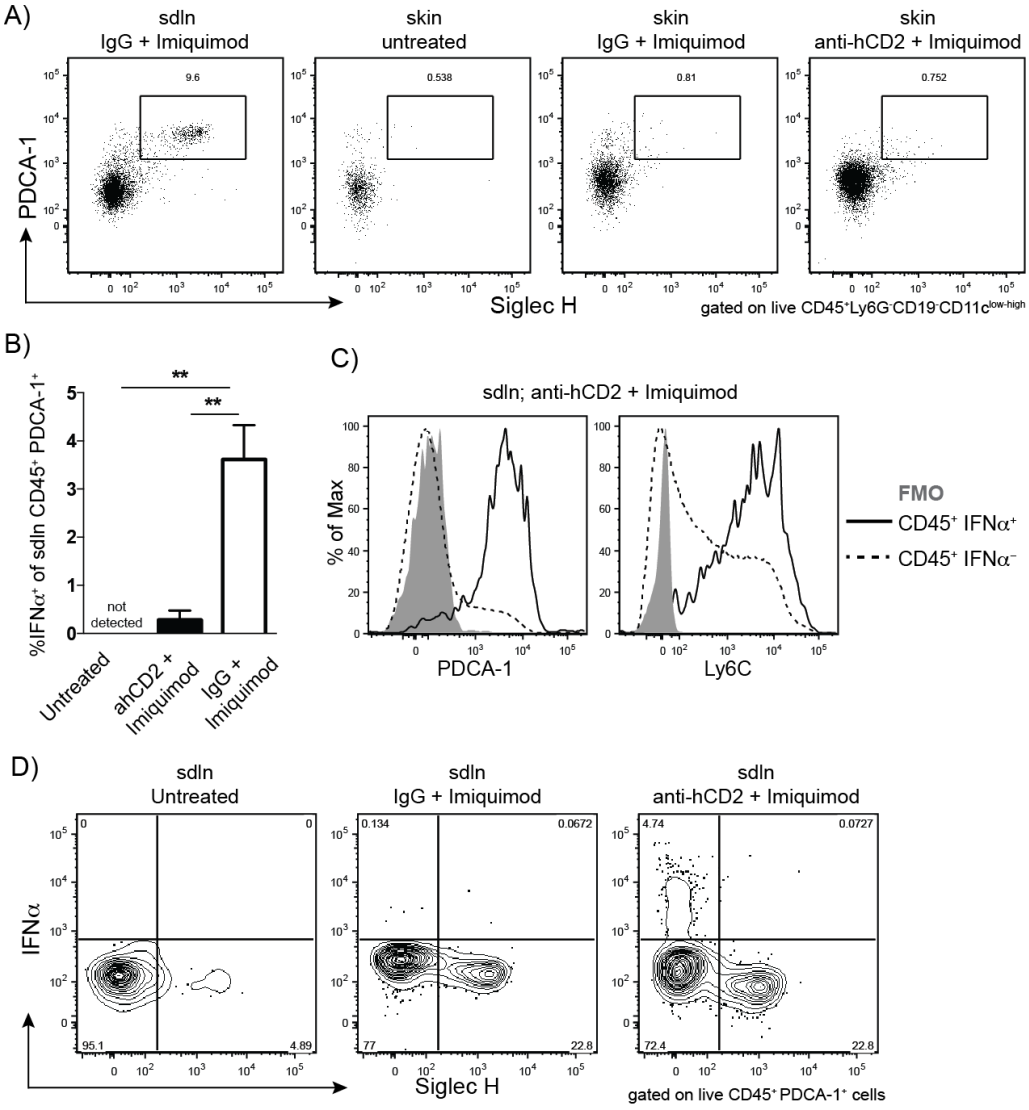

Figure 4.13. pDC and IFN-α secreting cells in the skin and lymph nodes

B6 Foxp3^{hCD2} mice were injected with anti-hCD2 depleting antibody or IgG control according to scheme in figure 4.5. 20.8mg of Imiqimod (Aldara) was applied to each ear for 7 consecutive days or left untreated. Mice were sacrificed on day 7 and single cell suspension from the ear and lymph nodes was stained with surface antibodies prior to analysis by FACS. For cytokine staining, lymph node cells were cultured for 4 hours in the presence of BFA prior to antibody staining.

(A) Representative FACS plot for pDC in skin draining lymph node (far left) and skin of mice undergoing treatment as indicated above the plot

(B) Frequency of IFNα$^+$ cells in the draining lymph nodes of respective groups.

(C) Representative histograms of PDCA-1 and Ly6C expression in CD45$^+$ IFNα$^+$ cells from the draining lymph node of Treg depleted imiquimod treated mice

(D) Representative FACS plots of IFNα$^+$ cells isolated from draining lymph nodes.

Bars represent means; error bars SEM. Statistical significance was determined using one-way Anova with Bonferroni post-hoc test. Data represent two independent experiments (n≥5 each).

4.2.8. PDCA-1^{+} inflammatory macrophages are increased in the absence of Tregs

We investigated if monocytes and monocyte-derived cells were changed in the tissue. In the skin it is particularly difficult to distinguish between monocytes, inflammatory macrophages and monocyte derived DC. In the steady state skin, very few macrophages are found and CD11b^{+} DC dominate the myeloid population. Malissen and colleagues proposed a gating strategy allowing the differentiation between these groups (Tamoutounour et al. 2013). Here, we use a similar gating strategy by first excluding dead cells and doublets and gating on CD45 expressing cells excluding B-cells and neutrophils for further analysis (Figure 4.14A). We then selected CD11b^{+}, CD64$^{low\text{-}high}$ and Ly6C$^{low\text{-}high}$ cells. The resulting population was divided into three subpopulations P1-P3: Ly6C^{high}MHCII^{-} (P1), Ly6C^{+}MHCII^{+} (P2) and Ly6C^{-}MHCII^{+} (P3), representing recently extravasated monocytes (P1), inflammatory monocytes (P2) and monocyte derived DC (moDC) (P3).

The overall population of mononuclear phagocytes is significantly increased in the imiquimod model, though this was not further increased in the absence of Tregs (Figure 4.14B). However, the distribution within this population was significantly altered. P1 was significantly decreased when Tregs were absent and was accompanied by a significant increase in inflammatory monocytes, suggesting an accelerated maturation process of extravasated monocytes to inflammatory monocytes (Figure 4.14C). Overall, moDC are proportionally reduced in imiquimod-induced inflammation in Treg deficient as well as sufficient animals.

When anti-hCD2 antibody and imiquimod was administered, all three populations expressed PDCA-1 at a higher level than their counterpart in Treg sufficient animals.

Taken together these data suggest that pDC are not the cell population responsible for IFN-I signature in the absence of Tregs. However, our data support the notion that the absence of Tregs allows inflammatory monocytes and macrophages to adopt a more proinflammatory phenotype and potentially become a source of IFN-I, driving excess inflammation.

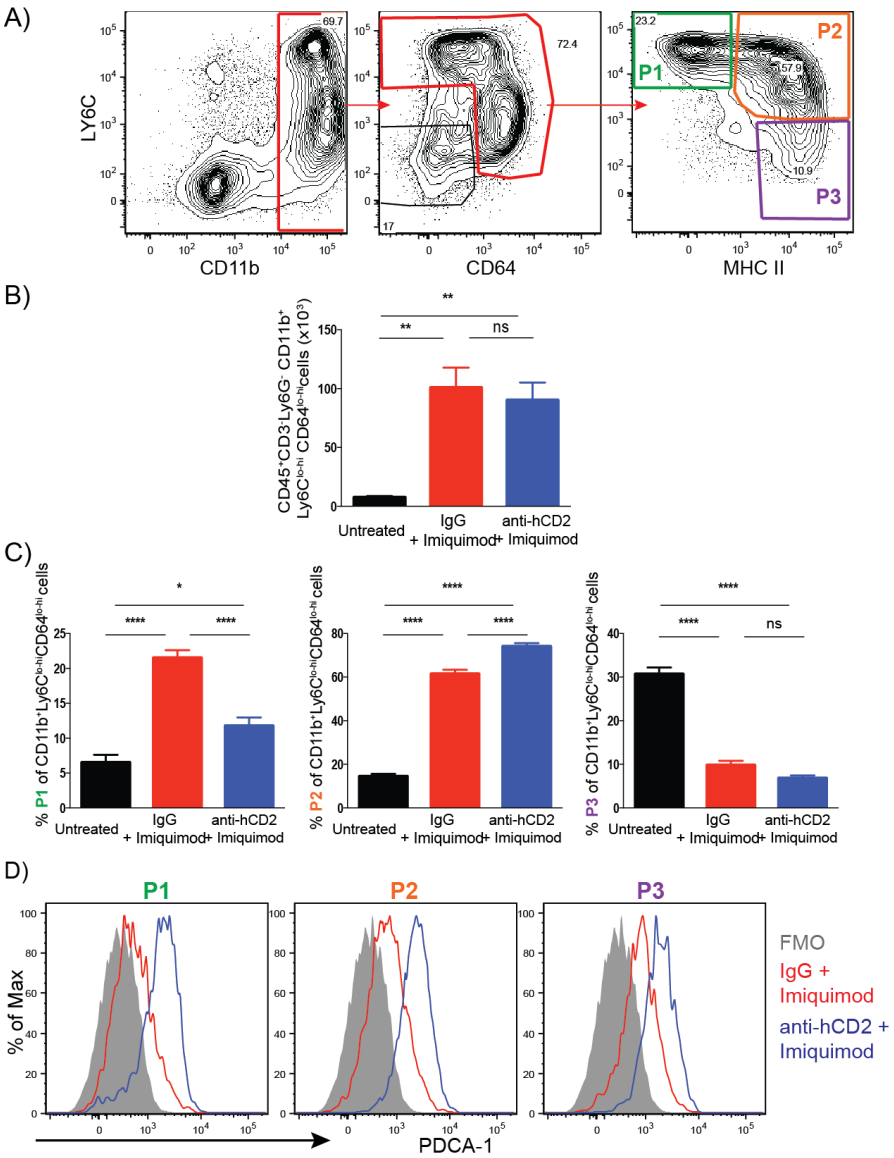

Figure 4.14. Activated macrophages are increased in Treg depleted skin

B6 Foxp3^{hCD2} mice were injected with anti-hCD2 depleting antibody or IgG control according to scheme in figure 4.5. 20.8mg of Imiqimod (Aldara) was applied to each ear for 7 consecutive days or left untreated. Mice were sacrificed on day 7 and single cell suspension from the ear and lymph nodes was stained with surface antibodies prior to analysis by FACS.

(A) Gating strategy for mononuclear phagocytes in the skin after exclusion of neutrophils (Ly6G), B-cells (CD19) and T cells (CD3)

(B) Total numbers of monocytes/macrophages in the skin

(C) Frequency of monocyte-derived populations in the skin (P1-P3 as per A)

(D) Representative FACS plots of PDCA-1 expression in monocyte-derived populations (P1-P3 as per A)

Data represent means; error bars SEM. Statistical significance was determined using one-way Anova with Bonferroni post-hoc test. Data representative of 3 experiments (n≥4 each)

4.2.9. IFN-I signature is confined to the skin tissue

We tested IFN-I signatures in the lymph node, to probe if an IFN-I signature was evident in the draining lymph node at various times in the inflammatory process or if it was confined to the inflamed tissue.

We observed that several genes associated with an IFN-I response such as *Stat1, Irf7, Isg15* and *Ifit2* were not significantly induced at any of the investigated time points (day 3, day 5 and day 7) (Figure 4.15). However, we did see an increase in *Ifng* and *Tbx21* mRNA, confirming an increase in Th1/Tc1 responses also present in the lymph node (Figure 4.15). These data suggest that the impact of IFN-I signalling is mainly confined to the skin tissue and does not extend to the draining lymph nodes. Simultaneously, an increase of genes indicative of Th1 and Tc1 cells is evident in the draining lymph nodes.

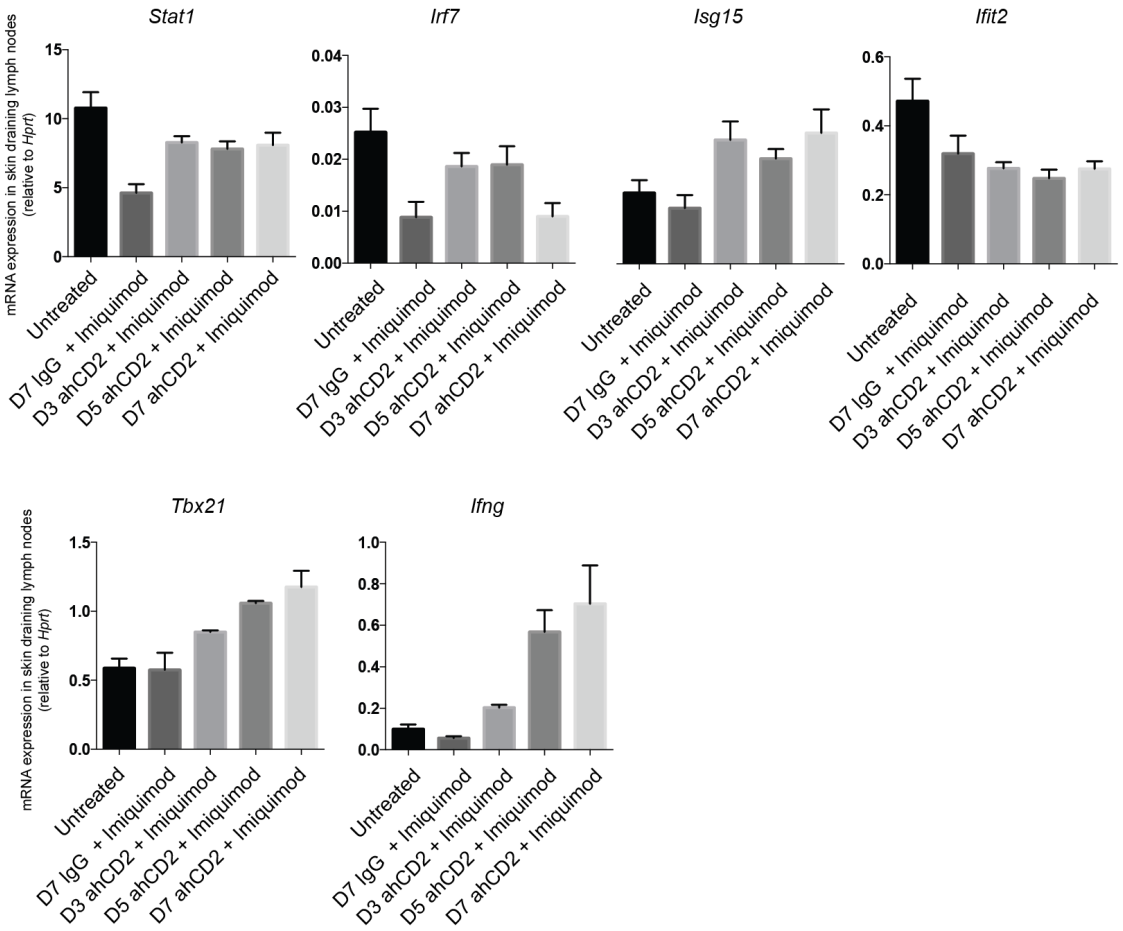

Figure 4.15. A IFN-I signature is not evident in the skin draining lymph nodes

(A) IFN-I regulated genes in the draining lymph node of untreated, day 7 Treg sufficient mice and day3, day 5 and day7 of Treg deficient mice when treated with imiquimod

(B) Th1/Tc1 defining transcription factor and cytokine in the draining lymph node.

Data represent means; error bars SEM. Data are representative of one single experiment (n=4).

4.3. Discussion

The mechanisms through which Tregs regulate inflammatory responses are not very well defined. In this chapter we addressed how Tregs are regulating the immune response in the skin by using the imiquimod-induced model of psoriasiform inflammation.

A cell depletion approach was used to address the role of Tregs. Throughout this chapter we utilized an antibody dependent depletion method in the B6 Foxp3^{hCD2} reporter mouse (Kendal et al., 2011). This mouse provides a reliable reporter and depletion system via hCD2 expression in Tregs. It has several advantages over the frequently published depletion system of Tregs through diphtheria toxin (DTx) and its receptor (DTR). DTx is injected in mice harbouring a Foxp3 bacterial artificial (BAC) driven transgene encoding DTR (DEREG) or DTR equipped with an internal ribosome entry site (IRES) in the translated Foxp3 region (Kim et al., 2007; Lahl et al., 2007). Even though these mice are very useful and widely utilized, the resulting spontaneous systemic immunopathology in these mice is often severe and restricts the use of this model as the mice develop severe multi-organ inflammation within a few days. The antibody dependent depletion of Tregs via hCD2 does not spontaneously show these severe effects as rapidly and has been used for several weeks in previous studies (Kendal et al., 2011).

The conducted experiments revealed that Tregs are crucial for dampening inflammation in the imiquimod model. In animals lacking Tregs the overall ear

thickness was increased and was significantly higher from four days after initiating imiquimod treatment until tissue harvest on day 7. Leukocyte influx was significantly increased in the absence of Tregs causing additional dermal and substantial epidermal infiltration. Treg depletion further led to increased systemic inflammation as shown by increased spleen weight and lymph node size.

A significant increase in the $CD3^+$ population was the most striking finding upon investigation of the skin infiltrate by flow cytometry. Upon further examination we found a highly significant increase in $CD8^+$ T cells and, to a significant but lesser extent, also $CD4^+$ T cells in the skin tissue. Interestingly, the isolated αβ T cells secreted large amounts of IFN-γ and TNF-α expressed the Th1/Tc1 transcription factor T-bet but did not produce IL-17A. In turn γδ T cells were significantly decreased in the absence of Tregs. The imiquimod model is strongly dependent on IL-23 and γδ T cells constitute the main source for the pathogenic IL-17 and IL-22 (Van Belle et al., 2012; van der Fits et al., 2009). Two reports have shown that $CD4^+$ $Foxp3^+$ T cells are capable of restraining responses in γδ T cells. One study investigated human Vδ2 T cells (Mahan et al., 2009) and the other colonic mouse γδ T cells (Yurchenko et al., 2011). Both investigations showed a Treg mediated suppression of IFN-γ production by these invariant T cells, and in the mouse model an additional reduction in IL-17A production was observed.

Our data demonstrate that the absence of Tregs clearly promotes an inflammatory response featuring high levels of T cells in lesional skin. However, in the absence of Tregs, γδ T cells remained at levels found in steady state skin and this finding was in stark contrast to the increase

observed in Treg sufficient inflamed skin. This highlights that Tregs in the skin are not primarily controlling the dermal γδ T cell response in the imiquimod model.

The increase in Th1/Tc1 cells that we observed in Treg depleted inflamed skin prompted closer investigation of Teff differentiating cytokines. In accordance, *Il23a* was decreased and *Il12a* significantly increased in the Treg deficient inflamed skin. These results highlight a distinct regulatory potential of Tregs in the skin with a preference for restraining Th1/Tc1 responses or their initiating cytokines.

Transcriptomic analysis of whole skin tissue was used to aid in the identification of genes and pathways that Tregs are controlling in the inflamed skin. Interestingly, at day 3 of the 7-day imiquimod treatment, Treg depleted and replete animals did not differ in their gene expression, suggesting that Tregs are more important for controlling the immune response at later stages. This time coincides with the beginning of increased ear thickness and increased leukocyte influx that we observe in this model.

The unique transcriptome at day 7 was demonstrated by a clear separation in a principal component and hierarchical clustering analysis. Gene Ontology (GO) pathway analysis found several processes upregulated in the Treg depleted skin. Confirming the RT-qPCR results, the search term “positive regulation of interleukin 12 production” was among the highest enriched terms and IL-17F was the most downregulated cytokine in the Treg replete skin. In addition, the genes encoding the IL-17A/IL-17F and IL-17C receptor subunits

Il17rc and *Il17re* were downregulated, further suggesting a role of Tregs in the regulation of IL-17 mediated inflammation.

An existing crossregulation between Tregs and Th17 cells has been suggested and Tregs could be promoting Th17 cells by providing TGFβ and/or limiting IL-2 availability as IL-2 inhibits Th17 differentiation (Chen & Oppenheim, 2014; Chen et al., 2011; Moore-Connors et al. 2013). γδ T cells are ontogenetically different from αβ T cells. They arise during embryonic development and do not undergo a differentiation process known for αβ T cells. However, TGFβ has been suggested to play a role, particularly in the thymic development of IL-17 producing γδ T cells (Do et al., 2010). As we have demonstrated in Chapter 3, many dermal γδ T cells express the IL-23R in steady state tissues. These invariant T cells do not need to undergo a differentiation programme and can immediately respond to innate signals (Do et al., 2010; Haas et al., 2012). However, it is not clear what additional signals γδ T cells receive in the tissues to become fully activated. It would be of interest to investigate if and how Tregs could contribute to the activation status and cytokine production of γδ T cells in tissues.

Strikingly, 6 pathways identified in our microarray analyses matched to interferon-regulated processes. Two pathways were related to production and signalling of IFN-γ, confirming the increased IFN-γ production that was observed in the absence of Tregs.

IFN-γ secreting T cells are elevated in the blood and plaques of psoriatic patients (Austin et al., 1999). Interestingly these cells were mainly found in the epidermis. This is similar to findings in a recently introduced mouse model of

psoriasiform inflammation using KC specific overexpression of H-Ras. The resulting inflammation was dependent on IFN-γ (Gunderson et al., 2013). Similar to our results, this model showed a significant increase pathogenic $CD8^+$ T cells. Tc1 cell involvement in psoriasis is further supported by a recent study showing the presence of LL-37 restricted $CD8^+$ T cells in psoriatic skin that produced IFN-γ upon antigen recognition (Lande et al., 2014). Together, the data presented in this chapter in the context of the literature highlight an important role for $CD8^+$ T cell derived IFN-γ in psoriasis and psoriasiform skin inflammation. The imiquimod model in Treg sufficient mice does not recapitulate this aspect of the disease. It can be speculated that Tregs play a critical role in constraining this disease defining feature and warrants further investigation.

Interestingly, the remaining four processes of the highlighted GO pathways all matched to IFN-I production or signalling pathways. IFN-I has long been suggested as a player in psoriasis (Nestle et al., 2005; van der Fits et al., 2004; Yao et al., 2008). In a xenotransplant model using uninvolved patient skin, IFN-I drove the initial development of the psoriatic plaque (Nestle et al., 2005). However, blocking antibodies for IFN-I did not prove successful in clinical studies (Bissonnette et al., 2010).

IFN-I is known to drive Th1 and Tc1 responses (McNab et al., 2015). Multiple MHC class Ib molecules were upregulated in the Treg depleted skin, which is likely a consequence of IFN-I exposure in the tissue. This further suggests an increased presentation of self-antigens in the absence of Tregs that is supported by the striking increase in $CD8^+$ T cells. Among the list of

differentially regulated genes, we identified *Bst2* encoding PDCA-1. Under homeostatic conditions it is a marker of pDC, the primary cell type considered responsible for secreting IFN-I in early plaque formation (Nestle et al., 2005).

Although this suggested an involvement of these professional interferon-producing cells, they were not elevated in the skin tissue of Treg depleted mice. However, a significant increase in PDCA-1 expressing cells was evident in the skin and draining lymph nodes of the Treg depleted inflamed mice that were absent in Treg replete animals. Interestingly, these did not express any other markers associated with pDC, but expressed markers associated with mononuclear phagocytes and produced significant amounts of IFNα in the skin draining lymph nodes. Monocytes and monocyte derived cells are a potent source of IFN-I and are crucial in maintaining anti-viral responses to influenza (Cao et al., 2012). The selective increase in monocyte derived inflammatory macrophages in the absence of Tregs in the skin supports the possibility of MNP as a source of IFN-I. Furthermore, pDC depletion in the imiquimod model has not shown an impact on skin inflammation (Wohn et al., 2013).

We were not able to identify an IFNα secreting population in the skin itself. This might be due to the often transient expression of IFN-I or could be due to the long isolation, culture, and staining process that could lead to cell death in highly activated cells. This of course can be equally true for pDC in the skin. However, the fact that the IFNα^{+} cells in the lymph node were Siglec H^{-} and B220^{-} points to a different source than pDC. The IFN-I signature was not detected at various time points in the lymph node. This could suggest that Ly6C^{high} cells are already poised to produce IFN-I, but only due so once they

enter the skin tissue. The identification of the cellular source will be important to identify a pathway though which Treg cells can suppress IFN-I in the tissue. The AMP LL-37 is highly expressed in psoriasis and can form complexes with self-nucleotides that result in TLR activation and the secretion of IFN-I (Ganguly et al., 2009; Lande et al., 2007). Recently LL-37 restricted $CD8^+$ T cells have been identified in patients suffering from psoriasis (Lande et al., 2014). It should be further investigated if AMP-self-NA complexes are increased in the skin of Treg depleted mice. These could be the target of the expanded $CD8^+$ T cells and trigger IFN-I from myeloid populations.

Type I and type II IFNs play an important role in recognising and eliminating pathogens and are vital host-defence mechanisms. However, they must be tightly regulated to protect from excessive tissue damage and autoimmunity (Ivashkiv & Donlin, 2014; Larkin et al., 2013). Regulatory functions of IFN-I on Tregs have been demonstrated. Interferon beta can promote regulatory T cell differentiation and has been suggested as a mechanism of action in IFNβ therapy in multiple sclerosis patients (Vandenbark et al., 2009). In a T cell transfer colitis model, IFN-I signalling is important for the suppressive capacity of Tregs and without IFN-I signalling, Tregs were not able to prevent colitis (Lee et al. 2012). In contrast, addition of IFN-I to activated human PBMCs *in vitro* led to a decrease of Treg:Teff ratios and blockade of IFN-I receptor (IFNAR1) reversed this effect (Golding et al., 2010). Furthermore, in a model of LCMV infection Campbell and colleagues have demonstrated that IFN-I can restrain regulatory T cell function by inhibiting co-stimulation-dependent cell

activation and consequently promoted viral clearance by $CD4^+$ and $CD8^+$ T cells (Srivastava et al. 2014).

The existing data show that IFN-I can have profound effects on Tregs. It can be speculated that this regulation is reciprocal and that Tregs can also restrain or promote IFN-I secretion. IL-10 is an important regulatory feature of tissue Tregs (Rubtsov et al., 2008), and the experiments in this chapter show that IL-10R blockade causes increased ear thickness in the imiquimod model. However, blockade of this pathway did not recapitulate the αβ T cell expansion triggered by Treg depletion. Furthermore, genetic deficiency of IL-33 signalling did not impact on the skin inflammation. The mechanistic tools Tregs use to control the inflammation triggered by their absence warrants further investigation and could assist in elucidating the role of Tregs in psoriatic skin.

In summary, the experiments described in this chapter identify a previously unappreciated role of $Foxp3^+$ cells in restraining $CD4^+$ and $CD8^+$ T cell influx in the imiquimod model of psoriasiform skin inflammation. Furthermore, Tregs restricted the emergence of IL-12 driven Th1/Tc1 differentiation and consequently secretion of IFN-γ. This was accompanied by a decrease of IL-23 and expression of IL-17 cytokines and receptors. Treg depletion further prevented the influx of γδ T cells, suggesting a distinct capacity of Tregs in controlling γδ and αβ T cells in the skin. The use of whole tissue transcriptomics led to in the identification of IFN-I as a key target of immunosuppression by Tregs. Further investigation pointed towards monocyte-derived cells being a likely source of IFNα.

Chapter 5. Identification and functional characterization of mechanisms controlled by Tregs

5.1. Introduction

Our studies presented in the previous chapters indicate that Tregs are crucial controllers of inflammation in the imiquimod model of psoriasiform skin inflammation. Those results highlight the capacity of Tregs to control $CD8^+$ and $CD4^+$ αβ T cells as well as type I and type II interferon secretion in the inflamed skin. Further experiments revealed an increase in inflammatory macrophages in the absence of Tregs. The final chapter of this thesis addresses the mechanistic basis of the observed changes and aims to test the hypothesis that Tregs control skin inflammation via restriction of MNP derived IFN-I.

Tregs can limit $CD8^+$ T cell expansion by limiting the availability of IL-2 (McNally et al., 2011), thereby determining the fate of $CD8^+$ Teff vs. memory generation (de Goër de Herve et al., 2012). In this context, Tregs influenced $CD8^+$ T cell fate at very early activation stages. In chronic viral infections, Tregs promote $CD8^+$ T cell exhaustion in a PDL-1 dependent manner and promote viral persistence (Penaloza-MacMaster et al., 2014). As previously discussed, $CD8^+$ T cells are a feature of psoriasis where they predominantly accumulate in the epidermis. However, their precise contribution to disease and a potential relationship with regulatory T cells in affected patients has not

been described and warrants further investigation. $CXCR3^+$ $T\text{-}bet^+$ Tregs are capable of restraining Th1 driven inflammation (Koch et al., 2009). However, we were unable to detect T-bet expression in the $Foxp3^+$ T cells in the skin at steady state and inflammation. This suggests that in our model, Tregs did not acquire these Th1 traits to control the increase of $CD4^+$ Teff that became evident in a Treg depleted inflamed setting.

Microarray analysis revealed that pathways regulating type I and type II interferon production and function were highly enriched in the skin tissue of Treg depleted inflamed mice. IFN-I are very potent inducers of immune responses and are beneficial as they promote clearance of infections. Conversely, chronically elevated levels can lead to impaired immune responses with resulting detrimental effects (González-Navajas et al. 2012). These seemingly contradictory effects highlight the complex immunomodulatory functions of IFN-I and suggest context and time dependent effects of IFN-I exposure. Most cell types, including both haematopoietic and non-haematopoietic populations, can produce IFN-I (Ivashkiv & Donlin, 2014). In addition to viral infections, these cytokines can also be induced in response to bacterial sensing and AMP-self-NA complexes via TLR-dependent pathways (Monroe et al., 2010).

The role of IFN-I in chronic inflammation is not very well established. As mentioned previously, IFN-I is used to treat MS and associated with improved outcome in models of colitis (Vandenbark et al., 2009). IFN-I can promote suppressive functions by inducing IL-10 and PDL1 in chronic infections such as tuberculosis and thus contribute to delayed and decreased pathogen

clearance (Teles et al., 2013). However, generally IFN-I are attributed a pathogenic role in many autoimmune diseases. Autoimmune diseases such as systemic lupus erythematosus, systemic sclerosis and rheumatoid arthritis are associated with chronically elevated IFN-I responses (Hall & Rosen, 2010). These data suggest that IFN-I are likely to elicit different responses during different phases of disease, especially as many autoimmune diseases are characterized by remitting and relapsing patterns and also differ in their cytokine profile during these times. In psoriasis, IFN-I from pDC are important during the plaque initiation phase (Nestle et al., 2005). Patients undergoing interferon therapy are prone to develop psoriasis-like lesions at injection sites, which further supports the role of IFN-I in psoriatic plaque initiation (Afshar et al., 2013). However, clinical trials targeting IFN-I signalling did not demonstrate positive results in chronic plaque psoriasis (Bissonnette et al., 2010). This indicates that in this complex disease IFN-I potentially play different roles in chronic and acute lesions. As previously mentioned, IFN-I trigger a complex autocrine feedback loop that shuts down further IFN-I production and allows restoration of homeostatic conditions following infection. However, the role of Tregs in control of IFN-I production has not been addressed.

The data we have presented so far suggest that Tregs restrain IFNs from exerting potentially harmful effects in skin inflammation. In this chapter we aim to identify which of the pathways activated in the absence of Tregs are crucial for the exacerbation of disease. We tested the hypothesis that IFN-I and IFN-γ are crucial for the inflammation in the absence of Tregs and set out to identify the cellular source of IFN-I in this setting.

5.2. Results

5.2.1. IFN-I drives inflammation in absence of Tregs

In order to assess the role of IFN-γ, we injected a cytokine neutralizing monoclonal antibody before and during imiquimod treatment (Figure 5.1 scheme). Neutralizing IFN-γ in Treg depleted imiquimod treated mice had no significant effect on ear thickness (Figure 5.1A). Furthermore, histology of the ear showed substantial leucocyte infiltration in the dermis and epidermis that was similar to the Treg depleted imiquimod treated control group (Figure 5.1B).

To address the role of IFN-I we used a monoclonal antibody that blocked the interferon-alpha/beta receptor alpha chain (IFNAR1) and thus blocked the effects of IFN-I (Figure 5.1 scheme). Blocking of IFNAR1 reversed the phenotype provoked by the absence of $Foxp3^+$ cells and imiquimod treatment (Figure 5.1 and 5.2). The ear thickness of the anti-IFNAR1 injected Treg depleted imiquimod treated group was similar to the Treg sufficient imiquimod treated control group and significantly lower than the IgG injected Treg depleted imiquimod treated group (Figure 5.1A). Blockade of IFNAR1 ameliorated the cellular and histological changes of the ear seen in Treg sufficient imiquimod treated animals (Figure 5.1B).

The splenomegaly observed in the Treg depleted imiquimod treated group was significantly improved by the addition of anti-IFNAR1 antibody and was similar to the Treg sufficient imiquimod treated control group (Figure 5.2A).

$CD8^+$ T cells in the tissue were also significantly decreased by blockade of IFN-I signalling (Figure 5.2B). However, anti-IFNAR1 treatment did not change the numbers of $CD4^+$ Teff in the skin (Figure 5.2C).

Together, these data show that IFN-1 but not IFN-γ enhance immune pathology in Treg depleted imiquimod treated mice.

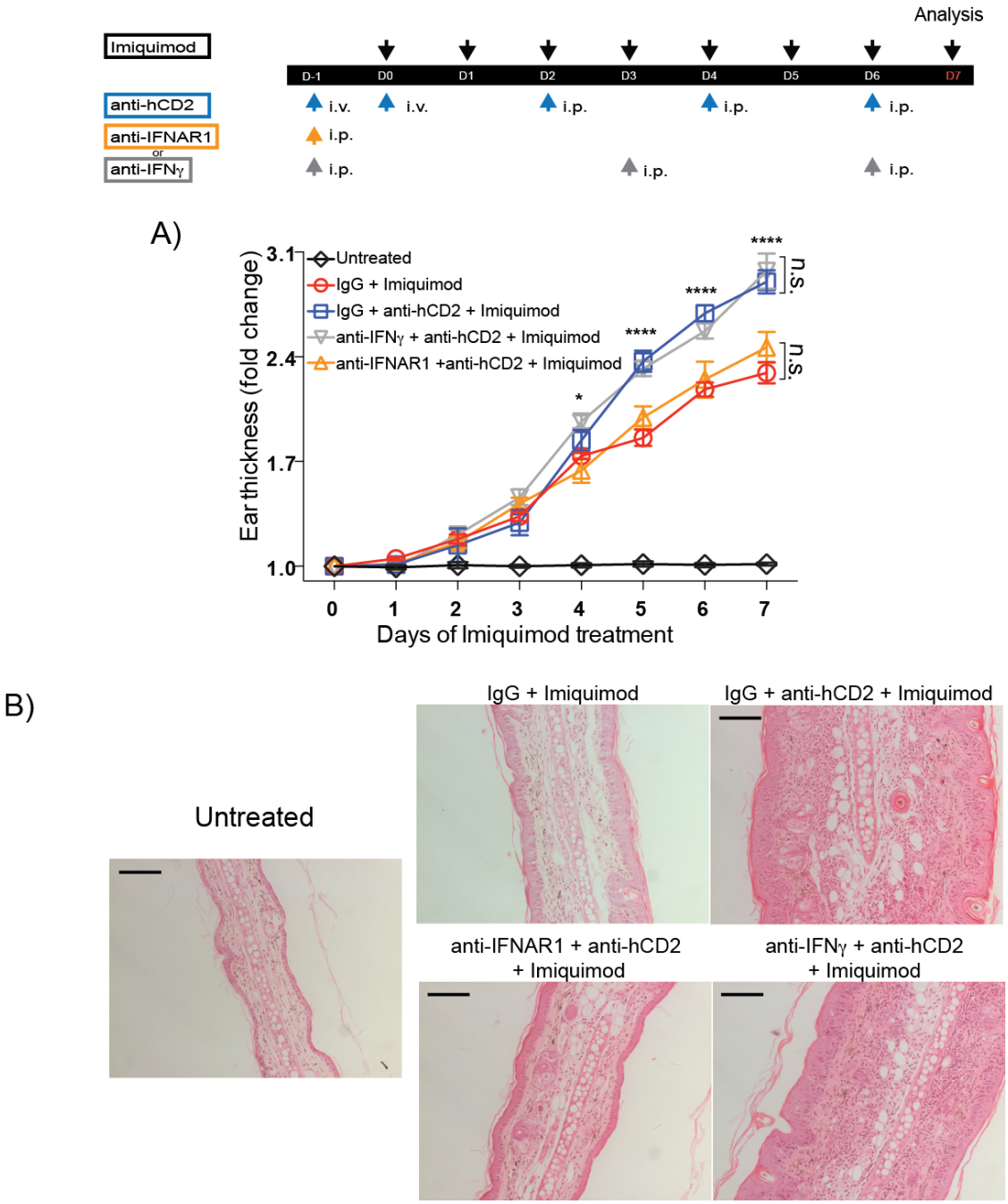

Figure 5.1. Blockade of IFN-I signalling reverses exacerbated inflammation

B6 Foxp3^{hCD2} mice were injected with depleting and blocking antibody or IgG control according to scheme. Anti-hCD2: 500µg /dose i.v. 250µg/dose i.p., anti-IFNAR1 1mg, anti-IFN-γ 500 µgD-1, 250µg D3&6. Imiqimod (Aldara) was applied to each ear for 7 consecutive days or left untreated. Mice were sacrificed on day 7, tissue was harvested and processed for histology assessment.

(A) Ear thickness measured over the imiquimod treatment period

(B) Representative photomicrographs of H&E stained ear tissue

Symbols represent means; error bars SEM. Statistical significance was determined using two-way Anova or one-way Anova with Bonferroni post-hoc test. Data are representative of 1 of 2 independent experiments with n≥4.

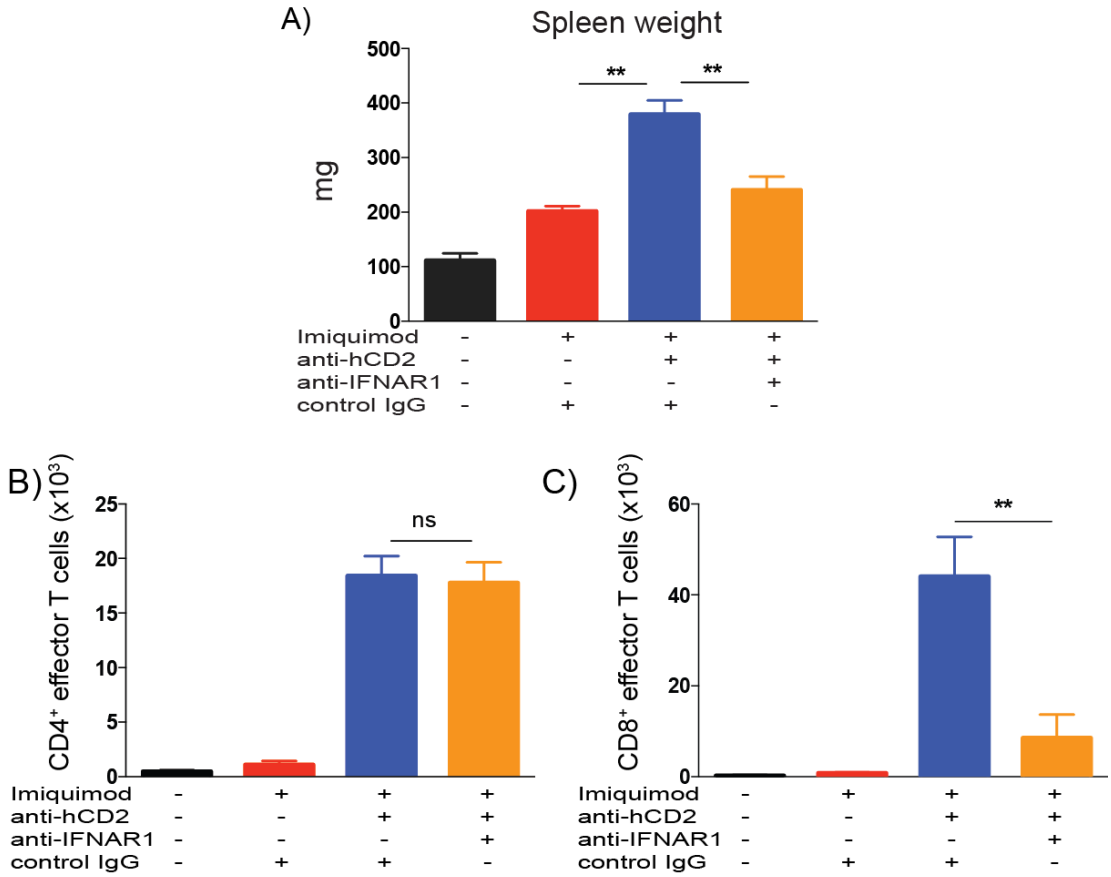

Figure 5.2. Skin histology and Teff infiltration after IFNAR1 blockade

B6 Foxp3^{hCD2} mice were injected with depleting and blocking antibody or IgG control according to scheme in figure 5.1. Anti-hCD2 500ug/dose i.v. 250ug/dose i.p., anti-IFNAR1 1mg, Imiqimod (Aldara) was applied to each ear for 7 consecutive days or left untreated. Mice were sacrificed on day 7, tissue was harvested and enzymatically digested and single cell suspension was stained with surface antibodies prior to analysis by FACS.

(A) Spleen weight of indicated groups

(B) CD4$^+$ Teff infiltration to the skin

(C) CD8$^+$ Teff infiltration to the skin

Data represent means; error bars SEM. Statistical significance was determined using one-way Anova with Bonferroni post-hoc test. Data are representative of 1 of 2 independent experiments with n≥4.

5.2.2. Interferon signalling controls the activation status and influx of monocytes and macrophages

Blocking IFN-I signalling had a profound effect on the histology and inflammatory response and restored the phenotype seen in Treg sufficient skin. In Chapter 4, we saw a change in frequency of infiltrating monocytes and inflammatory macrophages in the Treg depleted inflamed skin. We next set out to investigate the impact of anti-IFNAR1 blockade on MNP changes.

We used the gating strategy introduced in Chapter 4 and gated on live cells, excluded neutrophils (Ly6G), and T cells (CD3), followed by gating on $CD45^+CD11b^+CD64^+$ cells. We then used $Ly6C^+$ and $MHCII^+$ expression to distinguish between recently extravasated monocytes (P1), inflammatory monocytes (P2) and moDC (P3) (Figure 5.3A bottom right).

In all three populations IFNAR1 blockade was sufficient to reverse the PDCA-1 expression we observed in inflamed tissue in the absence of Tregs (Figure 5.3A). Furthermore, blocking IFN-I signalling reversed the increase in inflammatory monocytes as well as the decrease in recently extravasated monocytes caused by Treg depletion (Figure 5.3B).

Together, these data suggest that IFN-I is mediating the inflammatory phenotype of myeloid cells in the Treg depleted inflamed skin.

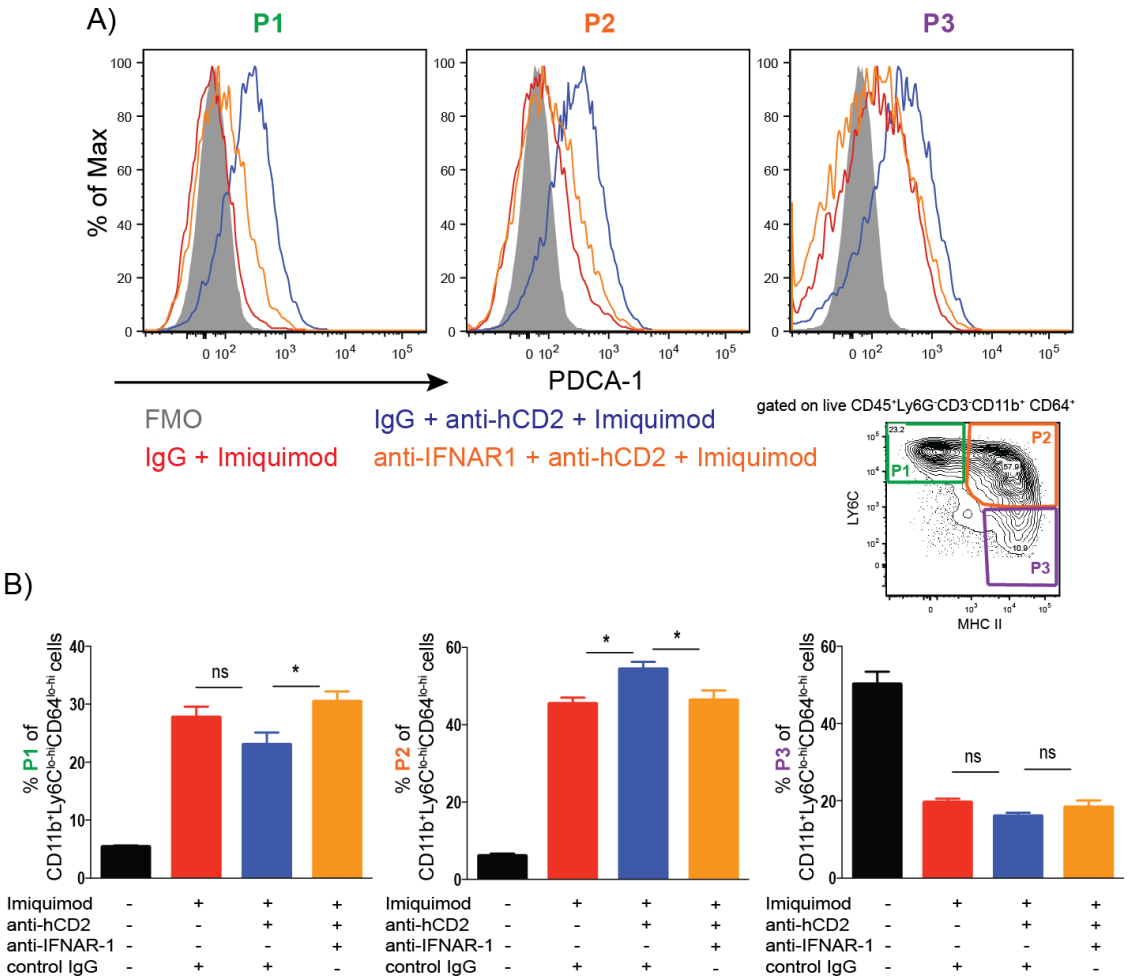

Figure 5.3. Blockade of IFN-I signalling reverses MNP phenotype and frequencies

B6 Foxp3^{hCD2} mice were injected with depleting and blocking antibody or IgG control according to scheme in figure 5.1. Anti-hCD2: 500µg /dose i.v. 250µg /dose i.p., anti-IFNAR1 1mg, Imiqimod (Aldara) was applied to each ear for 7 consecutive days or left untreated. Mice were sacrificed on day 7, tissue was harvested and enzymatically digested and single cell suspension was stained with surface antibodies prior to analysis by FACS.

(A) Representative histograms of PDCA-1 expression on myeloid populations gated according to FACS plot on bottom right. P1 extravasated monocytes, P2 inflammatory monocytes, and P3 moDC

(B) Frequency of myeloid populations P1, P2 and P3 gated according to FACS plot on bottom right of figure A

Data represent means; error bars SEM. Statistical significance was determined using one-way Anova with Bonferroni post-hoc test. Data are representative of 1 of 2 independent experiments with n≥4.

5.2.3. $CD4^+$ T cell help is required for Treg controlled inflammation

We next investigated whether $CD4^+$ T cell help is required for aggravated inflammation or if $CD4^+$ T cells are increased due to the increase in APC-derived inflammatory cytokines and chemokines. Therefore we depleted $CD4^+$ cells in the imiquimod model and compared CD4 depleted with Treg depleted animals (Figure 5.4 scheme). The ear thickness as well as the histology of the CD4 depleted group was similar to the Treg sufficient group (Figure 5.4A and B). Furthermore, in the absence of total $CD4^+$ T cells, $CD8^+$ T cells were not significantly increased compared to the Treg sufficient treated group. We confirmed that depletion of $CD4^+$ Treg and Teff cells was achieved (Figure 5.4D and E). However, further experiments including a double depletion of Foxp3 and CD4 to investigate an effect of CD4 depletion resistant Tregs should be conducted.

Together these data show that depletion of total CD4 expressing cells did not lead to a similar phenotype of amplified inflammation seen when $Foxp3^+$ cells are depleted. This suggests that $CD4^+$ T cell help is necessary for the inflammation seen in the absence of Tregs.

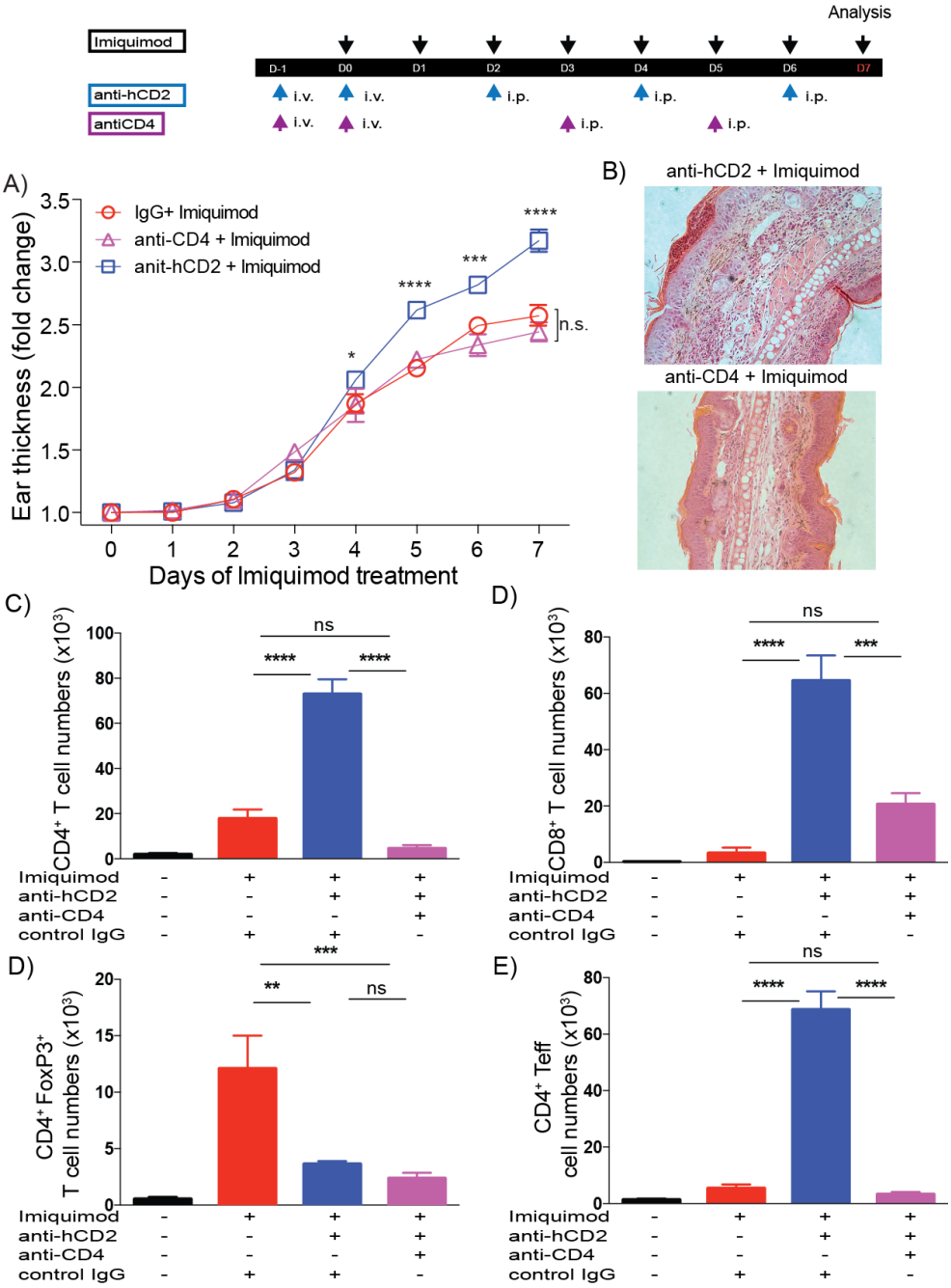

Figure 5.4. CD4$^+$ T cell help is required for IFN-I induced exacerbation

B6 Foxp3^{hCD2} mice were injected with anti-hCD2 depleting antibody (250µg each), anti-CD4 depleting antibody (200µg each) or IgG control according to scheme. 20.8mg of Imiqimod (Aldara) was applied to each ear for 7 days or left untreated. Mice were sacrificed on day 7 of treatment and single cell suspension from the ear was stained with surface antibodies prior to analysis by FACS.

(A) Ear thickness relative to values measured on day -1
(B) Representative photomicrographs of ear histology on day 7
(C) Total CD4$^+$ and CD8$^+$ T cell numbers in the skin
(D) CD4$^+$ Foxp3$^+$ (Treg) cells and CD4$^+$ Foxp3$^-$ Teff in the skin

Data represent means; error bars SEM Statistical significance was determined using two-way Anova or one-way Anova with Bonferroni post-hoc test. Data are representative of 1 of 2 independent experiments with n≥4.

5.2.4. $CD8^+$ T cells mediate skin inflammation suppressed by Tregs

As shown in Chapter 4, $CD8^+$ T cells expand in Treg depleted imiquimod treated skin where they aquire a Tc1 phenotype, express T-bet and secrete IFN-γ and make up the majority of T cells in the inflammatory infiltrate. To address the role of $CD8^+$ T cells in the Treg depleted skin inflammation we used an antibody depletion approach and administered an anti-CD8 monoclonal antibody before and during imiquimod application and Treg depletion in the $Foxp3^{hCD2}$ reporter strain (Figure 5.5 scheme).

Ear thickness in mice with combined Treg and $CD8^+$ T cell depletion was equivalent to that of Treg sufficient, imiquimod treated animals, indicating restoration of the normal imiquimod induced phenotype. This was also evident in the histology (Figure 5.5B). CD8 depletion did not change the total numbers of $CD4^+$ T effector cells, which remained at a similar level to Treg depleted skin (Figure 5.5C and D). These experiments confirmed that $CD8^+$ T cells are a crucial population mediating inflammation in the absence of Tregs.

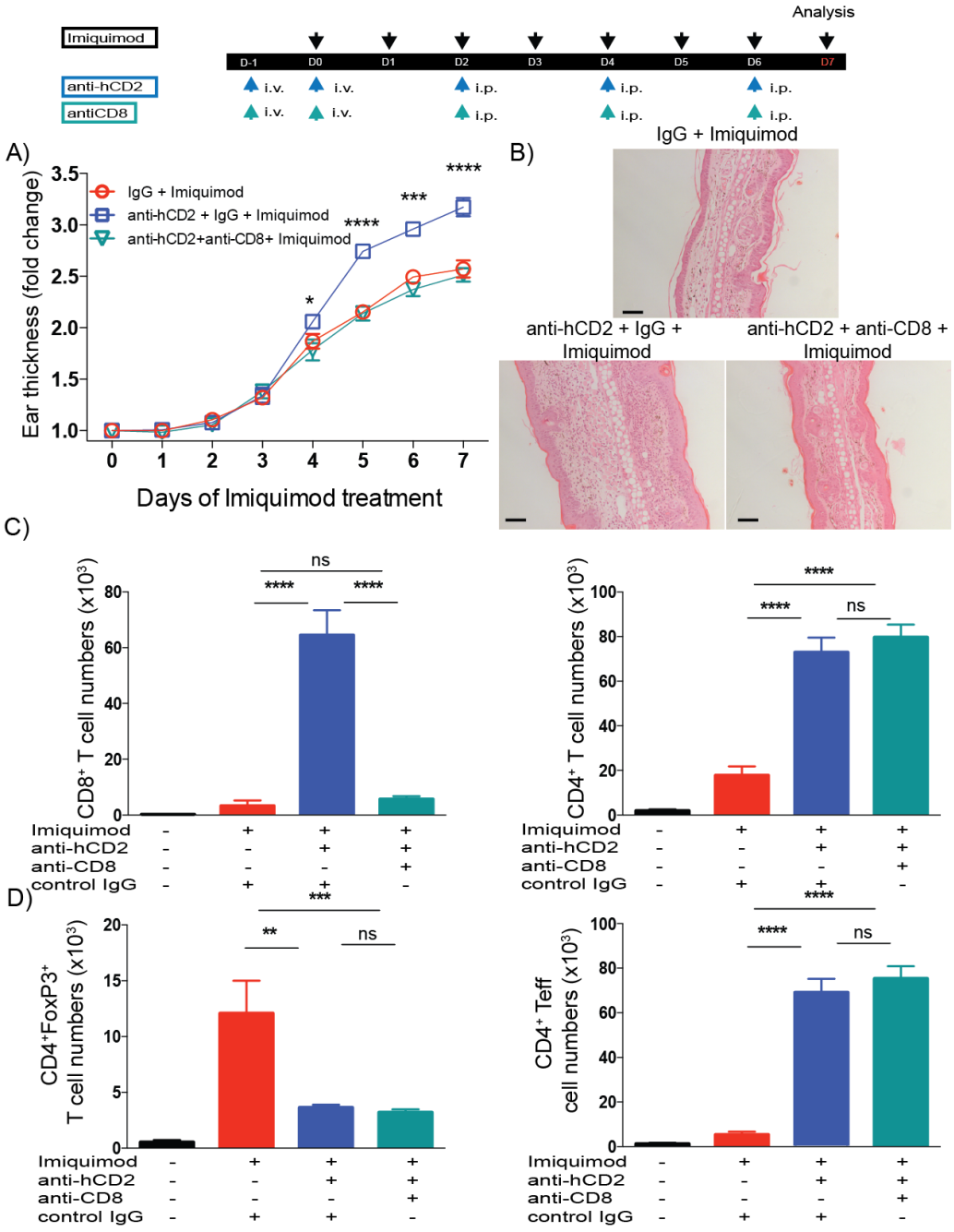

Figure 5.5. CD8$^+$ T cells mediate IFN-I dependent inflammation in the absence of Tregs

B6 Foxp3^{hCD2} mice were injected with anti-hCD2 depleting antibody, anti-CD8 depleting antibody or IgG control. 20.8mg of Imiqimod (Aldara) was applied to each ear for 7 consecutive days or left untreated. Mice were sacrificed on day 7 of imiquimod treatment, ears harvested and processed for histology and enzymatically digested. Single cell suspension from the ear was stained with surface antibodies prior to analysis by FACS.

(A) Ear thickness relative to values measured on day -1
(B) Representative photomicrographs of ear histology on day 7
(C) Total CD8$^+$ and CD4$^+$ T cell numbers in the skin
(D) Total numbers of CD4$^+$ Foxp3$^+$ (Treg) cells and CD4$^+$ Teff in the skin

Data represent means; error bars SEM. Statistical significance was determined using two-way Anova or one-way Anova with Bonferroni post-hoc test. Data are representative of 1 of 2 independent experiments with n≥4.

5.2.5. $CD8^+$ T cells in the skin are highly proliferative, but do not originate exclusively from resident cells

$CD8^+$ T cells in the steady state skin are mostly of memory phenotype (Clark, 2015). We wanted to establish if Tregs are controlling the expansion of a pre-existing $CD8^+$ T cell pool in the skin under inflammatory conditions. For this we injected $5x10^6$ CFSE labelled naïve ($CD44^-CD62L^+$) $CD45.1^+CD8^+$ T cells *i.v.* into B6 $Foxp3^{hCD2}$ reporter mice. We assessed the skin, spleen, and lymph nodes for T cell expansion at day 7 of inflammation.

We were unable to detect any of the injected cells in the skin of mice in the untreated group and also did not recover them from imiquimod treated Treg sufficient skin (Figure 5.6A). However, we observed an influx into the skin under Treg depleted imiquimod treated conditions. The percentage of $CD45.1^+$ cells among $CD8^+$ T cells was similar in the spleen, draining lymph nodes, and skin in this group (Figure 5.6A and B). $CD8^+$ T cells were proliferating in the spleen and the lymph nodes; however, the $CD8^+$ T cells that migrated to the skin showed significantly greater proliferation based on CSFE dilution (Figure 5.6C). However, if the $CD8^+$ T cells found in the skin proliferated after or before entering the tissue remains to be determined. Together these results suggest that $CD8^+$ T cells are recruited to the skin from the periphery and are highly proliferative.

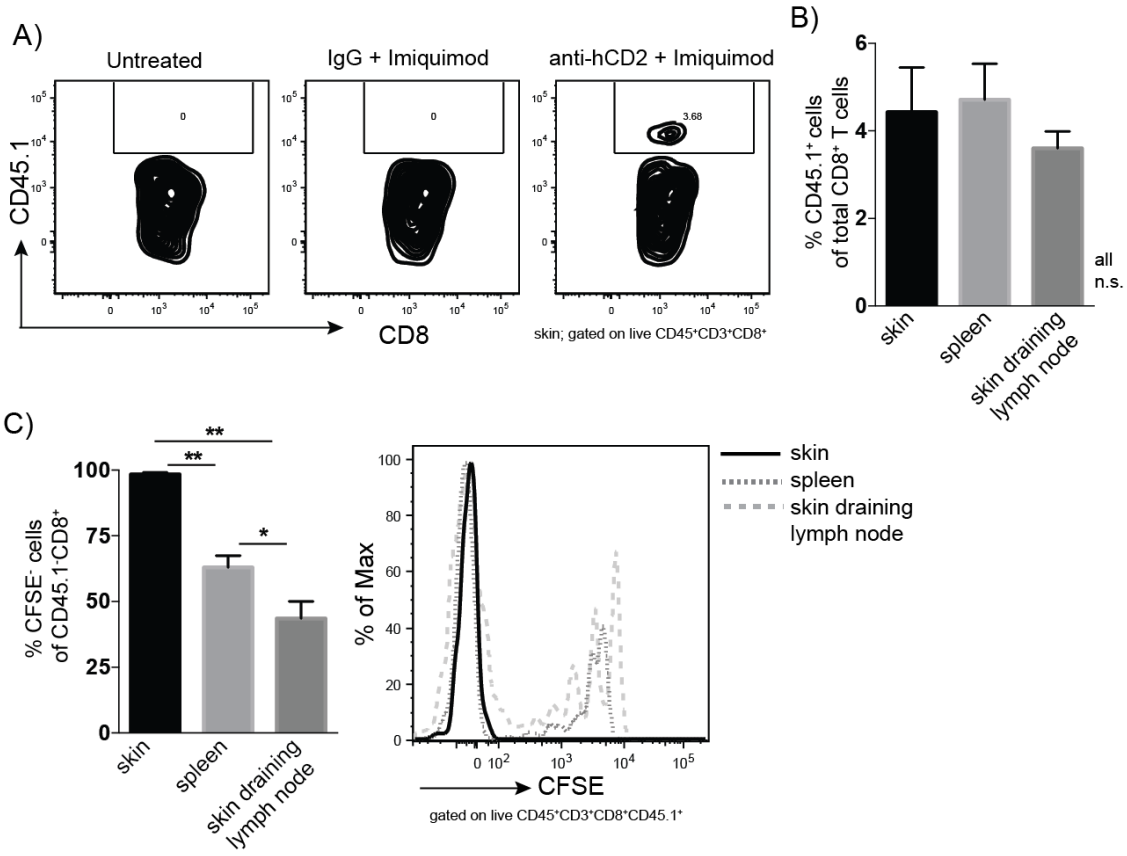

Figure 5.6. The CD8$^+$ T cell infiltrate doesn't exclusively originate from skin resident precursors

B6 Foxp3^{hCD2} mice were injected with anti-hCD2 depleting antibody. 20.8mg of Imiqimod (Aldara) was applied to each ear for 7 consecutive days or left untreated. Simultaneously with the first application, 5x 10^6 CFSE labeled CD45.1 CD44$^-$CD62$^+$ CD8$^+$ T cells were injected i.v. Mice were sacrificed on day 7 of imiquimod treatment and single cell suspension from the ear, spleen and draining lymph nodes were stained with surface antibodies prior to analysis by FACS.

(A) Representative FACS plots of CD45.1$^+$ cells of total CD8$^+$ T cells in the skin

(B) Frequency of CD45.1$^+$ cells of total CD8$^+$ T cells in indicated organs

(C) Frequency of CFSE negative cells and representative histogram of CFSE intensity at day 7 in the indicated organs

Data represent means; error bars SEM. Statistical significance was determined using one-way Anova with Bonferroni post-hoc test. Data are representative of 1 of 2 independent experiments with n≥3.

5.2.6. Absence of Tregs triggers epidermal $CD8^+$ T cell infiltration

As shown in Chapter 3, Tregs increase significantly during imiquimod-induced inflammation and $Foxp3^+$ cells also migrated into the epidermis of the inflamed skin. We therefore investigated where $CD8^+$ T cells located to in the absence of Tregs in inflamed skin. We sorted naïve ($CD44^-CD62L^+$) $CD8^+$ T cells from B6 $CD2^{dsRed}$ mice and injected $3.5x10^6$ cells *i.v.* into B6 $Foxp3^{hCD2}$ reporter mice. We depleted Tregs via anti-hCD2 antibody injection as previously described and treated the mice with imiquimod for 7 days. We then used *in vivo* imaging to assess the location of the $CD8^+$ T cells in the skin.

The transferred $CD8^+$ T cells largely located to the epidermal space (Figure 5.7A and B). As we showed in the previous experiment, naïve T cells homed to the skin draining lymph nodes, the spleen, and the skin equally. However, in Treg sufficient skin, no transferred $CD8^+$ T cells migrated to the ear (Figure 5.6A, imaging data not shown). After the *in vivo* imaging, we analysed single cell suspensions from the spleen of the mice and found $dsRed^+$ cells represented 3.08 ± 1.32 % of all $CD8^+$ T cells. Taking this into consideration, the epidermal space of the imaged ears is tightly packed with $CD8^+$ T effector cells. These data show that Tregs are locating to the same space that Tc1 cells are taking up in their absence. This suggests Tregs are preventing $CD8^+$ T cells from entering the epidermal space.

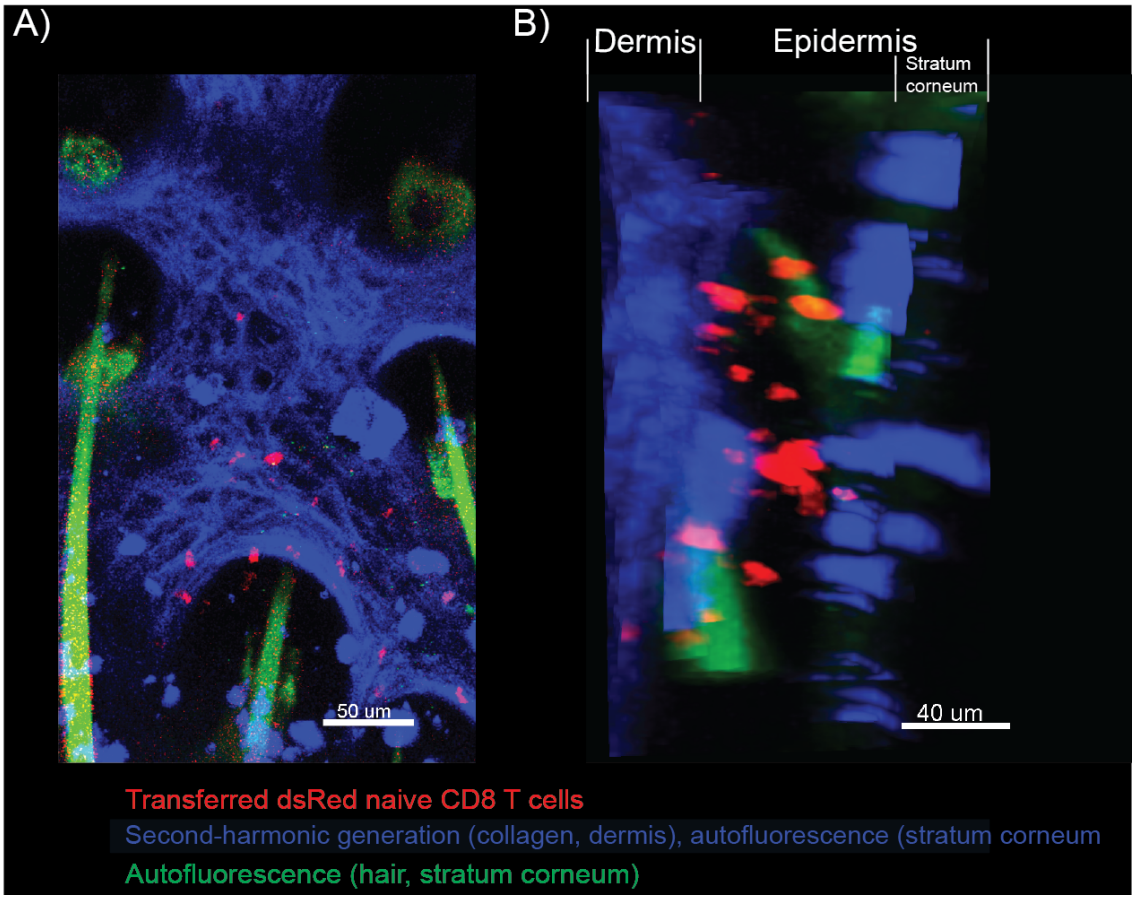

Figure 5.7. Location of $CD8^+$ T cells in the inflamed skin

B6 $Foxp3^{hCD2}$ mice were injected with anti-hCD2 depleting antibody. 20.8mg of Imiqimod (Aldara) was applied to each ear for 7 consecutive days or left untreated. Simultaneously with the first application, 3x 10^6 $CD44^-CD62^+$ $CD8^+$ T cells obtained from B6 $CD2^{dsRed}$ spleens were injected i.v. Mice were imaged on day 7 of imiquimod treatment

(A) Sagittal view of Treg depleted ears. $CD8^+$ T cells visible in red. Hair follicles (black) with autofluorescent hair (green)

(B) Transverse view of Treg depleted ears. $CD8^+$ T cells visible in red (from B6 $CD2^{dsRed}$mice), hair (autofluorescent, green), collagen (second harmonic generation, blue) and stratum corneum (autofluorescent, blue/green)

Data are representative of 1 of 3 imaged mice in one single experiment.

5.2.7. Phagocytic cells mediate IFN-I triggered inflammation

So far we have shown that Tregs control an IFN-I driven skin inflammation that depends on $CD4^+$ and $CD8^+$ Teff. We have further identified $CD45^+SiglecH^-$ $PDCA\text{-}1^+Ly6C^+$ cells as the main IFNα producing cells in the lymph node but did not find any IFNα secretion in cells extracted from the skin (Chapter 4). These data led to the hypothesis that a mononuclear phagocytic population could be responsible for the IFN-I signature we observed in the tissue.

An effective method to deplete phagocytic cells is via administration of dichloromethylene-bisphosphonate (clodronate) liposomes (Rooijen & Hendrikx, 2010). Systemic depletion can be achieved by either intravenous or intraperitoneal injection of liposomes. In order to avoid injecting liposomes and monoclonal antibodies via the same route on the same day, we depleted phagocytic cells by administration of 0.2 ml of clodronate liposomes *i.p.* 12 hours after anti-hCD2 injections (Figure 5.8 scheme).

Clodronate administration prevented the increase of ear thickness in the Treg depleted imiquimod treated group. The fold-change was similar to that observed in Treg sufficient treated animals (Figure 5.8A). Histological assessment of the ear tissue showed a decrease in dermal and epidermal thickness and a decrease in scale thickness when clodronate was administered. Furthermore, the dermo-epidermal junction showed a less disrupted architecture when compared to PBS liposome treated mice (Figure 5.8B). The histology showed similar infiltrates and thickness in the Treg sufficient groups that were treated with clodronate or PBS liposomes (Figure 5.8B).

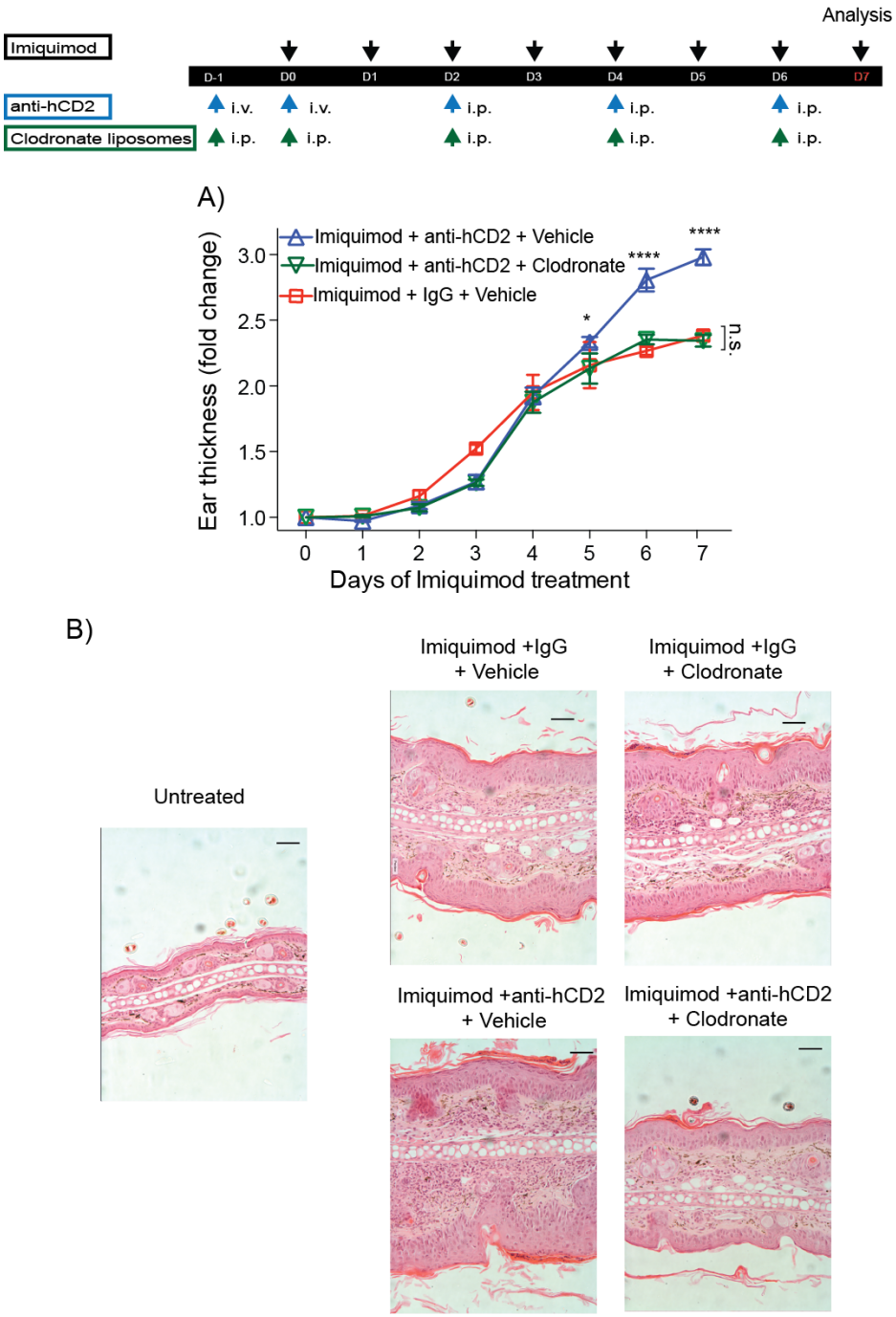

Figure 5.8. Phagocytic cells are driving IFN-I mediated exacerbation

B6 Foxp3^{hCD2} mice were injected with anti-hCD2 depleting antibody or IgG and clodronate or vehicle liposomes according to scheme. 20.8mg of Imiqimod (Aldara) was applied to each ear for 7 consecutive days or left untreated. Mice were sacrificed on day 7 of imiquimod treatment and processed for histology.

(A) Ear thickness relative to values measured on day -1

(B) Representative photomicrographs of ear histology on day 7

Symbols represent means; error bars SEM. Statistical significance was determined using two-way Anova with Bonferroni post-hoc test. Data are representative of 1 experiment (n≥4)

Clodronate injections led to a significant reduction in overall inflammation and infiltration into the skin. Therefore, we investigated which cells were reduced in the skin (Figure 5.9A). $CD11b^+$ $CD64^+$ skin cell numbers were significantly reduced and contained recently extravased monocytes (P1), inflammatory monocytes (P2) and moDC (P3). In order to identify the reduced populations $CD11b^+$ $CD64^+$ cells were subgated (Figure 5.9B). $Ly6C^+$ $MHCII^-$ monocytes (P1) and $Ly6C^+MHCII^+$ inflammatory monocytes (P2) were significantly reduced by clodronate injections (Figure 5.9C).

There were no differences in pDC numbers between imiquimod treated animals that received vehicle or clodronate injections (Figure 5.10A). The frequency of pDC was increased in the clodronate treated groups, reflecting the reduced phagocyte population (Figure 5.10B). However the frequency of pDC in the draining lymph nodes between untreated, imiquimod treated Treg sufficient and imiquimod treated Treg deficient animals were not different (Figure 5.10B).

Spleen weight was not significantly different between the Treg sufficient imiquimod treated animals and the Treg deficient treated animals that received clodronate (Figure 5.11A). $CD45^+$ cells infiltrated the skin at similar numbers in clodronate injected Treg deficient imiquimod treated animals and vehicle injected Treg sufficient imiquimod treated animals (Figure 5.11B). Furthermore, the influx of $CD8^+$ T cells as well as $CD4^+$ $Foxp3^-$ T cells was significantly lower in the clodronate vs. vehicle injected and imiquimod treated groups when Tregs were depleted (Figure 5.11D).

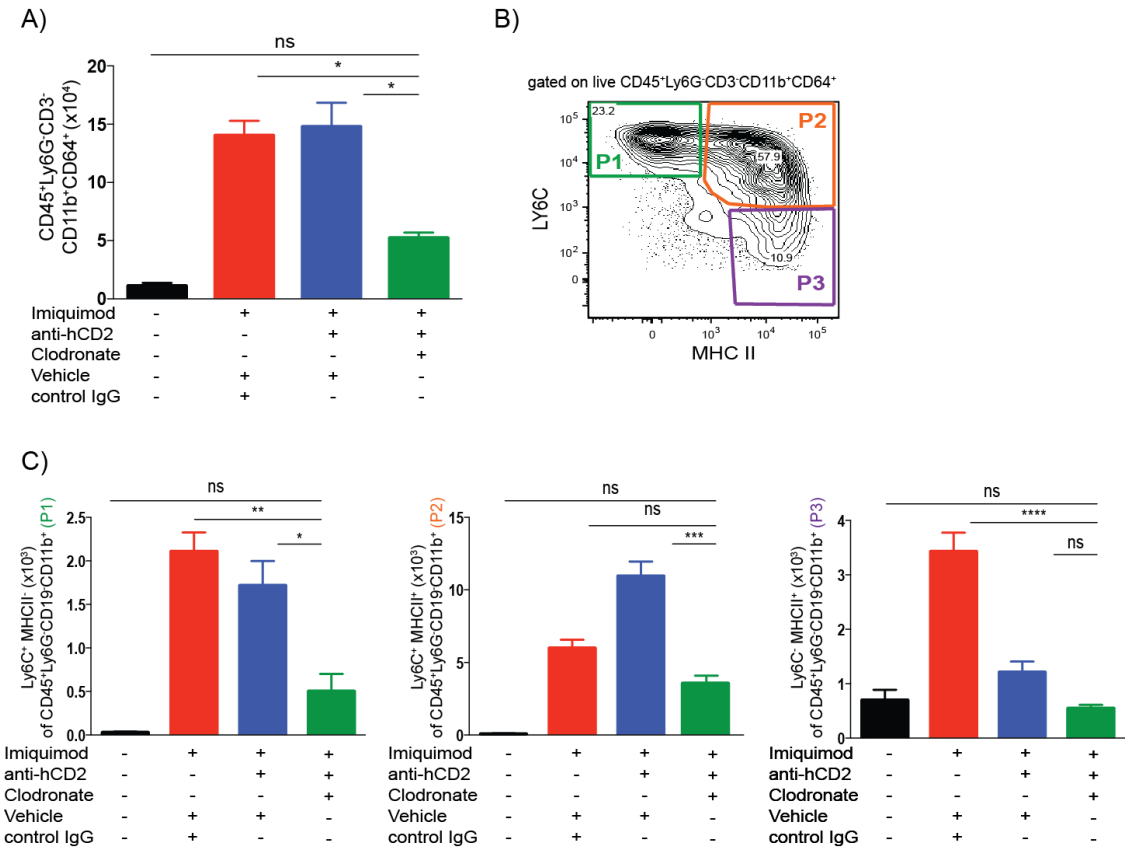

Figure 5.9. Clodronate treatment efficiently reduces CD11b^{+} myeloid cells

B6 Foxp3^{hCD2} mice were injected with anti-hCD2 depleting antibody or IgG and clodronate or vehicle liposomes according to scheme. 20.8mg of Imiqimod (Aldara) was applied to each ear for 7 consecutive days or left untreated. Mice were sacrificed on day 7 of imiquimod treatment and processed for histology.

(A) Total cell numbers of CD45^{+}Ly6G^{-}CD19^{-}CD11b^{+}CD64^{+} cells

(B) Gating strategy of (A) to identify monocyte derived cell subsets used in C

(C) Total sells of monocyte derived cell subsets: P1 Ly6C^{+}MHCII^{-}, P2 Ly6C^{+}MHCII^{+}, and P3 Ly6C^{-}MHCII^{+}

Data represent means; error bars SEM. Statistical significance was determined using one-way Anova with Bonferroni post-hoc test. Data are representative of 1 experiment (n≥4)

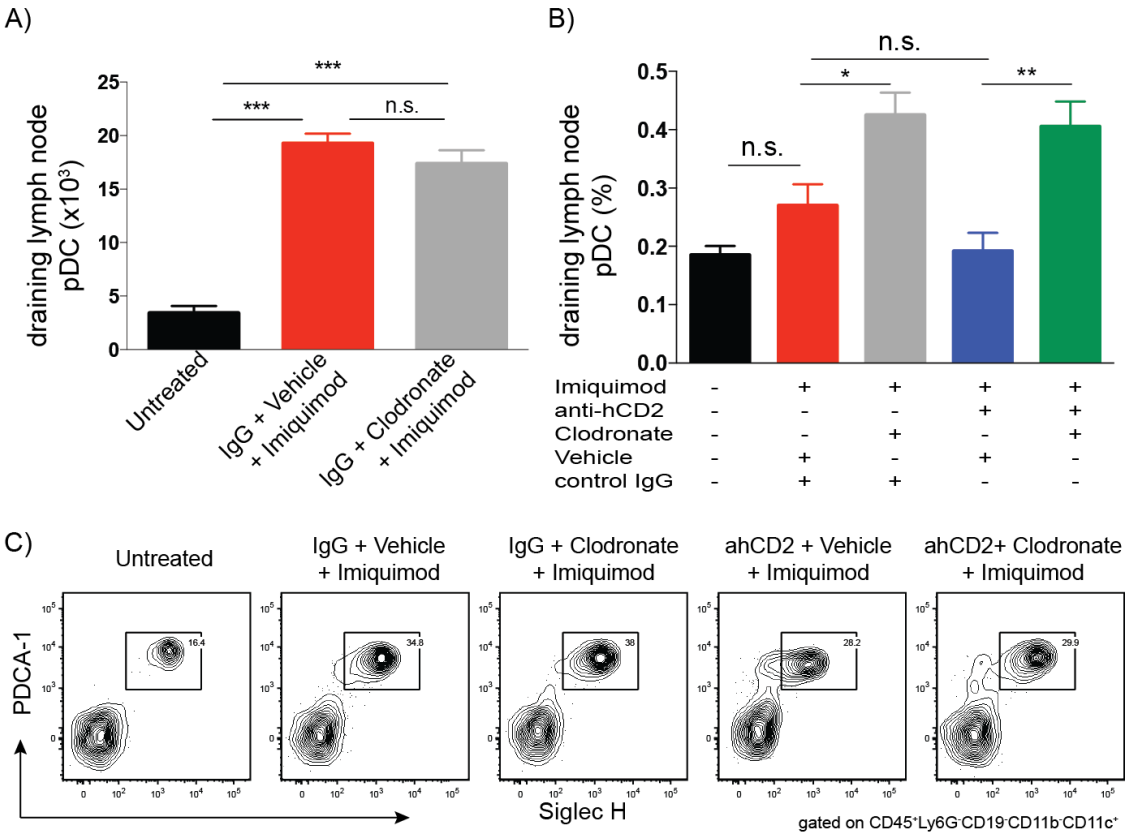

Figure 5.10. Clodronate treatment does not deplete pDC

B6 Foxp3^{hCD2} mice were injected with anti-hCD2 depleting antibody or IgG and clodronate or vehicle liposomes according to scheme. 20.8mg of Imiqimod (Aldara) was applied to each ear for 7 consecutive days or left untreated. Mice were sacrificed on day 7 of imiquimod treatment and processed for histology.

(A) Total cell numbers of pDC ($CD45^+Ly6G^-CD19^-CD11b^-CD11c^+PDCA\text{-}1^+SiglecH^+$cells) in the skin draining lymph nodes

(B) Frequency of pDC ($CD45^+Ly6G^-CD19^-CD11b^-CD11c^+PDCA\text{-}1^+SiglecH^+$cells) in the skin draining lymph nodes

(C) Representative FACS plots of $CD45^+Ly6G^-CD19^-CD11b^-CD11c^+$ cells

Data represent means; error bars SEM. Statistical significance was determined using one-way Anova with Bonferroni post-hoc test. Data are representative of 1 experiment (n≥4)

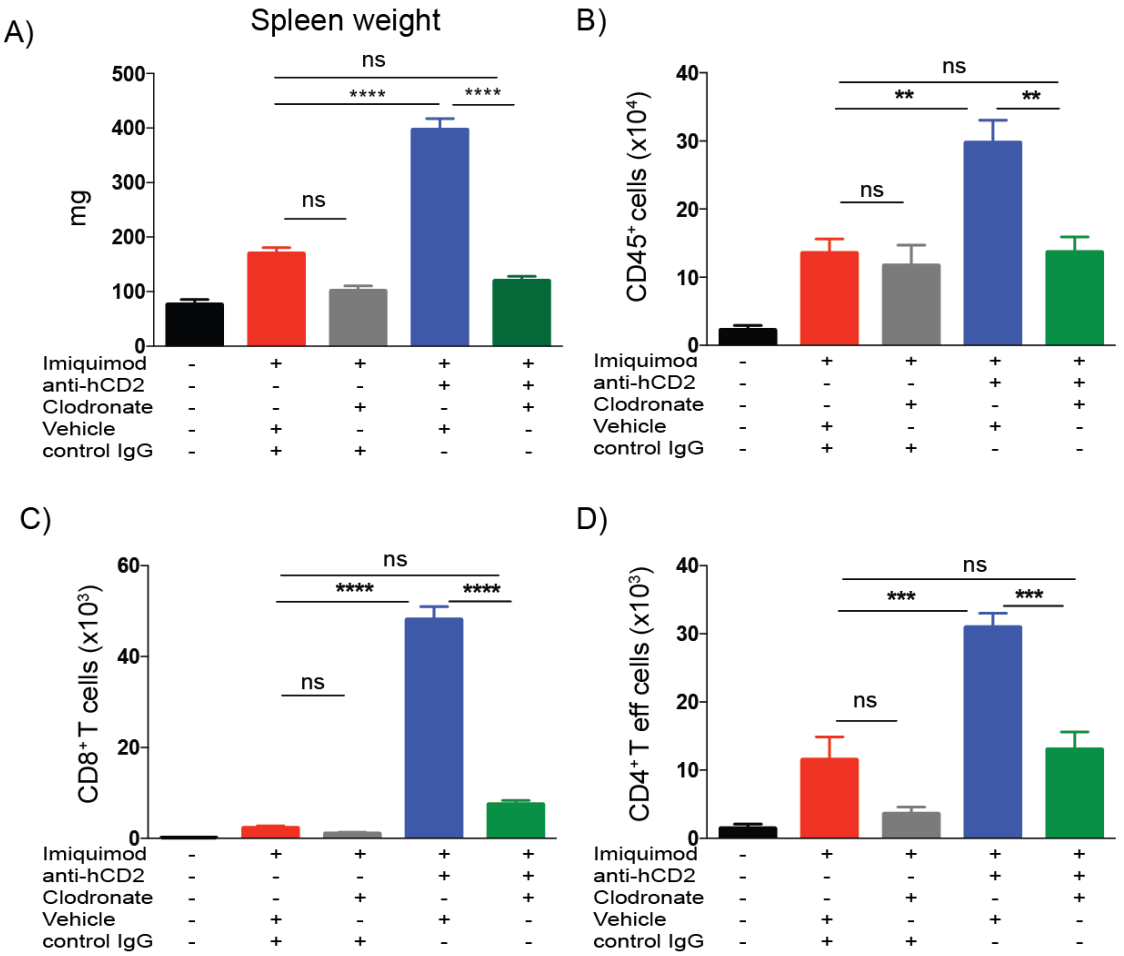

Figure 5.11. Phagocytic cells are driving IFN-I mediated exacerbation of inflammation

B6 Foxp3^{hCD2} mice were injected with anti-hCD2 depleting antibody or IgG and clodronate or vehicle liposomes according to scheme. 20.8mg of Imiqimod (Aldara) was applied to each ear for 7 consecutive days or left untreated. Mice were sacrificed on day 7 of imiquimod treatment, organs harvested and single cell suspension from ears stained with surface antibodies prior to analysis by flow cytometry

(A) Spleen weight of indicated groups on day 7 of treatment

(B) Total CD45$^+$ cells in the ears of indicated groups on day 7 of treatment

(C) Total CD8$^+$ T cells in the ears of indicated groups on day 7 of treatment

(D) Total CD4$^+$ T cells in the ears of indicated groups on day 7 of treatment

Data represent means; error bars SEM. Statistical significance was determined using one-way Anova with Bonferroni post-hoc test. Data are representative of 1 experiment (n≥4)

Consistent with these results, in RT-qPCR performed on mRNA from whole skin tissue showed that the administration of clodronate liposomes significantly reduced the IFN-I signature in the skin (Figure 5.12A). In addition, transcription of *Tbx21* (T-bet), *Il12a* (IL-12) and *Ifng* (IFN-γ) was significantly reduced (Figure 5.12B). Furthermore, the mRNA for the chemokines CCL5, CXCL9 and CXCL10 were also reduced to levels observed in Treg sufficient imiquimod treated skin (Figure 5.12C). Together these data demonstrate that depletion of phagocytic cells via clodronate liposomes prevents the phenotype observed in Treg depleted imiquimod treated mice.

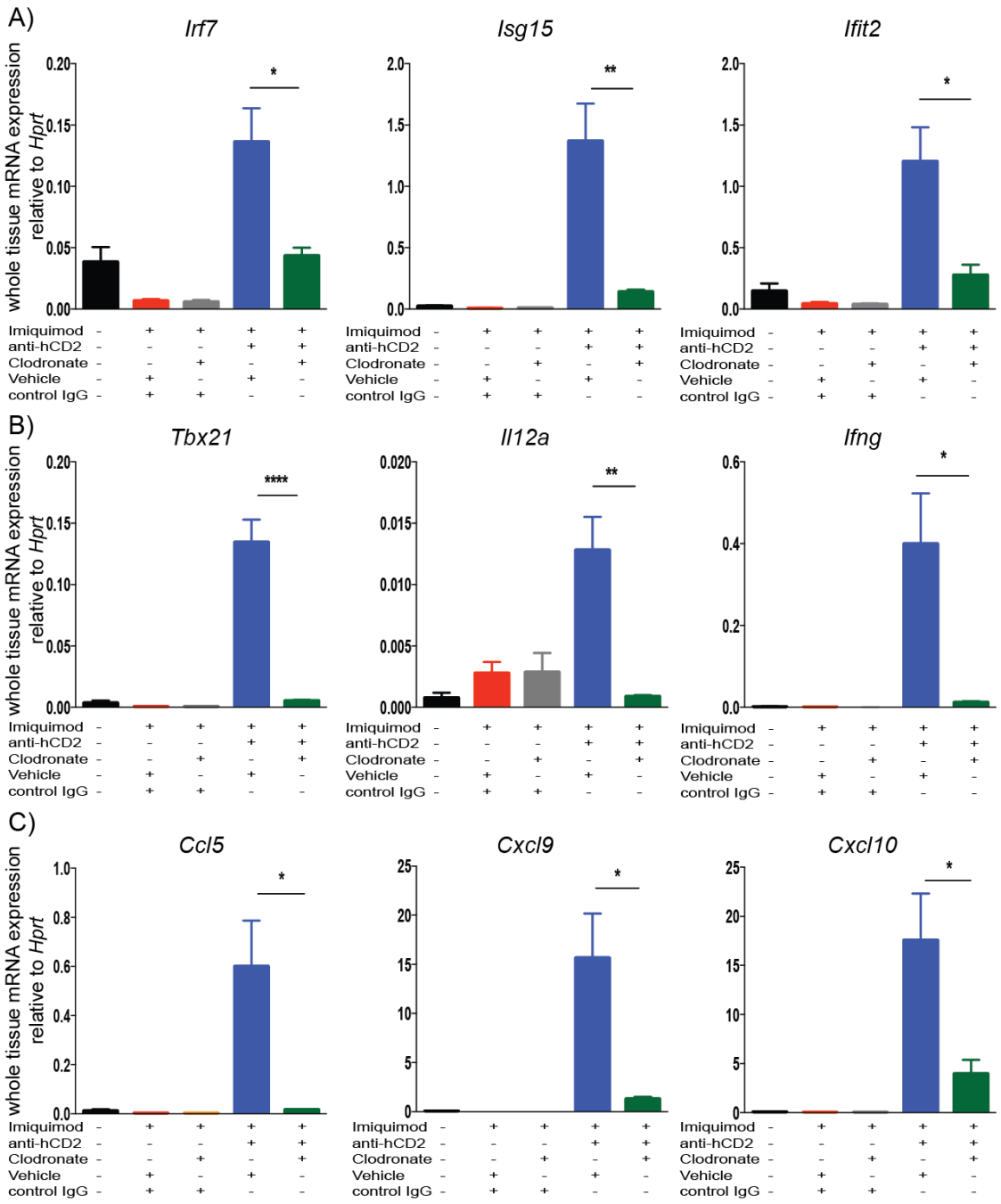

Figure 5.12. Clodronate administration abrogates IFN-I signature in the skin

B6 Foxp3^{hCD2} mice were injected with anti-hCD2 depleting antibody or IgG and clodronate or vehicle liposomes according to scheme in figure 5.8. 20.8mg of Imiqimod (Aldara) was applied to each ear for 7 consecutive days or left untreated. Mice were sacrificed on day 7 of imiquimod treatment and RNA extracted from ear tissue.

(A) Whole skin tissue mRNA expression of IFN-I induced genes relative to *Hprt*

(B) Whole skin tissue mRNA expression of Tc1/Th1 associated genes induced genes relative to *Hprt*

Data represent means; error bars SEM. Statistical significance was determined one-way Anova with Bonferroni post-hoc test. Data are representative of 1 experiment (n≥4)

5.2.8. Depletion of pDC does not alter skin inflammation

Plasmacytoid DC are a potent source of IFN-I and on a per cell basis can secrete higher amounts than other cell types (Swiecki & Colonna 2015). In Chapter 4, we demonstrated that pDC were not infiltrating the skin at day 7 of inflammation and that pDC were not the source of IFNα. However, as clodronate administration can also affect pDC numbers, we were not able to rule out that pDC could be of importance in the early phases of the Treg depleted inflammation. PDCA-1 is a reliable pDC marker at homeostatic conditions but can be upregulated on cells when they are exposed to IFN-I (Blasius et al., 2006).

We administered a depleting anti-PDCA-1 antibody 48 and 24 hours prior to imiquimod application to rule out depletion of any further populations that upregulated PDCA-1 during inflammation (Figure 5.13 scheme). PDCA-1 depletion prior to imiquimod treatment did not alter the ear thickness or histological phenotype of Treg depletion and imiquimod treatment (Figure 5.13A and B). Furthermore, we did not see a significant decrease in spleen weight. Similarly, infiltrating leukocytes were not reduced and $CD8^+$ T cells in the skin tissue remained at a high level compared to the IgG treated group (Figure 5.13C-E). Although the efficiency of the used antibody has been shown in multiple studies, we were not able to perform a control group to assess pDC numbers at the initiation of Imiquimod treatment. This should be highlighted when interpreting these preliminary results. In brief, these data show that depletion of pDC prior to onset of inflammation did not impact on the inflammatory phenotype controlled by Tregs in psoriasiform inflammation.

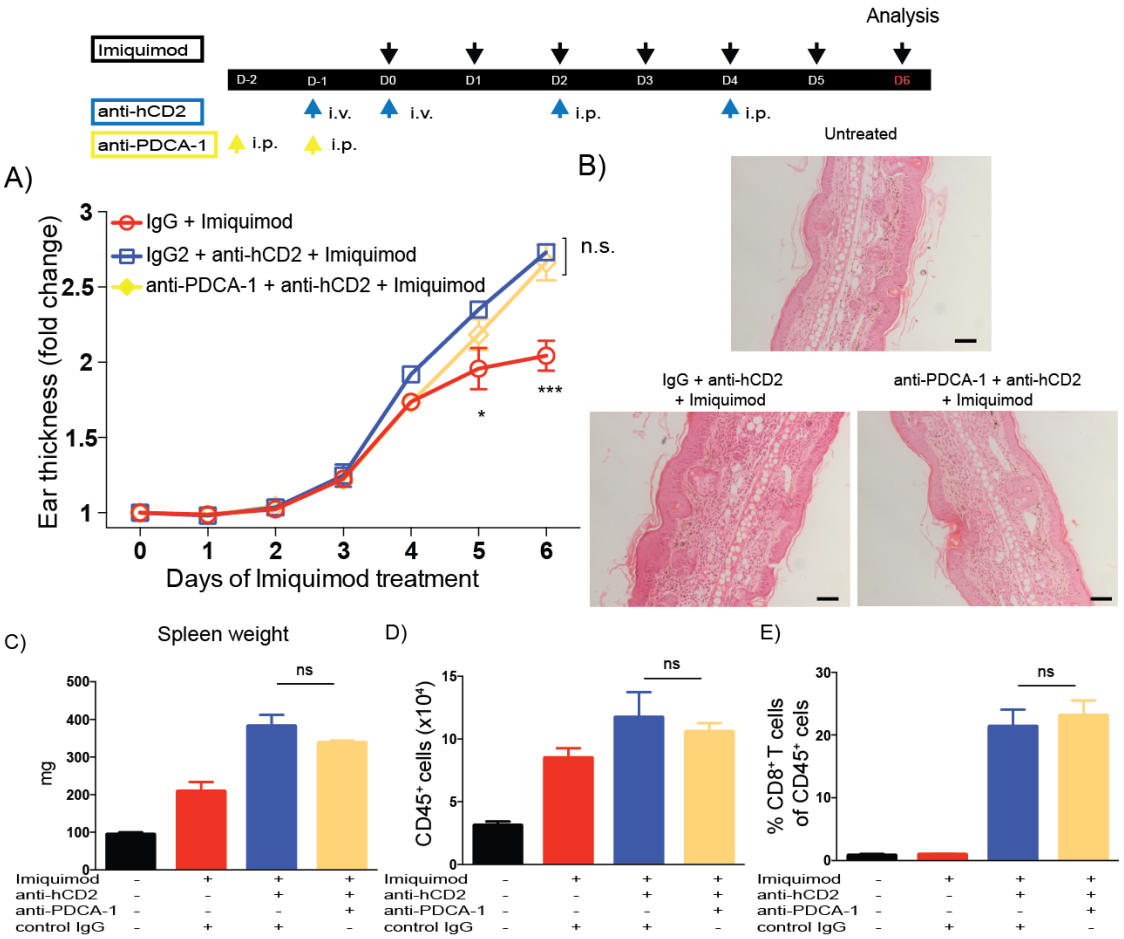

Figure 5.13. PDCA-1 depletion prior to imiquimod treatment does not alter interferon dependent inflammation

B6 Foxp3^{hCD2} mice were injected with anti-hCD2 depleting antibody or IgG and anti-PDCA-1 antibody according to scheme. 20.8mg of Imiqimod (Aldara) was applied to each ear for 6 consecutive days or left untreated. Mice were sacrificed on day 6 of imiquimod treatment, organs harvested and single cell suspension from the ear was stained with surface antibodies prior to analysis by FACS.

(A) Ear thickness relative to values measured on day -1

(B) Representative photomicrographs of ear histology on day 6

(C) Spleen weight of respective groups

(D) Total CD45$^+$ cells in the ears of respective groups

(E) Frequency of CD8$^+$ T cells in the ears of respective groups

Data represent means; error bars SEM. Statistical significance was determined using two-way or one-way Anova with Bonferroni post-hoc test. Data are representative of 1 experiment (n≥4)

5.3. Discussion

The principal objective of the experiments conducted in this chapter was to identify which of the observed changes in Treg depleted imiquimod treated skin are crucial to the exacerbated inflammation and changed inflammatory infiltrate in the skin.

We investigated if type1 and type 2 IFNs are responsible for the exacerbated inflammation. Neutralization of IFN-γ showed no changes to tissue or systemic inflammation in Treg deficient imiquimod treated mice. IFN-γ is a potent proinflammatory cytokine that is crucial for effective pathogen defence. It is elevated in psoriasis and several other autoimmune diseases (Lin & Young, 2013). Psoriasis is associated with a strong IFN-γ signature and was long regarded as a Th1 disease. This view has shifted since the discovery of IL-23 and description of Th17 cells and the successful treatment of psoriasis with drugs interfering in this pathway. Nevertheless, levels of IFN-γ in the blood of patients correlate with the severity of psoriasis and are reduced by successful therapy (Abdallah et al., 2009). Furthermore, IFN-γ associated gene signatures are elevated in psoriatic skin (Liu et al., 2007). However, the exact contribution of IFN-γ remains to be defined. IFN-γ and TNF-α can act in synergy to activate adhesion molecules and chemokines that facilitate leukocyte recruitment to the skin. IFN-γ promotes keratinocyte proliferation and expression of activation markers (Nickoloff & Nestle, 2004; Uyemura et al., 1993). A recently published study used a mouse model overexpressing RAS in suprabasal KCs that resulted in a psoriasis-like phenotype (Gunderson et al., 2013). The skin

infiltration was driven by $CD8^+$ T cells and could be rescued by neutralizing IFN-γ. Interestingly this study also reported infiltration of $CD8^+$ T cells into the epidermis, a prominent feature of human disease. The epidermal $CD8^+$ T cell infiltrate was also triggered by Treg depletion in the imiquimod model. It is likely that $CD8^+$ T cells in psoriatic plaques are mainly IFN-γ secreting epidermal $CD8^+$ T cells (Gunderson et al., 2013). These data warrant further analysis of the activation profile of KC and other epidermal cells in the epidermis under neutralization of IFN-γ in the Treg depleted imiquimod model. To date, no human data with anti-IFN-γ treatment in psoriasis is available. This would be of interest as it could assist the understanding of how Tregs could influence IFN-γ-driven changes in psoriasis.

IFN-I singling was abrogated by administration of a blocking antibody to IFNAR1, a crucial component of the IFNα/β receptor. Normalization of ear thickness, leukocyte infiltration and activation profile of αβ T cells as well as MNP to levels in Treg replete skin was observed. Reports from patients who develop psoriatic plaques near injection sites of therapeutic IFNα further support the role of IFN-I in psoriatic skin inflammation (Afshar et al., 2013). As described in Chapter 4, an increase in $CD11b^+Ly6C^+MHCII^+$ inflammatory monocytes was observed in the absence of Tregs in the inflamed skin. The transcriptomes of the different pools of monocyte derived cells in the skin have been recently investigated (Tamoutounour et al., 2013). This study showed that in a model of CHS, inflammatory monocytes expressed several IFN-stimulated genes such as *Irf7* and *Ifit2*, which was attributed to their capacity to produce IFN-I in the skin. The authors used phenotypic and transcriptomic

comparisons and showed that the Ly6C^{+}MHCII^{+} inflammatory monocytes were an intermediate population of recently extravasated Ly6C^{+}MHCII^{-} monocytes and Ly6C^{-}MHCII^{+} moDC. The data presented in the experiments here used a similar gating approach to Tamoutounour et al. The expanded population we observed in this and the previous chapter displays the same surface markers as the inflammatory monocyte population with the strongest IFN-I signature in the cited study. Investigation of genes associated with IFN-I production in sorted populations of skin MNP in the imiquimod model would therefore be of paramount interest in assessing their contribution to the phenotype in Treg depleted inflammation.

Uptake of clodronate containing liposomes via phagocytosis leads to apoptosis of phagocytic cells. Experiments conducted using clodronate depletion reversed the systemic as well as the tissue specific inflammation in Treg depleted imiquimod treated mice. Clodronate injections significantly reduced the overall CD45^{+}CD11b^{+}CD64^{+} MNP and in particular the Ly6C^{+}MHCII^{+} population. Furthermore, clodronate depletion reversed the IFN-I signature in the skin and normalized levels of Th1/Tc1 driving cytokines, transcription factors, and chemokines in the skin. However, clodronate treatment did not impact on pDC in the skin draining lymph nodes. The importance of MNP in psoriasiform inflammation is further supported by the paramount role of macrophages in two different mouse models of psoriasis (Stratis et al., 2006; Wang et al., 2006). In summary, this data suggest that Tregs control skin inflammation by restraining inflammatory MNP, who drive an IFN-I dependent exacerbation of inflammation. Experiments such as *in vitro* co-culture of these two populations and targeted *in vivo* depletion of *Ccr2* expressing cells should

be conducted to investigate how Tregs can control this accumulation of inflammatory monocytes in the skin

IFNα/β from pDC can contribute to psoriasis plaque formation (Nestle et al., 2005). The imiquimod model of psoriasiform inflammation used here is dependent on daily application of the TLR7 agonist imiquimod. pDC are highly reactive to TLR stimulation and produce large amounts of IFN-I (Lai & Gallo, 2008). However, previous studies have shown that depletion of pDC in the imiquimod model does not improve the imiquimod-induced skin inflammation and lack of IFN-I signalling by blocking or genetically depleting IFN-I shows little effect (Wohn et al., 2013). The imiquimod model has many similarities but also fundamental differences with human plaque psoriasis. These studies suggest that pDC in the imiquimod model play a different role than in human plaque psoriasis. The data presented in Chapter 4 further supports this difference, as we have shown that pDC depletion does not impact on the imiquimod-induced inflammation observed in the absence of Tregs. However, the pDC depletion experiment was only performed once and data was obtained on day 6 after imiquimod treatment. Further experiments should be performed before ruling out that pDC could contribute to the IFN-I driven inflammation in the Treg depleted imiquimod treated skin.

$CD8^+$ T cells are significantly expanded in the absence of Tregs and are crucial effector cells in the inflammation observed. Depletion of $CD8^+$ T cells reversed the excessive skin infiltration and reduced ear thickness. The inflammation seen in the absence of Tregs was at least in part dependent on $CD4^+$ T cell

help. Depletion of CD4 expressing cells did not phenocopy the inflammation observed in the Treg depleted group. However, in $CD8^+$ and Treg depleted skin $CD4^+$ T effector cells were still elevated, supporting that $CD4^+$ T cells are necessary but not sufficient in the observed exacerbation of inflammation. IL-2 from $CD4^+$ T cells could be contributing to the $CD8^+$ T cell expansion observed (Boyman & Sprent, 2012). The presence of Tregs could restrict IL-2 availability to $CD8^+$ T cells and this could be one of the mechanisms responsible for the exacerbated inflammation observed in their absence. Experimental blockade of CD25 could address this possibility. Further, changes in IL-2 levels in the different depletion setting should be measured and the role of $CD4^+$ T cell help in this setting should be explored further.

The data presented in Chapter 5 strengthens the link between IFN-I and Tregs in psoriasiform skin inflammation that was observed in Chapter 4. Our data together with further experiments could facilitate the understanding of the complex regulation of IFN-I in the acute phase of psoriatic plaque formation. The imiquimod model could assist in the identification of the time period during which Tregs are most important in psoriasis. Like other chronic and autoimmune diseases psoriasis is a long-term inflammation with phases of different disease activity (Lowes et al., 2014; Perera et al., 2012). The imiquimod model involves a 5-7 day application of imiquimod and hence is more comparable to acute plaque formation than long-term chronic plaques that patients often suffer from. A limitation of patient based research is the restricted access to tissues and many patient based studies use PBMCs for their investigations. This might fail to reflect the responses in the tissue and

imaging approaches are often descriptive and fail to address functionality. Furthermore, differences in duration of disease between individual patients studied as well as in individual plaques examined can pose a further challenge in the interpretation of results.

To date, the role of Tregs in psoriasis is not very clear. Tregs in the imiquimod model have a protective function and their absence leads to exacerbated disease. However, these data also raise critical new questions that involve the exact mechanism how Tregs control IFN-I mediated disease exacerbation. Further experiments will be necessary to identify the precise pathways Tregs use to control psoriasiform inflammation.

In summary, the data presented in this chapter demonstrates that Tregs control inflammation via regulation of MNP-derived IFN-I and suppression of $CD4^+$ and $CD8^+$ T effector populations.

Chapter 6. General Discussion

Regulatory T cells are important for tissue homeostasis and control of inflammation. Genetic defects in Foxp3 lead to the detrimental IPEX syndrome in which the skin is typically one of the first organs where symptoms arise in subjects affected by this disease. However, little is known about the contribution of Tregs to skin homeostasis and especially if and how they contribute to inflammatory diseases of the skin. Psoriasis is a multi-factorial disease and its pathogenesis is dependent on T cells. Nonetheless, the role of regulatory T cells in psoriasiform inflammation so far has been insufficiently addressed. The experiments presented in this thesis aim to investigate the phenotypic and transcriptomic characteristics of skin resident Tregs under homeostatic and psoriasis-like inflammatory conditions. It is within this context that I identified a novel role for regulatory T cells in controlling acute psoriasiform skin inflammation by harnessing IFN-I and $CD8^+$ and $CD4^+$ T cell activation in the tissue.

In the steady state skin, thymic-derived Tregs constitute the majority of the $CD4^+$ T cells. Tregs express a variety of surface molecules associated with high suppressive capacity. Microarray analyses revealed skin Tregs are equipped with an array of transcripts that have previously been characterized in other tissue derived regulatory T cells. Furthermore, this approach revealed several unique features of skin resident Tregs. Future experimental approaches will aide our understanding of the significance of these changes.

Studies of Tregs in psoriasis have suggested that they adapt an unstable Treg phenotype that could contribute to disease maintenance. Here we used an experimental approach to address the role of Tregs in a model of psoriasiform skin inflammation. Similar to human psoriasis, the imiquimod model is dependent on IL-23 and blocking of the IL-23/IL-17 axis reduces inflammation, thus making it a widely accepted and used model. The experiments revealed an increase in skin Tregs under inflammatory conditions and analysis of their transcriptome suggests that Tregs maintain a highly suppressive state during imiquimod-induced skin inflammation as evidenced by increased expression of *Lag3* and similar levels of *Il10, Tgfb1*,*Ctla4,* and others. Further, no change was observed in transcription factors and cytokines associated with Treg conversion or instability.

Treg depletion experiments in the imiquimod model of psoriasis-like inflammation revealed that Tregs are crucial for dampening inflammation. Absence of Tregs caused significantly increased leukocyte infiltration into the tissue and consequently a marked increase in ear thickness. $CD8^+$ T cells were the most prominent infiltrate in Treg deficient inflamed skin, a population that is rare in steady state and Treg replete imiquimod treated skin. $CD8^+$ T cell-infiltrates into the epidermis are a characteristic of human psoriasis and Treg depletion mimicked this pathological feature. A transcriptomic approach revealed that Tregs mainly control events 3 days after treatment initiation, which coincides with the visible and measurable changes in the inflammatory process. The depletion of Tregs revealed increased levels of IL-12 in the tissue and a Th1/Tc1 dominated skin infiltrate. IL-23 responsive dermal γδ T cells

drove the imiqumod-induced inflammation in the presence of Tregs via secretion of IL-17 and IL-22 (Cai et al., 2011; Van Belle et al., 2012; van der Fits et al., 2009). However, these cells and the associated cytokines were significantly decreased when Tregs were depleted. This suggests that Tregs in the imiquimod model are controlling Tc1 and Th1 cells, but not IL-17-producing dermal γδ T cells. The distinct contribution of IL-12 and IL-23 in the Treg depleted setting could help in our understanding of the role of IL-12 in psoriatic inflammation and warrants further investigation.

Furthermore, prominent gene signatures of type I and type II interferon were evident in the skin at the later stages of the inflamed Treg depleted mice. IFN-I and IFN-γ are both implicated in the pathogenesis of psoriasis, however their precise role is still elusive. Blockade of IFN-I signalling compensated for the absence of Tregs, ameliorated overall tissue inflammation, and markedly reduced cell infiltrates. However, neutralizing IFN-γ did not lead to significant changes in inflammation. The experiments presented here suggest that the most likely cell type responsible for the IFN-I driven inflammation were $Ly6C^{+}MHCII^{+}$ inflammatory monocytes. This population was significantly increased in the skin in the absence of Tregs. In addition, clodronate administration caused a clear reduction in these cells and prevented the excessive inflammation observed upon Treg depletion. While the presented data provide evidence for the role of $Ly6C^{+}MHCII^{+}$ inflammatory monocytes and their potential capacity to produce IFN-I, the exact mechanism how Tregs control this population needs to be further investigated.

Collectively, this study suggests that Tregs control myeloid derived IFN-I and consequent $CD4^+$ and $CD8^+$ T cell activation that drive initiation and exacerbation of skin inflammation. Although the imiquimod model does not recapitulate all aspects of human psoriasis, many pathways are similar. The imiquimod model is an acute model and could be regarded a good indicator of processes occurring in early plaque formation, which has proved difficult to study. It can be speculated that Tregs are of distinct importance at various time points throughout inflammation and our data suggest that Tregs play an important role in early disease during plaque development. This possibility warrants further investigations with patient samples that will aide our understanding of the pathophysiological process of psoriasis and could lead to targeted therapeutic intervention at different time points in the disease.

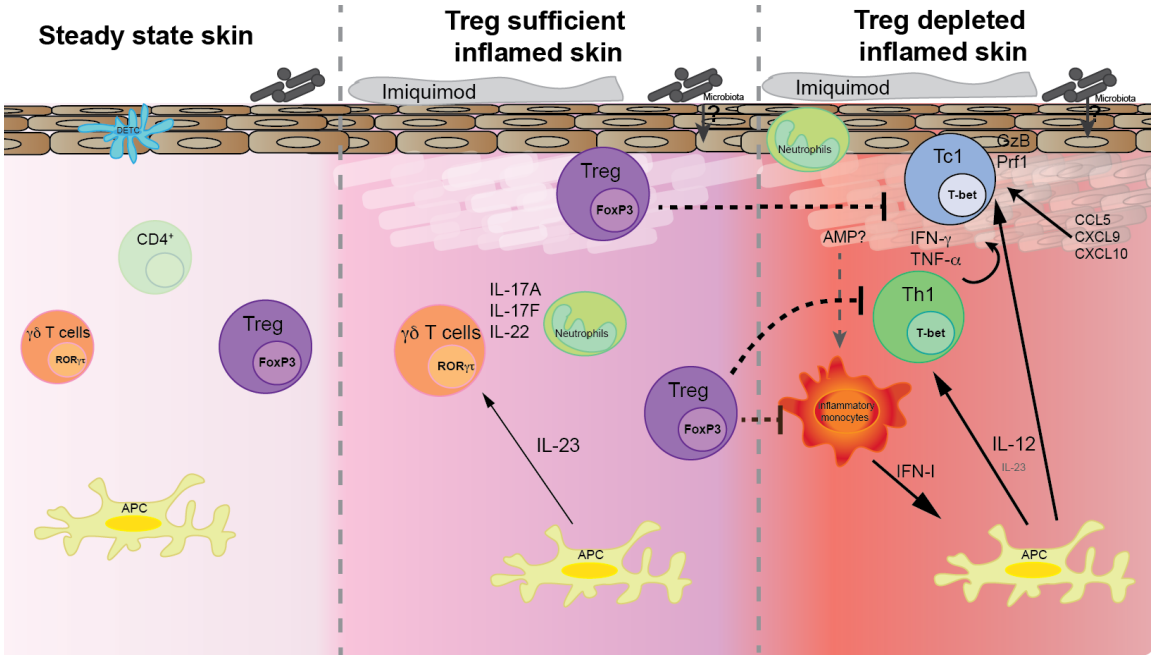

Figure 6.1. Working model - Tregs control skin inflammation in the imiquimod model of psoriasiform skin disease

At homeostatic conditions, Tregs constitute the majority of $CD4^+$ T cells in the skin. Epidermal γδ T cells are the main population of T cells in the skin and low numbers of dermal γδ T cells are present in the dermis.
Imiquimod treatment drives an IL-23-dependent IL-17 and IL-22 driven inflammation. Dermal γδ T cells are the main T cell population, and Treg cells increase significantly in the dermis and the epidermis.
In absence of Tregs, Imiquimod induced inflammation is driven by inflammatory monocyte derived IFN-I and is accompanied by increased levels of IL-12 and decreased levels of IL-23. αβ T cells produce significant amounts of IFN-γ and TNF-α and increased tissue levels of perforin and granzymeB are likely to contribute to the increased tissue inflammation.

References

Abdallah, M. A., Abdel-Hamid, M. F., Kotb, A. M., & Mabrouk, E. A. (2009). Serum interferon-gamma is a psoriasis severity and prognostic marker. *Cutis*, *84*(3), 163–168.

Abrams, J. R., Lebwohl, M. G., Guzzo, C. a., Jegasothy, B. V., Goldfarb, M. T., Goffe, B. S., Menter, A., Lowe, N. J., Krueger, G., Brown, M. J., Weiner, R. S., Birkhofer, M. J., Warner, G. L., Berry, K. K., Linsley, P. S., Krueger, J. G., Ochs, H. D., … Kang, S. (1999). CTLA4Ig-mediated blockade of T-cell costimulation in patients with psoriasis vulgaris. *Journal of Clinical Investigation*, *103*(9), 1243–1252.

Abtin, A., Jain, R., Mitchell, A. J., Roediger, B., Brzoska, A. J., Tikoo, S., Cheng, Q., Ng, L. G., Cavanagh, L. L., von Andrian, U. H., Hickey, M. J., Firth, N., & Weninger, W. (2013). Perivascular macrophages mediate neutrophil recruitment during bacterial skin infection. *Nature Immunology*, *15*(1), 1–12.

Acosta-Rodriguez, E. V, Napolitani, G., Lanzavecchia, A., & Sallusto, F. (2007). Interleukins 1beta and 6 but not transforming growth factor-beta are essential for the differentiation of interleukin 17-producing human T helper cells. *Nature Immunology*, *8*(9), 942–949.

Afkarian, M., Sedy, J. R., Yang, J., Jacobson, N. G., Cereb, N., Yang, S. Y., Murphy, T. L., & Murphy, K. M. (2002). T-bet is a STAT1-induced regulator of IL-12R expression in naïve CD4+ T cells. *Nature Immunology*, *3*(6), 549–557.

Afshar, M., Martinez, a. D., Gallo, R. L., & Hata, T. R. (2013). Induction and exacerbation of psoriasis with Interferon-alpha therapy for hepatitis C: A review and analysis of 36 cases. *Journal of the European Academy of Dermatology and Venereology*, *27*(6), 771–778.

Ahn, J., Gutman, D., Saijo, S., & Barber, G. N. (2012). STING manifests self DNA-dependent inflammatory disease. *Proceedings of the National Academy of Sciences of the United States of America*, *109*(47), 19386–19391.

Allison, J. P., & Havran, W. L. (1991). The immunobiology of T cells with invariant gd antigen receptors. *Annual Reviews of Immunology*, (1), 679–705.

Araújo-souza, P. S. De, Hanschke, S. C. H., & Viola, J. P. B. (2015). Epigenetic Control of Interferon-Gamma Expression in CD8 T Cells. *Journal of Immunology Research*, *2015*.

Ariotti, S., Hogenbirk, M. A., Dijkgraaf, F. E., Visser, L. L., Hoekstra, M. E., Song, J.-Y., Jacobs, H., Haanen, J. B., & Schumacher, T. N. (2014). Skin-resident memory CD8+ T cells trigger a state of tissue-wide pathogen alert. *Science*, *346*(6205), 101–105.

Arpaia, N., Green, J. A., Arvey, A., Hemmers, S., Yuan, S., Treuting, P. M., & Rudensky, A. Y. (2015). Distinct Function of Regulatory T Cells in Tissue Protection. *Cell*, *162*(5), 1078–1089.

Atarashi, K., Tanoue, T., Oshima, K., Suda, W., Nagano, Y., Nishikawa, H., Fukuda, S., Saito, T., Narushima, S., Hase, K., Kim, S., Fritz, J. V., Wilmes, P., Ueha, S., Matsushima, K., Ohno, H., Olle, B., … Honda, K. (2013). Treg induction by a rationally selected mixture of Clostridia strains from the human microbiota. *Nature*, *500*(7461), 232–236.

Austin, L. M., Ozawa, M., Kikuchi, T., Walters, I. B., & Krueger, J. G. (1999). The majority of epidermal T cells in Psoriasis vulgaris lesions can produce type 1 cytokines, interferon-gamma, interleukin-2, and tumor necrosis factor-alpha, defining TC1 (cytotoxic T lymphocyte) and TH1 effector populations: a type 1 differentiation bi. *The Journal of Investigative Dermatology*, *113*(5), 752–9.

Awasthi, A., Riol-Blanco, L., Jäger, A., Korn, T., Pot, C., Galileos, G., Bettelli, E., Kuchroo, V. K., & Oukka, M. (2009). Cutting edge: IL-23 receptor gfp reporter mice reveal distinct populations of IL-17-producing cells. *Journal of Immunology*, *182*(10), 5904–8.

Baker, B. S., Swain, A. F., Valdimarsson, H., & Fry, L. (1984). T-cell subpopulations in the blood and skin of patients with psoriasis. *The British Journal of Dermatology*, *110*(1), 37–44.

Barton, G. M., Kagan, J. C., & Medzhitov, R. (2006). Intracellular localization of Toll-like receptor 9 prevents recognition of self DNA but facilitates access to viral DNA. *Nature Immunology*, *7*(1), 49–56.

Belkaid, Y., Mendez, S., Lira, R., Kadambi, N., Milon, G., & Sacks, D. (2000). A natural model of Leishmania major infection reveals a prolonged “silent” phase of parasite amplification in the skin before the onset of lesion formation and immunity. *Journal of Immunology*, *165*(2), 969–977.

Belkaid, Y., & Segre, J. A. (2014). Dialogue between skin microbiota and immunity. *Science*, *346*(6212), 954–959.

Bernard, J. J., Cowing-Zitron, C., Nakatsuji, T., Muehleisen, B., Muto, J., Borkowski, A. W., Martinez, L., Greidinger, E. L., Yu, B. D., & Gallo, R. L. (2012). Ultraviolet radiation damages self noncoding RNA and is detected by TLR3. *Nature Medicine*, *18*(8), 1286–1290.

Bernink, J. H., Peters, C. P., Munneke, M., te Velde, A. a, Meijer, S. L., Weijer, K., Hreggvidsdottir, H. S., Heinsbroek, S. E., Legrand, N., Buskens, C. J., Bemelman, W. a, Mjösberg, J. M., & Spits, H. (2013). Human type 1 innate lymphoid cells accumulate in inflamed mucosal tissues. *Nature Immunology*, *14*(3), 221–9.

Bettelli, E., Carrier, Y., Gao, W., Korn, T., Strom, T. B., Oukka, M., Weiner, H. L., & Kuchroo, V. K. (2006). Reciprocal developmental pathways for the generation of pathogenic effector TH17 and regulatory T cells. *Nature*, *441*(7090), 235–238.

Bevan, M. J. (2004). Helping the CD8(+) T-cell response. *Nature Reviews. Immunology*, *4*(8), 595–602.

Beyer, M., Thabet, Y., Müller, R.-U., Sadlon, T., Classen, S., Lahl, K., Basu, S., Zhou, X., Bailey-Bucktrout, S. L., Krebs, W., Schönfeld, E. a, Böttcher, J., Golovina, T., Mayer, C. T., Hofmann, A., Sommer, D., Debey-Pascher, S., … Schultze, J. L. (2011). Repression of the genome organizer SATB1 in regulatory T cells is required for suppressive function and inhibition of effector differentiation. *Nature Immunology*, *12*(9), 898–907.

Bilate, A. M., & Lafaille, J. J. (2012). Induced CD4+FoxP3+ Regulatory T Cells in Immune Tolerance. *Annual Review of Immunology*, *30*(1), 733–758.

Bissonnette, R., Papp, K. A., Maari, C., Yao, Y., Robbie, G., White, W. I., Le, C., & White, B. (2010). A randomized, double-blind, placebo-controlled, phase I study of MEDI-545, an anti-interferon-alfa monoclonal antibody, in subjects with chronic psoriasis. *Journal of the American Academy of Dermatology*, *62*(3), 427–436.

Blasius, A. L., Giurisato, E., Cella, M., Schreiber, R. D., Shaw, A. S., & Colonna, M. (2006). Bone marrow stromal cell antigen 2 is a specific marker of type I IFN-producing cells in the naive mouse, but a promiscuous cell surface antigen following IFN stimulation. *Journal of Immunology*, *177*(5), 3260–3265.

Bobr, A., Olvera-Gomez, I., Igyarto, B. Z., Haley, K. M., Hogquist, K. a, & Kaplan, D. H. (2010). Acute ablation of Langerhans cells enhances skin immune responses. *Journal of Immunology*, *185*(8), 4724–4728.

Bodor, J., Bopp, T., Vaeth, M., Klein, M., Serfling, E., Hünig, T., Becker, C., Schild, H., & Schmitt, E. (2012). Cyclic AMP underpins suppression by regulatory T cells. *European Journal of Immunology*, *42*(6), 1375–1384.

Bopp, T., Becker, C., Klein, M., Klein-Hessling, S., Palmetshofer, A., Serfling, E., Heib, V., Becker, M., Kubach, J., Schmitt, S., Stoll, S., Schild, H., Staege, M. S., Stassen, M., Jonuleit, H., & Schmitt, E. (2007). Cyclic adenosine monophosphate is a key component of regulatory T cell-mediated suppression. *The Journal of Experimental Medicine*, *204*(6), 1303–1310.

Boulé, M. W., Broughton, C., Mackay, F., Akira, S., Marshak-Rothstein, A., & Rifkin, I. R. (2004). Toll-like receptor 9-dependent and -independent dendritic cell activation by chromatin-immunoglobulin G complexes. *The Journal of Experimental Medicine*, *199*(12), 1631–1640.

Bovenschen, H. J., van de Kerkhof, P. C., van Erp, P. E., Woestenenk, R., Joosten, I., & Koenen, H. J. P. M. (2011). Foxp3+ Regulatory T Cells of Psoriasis Patients Easily Differentiate into IL-17A-Producing Cells and Are Found in Lesional Skin. *The Journal of Investigative Dermatology*, *131*(9), 1853–1860.

Boyman, O., Hefti, H. P., Conrad, C., Nickoloff, B. J., Suter, M., & Nestle, F. O. (2004). Spontaneous development of psoriasis in a new animal model shows an essential role for resident T cells and tumor necrosis factor-alpha. *The Journal of Experimental Medicine*, *199*(5), 731–6.

Boyman, O., & Sprent, J. (2012). The role of interleukin-2 during homeostasis and activation of the immune system. *Nature Reviews Immunology*, *12*(3), 180–190.

Breitkreutz, D., Koxholt, I., Thiemann, K., & Nischt, R. (2013). Skin Basement Membrane: The Foundation of Epidermal Integrity. *BioMed Research International*, *2013*, 16.

Brencicova, E., & Diebold, S. S. (2013). Nucleic acids and endosomal pattern recognition: how to tell friend from foe? *Frontiers in Cellular and Infection Microbiology*, *3*(July), 37.

Breslin, J. W., Wu, M. H., Guo, M., Reynoso, R., & Yuan, S. Y. (2008). Toll-like receptor 4 contributes to microvascular inflammation and barrier dysfunction in thermal injury. *Shock*, *29*(3), 349–355.

Brunkow, M. E., Jeffery, E. W., Hjerrild, K. a, Paeper, B., Clark, L. B., Yasayko, S. a, Wilkinson, J. E., Galas, D., Ziegler, S. F., & Ramsdell, F. (2001). Disruption of a new forkhead/winged-helix protein, scurfin, results in the fatal lymphoproliferative disorder of the scurfy mouse. *Nature Genetics*, *27*(1), 68–73.

Brüstle, A., Brenner, D., Knobbe-Thomsen, C. B., Cox, M., Lang, P. A., Lang, K. S., & Mak, T. W. (2015). MALT1 is an intrinsic regulator of regulatory T cells. *Cell Death and Differentiation*, 1–10.

Buonocore, S., Ahern, P. P., Uhlig, H. H., Ivanov, I. I., Littman, D. R., Maloy, K. J., & Powrie, F. (2010). Innate lymphoid cells drive interleukin-23-dependent innate intestinal pathology. *Nature*, *464*(7293), 1371–5.

Burdette, D. L., Monroe, K. M., Sotelo-Troha, K., Iwig, J. S., Eckert, B., Hyodo, M., Hayakawa, Y., & Vance, R. E. (2011). STING is a direct innate immune sensor of cyclic di-GMP. *Nature*, *478*(7370), 515–518.

Burute, M., Gottimukkala, K., & Galande, S. (2012). Chromatin organizer SATB1 is an important determinant of T-cell differentiation. *Immunology and Cell Biology*, *90*(9), 852–859.

Burzyn, D., Benoist, C., & Mathis, D. (2013). Regulatory T cells in nonlymphoid tissues. *Nature Immunology*, *14*(10), 1007–1013.

Burzyn, D., Kuswanto, W., Kolodin, D., Shadrach, J. L., Cerletti, M., Jang, Y., Sefik, E., Tan, T. G., Wagers, A. J., Benoist, C., & Mathis, D. (2013). A Special Population of regulatory T Cells Potentiates muscle repair. *Cell*, *155*(6), 1282–1295.

Cai, Y., Shen, X., Ding, C., Qi, C., Li, K., Li, X., Jala, V. R., Zhang, H., Wang, T., Zheng, J., & Yan, J. (2011). Pivotal role of dermal IL-17-producing γδ T cells in skin inflammation. *Immunity*, *35*(4), 596–610.

Campbell, D. J., & Koch, M. A. (2011). Phenotypical and functional specialization of FOXP3+ regulatory T cells. *Nature Reviews. Immunology*, *11*(2), 119–30.

Cao, W., Taylor, a K., Biber, R. E., Davis, W. G., Kim, J. H., Reber, a J., Chirkova, T., De La Cruz, J. a, Pandey, a, Ranjan, P., Katz, J. M., Gangappa, S., & Sambhara, S. (2012). Rapid differentiation of monocytes into type I IFN-producing myeloid dendritic cells as an antiviral strategy against influenza virus infection. *J Immunol*, *189*(5), 2257–2265.

Cao, X., Cai, S. F., Fehniger, T. a., Song, J., Collins, L. I., Piwnica-Worms, D. R., & Ley, T. J. (2007). Granzyme B and Perforin Are Important for Regulatory T Cell-Mediated Suppression of Tumor Clearance. *Immunity*, *27*(4), 635–646.

Capon, F., Burden, a D., Trembath, R. C., & Barker, J. N. (2012). Psoriasis and other complex trait dermatoses: from Loci to functional pathways. *The Journal of Investigative Dermatology*, *132*(3 Pt 2), 915–22.

Capon, F., Di Meglio, P., Szaub, J., Prescott, N. J., Dunster, C., Baumber, L., Timms, K., Gutin, A., Abkevic, V., Burden, a. D., Lanchbury, J., Barker, J. N., Trembath, R. C., & Nestle, F. O. (2007). Sequence variants in the genes for the interleukin-23 receptor (IL23R) and its ligand (IL12B) confer protection against psoriasis. *Human Genetics*, *122*(2), 201–206.

Caproni, M., Antiga, E., Melani, L., Volpi, W., Del Bianco, E., & Fabbri, P. (2009). Serum levels of IL-17 and IL-22 are reduced by etanercept, but not by acitretin, in patients with psoriasis: a randomized-controlled trial. *Journal of Clinical Immunology*, *29*(2), 210–4.

Caramalho, I., Lopes-Carvalho, T., Ostler, D., Zelenay, S., Haury, M., & Demengeot, J. (2003). Regulatory T cells selectively express toll-like receptors and are activated by lipopolysaccharide. *The Journal of Experimental Medicine*, *197*(4), 403–411.

Cargill, M., Schrodi, S. J., Chang, M., Garcia, V. E., Brandon, R., Callis, K. P., Matsunami, N., Ardlie, K. G., Civello, D., Catanese, J. J., Leong, D. U., Panko, J. M., McAllister, L. B., Hansen, C. B., Papenfuss, J., Prescott, S. M., White, T. J., … Begovich, A. B. (2007). A large-scale genetic association study confirms IL12B and leads to the identification of IL23R as psoriasis-risk genes. *American Journal of Human Genetics*, *80*(2), 273–90.

Cases, S., Smith, S. J., Zheng, Y. W., Myers, H. M., Lear, S. R., Sande, E., Novak, S., Collins, C., Welch, C. B., Lusis, a J., Erickson, S. K., & Farese, R. V. (1998). Identification of a gene encoding an acyl CoA:diacylglycerol acyltransferase, a key enzyme in triacylglycerol synthesis. *Proceedings of the National Academy of Sciences of the United States of America*, *95*(22), 13018–13023.

Castellino, F., Huang, A. Y., Altan-Bonnet, G., Stoll, S., Scheinecker, C., & Germain, R. N. (2006). Chemokines enhance immunity by guiding naive CD8+ T cells to sites of CD4+ T cell-dendritic cell interaction. *Nature*, *440*(7086), 890–895.

Chamian, F., Lin, S.-L., Lee, E., Kikuchi, T., Gilleaudeau, P., Sullivan-Whalen, M., Cardinale, I., Khatcherian, A., Novitskaya, I., Wittkowski, K. M., Krueger, J. G., & Lowes, M. a. (2007). Alefacept (anti-CD2) causes a selective reduction in circulating effector memory T cells (Tem) and relative preservation of central memory T cells (Tcm) in psoriasis. *Journal of Translational Medicine*, *5*, 27.

Chamian, F., Lowes, M. a, Lin, S.-L., Lee, E., Kikuchi, T., Gilleaudeau, P., Sullivan-Whalen, M., Cardinale, I., Khatcherian, A., Novitskaya, I., Wittkowski, K. M., & Krueger, J. G. (2005). Alefacept reduces infiltrating T

cells, activated dendritic cells, and inflammatory genes in psoriasis vulgaris. *Proceedings of the National Academy of Sciences of the United States of America*, *102*(6), 2075–2080.

Chang, J. C., Smith, L. R., Froning, K. J., Schwabe, B. J., Laxer, J. a, Caralli, L. L., Kurland, H. H., Karasek, M. a, Wilkinson, D. I., Carlo, D. J., & Brostoff, S. W. (1994). CD8+ T cells in psoriatic lesions preferentially use T-cell receptor, *Abrams, J.*(September), 9282–9286.

Chang, Y.-J., Kim, H. Y., Albacker, L. a, Baumgarth, N., McKenzie, A. N. J., Smith, D. E., Dekruyff, R. H., & Umetsu, D. T. (2011). Innate lymphoid cells mediate influenza-induced airway hyper-reactivity independently of adaptive immunity. *Nature Immunology*, *12*(7), 631–638.

Chaudhry, A., Rudra, D., Treuting, P., Samstein, R. M., Liang, Y., Kas, A., & Rudensky, A. Y. (2009). CD4+ regulatory T cells control TH17 responses in a Stat3-dependent manner. *Science*, *326*(5955), 986–991.

Chen, W., Jin, W., Hardegen, N., Lei, K.-J., Li, L., Marinos, N., McGrady, G., & Wahl, S. M. (2003). Conversion of peripheral CD4+CD25- naive T cells to CD4+CD25+ regulatory T cells by TGF-beta induction of transcription factor Foxp3. *The Journal of Experimental Medicine*, *198*(12), 1875–1886.

Chen, X., & Oppenheim, J. J. (2014). Th17 cells and Tregs: unlikely allies. *Journal of Leukocyte Biology*, *95*(May), 723–731.

Chen, Y., Haines, C. J., Gutcher, I., Hochweller, K., Blumenschein, W. M., McClanahan, T., Hämmerling, G., Li, M. O., Cua, D. J., & McGeachy, M. J. (2011). Foxp3(+) regulatory T cells promote T helper 17 cell development in vivo through regulation of interleukin-2. *Immunity*, *34*(3), 409–21.

Cherwinski, H. M., Schumacher, J. H., Brown, K. D., & Mosmann, T. R. (1987). Two types of mouse helper T cell clone. III. Further differences in lymphokine synthesis between Th1 and Th2 clones revealed by RNA hybridization, functionally monospecific bioassays, and monoclonal antibodies. *The Journal of Experimental Medicine*, *166*(5), 1229–1244.

Chorro, L., Sarde, A., Li, M., Woollard, K. J., Chambon, P., Malissen, B., Kissenpfennig, A., Barbaroux, J.-B., Groves, R., & Geissmann, F. (2009). Langerhans cell (LC) proliferation mediates neonatal development, homeostasis, and inflammation-associated expansion of the epidermal LC network. *The Journal of Experimental Medicine*, *206*(13), 3089–3100.

Chow, Z., Mueller, S. N., Deane, J. a., & Hickey, M. J. (2013). Dermal Regulatory T Cells Display Distinct Migratory Behavior That Is Modulated during Adaptive and Innate Inflammation. *The Journal of Immunology*, *191*(6), 3049–3056.

Ciofani, M., Madar, A., Galan, C., Sellars, M., MacE, K., Pauli, F., Agarwal, A., Huang, W., Parkurst, C. N., Muratet, M., Newberry, K. M., Meadows, S., Greenfield, A., Yang, Y., Jain, P., Kirigin, F. K., Birchmeier, C., … Littman, D. R. (2012). A validated regulatory network for Th17 cell specification. *Cell*, *151*(2), 289–303.

Cipolletta, D., Feuerer, M., Li, A., Kamei, N., Lee, J., Shoelson, S. E., Benoist, C., & Mathis, D. (2012). PPAR-γ is a major driver of the accumulation and phenotype of adipose tissue Treg cells. *Nature*, *486*(7404), 549–553.

Clark, R. A. (2015). Resident memory T cells in human health and disease. *Science Translational Medicine*, *7*(269), 269rv1–269rv1.

Clark, R. A., Chong, B. F., Mirchandani, N., Brinster, N. K., Yamanaka, K.-I., Dowgiert, R. K., & Kupper, T. S. (2006). The vast majority of CLA+ T cells are resident in normal skin. *Journal of Immunology*, *176*(7), 4431–4439.

Clark, R. A., Chong, B. F., Mirchandani, N., Yamanaka, K.-I., Murphy, G. F., Dowgiert, R. K., & Kupper, T. S. (2006). A novel method for the isolation of skin resident T cells from normal and diseased human skin. *The Journal of Investigative Dermatology*, *126*(5), 1059–1070.

Clark, R. A., & Kupper, T. S. (2007). IL-15 and dermal fibroblasts induce proliferation of natural regulatory T cells isolated from human skin. *Blood*, *109*(1), 194–202.

Coombes, J. L., Siddiqui, K. R. R., Arancibia-Cárcamo, C. V, Hall, J., Sun, C.-M., Belkaid, Y., & Powrie, F. (2007). A functionally specialized population of mucosal CD103+ DCs induces Foxp3+ regulatory T cells via a TGF-beta and retinoic acid-dependent mechanism. *The Journal of Experimental Medicine*, *204*(8), 1757–1764.

Cowden, J. M., Zhang, M., Dunford, P. J., & Thurmond, R. L. (2010). The histamine H4 receptor mediates inflammation and pruritus in Th2-dependent dermal inflammation. *The Journal of Investigative Dermatology*, *130*(4), 1023–1033.

Crozat, K., Tamoutounour, S., Vu Manh, T.-P., Fossum, E., Luche, H., Ardouin, L., Guilliams, M., Azukizawa, H., Bogen, B., Malissen, B., Henri, S., & Dalod, M. (2011). Cutting Edge: Expression of XCR1 Defines Mouse Lymphoid-Tissue Resident and Migratory Dendritic Cells of the CD8 + Type. *The Journal of Immunology*, *187*(9), 4411–4415.

Curtsinger, J. M., Valenzuela, J. O., Agarwal, P., Lins, D., & Mescher, M. F. (2005). Type I IFNs provide a third signal to CD8 T cells to stimulate clonal expansion and differentiation. *Journal of Immunology*, *174*(8), 4465–4469.

D'Angelo, M. E., Bird, P. I., Peters, C., Reinheckel, T., Trapani, J. a, & Sutton, V. R. (2010). Cathepsin H is an additional convertase of pro-granzyme B. *The Journal of Biological Chemistry*, *285*(27), 20514–9.

Darrasse-Jèze, G., Deroubaix, S., Mouquet, H., Victora, G. D., Eisenreich, T., Yao, K., Masilamani, R. F., Dustin, M. L., Rudensky, A., Liu, K., & Nussenzweig, M. C. (2009). Feedback control of regulatory T cell homeostasis by dendritic cells in vivo. *The Journal of Experimental Medicine*, *206*(9), 1853–1862.

Dasu, M. R., Thangappan, R. K., Bourgette, A., DiPietro, L. a, Isseroff, R., & Jialal, I. (2010). TLR2 expression and signaling-dependent inflammation impair wound healing in diabetic mice. *Laboratory Investigation; a Journal of Technical Methods and Pathology*, *90*(11), 1628–1636.

De Cid, R., Riveira-Munoz, E., Zeeuwen, P. L. J. M., Robarge, J., Liao, W., Dannhauser, E. N., Giardina, E., Stuart, P. E., Nair, R., Helms, C., Escaramís, G., Ballana, E., Martín-Ezquerra, G., den Heijer, M., Kamsteeg, M., Joosten, I., Eichler, E. E., … Estivill, X. (2009). Deletion of the late cornified envelope LCE3B and LCE3C genes as a susceptibility factor for psoriasis. *Nature Genetics*, *41*(2), 211–215.

De Goër de Herve, M. G., Jaafoura, S., Vallée, M., & Taoufik, Y. (2012). FoxP3+ regulatory CD4 T cells control the generation of functional CD8 memory. *Nature Communications*, *3*, 986.

Demaria, O., Di Domizio, J., & Gilliet, M. (2014). Immune sensing of nucleic acids in inflammatory skin diseases. *Seminars in Immunopathology*, *36*(5), 519–529.

Di Meglio, P., Di Cesare, A., Laggner, U., Chu, C.-C., Napolitano, L., Villanova, F., Tosi, I., Capon, F., Trembath, R. C., Peris, K., & Nestle, F. O. (2011). The IL23R R381Q gene variant protects against immune-mediated diseases by impairing IL-23-induced Th17 effector response in humans. *PloS One*, *6*(2), e17160.

Do, J., Fink, P. J., Li, L., Spolski, R., Robinson, J., Leonard, W. J., Letterio, J. J., & Min, B. (2010). Cutting edge: spontaneous development of IL-17-producing gamma delta T cells in the thymus occurs via a TGF-beta 1-dependent mechanism. *Journal of Immunology*, *184*(4), 1675–1679.

Do, J., Visperas, a, Sanogo, Y. O., Bechtel, J. J., Dvorina, N., Kim, S., Jang, E., Stohlman, S. a, Shen, B., Fairchild, R. L., Baldwin III, W. M., Vignali, D. a a, & Min, B. (2015). An IL-27/Lag3 axis enhances Foxp3+ regulatory T cell–suppressive function and therapeutic efficacy. *Mucosal Immunology*, (April), 1–9.

Dudda, J. C., Perdue, N., Bachtanian, E., & Campbell, D. J. (2008). Foxp3+ regulatory T cells maintain immune homeostasis in the skin. *The Journal of Experimental Medicine*, *205*(7), 1559–65.

Duhen, R., Glatigny, S., Arbelaez, C. a, Blair, T. C., Oukka, M., & Bettelli, E. (2013). Cutting edge: the pathogenicity of IFN-γ-producing Th17 cells is independent of T-bet. *Journal of Immunology*, *190*(9), 4478–82.

Ephrem, A., Epstein, A. L., Stephens, G. L., Thornton, A. M., Glass, D., & Shevach, E. M. (2013). Modulation of Treg cells/T effector function by GITR signaling is context-dependent. *European Journal of Immunology*, *43*(9), 2421–2429.

Fallon, P. G., Ballantyne, S. J., Mangan, N. E., Barlow, J. L., Dasvarma, A., Hewett, D. R., McIlgorm, A., Jolin, H. E., & McKenzie, A. N. J. (2006). Identification of an interleukin (IL)-25-dependent cell population that provides IL-4, IL-5, and IL-13 at the onset of helminth expulsion. *The Journal of Experimental Medicine*, *203*(4), 1105–16.

Fan, X., Yang, S., Huang, W., Wang, Z. M., Sun, L. D., Liang, Y. H., Gao, M., Ren, Y. Q., Zhang, K. Y., Du, W. H., Shen, Y. J., Liu, J. J., & Zhang, X. J. (2008). Fine mapping of the psoriasis susceptibility locus PSORS1 supports HLA-C as the susceptibility gene in the Han Chinese population. *PLoS Genetics*, *4*(3).

Fanti, P. A., Dika, E., Vaccari, S., Miscial, C., & Varotti, C. (2006). Generalized psoriasis induced by topical treatment of actinic keratosis with imiquimod. *International Journal of Dermatology*, *45*(12), 1464–5.

Feldman, S. R. (2015). Treatment of psoriasis. Retrieved from http://www.uptodate.com/contents/treatment-of-psoriasis?source=search_result&search=psoriasis+treatment&selectedTitle=1~150

Feng, J., Zhang, Z., Kong, W., Liu, B., Xu, Q., & Wang, X. (2009). Regulatory T cells ameliorate hyperhomocysteinaemia-accelerated atherosclerosis in apoE-/- mice. *Cardiovascular Research*, *84*(1), 155–163.

Feng, T., Cao, A. T., Weaver, C. T., Elson, C. O., & Cong, Y. (2011). Interleukin-12 converts Foxp3+ regulatory T cells to interferonγ-producing Foxp3+ T cells that inhibit colitis. *Gastroenterology*, *140*(7), 2031–2043.

Fernandez, M. A., Uet Yu, Geoff Zhang, Rose White, Tim Sparwasser, Stephen I. Alexander, & Cheryl A. Jones. (2013). Treg depletion attenuates the severity of skin disease from ganglionic spread after HSV-2 flank infection. *Virology*, *447*(1-2), 9–20.

Fisson, S., Darrasse-Jèze, G., Litvinova, E., Septier, F., Klatzmann, D., Liblau, R., & Salomon, B. L. (2003). Continuous activation of autoreactive CD4+ CD25+ regulatory T cells in the steady state. *The Journal of Experimental Medicine*, *198*(5), 737–746.

Fontenot, J. D., Gavin, M. a, & Rudensky, A. Y. (2003). Foxp3 programs the development and function of CD4+CD25+ regulatory T cells. *Nature Immunology*, *4*(4), 330–336.

Fort, M. M., Cheung, J., Yen, D., Li, J., Zurawski, S. M., Lo, S., Menon, S., Clifford, T., Hunte, B., Lesley, R., Muchamuel, T., Hurst, S. D., Zurawski, G., Leach, M. W., Gorman, D. M., & Rennick, D. M. (2001). IL-25 Induces IL-4, IL-5, and IL-13 and Th2-associated pathologies in vivo. *Immunity*, *15*(6), 985–995.

Foster, A. M., Baliwag, J., Chen, C. S., Guzman, A. M., Stoll, S. W., Gudjonsson, J. E., Ward, N. L., & Johnston, A. (2014). IL-36 promotes myeloid cell infiltration, activation, and inflammatory activity in skin. *Journal of Immunology*, *192*(12), 6053–61.

Fu, W., Ergun, A., Lu, T., Hill, J. a, Haxhinasto, S., Fassett, M. S., Gazit, R., Adoro, S., Glimcher, L., Chan, S., Kastner, P., Rossi, D., Collins, J. J., Mathis, D., & Benoist, C. (2012). A multiply redundant genetic switch “locks in” the transcriptional signature of regulatory T cells. *Nature Immunology*, *13*(10), 972–980.

Fyhrquist, N., Lehtimäki, S., Lahl, K., Savinko, T., Lappeteläinen, A.-M., Sparwasser, T., Wolff, H., Lauerma, A., & Alenius, H. (2012). Foxp3+ cells control Th2 responses in a murine model of atopic dermatitis. *The Journal of Investigative Dermatology*, *132*(6), 1672–80.

Gagliani, N., Vesely, M. C. A., Iseppon, A., Brockmann, L., Xu, H., Palm, N. W., de Zoete, M. R., Licona-Limón, P., Paiva, R. S., Ching, T., Weaver, C., Zi, X., Pan, X., Fan, R., Garmire, L. X., Cotton, M. J., Drier, Y., …

Flavell, R. A. (2015). Th17 cells transdifferentiate into regulatory T cells during resolution of inflammation. *Nature*, *523*(7559), 221–5.

Gaide, O., Emerson, R. O., Xiaodong Jiang, Nicholas Gulati, Suzanne Nizza, Cindy Desmarais, Harlan Robins, James G Krueger, Rachael A Clark, & Thomas S Kupper. (2015). Common clonal origin of central and resident memory T cells following skin immunization. *Nature Medicine*, *21*(6), 647–653.

Gambineri, E., Torgerson, T. R., & Ochs, H. D. (2003). Immune dysregulation, polyendocrinopathy, enteropathy, and X-linked inheritance (IPEX), a syndrome of systemic autoimmunity caused by mutations of FOXP3, a critical regulator of T-cell homeostasis. *Current Opinion in Rheumatology*, *15*(4), 430–435.

Ganguly, D., Chamilos, G., Lande, R., Gregorio, J., Meller, S., Facchinetti, V., Homey, B., Barrat, F. J., Zal, T., & Gilliet, M. (2009). Self-RNA-antimicrobial peptide complexes activate human dendritic cells through TLR7 and TLR8. *The Journal of Experimental Medicine*, *206*(9), 1983–94.

Gartel, A. L., & Radhakrishnan, S. K. (2005). Lost in transcription: p21 repression, mechanisms, and consequences. *Cancer Research*, *65*(10), 3980–3985.

Gately, M. K., Wolitzky, a. G., Quinn, P. M., & Chizzonite, R. (1992). Regulation of human cytolytic lymphocyte responses by interleukin-12. *Cellular Immunology*, *143*(1), 127–142.

Gay, N. J., Symmons, M. F., Gangloff, M., & Bryant, C. E. (2014). Assembly and localization of Toll-like receptor signalling complexes. *Nature Reviews Immunology*, *14*(8), 546–558.

Gebhardt, T., Whitney, P. G., Zaid, A., Mackay, L. K., Brooks, A. G., Heath, W. R., Carbone, F. R., & Mueller, S. N. (2011). Different patterns of peripheral migration by memory CD4+ and CD8+ T cells. *Nature*, *477*(7363), 216–219.

Geisse, J. K., Rich, P., Pandya, A., Gross, K., Andres, K., Ginkel, A., & Owens, M. (2002). Imiquimod 5% cream for the treatment of superficial basal cell carcinoma: a double-blind, randomized, vehicle-controlled study. *Journal of the American Academy of Dermatology*, *47*(3), 390–8.

Geissmann, F., Manz, M. G., S. Jung, M. H. Sieweke, M. Merad, & K. Ley. (2010). Development of Monocytes, Macrophages, and Dendritic Cells. *Science*, *327*(5966), 656–661.

Gelfand, J. M., Troxel, A. B., Lewis, J. D., Kurd, S. K., Shin, D. B., Wang, X., Margolis, D. J., & Strom, B. L. (2007). The Risk of Mortality in Patients With Psoriasis. *Archives of Dermatological Researchh*, *143*(12), 1493–1499.

Geremia, A., Arancibia-Cárcamo, C. V, Fleming, M. P. P., Rust, N., Singh, B., Mortensen, N. J., Travis, S. P. L., & Powrie, F. (2011). IL-23-responsive innate lymphoid cells are increased in inflammatory bowel disease. *The Journal of Experimental Medicine*, *208*(6), 1127–33.

Gilliet, M., Conrad, C., Geiges, M., Cozzio, A., Thürlimann, W., Burg, G., Nestle, F. O., & Dummer, R. (2004). Psoriasis triggered by toll-like receptor 7 agonist imiquimod in the presence of dermal plasmacytoid dendritic cell precursors. *Archives of Dermatology*, *140*(12), 1490–1495.

Ginhoux, F., & Jung, S. (2014). Monocytes and macrophages: developmental pathways and tissue homeostasis. *Nature Reviews. Immunology*, *14*(6), 392–404.

Gladman, D. D., Antoni, C., Mease, P., Clegg, D. O., & Nash, P. (2005). Psoriatic arthritis: epidemiology, clinical features, course, and outcome. *Annals of the Rheumatic Diseases*, *64 Suppl 2*, ii14–i17.

Godfrey, V. L., Wilkinson, J. E., & Russell, L. B. (1991). X-linked lymphoreticular disease in the scurfy (sf) mutant mouse. *The American Journal of Pathology*, *138*(6), 1379–1387.

Golding, A., Rosen, A., Petri, M., Akhter, E., & Andrade, F. (2010). Interferon-alpha regulates the dynamic balance between human activated regulatory and effector T cells: Implications for antiviral and autoimmune responses. *Immunology*, *131*(1), 107–117.

Goldsmith, L. A., Katz, S. I., Gilchrist, B. A., Paller, A. S., Leffell, D. J., & Wolff, K. (2012). *Fitzpatrick's Dermatology in General Medicine*.

Gomez de Agüero, M., Vocanson, M., Hacini-Rachinel, F., Taillardet, M., Sparwasser, T., Kissenpfennig, A., Malissen, B., Kaiserlian, D., & Dubois, B. (2012). Langerhans cells protect from allergic contact dermatitis in mice by tolerizing CD8+ T cells and activating Foxp3+ regulatory T cells. *Journal of Clinical Investigation*, *122*(5), 1700–1711.

González-Granado, J. M., Silvestre-Roig, C., Rocha-Perugini, V., Trigueros-Motos, L., Cibrián, D., Morlino, G., Blanco-Berrocal, M., Osorio, F. G., Freije, J. M. P., López-Otín, C., Sánchez-Madrid, F., & Andrés, V. (2014). Nuclear envelope lamin-a couples actin dynamics with immunological synapse architecture and T cell activation. *Science Signaling*, *7*(322), ra37.

González-Navajas, J. M., Lee, J., David, M., & Raz, E. (2012). Immunomodulatory functions of type I interferons. *Nature Reviews Immunology*, *12*, 125–135.

Gordon, S. M., Chaix, J., Rupp, L. J., Wu, J., Madera, S., Sun, J. C., Lindsten, T., & Reiner, S. L. (2012). The Transcription Factors T-bet and Eomes Control Key Checkpoints of Natural Killer Cell Maturation. *Immunity*, *36*(1), 55–67.

Gottlieb, S. L., Gilleaudeau, P., Johnson, R., Estes, L., Woodworth, T. G., Gottlieb, a B., & Krueger, J. G. (1995). Response of psoriasis to a lymphocyte-selective toxin (DAB389IL-2) suggests a primary immune, but not keratinocyte, pathogenic basis. *Nature Medicine*, *1*(5), 442–447.

Gottschalk, R. a, Corse, E., & Allison, J. P. (2012). Expression of Helios in peripherally induced Foxp3+ regulatory T cells. *Journal of Immunology*, *188*(3), 976–80.

Goudy, K., Aydin, D., Barzaghi, F., Gambineri, E., Vignoli, M., Mannurita, S. C., Doglioni, C., Ponzoni, M., Cicalese, M. P., Assanelli, A., Tommasini, A., Brigida, I., Dellepiane, R. M., Martino, S., Olek, S., Aiuti, A., Ciceri, F., … Bacchetta, R. (2013). Human IL2RA null mutation mediates immunodeficiency with lymphoproliferation and autoimmunity. *Clinical Immunology*, *146*(3), 248–261.

Gratz, I. K., & Campbell, D. J. (2014). Organ-specific and memory Treg cells: Specificity, development, function, and maintenance. *Frontiers in Immunology*, *5*(JUL), 1–17.

Gratz, I. K., Truong, H. -a., Yang, S. H.-Y., Maurano, M. M., Lee, K., Abbas, a. K., & Rosenblum, M. D. (2013). Cutting Edge: Memory Regulatory T Cells Require IL-7 and Not IL-2 for Their Maintenance in Peripheral Tissues. *The Journal of Immunology*, 3–8.

Gregorio, J., Meller, S., Conrad, C., Di Nardo, A., Homey, B., Lauerma, A., Arai, N., Gallo, R. L., Digiovanni, J., & Gilliet, M. (2010). Plasmacytoid dendritic cells sense skin injury and promote wound healing through type I interferons. *The Journal of Experimental Medicine*, *207*(13), 2921–2930.

Grice, E. A., & Segre, J. A. (2011). The skin microbiome. *Nature Reviews. Microbiology*, *9*(4), 244–53.

Griseri, T., Asquith, M., Thompson, C., & Powrie, F. (2010). OX40 is required for regulatory T cell-mediated control of colitis. *The Journal of Experimental Medicine*, *207*(4), 699–709.

Grosso, J. F., Kelleher, C. C., Harris, T. J., Maris, C. H., Hipkiss, E. L., Marzo, A. De, Anders, R., Netto, G., Getnet, D., Bruno, T. C., Goldberg, M. V, Pardoll, D. M., & Drake, C. G. (2007). LAG-3 regulates CD8+ T cell accumulation and effector function in murine self- and tumor-tolerance systems. *Journal of Clinical Investigation*, *117*(11), 3383–3392.

Gudjonsson, J. E., Johnston, A., & Ellis, C. N. (2012). Novel systemic drugs under investigation for the treatment of psoriasis. *Journal of the American Academy of Dermatology*, *67*(1), 139–147.

Guilliams, M., Ginhoux, F., Jakubzick, C., Naik, S. H., Onai, N., Schraml, B. U., Segura, E., Tussiwand, R., & Yona, S. (2014). Dendritic cells, monocytes and macrophages: a unified nomenclature based on ontogeny. *Nature Reviews. Immunology*, *14*(8), 571–578.

Gunderson, A. J., Mohammed, J., Horvath, F. J., Podolsky, M. a, Anderson, C. R., & Glick, A. B. (2013). CD8(+) T cells mediate RAS-induced psoriasis-like skin inflammation through IFN-γ. *The Journal of Investigative Dermatology*, *133*(4), 955–63.

Guo, L., Wei, G., Zhu, J., Liao, W., Leonard, W. J., Zhao, K., & Paul, W. (2009). IL-1 family members and STAT activators induce cytokine production by Th2, Th17, and Th1 cells. *Proceedings of the National Academy of Sciences of the United States of America*, *106*(32), 13463–8.

Haas, J. D., Ravens, S., Düber, S., Sandrock, I., Oberdörfer, L., Kashani, E., Chennupati, V., Föhse, L., Naumann, R., Weiss, S., Krueger, A., Förster,

R., & Prinz, I. (2012). Development of Interleukin-17-Producing γδ T Cells Is Restricted to a Functional Embryonic Wave. *Immunity*, *37*(1), 48–59.

Halabi-Tawil, M., Ruemmele, F. M., Fraitag, S., Rieux-Laucat, F., Neven, B., Brousse, N., De Prost, Y., Fischer, a., Goulet, O., & Bodemer, C. (2009). Cutaneous manifestations of immune dysregulation, polyendocrinopathy, enteropathy, X-linked (IPEX) syndrome. *British Journal of Dermatology*, *160*(3), 645–651.

Hall, A. O., Daniel P. Beiting, Cristina Tato, Beena John, Guillaume Oldenhove, Claudia Gonzalez Lombana, Gretchen Harms Pritchard, Jonathan S. Silver, Nicolas Bouladoux, Jason S. Stumhofer, Tajie H. Harris, John Grainger, Elia D. Tait Wojno, Sagie Wagage, David S. Roos, Philip Scott, Laurence A. Turka, … Christopher A. Hunter. (2012). The Cytokines Interleukin 27 and Interferon-γ Promote Distinct Treg Cell Populations Required to Limit Infection-Induced Pathology. *Immunity*, *37*(3), 511–523.

Hall, J. C., & Rosen, A. (2010). Type I interferons: crucial participants in disease amplification in autoimmunity. *Nature Reviews. Rheumatology*, *6*(1), 40–9.

Hao, J.-Q. (2014). Targeting Interleukin-22 in Psoriasis. *Inflammation*, *37*(1), 94–99.

Harrison, O. J., Srinivasan, N., Pott, J., Schiering, C., Krausgruber, T., Ilott, N. E., & Maloy, K. J. (2015). Epithelial-derived IL-18 regulates Th17 cell differentiation and Foxp3+ Treg cell function in the intestine. *Mucosal Immunology*, (August 2014), 1–11.

Hartupee, J., Liu, C., Novotny, M., Li, X., & Hamilton, T. (2007). IL-17 enhances chemokine gene expression through mRNA stabilization. *Journal of Immunology*, *179*(6), 4135–4141.

Harvima, I. T., & Nilsson, G. (2011). Mast cells as regulators of skin inflammation and immunity. *Acta Dermato-Venereologica*, *91*(6), 644–650.

Hayday, A. C. (2009). γδ T Cells and the Lymphoid Stress-Surveillance Response. *Immunity*, *31*(2), 184–196.

Hayden, M. S., & Ghosh, S. (2012). NF-κB, the first quarter-century: Remarkable progress and outstanding questions. *Genes and Development*, *26*(3), 203–234.

Henderson, J. G., Opejin, A., Jones, A., Gross, C., & Hawiger, D. (2015). CD5 Instructs Extrathymic Regulatory T Cell Development in Response to Self and Tolerizing Antigens. *Immunity*, *42*(3), 471–483.

Hickman, H. D., Reynoso, G. V., Ngudiankama, B. F., Cush, S. S., Gibbs, J., Bennink, J. R., & Yewdell, J. W. (2015). CXCR3 Chemokine Receptor Enables Local CD8+ T Cell Migration for the Destruction of Virus-Infected Cells. *Immunity*, *42*(3), 524–537.

Himmel, M. E., MacDonald, K. G., Garcia, R. V, Steiner, T. S., & Levings, M. K. (2013). Helios+ and Helios- cells coexist within the natural FOXP3+ T regulatory cell subset in humans. *Journal of Immunology*, *190*(5), 2001–8.

Hirahara, K., Liu, L., & Clark, R. (2006). The Majority of Human Peripheral Blod CD4+ CD25highFoxp3+ Regulatory T Cells Bear Functional Skin-Homing Receptors. *The Journal of Immunology*, *177*, 4488–4494.

Hirota, K., Yoshitomi, H., Hashimoto, M., Maeda, S., Teradaira, S., Sugimoto, N., Yamaguchi, T., Nomura, T., Ito, H., Nakamura, T., Sakaguchi, N., & Sakaguchi, S. (2007). Preferential recruitment of CCR6-expressing Th17 cells to inflamed joints via CCL20 in rheumatoid arthritis and its animal model. *The Journal of Experimental Medicine*, *204*(12), 2803–2812.

Honda, T., Egawa, G., Grabbe, S., & Kabashima, K. (2012). Update of Immune Events in the Murine Contact Hypersensitivity Model: Toward the Understanding of Allergic Contact Dermatitis. *Journal of Investigative Dermatology*, *133*(2), 303–315.

Hori, S. (2003). Control of Regulatory T Cell Development by the Transcription Factor Foxp3. *Science*, *299*, 1057–1061.

Howie, D., Waldmann, H., & Cobbold, S. (2014). Nutrient Sensing via mTOR in T Cells Maintains a Tolerogenic Microenvironment. *Frontiers in Immunology*, *5*(August), 1–14.

Huang, C. T., Workman, C. J., Flies, D., Pan, X., Marson, A. L., Zhou, G., Hipkiss, E. L., Ravi, S., Kowalski, J., Levitsky, H. I., Powell, J. D., Pardoll, D. M., Drake, C. G., & Vignali, D. a a. (2004). Role of LAG-3 in regulatory T cells. *Immunity*, *21*(4), 503–513.

Huang, W., Na, L., Fidel, P. L., & Schwarzenberger, P. (2004). Requirement of interleukin-17A for systemic anti-Candida albicans host defense in mice. *The Journal of Infectious Diseases*, *190*(3), 624–31.

Hufford, M. M., Kim, T. S., Sun, J., & Braciale, T. J. (2011). Antiviral CD8+ T cell effector activities in situ are regulated by target cell type. *The Journal of Experimental Medicine*, *208*(1), 167–180.

Huppler, A. R., Bishu, S., & Gaffen, S. L. (2012). Mucocutaneous candidiasis: the IL-17 pathway and implications for targeted immunotherapy. *Arthritis Research & Therapy*, *14*(4), 217.

Hurst, S. D., Muchamuel, T., Gorman, D. M., Gilbert, J. M., Clifford, T., Kwan, S., Menon, S., Seymour, B., Jackson, C., Kung, T. T., Brieland, J. K., Zurawski, S. M., Chapman, R. W., Zurawski, G., & Coffman, R. L. (2002). New IL-17 family members promote Th1 or Th2 responses in the lung: in vivo function of the novel cytokine IL-25. *Journal of Immunology*, *169*(1), 443–453.

Igyártó, B. Z., Haley, K., Ortner, D., Bobr, A., Gerami-Nejad, M., Edelson, B. T., Zurawski, S. M., Malissen, B., Zurawski, G., Berman, J., & Kaplan, D. H. (2011). Skin-Resident Murine Dendritic Cell Subsets Promote Distinct and Opposing Antigen-Specific T Helper Cell Responses. *Immunity*, *35*(2), 260–272.

Ishikawa, H., Ma, Z., & Barber, G. N. (2009). STING regulates intracellular DNA-mediated, type I interferon-dependent innate immunity. *Nature*, *461*(7265), 788–792.

Ishizaki, K., Yamada, A., Yoh, K., Nakano, T., Shimohata, H., Maeda, A., Fujioka, Y., Morito, N., Kawachi, Y., Shibuya, K., Otsuka, F., Shibuya, A., & Takahashi, S. (2007). Th1 and type 1 cytotoxic T cells dominate responses in T-bet overexpression transgenic mice that develop contact dermatitis. *Journal of Immunology*, *178*(1), 605–612.

Itoh, M., Takahashi, T., Sakaguchi, N., Kuniyasu, Y., Shimizu, J., Otsuka, F., & Sakaguchi, S. (1999). Thymus and autoimmunity: production of CD25+CD4+ naturally anergic and suppressive T cells as a key function of the thymus in maintaining immunologic self-tolerance. *J Immunol*, *162*(9), 5317–5326.

Ivanov, I. I., McKenzie, B. S., Zhou, L., Tadokoro, C. E., Lepelley, A., Lafaille, J. J., Cua, D. J., & Littman, D. R. (2006). The Orphan Nuclear Receptor RORγt Directs the Differentiation Program of Proinflammatory IL-17+ T Helper Cells. *Cell*, *126*(6), 1121–1133.

Ivashkiv, L. B., & Donlin, L. T. (2014). Regulation of type I interferon responses. *Nature Reviews. Immunology*, *14*(1), 36–49.

Izcue, A., Hue, S., Buonocore, S., Arancibia-Cárcamo, C. V, Ahern, P. P., Iwakura, Y., Maloy, K. J., & Powrie, F. (2008). Interleukin-23 restrains regulatory T cell activity to drive T cell-dependent colitis. *Immunity*, *28*(4), 559–70.

Jakubzick, C., Gautier, E. L., Gibbings, S. L., Dorothy K. Sojka, Andreas Schlitzer, Theodore E. Johnson, Stoyan Ivanov, Qiaonan Duan, Shashi Bala, Tracy Condon, Nico van Rooijen, John R. Grainger, Yasmine Belkaid, Avi Ma'ayan, David W.H. Riches, Wayne M. Yokoyama, Florent Ginhoux, … Gwendalyn J. Randolph. (2013). Minimal Differentiation of Classical Monocytes as They Survey Steady-State Tissues and Transport Antigen to Lymph Nodes. *Immunity*, *39*(3), 599–610.

Jameson, J., & Havran, W. L. (2007). Skin gd T-cell functions in homeostasis and wound healing. *Immunological Reviews*, *215*(1), 114–122.

Janeway, C. A., & Medzhitov, R. (2002). Innate immune recognition. *Annual Review of Immunology*, *20*(2), 197–216.

Johnston, A., Fritz, Y., Dawes, S. M., Diaconu, D., Al-Attar, P. M., Guzman, A. M., Chen, C. S., Fu, W., Gudjonsson, J. E., McCormick, T. S., & Ward, N. L. (2013). Keratinocyte Overexpression of IL-17C Promotes Psoriasiform Skin Inflammation. *Journal of Immunology*.

Johnston, A., Guzman, A. M., Swindell, W. R., Wang, F., Kang, S., & Gudjonsson, J. E. (2014). Early tissue responses in psoriasis to the antitumour necrosis factor-α biologic etanercept suggest reduced interleukin-17 receptor expression and signalling. *British Journal of Dermatology*, *171*(1), 97–107.

Johnston, A., Xing, X., Guzman, A. M., Riblett, M., Loyd, C. M., Ward, N. L., Wohn, C., Prens, E. P., Wang, F., Maier, L. E., Kang, S., Voorhees, J. J., Elder, J. T., & Gudjonsson, J. E. (2011). IL-1F5, -F6, -F8, and -F9: a novel IL-1 family signaling system that is active in psoriasis and promotes keratinocyte antimicrobial peptide expression. *Journal of Immunology*, *186*(4), 2613–22.

Johnston, A., Xing, X., Swindell, W. R., Kochkodan, J., Riblett, M., Nair, R. P., Stuart, P. E., Ding, J., Voorhees, J. J., Elder, J. T., & Gudjonsson, J. E. (2013). Susceptibility-associated genetic variation at IL12B enhances Th1 polarization in psoriasis. *Human Molecular Genetics*, *22*(9), 1807–1815.

Josefowicz, S. Z., Lu, L.-F., & Rudensky, A. Y. (2012). Regulatory T cells: mechanisms of differentiation and function. *Annual Review of Immunology*, *30*, 531–64.

Jung, N., Hellmann, M., Hoheisel, R., Lehmann, C., Haase, I., Perniok, A., Hallek, M., & Rubbert, A. (2010). An open-label pilot study of the efficacy and safety of anakinra in patients with psoriatic arthritis refractory to or intolerant of methotrexate (MTX). *Clinical Rheumatology*, *29*(10), 1169–1173.

Kaesler, S., Volz, T., Skabytska, Y., Köberle, M., Hein, U., Chen, K. M., Guenova, E., Wölbing, F., Röcken, M., & Biedermann, T. (2014). Toll-like receptor 2 ligands promote chronic atopic dermatitis through IL-4-mediated suppression of IL-10. *Journal of Allergy and Clinical Immunology*, *134*(1).

Kamanaka, M., Kim, S. T., Wan, Y. Y., Sutterwala, F. S., Lara-Tejero, M., Galán, J. E., Harhaj, E., & Flavell, R. a. (2006). Expression of Interleukin-10 in Intestinal Lymphocytes Detected by an Interleukin-10 Reporter Knockin tiger Mouse. *Immunity*, *25*(6), 941–952.

Kariniemi, A.-L. (1977). Effect of human leukocyte interferon on DNA synthesis in human psoriatic skin cultured in diffucion chambers. *Acta Pathologica Microbiologica Scandinavica Section A Pathology*, *85A*(2), 270–272.

Kauffman, C. L., Aria, N., Toichi, E., McCormick, T. S., Cooper, K. D., Gottlieb, A. B., Everitt, D. E., Frederick, B., Zhu, Y., Graham, M. a, Pendley, C. E., & Mascelli, M. A. (2004). A phase I study evaluating the safety, pharmacokinetics, and clinical response of a human IL-12 p40 antibody in subjects with plaque psoriasis. *The Journal of Investigative Dermatology*, *123*(6), 1037–1044.

Keijsers, R. R. M. C., van der Velden, H. M. J., van Erp, P. E. J., de Boer-van Huizen, R. T., Joosten, I., Koenen, H. J. P. M., & van de Kerkhof, P. C. M. (2013). Balance of Treg vs. T-helper cells in the transition from symptomless to lesional psoriatic skin. *The British Journal of Dermatology*, *168*(6), 1294–1302.

Kendal, A. R., Chen, Y., Regateiro, F. S., Ma, J., Adams, E., Cobbold, S. P., Hori, S., & Waldmann, H. (2011). Sustained suppression by Foxp3+ regulatory T cells is vital for infectious transplantation tolerance. *Journal of Experimental Medicine*, *208*(10), 2043–2053.

Kikonomou, K. G., Zachou, K., & Dalekos, G. N. (2011). Alpha-actinin: A multidisciplinary protein with important role in B-cell driven autoimmunity. *Autoimmunity Reviews*, *10*(7), 389–396.

Kim, B. S. (2014). Innate Lymphoid Cells in the Skin. *Journal of Investigative Dermatology*, *135*(3), 673–678.

Kim, B. S., Siracusa, M. C., Saenz, S. a, Noti, M., Monticelli, L. a, Sonnenberg, G. F., Hepworth, M. R., Van Voorhees, A. S., Comeau, M. R., & Artis, D. (2013). TSLP elicits IL-33-independent innate lymphoid cell responses to promote skin inflammation. *Science Translational Medicine*, *5*(170), 170ra16.

Kim, H.-P., & Leonard, W. J. (2007). CREB/ATF-dependent T cell receptor-induced FoxP3 gene expression: a role for DNA methylation. *The Journal of Experimental Medicine*, *204*(7), 1543–1551.

Kim, J. M., Rasmussen, J. P., & Rudensky, A. Y. (2007). Regulatory T cells prevent catastrophic autoimmunity throughout the lifespan of mice. *Nature Immunology*, *8*(2), 191–197.

Kim, S. V, Xiang, W. V, Kwak, C., Yang, Y., Lin, X. W., Ota, M., Sarpel, U., Rifikin, D. B., Xu, R., & Littman, D. R. (2013). GPR15-mediated homing controls immune homeostasis in the large intestine mucosa. *Science*, *340*, 1456–1459.

Kissenpfennig, A., Henri, S., Dubois, B., Laplace-Builhé, C., Perrin, P., Romani, N., Tripp, C. H., Douillard, P., Leserman, L., Kaiserlian, D., Saeland, S., Davoust, J., & Malissen, B. (2005). Dynamics and function of langerhans cells in vivo: Dermal dendritic cells colonize lymph node areasdistinct from slower migrating langerhans cells. *Immunity*, *22*(5), 643–654.

Koch, M. a, Tucker-Heard, G., Perdue, N. R., Killebrew, J. R., Urdahl, K. B., & Campbell, D. J. (2009). The transcription factor T-bet controls regulatory T cell homeostasis and function during type 1 inflammation. *Nature Immunology*, *10*(6), 595–602.

Koenecke, C., Lee, C.-W., Thamm, K., Föhse, L., Schafferus, M., Mittrücker, H.-W., Floess, S., Huehn, J., Ganser, A., Förster, R., & Prinz, I. (2012). IFN-γ Production by Allogeneic Foxp3+ Regulatory T Cells Is Essential for Preventing Experimental Graft-versus-Host Disease. *The Journal of Immunology* , *189* (6), 2890–2896.

Koenen, H. J. P. M., Smeets, R. L., Vink, P. M., Rijssen, E. Van, Boots, A. M. H., & Joosten, I. (2008). Human CD25 high Foxp3 pos regulatory T cells differentiate into IL-17 – producing cells. *Blood*, *112*(6), 2340–2352.

Komatsu, N., Mariotti-Ferrandiz, M. E., Wang, Y., Malissen, B., Waldmann, H., & Hori, S. (2009). Heterogeneity of natural Foxp3+ T cells: a committed regulatory T-cell lineage and an uncommitted minor population retaining plasticity. *Proceedings of the National Academy of Sciences of the United States of America*, *106*(6), 1903–1908.

Komatsu, N., Okamoto, K., Sawa, S., Nakashima, T., Oh-hora, M., Kodama, T., Tanaka, S., Bluestone, J. a, & Takayanagi, H. (2014). Pathogenic conversion of Foxp3+ T cells into TH17 cells in autoimmune arthritis. *Nature Medicine*, *20*(1), 62–8.

Kool, M., van Loo, G., Waelput, W., De Prijck, S., Muskens, F., Sze, M., van Praet, J., Branco-Madeira, F., Janssens, S., Reizis, B., Elewaut, D., Beyaert, R., Hammad, H., & Lambrecht, B. N. (2011). The ubiquitin-editing

protein a20 prevents dendritic cell activation, recognition of apoptotic cells, and systemic autoimmunity. *Immunity*, *35*(1), 82–96.

Koonpaew, S., Shen, S., Flowers, L., & Zhang, W. (2006). LAT-mediated signaling in CD4+CD25+ regulatory T cell development. *The Journal of Experimental Medicine*, *203*(1), 119–129.

Kopp, T., Riedl, E., Bangert, C., Bowman, E. P., Greisenegger, E., Horowitz, A., Kittler, H., Blumenschein, W. M., McClanahan, T. K., Marbury, T., Zachariae, C., Xu, D., Hou, X. S., Mehta, A., Zandvliet, A. S., Montgomery, D., van Aarle, F., & Khalilieh, S. (2015). Clinical improvement in psoriasis with specific targeting of interleukin-23. *Nature*, *521*, 222–226.

Kothary, N., Diak, I. L., Brinker, A., Bezabeh, S., Avigan, M., & Dal Pan, G. (2011). Progressive multifocal leukoencephalopathy associated with efalizumab use in psoriasis patients. *Journal of the American Academy of Dermatology*, *65*(3), 546–551.

Kretschmer, K., Apostolou, I., Hawiger, D., Khazaie, K., Nussenzweig, M. C., & von Boehmer, H. (2005). Inducing and expanding regulatory T cell populations by foreign antigen. *Nature Immunology*, *6*(12), 1219–1227.

Kryczek, I., Bruce, A. T., Gudjonsson, J. E., Johnston, A., Aphale, A., Vatan, L., Szeliga, W., Wang, Y., Liu, Y., Welling, T. H., Elder, J. T., & Zou, W. (2008). Induction of IL-17+ T cell trafficking and development by IFN-gamma: mechanism and pathological relevance in psoriasis. *Journal of Immunology*, *181*(7), 4733–4741.

Kullberg, M. C., Jankovic, D., Feng, C. G., Hue, S., Gorelick, P. L., McKenzie, B. S., Cua, D. J., Powrie, F., Cheever, A. W., Maloy, K. J., & Sher, A. (2006). IL-23 plays a key role in Helicobacter hepaticus-induced T cell-dependent colitis. *The Journal of Experimental Medicine*, *203*(11), 2485–94.

Lahl, K., Loddenkemper, C., Drouin, C., Freyer, J., Arnason, J., Eberl, G., Hamann, A., Wagner, H., Huehn, J., & Sparwasser, T. (2007). Selective depletion of Foxp3+ regulatory T cells induces a scurfy-like disease. *The Journal of Experimental Medicine*, *204*(1), 57–63.

Lai, Y., & Gallo, R. L. (2008). Toll-like receptors in skin infections and inflammatory diseases. *Infectious Disorders Drug Targets*, *8*(3), 144–155.

Lande, R., Botti, E., Jandus, C., Dojcinovic, D., Fanelli, G., Conrad, C., Chamilos, G., Feldmeyer, L., Marinari, B., Chon, S., Vence, L., Riccieri, V., Guillaume, P., Navarini, A. a., Romero, P., Costanzo, A., Piccolella, E., … Frasca, L. (2014). The antimicrobial peptide LL37 is a T-cell autoantigen in psoriasis. *Nature Communications*, *5*(May), 5621.

Lande, R., Ganguly, D., Facchinetti, V., Frasca, L., Conrad, C., Gregorio, J., Meller, S., Chamilos, G., Sebasigari, R., Riccieri, V., Bassett, R., Amuro, H., Fukuhara, S., Ito, T., Liu, Y.-J., & Gilliet, M. (2011). Neutrophils activate plasmacytoid dendritic cells by releasing self-DNA-peptide complexes in systemic lupus erythematosus. *Science Translational Medicine*, *3*(73), 73ra19.

Lande, R., Gregorio, J., Facchinetti, V., Chatterjee, B., Wang, Y.-H., Homey, B., Cao, W., Wang, Y.-H., Su, B., Nestle, F. O., Zal, T., Mellman, I., Schröder, J.-M., Liu, Y.-J., & Gilliet, M. (2007). Plasmacytoid dendritic cells sense self-DNA coupled with antimicrobial peptide. *Nature*, *449*(7162), 564–569.

Langley, R. G., Elewski, B. E., Lebwohl, M., Reich, K., Griffiths, C. E. M., Papp, K. A., Puig, L., Nakagawa, H., Spelman, L., Sigurgeirsson, B., Rivas, E., Tsai, T.-F., Wasel, N., Tyring, S., Salko, T., Hampele, I., Notter, M., … Papavassilis, C. (2014). Secukinumab in Plaque Psoriasis - Results of Two Phase 3 Trials. *The New England Journal of Medicine*, 3–8.

Langrish, C. L., Chen, Y., Blumenschein, W. M., Mattson, J., Basham, B., Sedgwick, J. D., McClanahan, T., Kastelein, R. A., & Cua, D. J. (2005). IL-23 drives a pathogenic T cell population that induces autoimmune inflammation. *The Journal of Experimental Medicine*, *201*(2), 233–40.

Larkin, J., Ahmed, C. M., Wilson, T. D., & Johnson, H. M. (2013). Regulation of interferon gamma signaling by suppressors of cytokine signaling and regulatory T cells. *Frontiers in Immunology*, *4*(DEC), 1–8.

Le Gros, G. (1990). Generation of interleukin 4 (IL-4)-producing cells in vivo and in vitro: IL-2 and IL-4 are required for in vitro generation of IL-4-producing cells. *Journal of Experimental Medicine*, *172*(3), 921–929.

Lebwohl, M., Strober, B., Menter, A., Gordon, K., Weglowska, J., Puig, L., Papp, K. A., Spelman, L., Toth, D., Kerdel, F., Armstrong, A. W., Stingl, G., Kimball, A. B., Bachelez, H., Wu, J. J., Crowley, J., Langley, R. G., … Nirula, A. (2015). Phase 3 Studies Comparing Brodalumab with Ustekinumab in Psoriasis. *New England Journal of Medicine*, *373*(14), 1318–1328.

Lee, E. G., Boone, D. L., Chai, S., Libby, S. L., Chien, M., Lodolce, J. P., & Ma, A. (2000). Failure to regulate TNF-induced NF-kappaB and cell death responses in A20-deficient mice. *Science*, *289*(5488), 2350–2354.

Lee, E., Trepicchio, W. L., Oestreicher, J. L., Pittman, D., Wang, F., Chamian, F., Dhodapkar, M., & Krueger, J. G. (2004). Increased expression of interleukin 23 p19 and p40 in lesional skin of patients with psoriasis vulgaris. *The Journal of Experimental Medicine*, *199*(1), 125–30.

Lee, H. M., Bautista, J. L., Scott-Browne, J., Mohan, J. F., & Hsieh, C. S. (2012). A Broad Range of Self-Reactivity Drives Thymic Regulatory T Cell Selection to Limit Responses to Self. *Immunity*, *37*(3), 475–486.

Lee, S. E., Li, X., Kim, J. C. K., Lee, J., González-Navajas, J. M., Hong, S. H., Park, I. K., Rhee, J. H., & Raz, E. (2012). Type i interferons maintain Foxp3 expression and T-regulatory cell functions under inflammatory conditions in mice. *Gastroenterology*, *143*(1), 145–154.

Lee, Y., Awasthi, A., Yosef, N., Quintana, F. J., Xiao, S., Peters, A., Wu, C., Kleinewietfeld, M., Kunder, S., Hafler, D. a, Sobel, R. a, Regev, A., & Kuchroo, V. K. (2012). Induction and molecular signature of pathogenic TH17 cells. *Nature Immunology*, *13*(10), 991–999.

Lehtimäki, S., Savinko, T., Lahl, K., Sparwasser, T., Wolff, H., Lauerma, A., Alenius, H., & Fyhrquist, N. (2012). The Temporal and Spatial Dynamics of Foxp3+ Treg Cell–Mediated Suppression during Contact Hypersensitivity Responses in a Murine Model. *Journal of Investigative Dermatology*, *132*, 2744–2751.

Leonardi, C. L., Powers, J. L., Matheson, R. T., Goffe, B. S., Zitnik, R., Wang, A., & Gottlieb, A. B. (2003). Etanercept as monotherapy in patients with psoriasis. *The New England Journal of Medicine*, *349*(21), 2014–2022.

Leonardi, C., Matheson, R., Zachariae, C., Cameron, G., Li, L., Edson-Heredia, E., Braun, D., & Banerjee, S. (2012). Anti-interleukin-17 monoclonal antibody ixekizumab in chronic plaque psoriasis. *The New England Journal of Medicine*, *366*(13), 1190–9.

Leyva-Castillo, J. M., Hener, P., Michea, P., Karasuyama, H., Chan, S., Soumelis, V., & Li, M. (2013). Skin thymic stromal lymphopoietin initiates Th2 responses through an orchestrated immune cascade. *Nature Communications*, *4*(May), 2847.

Liang, S. C., Tan, X.-Y., Luxenberg, D. P., Karim, R., Dunussi-Joannopoulos, K., Collins, M., & Fouser, L. a. (2006). Interleukin (IL)-22 and IL-17 are coexpressed by Th17 cells and cooperatively enhance expression of antimicrobial peptides. *The Journal of Experimental Medicine*, *203*(10), 2271–2279.

Lin, F.-C., & Young, H. a. (2013). The talented interferon-gamma. *Advances in Bioscience and Biotechnology*, *04*(07), 6–13.

Lin, W. J., Norris, D. a., Achziger, M., Kotzin, B. L., & Tomkinson, B. (2001). Oligoclonal expansion of intraepidermal t cells in psoriasis skin lesions. *Journal of Investigative Dermatology*, *117*(6), 1546–1553.

Liu, K., Victora, G. D., Schwickert, T. A., Guermonprez, P., Meredith, M. M., Yao, K., Chu, F.-F., Randolph, G. J., Rudensky, A. Y., & Nussenzweig, M. (2009). In vivo analysis of dendritic cell development and homeostasis. *Science*, *324*(5925), 392–397.

Liu, P. T., Stenger, S., Li, H., Wenzel, L., Tan, B. H., Krutzik, S. R., Ochoa, M. T., Schauber, J., Wu, K., Meinken, C., Kamen, D. L., Wagner, M., Bals, R., Steinmeyer, A., Zügel, U., Gallo, R. L., Eisenberg, D., … Modlin, R. L. (2006). Toll-like receptor triggering of a vitamin D-mediated human antimicrobial response. *Science*, *311*(5768), 1770–1773.

Liu, Y., Helms, C., Liao, W., Zaba, L. C., Duan, S., Gardner, J., Wise, C., Miner, A., Malloy, M. J., Pullinger, C. R., Kane, J. P., Saccone, S., Worthington, J., Bruce, I., Kwok, P. Y., Menter, A., Krueger, J., … Bowcock, A. M. (2008). A genome-wide association study of psoriasis and psoriatic arthritis identifies new disease loci. *PLoS Genetics*, *4*(3).

Liu, Y., Krueger, J. G., & Bowcock, a M. (2007). Psoriasis: genetic associations and immune system changes. *Genes and Immunity*, *8*(1), 1–12.

Lizzul, P. F., Aphale, A., Malaviya, R., Sun, Y., Masud, S., Dombrovskiy, V., & Gottlieb, A. B. (2005). Differential expression of phosphorylated NF-kappaB/RelA in normal and psoriatic epidermis and downregulation of NF-

kappaB in response to treatment with etanercept. *The Journal of Investigative Dermatology*, *124*(6), 1275–1283.

Long, M., Park, S.-G., Strickland, I., Hayden, M. S., & Ghosh, S. (2009). Nuclear factor-kappaB modulates regulatory T cell development by directly regulating expression of Foxp3 transcription factor. *Immunity*, *31*(6), 921–931.

Lövgren, T., Eloranta, M.-L., Kastner, B., Wahren-Herlenius, M., Alm, G. V, & Rönnblom, L. (2006). Induction of interferon-alpha by immune complexes or liposomes containing systemic lupus erythematosus autoantigen- and Sjögren's syndrome autoantigen-associated RNA. *Arthritis and Rheumatism*, *54*(6), 1917–1927.

Lowes, M. a, Kikuchi, T., Fuentes-Duculan, J., Cardinale, I., Zaba, L. C., Haider, A. S., Bowman, E. P., & Krueger, J. G. (2008). Psoriasis vulgaris lesions contain discrete populations of Th1 and Th17 T cells. *The Journal of Investigative Dermatology*, *128*(5), 1207–1211.

Lowes, M. a, Suárez-Fariñas, M., & Krueger, J. G. (2014). Immunology of Psoriasis. *Annual Review of Immunology*, *32*, 227–55.

Lowes, M. A., Chamian, F., Abello, M. V., Fuentes-Duculan, J., Lin, S.-L., Nussbaum, R., Novitskaya, I., Carbonaro, H., Cardinale, I., Kikuchi, T., Gilleaudeau, P., Sullivan-Whalen, M., Wittkowski, K. M., Papp, K. A., Garovoy, M., Dummer, W., Steinman, R. M., & Krueger, J. G. (2005). Increase in TNF-alpha and inducible nitric oxide synthase-expressing dendritic cells in psoriasis and reduction with efalizumab (anti-CD11a). *Proceedings of the National Academy of Sciences of the United States of America*, *102*(52), 19057–19062.

Lu, B., Ferrandino, A. F., & Flavell, R. a. (2004). Gadd45beta is important for perpetuating cognate and inflammatory signals in T cells. *Nature Immunology*, *5*(1), 38–44.

Luger, T. A., Stadler, B. M., Luger, B. M., Mathieson, B. J., Mage, M., Schmidt, J. A., & Oppenheim, J. J. (1982). Murine epidermal cell-derived thymocyte-activating factor resembles murine interleukin 1. *Journal of Immunology*, *128*(5), 2147–2152.

Mackay, L. K., Rahimpour, A., Ma, J. Z., Collins, N., Stock, A. T., Hafon, M.-L., Vega-Ramos, J., Lauzurica, P., Mueller, S. N., Stefanovic, T., Tscharke, D. C., Heath, W. R., Inouye, M., Carbone, F. R., & Gebhardt, T. (2013). The developmental pathway for CD103(+)CD8+ tissue-resident memory T cells of skin. *Nature Immunology*, *14*(12), 1294–301.

Mahan, C. S., Thomas, J. J., Boom, W. H., & Rojas, R. E. (2009). CD4 + CD25 high Foxp3 + regulatory T cells downregulate human Vd2 + T-lymphocyte function triggered by anti-CD3 or phosphoantigen. *Immunology*, *127*(3), 398–407.

Malissen, B., Tamoutounour, S., & Henri, S. (2014). The origins and functions of dendritic cells and macrophages in the skin. *Nature Reviews. Immunology*, *14*(6), 417–28.

Mangan, P. R., Harrington, L. E., O'Quinn, D. B., Helms, W. S., Bullard, D. C., Elson, C. O., Hatton, R. D., Wahl, S. M., Schoeb, T. R., & Weaver, C. T. (2006). Transforming growth factor-beta induces development of the T(H)17 lineage. *Nature*, *441*(7090), 231–4.

Marson, A., Kretschmer, K., Frampton, G. M., Jacobsen, E. S., Polansky, J. K., MacIsaac, K. D., Levine, S. S., Fraenkel, E., von Boehmer, H., & Young, R. a. (2007). Foxp3 occupancy and regulation of key target genes during T-cell stimulation. *Nature*, *445*(7130), 931–935.

Mccully, M. L., Ladell, K., Hakobyan, S., Mansel, R. E., Price, D. a, Dc, W., & Moser, B. (2013). Epidermis instructs skin homing receptor expression in human T cells Epidermis instructs skin homing receptor expression in human T cells, *120*(23), 4591–4598.

McCully, M. L., Ladell, K., Hakobyan, S., Mansel, R. E., Price, D. a, & Moser, B. (2012). Epidermis instructs skin homing receptor expression in human T cells. *Blood*, *120*(23), 4591–8.

McGeachy, M. J., Bak-Jensen, K. S., Chen, Y., Tato, C. M., Blumenschein, W., McClanahan, T., & Cua, D. J. (2007). TGF-beta and IL-6 drive the production of IL-17 and IL-10 by T cells and restrain T(H)-17 cell-mediated pathology. *Nature Immunology*, *8*(12), 1390–1397.

McGeachy, M. J., Chen, Y., Tato, C. M., Laurence, A., Joyce-Shaikh, B., Blumenschein, W. M., McClanahan, T. K., O'Shea, J. J., & Cua, D. J. (2009). The interleukin 23 receptor is essential for the terminal differentiation of interleukin 17-producing effector T helper cells in vivo. *Nature Immunology*, *10*(3), 314–24.

McGill, J., & Legge, K. L. (2009). Cutting edge: contribution of lung-resident T cell proliferation to the overall magnitude of the antigen-specific CD8 T cell response in the lungs following murine influenza virus infection. *Journal of Immunology*, *183*(7), 4177–4181.

McNab, F., Mayer-barber, K., Sher, A., Wack, A., & Garra, A. O. (2015). Type I interferons in infectious disease. *Nature Reviews Immunology*, *15*(2), 87–103.

McNally, A., Hill, G. R., Sparwasser, T., Thomas, R., & Steptoe, R. J. (2011). CD4+CD25+ regulatory T cells control CD8+ T-cell effector differentiation by modulating IL-2 homeostasis. *Proceedings of the National Academy of Sciences of the United States of America*, *108*(18), 7529–7534.

Means, T. K., Latz, E., Hayashi, F., Murali, M. R., Golenbock, D. T., & Luster, A. D. (2005). Human lupus autoantibody-DNA complexes activate DCs through cooperation of CD32 and TLR9. *Journal of Clinical Investigation*, *115*(2), 407–417.

Medoff, B. D., Sandall, B. P., Landry, A., Nagahama, K., Mizoguchi, A., Luster, A. D., & Xavier, R. J. (2009). Differential requirement for CARMA1 in agonist-selected T-cell development. *European Journal of Immunology*, *39*(1), 78–84.

Meir, K. S. (2004). Atherosclerosis in the Apolipoprotein E-Deficient Mouse: A Decade of Progress. *Arteriosclerosis, Thrombosis, and Vascular Biology*, *24*(6), 1006–1014.

Merad, M., Sathe, P., Helft, J., Miller, J., & Mortha, A. (2013). The dendritic cell lineage: ontogeny and function of dendritic cells and their subsets in the steady state and the inflamed setting. *Annual Review of Immunology*, *31*, 563–604.

Miller, L. S. (2008). Toll-Like Receptors in Skin. *Advances in Dermatology*, *24*(C), 71–87.

Miyao, T., Floess, S., Setoguchi, R., Luche, H., Fehling, H. J., Waldmann, H., Huehn, J., & Hori, S. (2012). Plasticity of Foxp3 + T Cells Reflects Promiscuous Foxp3 Expression in Conventional T Cells but Not Reprogramming of Regulatory T Cells. *Immunity*, *36*(2), 262–275.

Monroe, K. M., McWhirter, S. M., & Vance, R. E. (2010). Induction of type I interferons by bacteria. *Cellular Microbiology*, *12*(7), 881–890.

Monticelli, L. a, Sonnenberg, G. F., Abt, M. C., Alenghat, T., Ziegler, C. G. K., Doering, T. a, Angelosanto, J. M., Laidlaw, B. J., Yang, C. Y., Sathaliyawala, T., Kubota, M., Turner, D., Diamond, J. M., Goldrath, A. W., Farber, D. L., Collman, R. G., Wherry, E. J., & Artis, D. (2011). Innate lymphoid cells promote lung-tissue homeostasis after infection with influenza virus. *Nature Immunology*, *12*(11), 1045–1054.

Moore-Connors, J. M., Fraser, R., Halperin, S. a, & Wang, J. (2013). CD4+CD25+Foxp3+ Regulatory T Cells Promote Th17 Responses and Genital Tract Inflammation upon Intracellular Chlamydia muridarum Infection. *Journal of Immunology*, *191*(6), 3430–9.

Mor, A., Planer, D., Luboshits, G., Afek, A., Metzger, S., Chajek-Shaul, T., Keren, G., & George, J. (2007). Role of naturally occurring CD4+ CD25+ regulatory T cells in experimental atherosclerosis. *Arteriosclerosis, Thrombosis, and Vascular Biology*, *27*(4), 893–900.

Morrissey, P. J., Charrier, K., Braddy, S., Liggitt, D., & Watson, J. D. (1993). CD4+ T cells that express high levels of CD45RB induce wasting disease when transferred into congenic severe combined immunodeficient mice. Disease development is prevented by cotransfer of purified CD4+ T cells. *The Journal of Experimental Medicine*, *178*(1), 237–244.

Mosmann, T. R. R., Cherwinski, H. M., Bond, M. W., Giedlin, M. A., & Coffman, R. L. (1986). Two types of murine helper T cell clone. I. Definition according to profiles of lymphokine activities and secreted proteins. *The Journal of Immunology*, *136*(7), 2348.

Mullen, a C., High, F. a, Hutchins, a S., Lee, H. W., Villarino, a V, Livingston, D. M., Kung, a L., Cereb, N., Yao, T. P., Yang, S. Y., & Reiner, S. L. (2001). Role of T-bet in commitment of TH1 cells before IL-12-dependent selection. *Science*, *292*(5523), 1907–1910.

Murai, M., Turovskaya, O., Kim, G., Madan, R., Karp, C. L., Cheroutre, H., & Kronenberg, M. (2009). Interleukin 10 acts on regulatory T cells to

maintain expression of the transcription factor Foxp3 and suppressive function in mice with colitis. *Nature Immunology*, *10*(11), 1178–1184.

Murali-Krishna, K., Altman, J. D., Suresh, M., Sourdive, D. J. D., Zajac, A. J., Miller, J. D., Slansky, J., & Ahmed, R. (1998). Counting antigen-specific CD8 T cells: A reevaluation of bystander activation during viral infection. *Immunity*, *8*(2), 177–187.

Muranski, P., & Restifo, N. P. (2013). Essentials of Th17 cell commitment and plasticity. *Blood*, *121*(13), 2402–2414.

Murphy, J. E., Robert, C., & Kupper, T. S. (2000). Interleukin-1 and cutaneous inflammation: A crucial link between innate and acquired immunity. *Journal of Investigative Dermatology*, *114*(3), 602–608.

Murray, H. W. (1979). Macrophage oxygen-dependent antimicrobial activity. II. The role of oxygen intermediates. *Journal of Experimental Medicine*, *150*(4), 950–964.

Muth, S., Schutze, K., Schild, H., & Probst, H. C. (2012). Release of dendritic cells from cognate CD4+ T-cell recognition results in impaired peripheral tolerance and fatal cytotoxic T-cell mediated autoimmunity. *Proceedings of the National Academy of Sciences*, *109*(23), 9059–9064.

Nair, R. P., Duffin, K. C., Helms, C., Ding, J., Stuart, P. E., Goldgar, D., Gudjonsson, J. E., Li, Y., Tejasvi, T., Feng, B.-J., Ruether, A., Schreiber, S., Weichenthal, M., Gladman, D., Rahman, P., Schrodi, S. J., Prahalad, S., … Abecasis, G. R. (2009). Genome-wide scan reveals association of psoriasis with IL-23 and NF-kappaB pathways. *Nature Genetics*, *41*(2), 199–204.

Nair, R. P., Ruether, A., Stuart, P. E., Jenisch, S., Tejasvi, T., Hiremagalore, R., Schreiber, S., Kabelitz, D., Lim, H. W., Voorhees, J. J., Christophers, E., Elder, J. T., & Weichenthal, M. (2008). Polymorphisms of the IL12B and IL23R genes are associated with psoriasis. *The Journal of Investigative Dermatology*, *128*(7), 1653–1661.

Nair, R. P., Stuart, P. E., Nistor, I., Hiremagalore, R., Chia, N. V. C., Jenisch, S., Weichenthal, M., Abecasis, G. R., Lim, H. W., Christophers, E., Voorhees, J. J., & Elder, J. T. (2006). Sequence and haplotype analysis supports HLA-C as the psoriasis susceptibility 1 gene. *American Journal of Human Genetics*, *78*(5), 827–851.

Nakanishi, Y., Lu, B., Gerard, C., & Iwasaki, A. (2009). CD8(+) T lymphocyte mobilization to virus-infected tissue requires CD4(+) T-cell help. *Nature*, *462*(7272), 510–513.

Natsuaki, Y., Egawa, G., Satoshi Nakamizo, Sachiko Ono, Sho Hanakawa, Takaharu Okada, Nobuhiro Kusuba, Atsushi Otsuka, Akihiko Kitoh, Tetsuya Honda, Saeko Nakajima, Soken Tsuchiya, Yukihiko Sugimoto, Ken J Ishii, Hiroko Tsutsui, Hideo Yagita, Yoichiro Iwakura, … Kenji Kabashima. (2014). Perivascular leukocyte clusters are essential for efficient activation of effector T cells in the skin. *Nature Immunology*, *15*(11), 1064–1069.

Nestle, F. O., Conrad, C., Tun-Kyi, A., Homey, B., Gombert, M., Boyman, O., Burg, G., Liu, Y.-J., & Gilliet, M. (2005). Plasmacytoid predendritic cells initiate psoriasis through interferon-alpha production. *The Journal of Experimental Medicine*, *202*(1), 135–143.

Nestle, F. O., Kaplan, D. H., & Barker, J. (2009). Psoriasis. *New England Journal of Medicine*, *361*(5), 496–509.

Nguyen, L. P., Pan, J., Dinh, T. T., Hadeiba, H., O'Hara, E., Ebtikar, A., Hertweck, A., Gökmen, M. R., Lord, G. M., Jenner, R. G., Butcher, E. C., & Habtezion, A. (2014). Role and species-specific expression of colon T cell homing receptor GPR15 in colitis. *Nature Immunology*, *16*(2), 207–213.

Nguyen, L. T., & Ohashi, P. S. (2015). Clinical blockade of PD1 and LAG3 — potential mechanisms of action. *Nature Reviews Immunology*, *15*(1), 45–56.

Nickoloff, B. J., & Nestle, F. O. (2004). Science in medicine Recent insights into the immunopathogenesis of psoriasis provide new therapeutic opportunities. *Journal of Clinical Investigation*, *113*(12), 1664–1675.

Nishizuka, Y., & Sakakura, T. (1969). Thymus and reproduction: sex-linked dysgenesia of the gonad after neonatal thymectomy in mice. *Science*, *166*(906), 753–755.

Nurieva, R. I., Chung, Y., Martinez, G. J., Yang, X. O., Tanaka, S., Matskevitch, T. D., Wang, Y.-H., & Dong, C. (2009). Bcl6 mediates the development of T follicular helper cells. *Science*, *325*(5943), 1001–1005.

Ohnmacht, C., Park, J.-H., Cording, S., Wing, J. B., Atarashi, K., Obata, Y., Gaboriau-Routhiau, V., Marques, R., Dulauroy, S., Fedoseeva, M., Busslinger, M., Cerf-Bensussan, N., Boneca, I. G., Voehringer, D., Hase, K., Honda, K., Sakaguchi, S., & Eberl, G. (2015). The microbiota regulates type 2 immunity through RORgt+ T cells. *Science*, *349*(6251), 989–993.

Oldenhove, G., Bouladoux, N., Wohlfert, E. a., Hall, J. a., Chou, D., Dos santos, L., O'Brien, S., Blank, R., Lamb, E., Natarajan, S., Kastenmayer, R., Hunter, C., Grigg, M. E., & Belkaid, Y. (2009). Decrease of Foxp3+ Treg Cell Number and Acquisition of Effector Cell Phenotype during Lethal Infection. *Immunity*, *31*(5), 772–786.

Oliphant, C. J., Hwang, Y. Y., Walker, J. A., Salimi, M., Wong, S. H., Brewer, J. M., Englezakis, A., Barlow, J. L., Hams, E., Scanlon, S. T., Ogg, G. S., Fallon, P. G., & McKenzie, A. N. J. (2014). MHCII-Mediated Dialog between Group 2 Innate Lymphoid Cells and CD4+ T Cells Potentiates Type 2 Immunity and Promotes Parasitic Helminth Expulsion. *Immunity*, *41*(2), 283–295.

Onishi, Y., Fehervari, Z., Yamaguchi, T., & Sakaguchi, S. (2008). Foxp3+ natural regulatory T cells preferentially form aggregates on dendritic cells in vitro and actively inhibit their maturation. *Proceedings of the National Academy of Sciences of the United States of America*, *105*(29), 10113–10118.

Ortega, C., Fernández-A, S., Carrillo, J. M., Romero, P., Molina, I. J., Moreno, J. C., & Santamaría, M. (2009). IL-17-producing CD8+ T lymphocytes from psoriasis skin plaques are cytotoxic effector cells that secrete Th17-related cytokines. *Journal of Leukocyte Biology*, *86*(2), 435–443.

Ouchi, T., Kubo, A., Yokouchi, M., Adachi, T., Kobayashi, T., Kitashima, D. Y., Fujii, H., Clausen, B. E., Koyasu, S., Amagai, M., & Nagao, K. (2011). Langerhans cell antigen capture through tight junctions confers preemptive immunity in experimental staphylococcal scalded skin syndrome. *The Journal of Experimental Medicine*, *208*(13), 2607–13.

Ouyang, W., Liao, W., Luo, C. T., Yin, N., Huse, M., Kim, M. V, Peng, M., Chan, P., Ma, Q., Mo, Y., Meijer, D., Zhao, K., Rudensky, A. Y., Atwal, G., Zhang, M. Q., & Li, M. O. (2012). Novel Foxo1-dependent transcriptional programs control T(reg) cell function. *Nature*, *491*(7425), 554–9.

Pantelyushin, S., Haak, S., Ingold, B., Kulig, P., Heppner, F. L., Navarini, A. A., & Becher, B. (2012). Rorγt + innate lymphocytes and γδ T cells initiate psoriasiform plaque formation in mice. *The Journal of Clinical Investigation*, *122*(6), 2252–2256.

Papp, K. A., Langley, R. G., Lebwohl, M., Krueger, G. G., Szapary, P., Yeilding, N., Guzzo, C., Hsu, M.-C., Wang, Y., Li, S., Dooley, L. T., & Reich, K. (2008). Efficacy and safety of ustekinumab, a human interleukin-12/23 monoclonal antibody, in patients with psoriasis: 52-week results from a randomised, double-blind, placebo-controlled trial (PHOENIX 2). *Lancet*, *371*(9625), 1675–84.

Papp, K. A., Leonardi, C., Menter, A., Ortonne, J.-P., Krueger, J. G., Kricorian, G., Aras, G., Li, J., Russell, C. B., Thompson, E. H. Z., & Baumgartner, S. (2012). Brodalumab, an anti-interleukin-17-receptor antibody for psoriasis. *The New England Journal of Medicine*, *366*(13), 1181–9.

Papp, K. A., Poulin, Y., Bissonnette, R., Bourcier, M., Toth, D., Rosoph, L., Poulin-Costello, M., Setterfield, M., & Syrotuik, J. (2012). Assessment of the long-term safety and effectiveness of etanercept for the treatment of psoriasis in an adult population. *Journal of the American Academy of Dermatology*, *66*(2), e33–e45.

Parisi, R., Symmons, D. P. M., Griffiths, C. E. M., & Ashcroft, D. M. (2012). Global Epidemiology of Psoriasis: A Systematic Review of Incidence and Prevalence. *Journal of Investigative Dermatology*, *133*(2), 377–385.

Pasparakis, M., Haase, I., & Nestle, F. O. (2014). Mechanisms regulating skin immunity and inflammation. *Nature Reviews Immunology*, *14*(5), 289–301.

Penaloza-MacMaster, P., Kamphorst, a. O., Wieland, a., Araki, K., Iyer, S. S., West, E. E., O'Mara, L., Yang, S., Konieczny, B. T., Sharpe, a. H., Freeman, G. J., Rudensky, a. Y., & Ahmed, R. (2014). Interplay between regulatory T cells and PD-1 in modulating T cell exhaustion and viral control during chronic LCMV infection. *Journal of Experimental Medicine*, *211*(9), 1905–1918.

Perera, G. K., Di Meglio, P., & Nestle, F. O. (2012). Psoriasis. *Annual Review of Pathology*, *7*, 385–422.

Pipkin, M. E., Sacks, J. a., Cruz-Guilloty, F., Lichtenheld, M. G., Bevan, M. J., & Rao, A. (2010). Interleukin-2 and Inflammation Induce Distinct Transcriptional Programs that Promote the Differentiation of Effector Cytolytic T Cells. *Immunity*, *32*(1), 79–90.

Poulin, L. F., Henri, S., de Bovis, B., Devilard, E., Kissenpfennig, A., & Malissen, B. (2007). The dermis contains langerin+ dendritic cells that develop and function independently of epidermal Langerhans cells. *The Journal of Experimental Medicine*, *204*(13), 3119–31.

Powrie, F., Leach, M. W., Mauze, S., Caddle, L. B., & Coffman, R. L. (1993). Phenotypically distinct subsets of CD4+ T cells induce or protect from chronic intestinal inflammation in C. B-17 scid mice. *International Immunology*, *5*(11), 1461–1471.

Powrie, F., & Mason, D. (1990). OX-22high CD4+ T cells induce wasting disease with multiple organ pathology: prevention by the OX-22low subset. *The Journal of Experimental Medicine*, *172*(6), 1701–1708.

Puel, A., Cypowyj, S., Maródi, L., Abel, L., Picard, C., & Casanova, J.-L. (2012). Inborn errors of human IL-17 immunity underlie chronic mucocutaneous candidiasis. *Current Opinion in Allergy and Clinical Immunology*, *12*(6), 616–622.

Rajan, N., & Langtry, J. A. A. (2006). Generalized exacerbation of psoriasis associated with imiquimod cream treatment of superficial basal cell carcinomas. *Clinical and Experimental Dermatology*, *31*(1), 140–1.

Ramirez, K., Witherden, D. a., & Havran, W. L. (2015). All hands on DE(T)C: Epithelial-resident γδ T cells respond to tissue injury. *Cellular Immunology*, *296*(1), 57–61.

Rao, R. R., Li, Q., Odunsi, K., & Shrikant, P. a. (2010). The mTOR Kinase Determines Effector versus Memory CD8+ T Cell Fate by Regulating the Expression of Transcription Factors T-bet and Eomesodermin. *Immunity*, *32*(1), 67–78.

Rashighi, M., Agarwal, P., Richmond, J. M., Harris, T. H., Dresser, K., Su, M.-W., Zhou, Y., Deng, A., Hunter, C. a, Luster, A. D., & Harris, J. E. (2014). CXCL10 is critical for the progression and maintenance of depigmentation in a mouse model of vitiligo. *Science Translational Medicine*, *6*(223), 223ra23.

Res, P. C. M., Piskin, G., de Boer, O. J., van der Loos, C. M., Teeling, P., Bos, J. D., & Teunissen, M. B. M. (2010). Overrepresentation of IL-17A and IL-22 Producing CD8 T Cells in Lesional Skin Suggests Their Involvement in the pathogenesis of psoriasis. *PLoS ONE*, *5*(11).

Rodriguez, R. S., Pauli, M. L., Neuhaus, I. M., Yu, S. S., Arron, S. T., Harris, H. W., Yang, S. H.-Y., Anthony, B. A., Sverdrup, F. M., Krow-Lucal, E., Mackenzie, T. C., Johnson, D. S., Meyer, E. H., Löhr, A., Hsu, A., Koo, J., Liao, W., … Rosenblum, M. D. (2014). Memory regulatory T cells reside in human skin. *The Journal of Clinical Investigation*, *124*(3), 1–10.

Roediger, B., Kyle, R., Yip, K. H., Nital Sumaria, Thomas V Guy, Brian S Kim, Andrew J Mitchell, Szun S Tay, Rohit Jain, Elizabeth Forbes-Blom, Xi

Chen, Philip L Tong, Holly A Bolton, David Artis, William E Paul, Barbara Fazekas de St Groth, Michele A Grimbaldeston, … Wolfgang Weninger. (2013). Cutaneous immunosurveillance and regulation of inflammation by group 2 innate lymphoid cells. *Nature Immunology*, *14*(6), 564–573.

Rooijen, N. Van, & Hendrikx, E. (2010). *Chapter 13: Liposomes, Methods in Molecular Biology* (Vol. 605).

Rosenblum, M. D., Gratz, I. K., Paw, J. S., Lee, K., Marshak-Rothstein, A., & Abbas, A. K. (2011). Response to self antigen imprints regulatory memory in tissues. *Nature*, *480*(7378), 538–542.

Ross, E. M., Bourges, D., Hogan, T. V., Gleeson, P. a., & van Driel, I. R. (2014). Helios defines T cells being driven to tolerance in the periphery and thymus. *European Journal of Immunology*, *44*(7), 2048–2058.

Rubtsov, Y. P., Rasmussen, J. P., Chi, E. Y., Fontenot, J., Castelli, L., Ye, X., Treuting, P., Siewe, L., Roers, A., Henderson, W. R., Muller, W., & Rudensky, A. Y. (2008). Regulatory T Cell-Derived Interleukin-10 Limits Inflammation at Environmental Interfaces. *Immunity*, *28*(4), 546–558.

Rudra, D., deRoos, P., Chaudhry, A., Niec, R. E., Arvey, A., Samstein, R. M., Leslie, C., Shaffer, S. a, Goodlett, D. R., & Rudensky, A. Y. (2012). Transcription factor Foxp3 and its protein partners form a complex regulatory network. *Nature Immunology*, *13*(10), 1010–1019.

Ruefli-Brasse, A. A., French, D. M., & Dixt, V. M. (2003). Regulation of NF-kB – Dependent Lymphocyte Activation and Development by Paracaspase. *Science*, *302*, 1581–1584.

Ruland, J., Duncan, G. S., Wakeham, A., & Mak, T. W. (2003). Differential requirement for Malt1 in T and B cell antigen receptor signaling. *Immunity*, *19*(5), 749–758.

Russel, T. J., Schultes, L. M., & Kuban, D. J. (1972). Histocompatibility (HL-A) Antigens Associated with Psoriasis. *New England Journal of Medicine*, 738–740.

Sakaguchi, S., Sakaguchi, N., Asano, M., Itoh, M., & Toda, M. (1995). Immunologic Self-Tolerance Maintained by Activated T Cells Expressing IL-2 Receptor a-Chains (CD25). *The Journal of Immunoloy*, *155*, 1151–1164.

Sakaguchi, S., Takahashi, T., & Nishizuka, Y. (1982). Study on cellular events in post-thymectomy autoimmune oophoritis in mice. II. Requirement of Lyt-1 cells in normal female mice for the prevention of oophoritis. *The Journal of Experimental Medicine*, *156*(6), 1577–1586.

Sakaguchi, S., Yamaguchi, T., Nomura, T., & Ono, M. (2008). Regulatory T Cells and Immune Tolerance. *Cell*, *133*(5), 775–787.

Salimi, M., Barlow, J. L., Saunders, S. P., Xue, L., Gutowska-Owsiak, D., Wang, X., Huang, L.-C., Johnson, D., Scanlon, S. T., McKenzie, A. N. J., Fallon, P. G., & Ogg, G. S. (2013). A role for IL-25 and IL-33-driven type-2 innate lymphoid cells in atopic dermatitis. *The Journal of Experimental Medicine*, *210*(13), 2939–50.

Sanford, M., & McKeage, K. (2015). Secukinumab: First Global Approval. *Drugs*, *75*(3), 329–338.

Sather, B. D., Treuting, P., Perdue, N., Miazgowicz, M., Fontenot, J. D., Rudensky, A. Y., & Campbell, D. J. (2007). Altering the distribution of Foxp3+ regulatory T cells results in tissue-specific inflammatory disease. *The Journal of Experimental Medicine*, *204*(6), 1335–1347.

Savinko, T., Matikainen, S., Saarialho-Kere, U., Lehto, M., Wang, G., Lehtimäki, S., Karisola, P., Reunala, T., Wolff, H., Lauerma, A., & Alenius, H. (2012). IL-33 and ST2 in Atopic Dermatitis: Expression Profiles and Modulation by Triggering Factors. *The Journal of Investigative Dermatology*, *132*.

Sawant, D. V, Sehra, S., Nguyen, E. T., Jadhav, R., Englert, K., Shinnakasu, R., Hangoc, G., Broxmeyer, H. E., Nakayama, T., Perumal, N. B., Kaplan, M. H., & Dent, A. L. (2012). Bcl6 controls the Th2 inflammatory activity of regulatory T cells by repressing Gata3 function. *Journal of Immunology*, *189*(10), 4759–69.

Schauber, J., Dorschner, R. A., Coda, A. B., Büchau, A. S., Liu, P. T., Kiken, D., Helfrich, Y. R., Kang, S., Elalieh, H. Z., Steinmeyer, A., Zügel, U., Bikle, D. D., Modlin, R. L., & Gallo, R. L. (2007). Injury enhances TLR2 function and antimicrobial peptide expression through a vitamin D–dependent mechanism. *Journal of Clinical Investigation*, *3*(17), 803–811.

Schenkel, J. M., Fraser, K. A., Beura, L. K., Pauken, K. E., Vezys, V., & Masopust, D. (2014). Resident memory CD8 T cells trigger protective innate and adaptive immune responses. *Science*, *346*(6205), 98–101.

Schiering, C., Krausgruber, T., Chomka, A., Fröhlich, A., Adelmann, K., Wohlfert, E. A., Pott, J., Griseri, T., Bollrath, J., Hegazy, A. N., Harrison, O. J., Owens, B. M. J., Löhning, M., Belkaid, Y., Fallon, P. G., & Powrie, F. (2014). The alarmin IL-33 promotes regulatory T-cell function in the intestine. *Nature*, *513*(7519), 564–568.

Schmid, P., Itin, P., Cox, D., McMaster, G. K., & Horisberger, M. A. (1994). The type I interferon system is locally activated in psoriatic lesions. *Journal of Interferon Research*, *14*(5), 229–234.

Schmidt-Supprian, M., Courtois, G., Tian, J., Coyle, A. J., Israël, A., Rajewsky, K., & Pasparakis, M. (2003). Mature T cells depend on signaling through the IKK complex. *Immunity*, *19*(3), 377–389.

Schmidt-Supprian, M., Tian, J., Grant, E. P., Pasparakis, M., Maehr, R., Ovaa, H., Ploegh, H. L., Coyle, A. J., & Rajewsky, K. (2004). Differential dependence of CD4+CD25+ regulatory and natural killer-like T cells on signals leading to NF-kappaB activation. *Proceedings of the National Academy of Sciences of the United States of America*, *101*(13), 4566–4571.

Schmitz, J., Owyang, A., Oldham, E., Song, Y., Murphy, E., McClanahan, T. K., Zurawski, G., Moshrefi, M., Qin, J., Li, X., Gorman, D. M., Bazan, J. F., & Kastelein, R. a. (2005). IL-33, an interleukin-1-like cytokine that signals via the IL-1 receptor-related protein ST2 and induces T helper type 2-associated cytokines. *Immunity*, *23*(5), 479–490.

Schmolka, N., Wencker, M., Hayday, A. C., & Silva-Santos, B. (2015). Epigenetic and transcriptional regulation of γδ T cell differentiation: Programming cells for responses in time and space. *Seminars in Immunology*, *27*(1), 19–25.

Schug, Z. T., Peck, B., Jones, D. T., Zhang, Q., Grosskurth, S., Alam, I. S., Goodwin, L. M., Smethurst, E., Mason, S., Blyth, K., McGarry, L., James, D., Shanks, E., Kalna, G., Saunders, R. E., Jiang, M., Howell, M., … Gottlieb, E. (2015). Acetyl-CoA Synthetase 2 Promotes Acetate Utilization and Maintains Cancer Cell Growth under Metabolic Stress. *Cancer Cell*, *27*(1), 57–71.

Sefik, E., Geva-zatorsky, N., Oh, S., Konnikova, L., Zemmour, D., Mcguire, A. M., Burzyn, D., Ortiz-lopez, A., Lobera, M., Yang, J., Ghosh, S., Earl, A., Snapper, S. B., Jupp, R., Kasper, D., Mathis, D., & Benoist, C. (2015). Individual intestinal symbionts induce a distinct population of ROR g + regulatory T cells, (January), 13–18.

Seneschal, J., Clark, R. a., Gehad, A., Baecher-Allan, C. M., & Kupper, T. S. (2012). Human Epidermal Langerhans Cells Maintain Immune Homeostasis in Skin by Activating Skin Resident Regulatory T Cells. *Immunity*, *36*(5), 873–884.

Serbina, N. V, Salazar-mather, T. P., Biron, C. a, Kuziel, W. a, & Pamer, E. G. (2003). TNF / iNOS-Producing Dendritic Cells Mediate Innate Immune Defense against Bacterial Infection University of Texas at Austin, *19*, 59–70.

Shaw, F. L., Cumberbatch, M., Kleyn, C. E., Begum, R., Dearman, R. J., Kimber, I., & Griffiths, C. E. M. (2010). Langerhans cell mobilization distinguishes between early-onset and late-onset psoriasis. *The Journal of Investigative Dermatology*, *130*(7), 1940–1942.

Shaw, F. L., Mellody, K. T., Ogden, S., Dearman, R. J., Kimber, I., & Griffiths, C. E. M. (2013). Treatment-Related Restoration of Langerhans Cell Migration in Psoriasis. *The Journal of Investigative Dermatology*, *134*(July), 2–4.

Shi-Wen, X., Leask, A., & Abraham, D. (2008). Regulation and function of connective tissue growth factor/CCN2 in tissue repair, scarring and fibrosis. *Cytokine and Growth Factor Reviews*, *19*, 133–144.

Sigmundsdóttir, H., Johnston, A., Gudjónsson, J. E., & Valdimarsson, H. (2004). Differential effects of interleukin 12 and interleukin 10 on superantigen-induced expression of cutaneous lymphocyte-associated antigen (CLA) and αEβ7 integrin (CD103) by CD8+ T cells. *Clinical Immunology*, *111*(1), 119–125.

Sims, J. E., & Smith, D. E. (2010). The IL-1 family: regulators of immunity. *Nature Reviews. Immunology*, *10*(2), 89–102.

Singh, K., Hjort, M., Thorvaldson, L., & Sandler, S. (2015). Concomitant analysis of Helios and Neuropilin-1 as a marker to detect thymic derived regulatory T cells in naïve mice. *Scientific Reports*, *5*, 7767.

Skabytska, Y., Wölbing, F., Günther, C., Köberle, M., Kaesler, S., Chen, K.-M., Guenova, E., Demircioglu, D., Kempf, W. E., Volz, T., Rammensee, H.-G., Schaller, M., Röcken, M., Götz, F., & Biedermann, T. (2014). Cutaneous Innate Immune Sensing of Toll-like Receptor 2-6 Ligands Suppresses T Cell Immunity by Inducing Myeloid-Derived Suppressor Cells. *Immunity*, *41*(5), 762–775.

Sonkoly, E., Muller, A., Lauerma, A. I., Pivarcsi, A., Soto, H., Kemeny, L., Alenius, H., Dieu-Nosjean, M. C., Meller, S., Rieker, J., Steinhoff, M., Hoffmann, T. K., Ruzicka, T., Zlotnik, A., & Homey, B. (2006). IL-31: A new link between T cells and pruritus in atopic skin inflammation. *Journal of Allergy and Clinical Immunology*, *117*(2), 411–417.

Soumelis, V., Reche, P. A., Kanzler, H., Yuan, W., Edward, G., Homey, B., Gilliet, M., Ho, S., Antonenko, S., Lauerma, A., Smith, K., Gorman, D., Zurawski, S., Abrams, J., Menon, S., McClanahan, T., de Waal-Malefyt Rd, R., … Liu, Y.-J. (2002). Human epithelial cells trigger dendritic cell mediated allergic inflammation by producing TSLP. *Nature Immunology*, *3*(7), 673–680.

Spits, H., Artis, D., Colonna, M., Diefenbach, A., Di Santo, J. P., Eberl, G., Koyasu, S., Locksley, R. M., McKenzie, A. N. J., Mebius, R. E., Powrie, F., & Vivier, E. (2013). Innate lymphoid cells--a proposal for uniform nomenclature. *Nature Reviews. Immunology*, *13*(2), 145–9.

Srivastava, S., Koch, M. A., Pepper, M., & Campbell, D. J. (2014). Type I interferons directly inhibit regulatory T cells to allow optimal antiviral T cell responses during acute LCMV infection, *211*(5), 961–974.

Stetson, D. B., Ko, J. S., Heidmann, T., & Medzhitov, R. (2008). Trex1 Prevents Cell-Intrinsic Initiation of Autoimmunity. *Cell*, *134*(4), 587–598.

Stifano, G., Affandi, A. J., Mathes, A. L., Rice, L. M., Nakerakanti, S., Nazari, B., Lee, J., Christmann, R. B., & Lafyatis, R. (2014). Chronic Toll-like receptor 4 stimulation in skin induces inflammation, macrophage activation, transforming growth factor beta signature gene expression, and fibrosis. *Arthritis Research & Therapy*, *16*(4), R136.

Stratis, A., Pasparakis, M., Rupec, R. A., Markur, D., Hartmann, K., Scharffetter-Kochanek, K., Peters, T., Van Rooijen, N., Krieg, T., & Haase, I. (2006). Pathogenic role for skin macrophages in a mouse model of keratinocyte-induced psoriasis-like skin inflammation. *Journal of Clinical Investigation*, *116*(8), 2094–2104.

Suffia, I., Reckling, S. K., Salay, G., & Belkaid, Y. (2005). A role for CD103 in the retention of CD4+CD25+ Treg and control of Leishmania major infection. *Journal of Immunology*, *174*(9), 5444–5455.

Sugiyama, H., Gyulai, R., Toichi, E., Garaci, E., Shimada, S., Stevens, S. R., McCormick, T. S., & Cooper, K. D. (2005). Dysfunctional blood and target tissue CD4+ CD25high regulatory T cells in psoriasis: mechanism underlying unrestrained pathogenic effector T cell proliferation. *The Journal of Immunology*, (174), 164–173.

Sumaria, N., Roediger, B., Ng, L. G., Qin, J., Pinto, R., Cavanagh, L. L., Shklovskaya, E., Fazekas de St Groth, B., Triccas, J. a, & Weninger, W.

(2011). Cutaneous immunosurveillance by self-renewing dermal gammadelta T cells. *The Journal of Experimental Medicine*, *208*(3), 505–518.

Swain, S. L., Weinberg, a D., English, M., & Huston, G. (1990). IL-4 directs the development of Th2-like helper effectors. *Journal of Immunology*, *145*(11), 3796–3806.

Swiecki, M., & Colonna, M. (2015). The multifaceted biology of plasmacytoid dendritic cells. *Nature Reviews Immunology*, *15*(8), 471–485.

Swindell, W. R., Johnston, A., Carbajal, S., Han, G., Wohn, C., Lu, J., Xing, X., Nair, R. P., Voorhees, J. J., Elder, J. T., Wang, X.-J., Sano, S., Prens, E. P., DiGiovanni, J., Pittelkow, M. R., Ward, N. L., & Gudjonsson, J. E. (2011). Genome-wide expression profiling of five mouse models identifies similarities and differences with human psoriasis. *PloS One*, *6*(4), e18266.

Szabo, S. J., Kim, S. T., Costa, G. L., Zhang, X., Fathman, C. G., & Glimcher, L. H. (2000). A novel transcription factor, T-bet, directs Th1 lineage commitment. *Cell*, *100*(6), 655–669.

Szabo, S. J., Sullivan, B. M., Stemmann, C., Satoskar, A. R., Sleckman, B. P., & Glimcher, L. H. (2002). Distinct effects of T-bet in TH1 lineage commitment and IFN-gamma production in CD4 and CD8 T cells. *Science*, *295*(5553), 338–342.

Szeimies, R.-M., Gerritsen, M.-J. P., Gupta, G., Ortonne, J. P., Serresi, S., Bichel, J., Lee, J. H., Fox, T. L., & Alomar, A. (2004). Imiquimod 5% cream for the treatment of actinic keratosis: results from a phase III, randomized, double-blind, vehicle-controlled, clinical trial with histology. *Journal of the American Academy of Dermatology*, *51*(4), 547–55.

Takemoto, N., Intlekofer, A. M., Northrup, J. T., Wherry, E. J., & Reiner, S. L. (2006). Cutting Edge: IL-12 inversely regulates T-bet and eomesodermin expression during pathogen-induced CD8+ T cell differentiation. *Journal of Immunology*, *177*(11), 7515–7519.

Tamoutounour, S., Guilliams, M., Montanana Sanchis, F., Liu, H., Terhorst, D., Malosse, C., Pollet, E., Ardouin, L., Luche, H., Sanchez, C., Marc Dalod, Malissen, B., & Henri, S. (2013). Origins and Functional Specialization of Macrophages and of Conventional and Monocyte-Derived Dendritic Cells in Mouse Skin. *Immunity*, *39*(5), 925–938.

Tanaka, Y., & Chen, Z. J. (2012). STING Specifies IRF3 Phosphorylation by TBK1 in the Cytosolic DNA Signaling Pathway. *Science Signaling*, *5*(214), ra20–ra20.

Tang, W., Wang, H., Claudio, E., Tassi, I., Ha, H.-L., Saret, S., & Siebenlist, U. (2014). The oncoprotein and transcriptional regulator bcl-3 governs plasticity and pathogenicity of autoimmune T cells. *Immunity*, *41*(4), 555–66.

Tassi, I., Rikhi, N., Claudio, E., Wang, H., Tang, W., Ha, H.-L., Saret, S., Kaplan, D. H., & Siebenlist, U. (2015). The NF-κB regulator Bcl-3 modulates inflammation during contact hypersensitivity reactions in radioresistant cells. *European Journal of Immunology*, *45*(4), 1059–68.

Teles, R. M. B., Graeber, T. G., Krutzik, S. R., Montoya, D., Schenk, M., Lee, D. J., Komisopoulou, E., Kelly-Scumpia, K., Chun, R., Iyer, S. S., Sarno, E. N., Rea, T. H., Hewison, M., Adams, J. S., Popper, S. J., Relman, D. A., Stenger, S., … Modlin, R. L. (2013). Type I interferon suppresses type II interferon-triggered human anti-mycobacterial responses. *Science*, *339*(6126), 1448–53.

Teunissen, M. B. M., Munneke, J. M., Bernink, J. H., Spuls, P. I., Res, P. C. M., Te Velde, A., Cheuk, S., Brouwer, M. W. D., Menting, S. P., Eidsmo, L., Spits, H., Hazenberg, M. D., & Mjösberg, J. (2014). Composition of Innate Lymphoid Cell Subsets in the Human Skin: Enrichment of NCR(+) ILC3 in Lesional Skin and Blood of Psoriasis Patients. *The Journal of Investigative Dermatology*, *13*.

Thornton, A. M., Korty, P. E., Tran, D. Q., Wohlfert, E. a, Murray, P. E., Belkaid, Y., & Shevach, E. M. (2010). Expression of Helios, an Ikaros transcription factor family member, differentiates thymic-derived from peripherally induced Foxp3+ T regulatory cells. *Journal of Immunology*, *184*(7), 3433–41.

Tomura, M., Honda, T., Tanizaki, H., Otsuka, A., Egawa, G., Tokura, Y., Waldmann, H., Hori, S., Cyster, J. G., Watanabe, T., Miyachi, Y., Kanagawa, O., & Kabashima, K. (2010). Activated regulatory T cells are the major T cell type emigrating from the skin during a cutaneous immune response in mice. *Journal of Clinical Investigation*, *120*(3), 883–893.

Tone, Y., Furuuchi, K., Kojima, Y., Tykocinski, M. L., Greene, M. I., & Tone, M. (2008). Smad3 and NFAT cooperate to induce Foxp3 expression through its enhancer. *Nature Immunology*, *9*(2), 194–202.

Tortola, L., Rosenwald, E., Abel, B., Blumberg, H., Schäfer, M., Coyle, A. J., Renauld, J. C., Werner, S., Kisielow, J., & Kopf, M. (2012). Psoriasiform dermatitis is driven by IL-36-mediated DC-keratinocyte crosstalk. *Journal of Clinical Investigation*, *122*(11), 3965–3976.

Toulon, A., Breton, L., Taylor, K. R., Tenenhaus, M., Bhavsar, D., Lanigan, C., Rudolph, R., Jameson, J., & Havran, W. L. (2009). A role for human skin-resident T cells in wound healing. *Journal of Experimental Medicine*, *206*(4), 743–750.

Trinchieri, G. (2003). Interleukin-12 and the regulation of innate resistance and adaptive immunity. *Nature Reviews. Immunology*, *3*(2), 133–46.

Tsoi, L. C., Spain, S. L., Knight, J., Ellinghaus, E., Stuart, P. E., Capon, F., Ding, J., Li, Y., Tejasvi, T., Gudjonsson, J. E., Kang, H. M., Allen, M. H., McManus, R., Novelli, G., Samuelsson, L., Schalkwijk, J., Ståhle, M., … Trembath, R. C. (2012). Identification of 15 new psoriasis susceptibility loci highlights the role of innate immunity. *Nature Genetics*, *advance on*.

Turnquist, H. R., Zhao, Z., Rosborough, B. R., Liu, Q., Castellaneta, A., Isse, K., Wang, Z., Lang, M., Stolz, D. B., Zheng, X. X., Demetris, a J., Liew, F. Y., Wood, K. J., & Thomson, A. W. (2011). IL-33 expands suppressive CD11b+ Gr-1(int) and regulatory T cells, including ST2L+ Foxp3+ cells, and mediates regulatory T cell-dependent promotion of cardiac allograft survival. *Journal of Immunology*, *187*(9), 4598–610.

Uldrich, A. P., Le Nours, J., Pellicci, D. G., Gherardin, N. a, McPherson, K. G., Lim, R. T., Patel, O., Beddoe, T., Gras, S., Rossjohn, J., & Godfrey, D. I. (2013). CD1d-lipid antigen recognition by the γδ TCR. *Nature Immunology*, *14*(11), 1137–45.

Uyemura, K., Yamamura, M., Fivenson, D. F., Modlin, R. L., & Nickoloff, B. J. (1993). The cytokine network in lesional and lesion-free psoriatic skin is characterized by a T-helper type 1 cell-mediated response. *Journal of Investigative Dermatology*.

Valdimarsson, H., Thorleifsdottir, R. H., Sigurdardottir, S. L., Gudjonsson, J. E., & Johnston, A. (2009). Psoriasis - as an autoimmune disease caused by molecular mimicry. *Trends in Immunology*, *30*(10), 494–501.

Van Belle, A. B., de Heusch, M., Lemaire, M. M., Hendrickx, E., Warnier, G., Dunussi-Joannopoulos, K., Fouser, L. a., Renauld, J.-C. J.-C., & Dumoutier, L. (2012). IL-22 is required for imiquimod-induced psoriasiform skin inflammation in mice. *Journal of Immunology*, *188*(1), 462–9.

Van der Fits, L., Mourits, S., Voerman, J. S. a, Kant, M., Boon, L., Laman, J. D., Cornelissen, F., Mus, A.-M., Florencia, E., Prens, E. P., & Lubberts, E. (2009). Imiquimod-induced psoriasis-like skin inflammation in mice is mediated via the IL-23/IL-17 axis. *Journal of Immunology*, *182*(9), 5836–45.

Van der Fits, L., van der Wel, L. I., Laman, J. D., Prens, E. P., & Verschuren, M. C. M. (2004). In Psoriasis Lesional Skin the Type I Interferon Signaling Pathway Is Activated, whereas Interferon-a Sensitivity Is Unaltered. *Journal of Investigative Dermatology*, *122*(1), 51–60.

Van Furth, R., & Cohn, Z. a. (1968). The origin and kinetics of mononuclear phagocytes. *The Journal of Experimental Medicine*, *128*(3), 415–435.

Vandenbark, A. a., Huan, J., Agotsch, M., La Tocha, D., Goelz, S., Offner, H., Lanker, S., & Bourdette, D. (2009). Interferon-beta-1a treatment increases CD56bright natural killer cells and CD4+CD25+ Foxp3 expression in subjects with multiple sclerosis. *Journal of Neuroimmunology*, *215*(1-2), 125–128.

Vasanthakumar, A., Moro, K., Xin, A., Liao, Y., Gloury, R., Kawamoto, S., Fagarasan, S., Mielke, L. a, Afshar-sterle, S., Masters, S. L., Nakae, S., Saito, H., Wentworth, J. M., Li, P., Liao, W., Leonard, W. J., Smyth, G. K., … Kallies, A. (2015). The transcriptional regulators IRF4 , BATF and IL-33 orchestrate development and maintenance of adipose tissue – resident regulatory T cells. *Nature Immunology*, *16*(3).

Villanova, F., Flutter, B., Tosi, I., Grys, K., Sreeneebus, H., Perera, G. K., Chapman, A., Smith, C. H., Di Meglio, P., & Nestle, F. O. (2014). Characterization of innate lymphoid cells in human skin and blood demonstrates increase of NKp44+ ILC3 in psoriasis. *The Journal of Investigative Dermatology*, *134*(4), 984–91.

Villarroel, V. a, Okiyama, N., Tsuji, G., Linton, J. T., & Katz, S. I. (2014). CXCR3-mediated skin homing of autoreactive CD8 T cells is a key determinant in murine graft-versus-host disease. *The Journal of Investigative Dermatology*, *134*(6), 1552–60.

Wachstein, J., Tischer, S., Figueiredo, C., Limbourg, A., Falk, C., Immenschuh, S., Blasczyk, R., & Eiz-Vesper, B. (2012). HSP70 Enhances Immunosuppressive Function of CD4+CD25+FoxP3+ T Regulatory Cells and Cytotoxicity in CD4+CD25- T Cells. *PLoS ONE*, *7*(12).

Wagner, E. F., Schonthaler, H. B., Guinea-Viniegra, J., & Tschachler, E. (2010). Psoriasis: what we have learned from mouse models. *Nature Reviews Rheumatology*, *6*(12), 704–714.

Walter, A., Schäfer, M., Cecconi, V., Matter, C., Urosevic-Maiwald, M., Belloni, B., Schönewolf, N., Dummer, R., Bloch, W., Werner, S., Beer, H.-D., Knuth, A., & van den Broek, M. (2013). Aldara activates TLR7-independent immune defence. *Nature Communications*, *4*, 1560.

Wan, Y. Y., Chi, H., Xie, M., Schneider, M. D., & Flavell, R. a. (2006). The kinase TAK1 integrates antigen and cytokine receptor signaling for T cell development, survival and function. *Nature Immunology*, *7*(8), 851–858.

Wang, H., Peters, T., Kess, D., Sindrilaru, A., Oreshkova, T., Van Rooijen, N., Stratis, A., Renkl, A. C., Sunderkötter, C., Wlaschek, M., Haase, I., & Scharffetter-Kochanek, K. (2006). Activated macrophages are essential in a murine model for T cell-mediated chronic psoriasiform skin inflammation. *The Journal of Clinical Investigation*, *116*(8), 2105–14.

Wang, Y., Godec, J., Ben-Aissa, K., Cui, K., Zhao, K., Pucsek, A. B., Lee, Y. K., Weaver, C. T., Yagi, R., & Lazarevic, V. (2014). The transcription factors T-bet and runx are required for the ontogeny of pathogenic interferon-??-producing T helper 17 cells. *Immunity*, *40*(3), 355–366.

Watanabe, R., Gehad, A., C. Yang, L. L. Scott, J. E. Teague, C. Schlapbach, C. P. Elco, V. Huang, T. R. Matos, T. S. Kupper, & R. A. Clark. (2015). Human skin is protected by four functionally and phenotypically discrete populations of resident and recirculating memory T cells. *Science Translational Medicine*, *7*(279), 279ra39–279ra39.

Weaver, C. T., Elson, C. O., Fouser, L. A., & Kolls, J. K. (2013). The Th17 pathway and inflammatory diseases of the intestines, lungs, and skin. *Annual Review of Pathology*, *8*(1), 477–512.

Weiss, J. M., Bilate, a. M., Gobert, M., Ding, Y., Curotto de Lafaille, M. a., Parkhurst, C. N., Xiong, H., Dolpady, J., Frey, a. B., Ruocco, M. G., Yang, Y., Floess, S., Huehn, J., Oh, S., Li, M. O., Niec, R. E., Rudensky, a. Y., … Lafaille, J. J. (2012). Neuropilin 1 is expressed on thymus-derived natural regulatory T cells, but not mucosa-generated induced Foxp3+ T reg cells. *Journal of Experimental Medicine*, *209*(10), 1723–1742.

Weissler, K. a, & Caton, A. J. (2014). The role of T-cell receptor recognition of peptide:MHC complexes in the formation and activity of Foxp3(+) regulatory T cells. *Immunological Reviews*, *259*(1), 11–22.

Weller, R., Hunter, H., & Mann, M. W. (2015). *Clinical Dermatology* (Vol. 5).

Wikramanayake, T. C., Stojadinovic, O., & Tomic-Canic, M. (2014). Epidermal Differentiation in Barrier Maintenance and Wound Healing. *Advances in Wound Care*, *3*(3), 272–280.

Wilson, N. S., Young, L. J., Kupresanin, F., Naik, S. H., Vremec, D., Heath, W. R., Akira, S., Shortman, K., Boyle, J., Maraskovsky, E., Belz, G. T., & Villadangos, J. a. (2008). Normal proportion and expression of maturation markers in migratory dendritic cells in the absence of germs or Toll-like receptor signaling. *Immunology and Cell Biology*, *86*(2), 200–205.

Wing, J. B., & Sakaguchi, S. (2012). Multiple treg suppressive modules and their adaptability. *Frontiers in Immunology*, *3*(June), 178.

Wohlfert, E., Grainger, J., Bouladoux, N., Konkel, J. E., Oldenhove, G., Ribeiro, C. H., Hall, J. A., Yagi, R., Naik, S., Bhairavabhotla, R., Paul, W. E., Bosselut, R., Wei, G., Zhao, K., Oukka, M., Zhu, J., & Belkaid, Y. (2011). GATA3 controls Foxp3+ regulatory T cell fate during inflammation in mice. *The Journal of Clinical*, *121*(11), 4503–4515.

Wohn, C., Ober-Blöbaum, J. L., Haak, S., Pantelyushin, S., Cheong, C., Zahner, S. P., Onderwater, S., Kant, M., Weighardt, H., Holzmann, B., Reizis, B., Becher, B., Prens, E. P., & Clausen, B. E. (2013). Langerin(neg) conventional dendritic cells produce IL-23 to drive psoriatic plaque formation in mice. *Proceedings of the National Academy of Sciences of the United States of America*, *110*(26), 10723–10728.

Xu, L., Kitani, A., Fuss, I., & Strober, W. (2007). Cutting edge: regulatory T cells induce CD4+CD25-Foxp3- T cells or are self-induced to become Th17 cells in the absence of exogenous TGF-beta. *Journal of Immunology*, *178*(11), 6725–6729.

Xue, L., Salimi, M., Panse, I., Mjösberg, J. M., McKenzie, A. N. J., Spits, H., Klenerman, P., & Ogg, G. (2014). Prostaglandin D2 activates group 2 innate lymphoid cells through chemoattractant receptor-homologous molecule expressed on TH2 cells. *Journal of Allergy and Clinical Immunology*, *133*(4).

Yadav, M., Louvet, C., D. Davini, J. M. Gardner, M. Martinez-Llordella, S. Bailey-Bucktrout, B. A. Anthony, F. M. Sverdrup, R. Head, D. J. Kuster, P. Ruminski, D. Weiss, D. Von Schack, & J. A. Bluestone. (2012). Neuropilin-1 distinguishes natural and inducible regulatory T cells among regulatory T cell subsets in vivo. *Journal of Experimental Medicine*, *209*(10), 1713–1722.

Yang, S., Fujikado, N., Kolodin, D., Benoist, C., & Mathis, D. (2015). Regulatory T cells generated early in life play a distinct role in maintaining self-tolerance. *Science*, *348*(6234), 589–594.

Yao, Y., Richman, L., Morehouse, C., de los Reyes, M., Higgs, B. W., Boutrin, A., White, B., Coyle, A., Krueger, J., Kiener, P. a., & Jallal, B. (2008). Type I Interferon: Potential Therapeutic Target for Psoriasis? *PLoS ONE*, *3*(7), e2737.

Yawalkar, N., Karlen, S., Hunger, R., Brand, C. U., & Braathen, L. R. (1998). Expression of interleukin-12 is increased in psoriatic skin. *Journal of Investigative Dermatology*, *111*, 1053–1057.

Yeilding, N., Guzzo, C., Wang, Y., Ph, D., Dooley, L. T., & Lebwohl, M. (2007). Antibody for the Treatment of Psoriasis.

Yoneyama, M., Kikuchi, M., Natsukawa, T., Shinobu, N., Imaizumi, T., Miyagishi, M., Taira, K., Akira, S., & Fujita, T. (2004). The RNA helicase RIG-I has an essential function in double-stranded RNA-induced innate antiviral responses. *Nature Immunology*, *5*(7), 730–737.

Yoon, H., Kim, T. S., & Braciale, T. J. (2010). The cell cycle time of CD8+ T cells responding in Vivo is controlled by the type of antigenic stimulus. *PLoS ONE*, *5*(11).

Yun, W.-J., Lee, D.-W., Chang, S.-E., Yoon, G.-S., Huh, J.-R., Won, C.-H., Lee, M.-W., Kim, S.-E., Kim, B.-J., Moon, K.-C., & Choi, J.-H. (2010). Role of CD4CD25FOXP3 Regulatory T Cells in Psoriasis. *Annals of Dermatology*, *22*(4), 397–403.

Yurchenko, E., Levings, M. K., & Piccirillo, C. a. (2011). CD4+ Foxp3+ regulatory T cells suppress gammadelta T-cell effector functions in a model of T-cell-induced mucosal inflammation. *Eur J Immunol*, *41*(12), 3455–3466.

Zaba, L. C., Cardinale, I., Gilleaudeau, P., Sullivan-Whalen, M., Suárez-Fariñas, M., Fuentes-Duculan, J., Novitskaya, I., Khatcherian, A., Bluth, M. J., Lowes, M. a, & Krueger, J. G. (2007). Amelioration of epidermal hyperplasia by TNF inhibition is associated with reduced Th17 responses. *The Journal of Experimental Medicine*, *204*(13), 3183–3194.

Zaba, L. C., Fuentes-Duculan, J., Eungdamrong, N. J., Abello, M. V., Novitskaya, I., Pierson, K. C., Gonzalez, J., Krueger, J. G., & Lowes, M. a. (2009). Psoriasis is characterized by accumulation of immunostimulatory and Th1/Th17 cell-polarizing myeloid dendritic cells. *The Journal of Investigative Dermatology*, *129*(1), 79–88.

Zaba, L. C., Krueger, J. G., & Lowes, M. a. (2009). Resident and “inflammatory” dendritic cells in human skin. *The Journal of Investigative Dermatology*, *129*(2), 302–308.

Zanoni, I., Ostuni, R., Marek, L. R., Barresi, S., Barbalat, R., Barton, G. M., Granucci, F., & Kagan, J. C. (2011). CD14 controls the LPS-induced endocytosis of toll-like receptor 4. *Cell*, *147*(4), 868–880.

Zasloff, M. (2002). Antimicrobial peptides of multicellular organisms. *Nature*, *415*(January), 389–395.

Zhang, J., Raper, A., Sugita, N., Hingorani, R., Salio, M., Palmowski, M. J., Cerundolo, V., Crocker, P. R., & Dc, W. (2006). Characterization of Siglec-H as a novel endocytic receptor expressed on murine plasmacytoid dendritic cell precursors Characterization of Siglec-H as a novel endocytic receptor expressed on murine plasmacytoid dendritic cell precursors. *Blood*, *107*(9), 3600–3608.

Zhang, N., & Bevan, M. J. (2011). CD8+ T Cells: Foot Soldiers of the Immune System. *Immunity*, *35*(2), 161–168.

Zhang, X.-J., Huang, W., Yang, S., Sun, L.-D., Zhang, F.-Y., Zhu, Q.-X., Zhang, F.-R., Zhang, C., Du, W.-H., Pu, X.-M., Li, H., Xiao, F.-L., Wang, Z.-X., Cui, Y., Hao, F., Zheng, J., Yang, X.-Q., … Liu, J.-J. (2009).

Psoriasis genome-wide association study identifies susceptibility variants within LCE gene cluster at 1q21. *Nature Genetics*, *41*(2), 205–210.

Zheng, W., & Flavell, R. A. (1997). The Transcription Factor GATA-3 is Necessary and Sufficient for Th2 Cytokine Gene Expression in CD4 T cells. *Cell*, *89*(4), 587–596.

Zheng, Y., Chaudhry, A., Kas, A., deRoos, P., Kim, J. M., Chu, T.-T., Corcoran, L., Treuting, P., Klein, U., & Rudensky, A. Y. (2009). Regulatory T-cell suppressor program co-opts transcription factor IRF4 to control T(H)2 responses. *Nature*, *458*(7236), 351–356.

Zheng, Y., Danilenko, D. M., Valdez, P., Kasman, I., Eastham-Anderson, J., Wu, J., & Ouyang, W. (2007). Interleukin-22, a T(H)17 cytokine, mediates IL-23-induced dermal inflammation and acanthosis. *Nature*, *445*(7128), 648–51.

Zhou, L., Ivanov, I. I., Spolski, R., Min, R., Shenderov, K., Egawa, T., Levy, D. E., Leonard, W. J., & Littman, D. R. (2007). IL-6 programs T(H)-17 cell differentiation by promoting sequential engagement of the IL-21 and IL-23 pathways. *Nature Immunology*, *8*(9), 967–974.

Zhou, X., Bailey-Bucktrout, S. L., Jeker, L. T., Penaranda, C., Martínez-Llordella, M., Ashby, M., Nakayama, M., Rosenthal, W., & Bluestone, J. a. (2009). Instability of the transcription factor Foxp3 leads to the generation of pathogenic memory T cells in vivo. *Nature Immunology*, *10*(9), 1000–1007.

Zhu, C., Sakuishi, K., Xiao, S., Sun, Z., Zaghouani, S., Gu, G., Wang, C., Tan, D. J., Wu, C., Rangachari, M., Pertel, T., Jin, H.-T., Ahmed, R., Anderson, A. C., & Kuchroo, V. K. (2015). An IL-27/NFIL3 signalling axis drives Tim-3 and IL-10 expression and T-cell dysfunction. *Nature Communications*, *6*, 6072.

Zielinski, C. E., Mele, F., Aschenbrenner, D., Jarrossay, D., Ronchi, F., Gattorno, M., Monticelli, S., Lanzavecchia, A., & Sallusto, F. (2012). Pathogen-induced human TH17 cells produce IFN-γ or IL-10 and are regulated by IL-1β. *Nature*, *484*(7395), 514–518.

Zorn, E., Nelson, E. A., Mohseni, M., Porcheray, F., Kim, H., Litsa, D., Bellucci, R., Raderschall, E., Canning, C., Soiffer, R. J., Frank, D. a, & Ritz, J. (2006). IL-2 regulates FOXP3 expression in human CD4+CD25+ regulatory T cells through a STAT-dependent mechanism and induces the expansion of these cells in vivo. *Blood*, *108*(5), 1571–1579.

Supplementary Data

Supplementary Table 1

Probe ID	log 2 fold change	adj. p value	gene
4120753	4.64074	0.000714676	LMNA
1260632	4.41108	0.004935349	IL10
650711	4.34991	0.000144248	DGAT2
7400044	4.05183	0.010147063	FOSL2
5220279	3.96709	0.003631708	MT1
3370377	3.58853	0.001551317	GADD45B
5420739	3.34850	0.001216186	FES
3130630	3.34746	0.001086164	CDKN1A
2350017	3.32895	0.011202546	HSPA1A
1990373	3.30481	0.031243361	AREG
6520075	3.29900	0.041834984	IER3
6250373	3.27250	0.008983499	CREM
3290427	3.19922	0.009108712	SLC15A3
6270131	3.14112	0.011060061	2310009N05RIK
630730	3.10921	0.000701651	IGK-C
7160167	3.07671	0.000291855	EMP1
3840521	2.97792	0.007863907	NFIL3
4590341	2.92250	0.004199830	AI115600
2750326	2.86629	0.025623378	EGLN3
6840112	2.85805	0.000334940	UAP1
580746	2.83529	0.006289940	RASGRF1
4150592	2.82555	0.016747600	DGAT1
460754	2.79178	0.032521537	TFF1
3870291	2.77687	0.009745488	IL1RL1
6480554	2.72307	0.004233032	BC023892
4570368	2.69183	0.009466080	1300002F13RIK
60603	2.66449	0.005040264	HAVCR2
5700014	2.63538	0.002071210	KLRG1
1300373	2.62268	0.000482653	TNFRSF9
2100358	2.57697	0.000217816	MAP2K3
1090228	2.57397	0.000256681	5430432M24RIK
6020400	2.56983	0.003397973	SAMSN1
630192	2.55322	0.000232010	MPP7
1580349	2.55254	0.000009375	1810006K23RIK
2260471	2.54662	0.002930829	CRIP2
510474	2.54147	0.006145506	LGALS3
2000139	2.51686	0.000554560	CENPL
3890022	2.49909	0.022701862	NDRL
1090438	2.49588	0.000244609	ATF3
1090112	2.47535	0.013972166	ADARB1
4290324	2.46637	0.001198205	9130404D14RIK
2600377	2.45702	0.006943586	EBI2
6660039	2.45410	0.005263016	MAD
6330195	2.42786	0.000009375	CAMK2N1
6940451	2.42337	0.013740963	MYADM
2360703	2.41509	0.001923996	ITGA3
6100494	2.41242	0.004317141	2610300B10RIK
6940037	2.41134	0.027571046	LTF
1450095	2.40515	0.000079564	ICAM1
6330377	2.36737	0.000404168	GADD45G
4120703	2.35626	0.000933265	VCL
4850079	2.34091	0.000235407	KIF23
2360343	2.32480	0.006943586	C330006P03RIK
5050008	2.29501	0.000006874	SMOX
6760209	2.29159	0.014714914	RAB26
6960189	2.28414	0.000009375	FURIN

1690091	2.23949	0.000118297	VIM
3190379	2.23932	0.019072747	SYTL3
6620187	2.23051	0.026398092	NDRG1
4220239	2.21635	0.001634702	COQ10B
840673	2.21397	0.001178227	LMNB1
360674	2.20715	0.001270564	TRP53INP2
4290152	2.16555	0.004199830	2310016C08RIK
5720523	2.12322	0.000079787	S100A11
3140041	2.11337	0.001138515	2310046K01RIK
6270181	2.09278	0.020199312	DUSP4
4230348	2.08068	0.000191088	CEBPB
4230402	2.07209	0.024463933	LTB4R1
7330278	2.04930	0.007645409	LGALS1
7330228	2.02345	0.000009782	2810439F02RIK
2470086	2.01625	0.003802097	SLC39A4
4830612	1.99799	0.013972166	1110018K11RIK
1070484	1.99107	0.027553444	HSPA2
4010082	1.98601	0.001923996	CTGF
1340301	1.98492	0.000232010	MIF4GD
430523	1.97343	0.004003341	TNFAIP3
5900370	1.96997	0.000728170	LOC381140
270341	1.96913	0.013198442	EMB
2760341	1.96896	0.018980144	6230400I06RIK
3360520	1.96843	0.003191079	TMEM49
4880138	1.96584	0.000099042	CD44
160390	1.96425	0.000009375	IL2RA
630707	1.94985	0.039676977	RAPGEF3
3870270	1.93766	0.019072747	BC004022
6510463	1.93375	0.045698757	ANTXR2
4290403	1.93336	0.002660100	ZFHX1A
3420600	1.92791	0.007620567	1110060I01RIK
2450239	1.92524	0.000334940	ICOS
3840324	1.90834	0.000096191	BLCAP
4880288	1.90815	0.000703866	SYTL3
5310050	1.90722	0.000334940	JAK2
5960471	1.89688	0.000561805	X83328
1470121	1.89681	0.001324684	SDC4
5550035	1.89613	0.001176224	RRAD
2900373	1.89264	0.000666109	1190002H23RIK
3800274	1.88699	0.005252639	SKIL
1990639	1.88688	0.014357784	APAF1
3360338	1.86701	0.000305615	Il
3120014	1.86381	0.003010695	JUNB
1710400	1.85579	0.043883471	2810439F02RIK
3450370	1.85378	0.007882696	TUFT1
3310474	1.85044	0.022028327	SGIP1
1260164	1.85042	0.003191079	ASNS
670608	1.83939	0.010209972	ELOVL6
1470465	1.82747	0.003454357	CALCA
5130156	1.81534	0.018635615	CCRL2
4070020	1.81334	0.000142613	BCL3
2360711	1.78802	0.000099042	4930519N16RIK
520102	1.78745	0.010219882	9130604K18RIK
6840121	1.78449	0.019072747	ODC1
160519	1.77411	0.000869098	TMEM65
5290360	1.76476	0.000275886	PICALM
1710193	1.76161	0.029510041	GJA1
1660504	1.75147	0.002948735	IL7R
4900519	1.75120	0.007462814	SGK
7200242	1.74961	0.002742171	HAK
5570240	1.74478	0.008533524	BB128963
5670722	1.74477	0.000283496	HSPB1
6100520	1.74381	0.001353700	CNNM2
6220026	1.73018	0.001312273	ZFP36
3140500	1.72095	0.003656342	H2AFZ
6020224	1.71122	0.006511882	IL4I1

5260195	1.71059	0.007834379	ISY1
5670687	1.70315	0.019534045	GPR65
3450470	1.70117	0.000183195	SERINC1
6220037	1.69740	0.001719207	BC019206
4560619	1.69340	0.000342477	SQSTM1
3180156	1.68600	0.002054283	TNFRSF18
4900142	1.68404	0.001780381	MAPKAPK2
6660653	1.68299	0.002505005	BAG3
2480372	1.68292	0.019072747	PLCD1
730193	1.68160	0.000079564	KIT
520121	1.67528	0.001399696	RAB6IP1
610463	1.67459	0.048896696	NPN3
6200367	1.66954	0.023695807	NCAPH
3710242	1.66719	0.000708768	ARPC3
1230341	1.66515	0.000426990	BHLHB2
2070427	1.66221	0.000961444	CDC42BPB
5820626	1.65665	0.001439777	TMBIM1
1230681	1.65613	0.003359422	LOC268569
2480241	1.65153	0.000367096	MUC1
4220162	1.64936	0.022000847	STX11
160035	1.64860	0.001040147	BATF
4040382	1.64467	0.004468565	LOC240672
2190743	1.64354	0.019343889	OSBPL3
2510164	1.63204	0.032972619	TRAF1
6370204	1.63021	0.000945620	TAGLN2
290358	1.62417	0.020741182	GCNT1
670360	1.62348	0.013633498	2310057H16RIK
2490201	1.61735	0.007628112	GNA13
7550053	1.61656	0.032012956	GAD1
6650458	1.61578	0.001357448	NFKBIZ
4390564	1.61576	0.001037272	ORMDL3
6840594	1.60920	0.001828797	RGS1
4070184	1.60230	0.000717670	BIRC2
1940288	1.60049	0.013090157	D830014E11RIK
4210192	1.60006	0.043608796	EHD4
60553	1.59653	0.002299262	GBP4
1230722	1.58791	0.001599140	WSB1
2900594	1.56569	0.002595365	2810405I11RIK
3290747	1.56244	0.000431852	BEX2
770577	1.55764	0.001021362	ARHGAP21
580685	1.55410	0.001282865	TGN
7040619	1.55101	0.011564491	CLIC4
3460296	1.54338	0.031460892	ANXA2
4850682	1.54180	0.001218239	TGIF
940129	1.54125	0.000342477	4930486L24RIK
6100132	1.53879	0.004811412	2610024H22RIK
2230463	1.53771	0.002004059	TNFRSF1B
540647	1.52615	0.003099525	CD69
630706	1.52511	0.000232010	HEMK1
3420086	1.52450	0.019072747	2610024E20RIK
3360653	1.52321	0.001159526	OSTF1
5360477	1.52226	0.000009375	MAPKAPK3
6350044	1.51969	0.030843615	SLC2A1
3060647	1.50853	0.000276034	RELB
5080326	1.50488	0.010524278	S100A6
240168	1.50316	0.001980830	CMKBR2
4880187	1.49213	0.001778407	ERDR1
5690270	1.49147	0.039755072	COL18A1
3310577	1.48842	0.023901775	GNA15
5890221	1.48318	0.000482270	FAS
3170689	1.48144	0.004199830	AXUD1
5340446	1.47650	0.034462946	6330439P19RIK
670647	1.47267	0.001032998	RGS9
10768	1.47071	0.000059952	GM2A
7040044	1.46843	0.001728403	TRF
5670259	1.46512	0.014496712	5033421J10RIK

1010397	1.46423	0.001754877	IRF4
6420762	1.46087	0.001981929	A530026H04RIK
6560477	1.46023	0.039476752	STK2
2070307	1.45740	0.004426953	GOT1
3400014	1.44726	0.043883471	SLK
4880253	1.44385	0.018196473	JMJD3
3890767	1.43562	0.038427759	SV2C
5820292	1.42670	0.027553444	BC026744
2140148	1.41942	0.031629101	COL17A1
3890102	1.41843	0.001334514	MRPS6
3890673	1.41216	0.001334514	3830408P04RIK
4900053	1.41175	0.004426953	IER5L
6620131	1.41139	0.000703866	TNIP2
7650242	1.40918	0.008163435	IL18R1
1500722	1.40606	0.000122598	PLD3
510368	1.40347	0.018073026	FOS
5490561	1.40303	0.044645660	SLC25A19
5700168	1.40254	0.009548321	VAMP3
5870671	1.39804	0.000717670	D11BWG0414E
1850725	1.39778	0.000255073	SDCBP2
1690537	1.39400	0.001873789	ALDOA
3460026	1.39328	0.028797154	LOC269941
4890113	1.39048	0.003631708	PNP
4150463	1.38628	0.005714380	MRPL33
1770424	1.38468	0.001983180	EPB4.1L2
3940333	1.37912	0.029629771	RNF36
6420040	1.37839	0.008573273	SRC
4250066	1.37751	0.027227711	GGTA1
3520114	1.37070	0.027755893	BRRN1
2600301	1.37060	0.001344471	1810007I17RIK
2070274	1.36435	0.014897209	APP
1170474	1.35673	0.001922028	FBXO33
4880112	1.35589	0.001117080	TDE2
4150669	1.35568	0.005291033	AW742319
2070615	1.34901	0.000463340	ANXA11
5130139	1.34761	0.003309434	TGFB1
5870201	1.34701	0.011304223	MYO1E
1780524	1.34029	0.005039803	TFRC
4540070	1.34012	0.005285140	1600019D15RIK
620372	1.33585	0.027761552	SPHK1
3310270	1.33348	0.010785737	SLC19A2
4200086	1.32832	0.033283246	AEBP2
780475	1.32659	0.046104171	PRC1
2370039	1.32307	0.014288110	GPR171
5490452	1.32165	0.003104600	GALNT2
380035	1.32044	0.001545687	2810026P18RIK
4610373	1.32021	0.010886400	ICSBP1
6400017	1.31866	0.002375381	HIST1H2BC
4010348	1.31849	0.028586480	COL4A3BP
150022	1.31649	0.000793098	NFKBIA
6480703	1.31368	0.019038495	BTG1
1770458	1.31106	0.002897957	SLAMF1
3460468	1.31080	0.001890732	NPTN
1510739	1.30694	0.002375381	KAI1
2630647	1.30688	0.001157031	PREP
4280471	1.30675	0.045926115	TLCD1
4810487	1.30365	0.045340761	SNAG1
6560327	1.30293	0.000703866	LAMP2
3400491	1.30248	0.002014415	CLIC4
4480543	1.29713	0.018907499	MTF1
6270682	1.29528	0.027300973	SLC15A2
3310215	1.29204	0.000144248	1200016E24RIK
20079	1.29144	0.011192052	PTP4A1
2190544	1.28618	0.000473214	YWHAH
4150682	1.28449	0.030738152	0610009F02RIK
4070706	1.28409	0.001463719	PDE4D

110026	1.28363	0.046647622	A930004K21RIK
1050541	1.27868	0.000178800	RHEB
5700017	1.27232	0.007882696	ITGAE
6060564	1.27150	0.002392428	ARRDC4
4050112	1.27034	0.018575821	GLRX
1850270	1.26873	0.002394733	HSPA8
2850482	1.26834	0.006130384	CIAPIN1
150164	1.26767	0.002003822	SAMD11
2370189	1.26682	0.000945620	LOC218482
4200100	1.26532	0.025568331	DUSP1
3290202	1.25925	0.001526116	1110008P08RIK
7200403	1.25820	0.004021025	EG622339
6980021	1.25594	0.001389757	PLP2
5690181	1.25382	0.000394228	DNAJA4
3420037	1.25137	0.013434867	CDR2
6280504	1.25002	0.000068309	CRSP9
6450349	1.24986	0.016079834	ANKRD6
150458	1.24868	0.022034960	TRP53RK
2630605	1.24811	0.016163278	F730031O20RIK
430044	1.24790	0.050265008	TEX2
1990377	1.24299	0.028110511	N4WBP5-PENDING
1440192	1.24202	0.002936639	RAB8B
7150377	1.24098	0.000706279	CD83
6520240	1.23981	0.014288110	1110059G02RIK
1400170	1.23886	0.004671474	AA407930
2000747	1.23748	0.000083553	TNFRSF4
2350139	1.23303	0.024293609	DENR
4040440	1.23261	0.000482653	TNFAIP8
2940138	1.23203	0.000817764	CTLA2B
2370630	1.22989	0.001374811	2610204M08RIK
3360669	1.22847	0.004468565	H3F3A
1850494	1.22215	0.015042846	3300001A09RIK
4880600	1.21344	0.024238008	CSNK1G3
5080634	1.20607	0.009105953	PPP1R3B
4260333	1.20549	0.025623378	NDFIP1
7200519	1.20185	0.024641864	CENPA
1500706	1.19952	0.020264731	STIP1
2680035	1.19921	0.002911434	AI849286
3290008	1.19873	0.018389352	SH3MD2
6580553	1.19256	0.004624219	STAT3
6840270	1.18879	0.019291555	4930431B09RIK
5560603	1.18737	0.023225275	A630072M18RIK
5360047	1.18654	0.000831537	ATP6V0D1
2070537	1.18474	0.000872699	EBI3
150066	1.18302	0.000362087	1810055G02RIK
2340364	1.18272	0.000067798	SLC25A3
4180369	1.18002	0.008624703	SYAP1
5560328	1.17972	0.012659920	MYD116
6980064	1.17914	0.003040363	9130427A09RIK
3310672	1.17870	0.002299262	NR1D1
2600446	1.17522	0.000367096	EIF4EL3
7550041	1.17468	0.000450230	ATP6V0A1
6350086	1.17162	0.038453175	SLC6A8
3170477	1.16921	0.013042947	TAX1BP3
4150184	1.16865	0.002375381	ELOVL5
1430445	1.16828	0.003022594	PPP1R10
4390026	1.16748	0.007146668	LOC218814
1030152	1.16109	0.010679911	IFNGR1
3830291	1.15939	0.004199051	VPS29
6420520	1.15686	0.033666673	FOSB
1690719	1.15262	0.001808841	LGMN
2320168	1.15246	0.019072747	CATNAL1
2070563	1.15031	0.002684685	POR
1770201	1.14894	0.049427606	SERINC3
2850609	1.14790	0.036839820	FAIM
6760546	1.14532	0.003517968	RBBP5

3180739	1.14076	0.004875067	VDR
520072	1.13827	0.045711649	H2-EB1
6060452	1.13785	0.012153101	FGFR2
3940129	1.13780	0.004021025	MELA
7330719	1.13681	0.016685967	2010012F05RIK
3420372	1.13540	0.002916771	TGOLN1
3140646	1.13215	0.008310143	IRF5
1240538	1.13116	0.011227768	P2RY14
160392	1.12960	0.000204685	CXCR4
5720494	1.12821	0.001334514	LINCR
1030497	1.12783	0.020732261	IRAK3
4920196	1.12550	0.002776564	D330008I21RIK
6560465	1.12549	0.013972166	LOC238836
5560288	1.12549	0.030508388	CTLA4
1400041	1.12408	0.027113430	GBP2
5960594	1.12235	0.001987910	LIN54
5270132	1.12192	0.005332682	PDE8A
4780066	1.11652	0.010936511	CSRP1
2690259	1.11603	0.000296765	WBP5
6510112	1.11404	0.001780381	YBX3
5290017	1.11098	0.002394733	CASP4
6510142	1.11044	0.036913151	D730019B10RIK
3710563	1.10980	0.009105953	SYTL2
1030519	1.10888	0.000232010	ID2
4120524	1.10769	0.030382779	C130033B18RIK
1690768	1.10497	0.002392428	CCL5
2120286	1.10343	0.011108317	MFGE8
4900470	1.09595	0.004706008	4833438C02RIK
4480180	1.09594	0.000812100	PHLDA1
2850487	1.09587	0.003397973	EIF1A
4050619	1.09556	0.000342477	STAT5A
510367	1.09438	0.001392577	SPHK2
670554	1.09186	0.001156726	CHRNB1
4540500	1.08474	0.001977710	TFIP11
5820168	1.08469	0.007873483	BCL2L11
5420441	1.08392	0.019586584	TRAF3
2760053	1.08163	0.001178227	6430704N06
2970703	1.08085	0.004796886	MLF1
4200017	1.07982	0.008685430	CISH
5340121	1.07936	0.007628112	1500003O03RIK
5260201	1.07386	0.014230433	TRP53INP1
7100608	1.07347	0.006377802	2310032D16RIK
870707	1.07264	0.013972166	BCL6
4040037	1.07120	0.000178800	TPM4
2570368	1.06666	0.001917324	GLUD1
620360	1.06651	0.005427358	D530030D03RIK
3290020	1.06571	0.006765216	GAPD
5050427	1.06169	0.001137066	LAMC1
3420689	1.06116	0.005516518	AP3S1
1770541	1.06038	0.000144248	TNFRSF12A
160142	1.05992	0.006511882	ARPP19
3830377	1.05915	0.033097557	IQGAP1
1260039	1.05828	0.000787843	NR1D2
1580008	1.05744	0.002193463	AIM1
7560093	1.05546	0.010579954	NOL10
7210687	1.05477	0.019320393	APOE
3780291	1.05464	0.001710999	PKM2
7650152	1.05389	0.049101202	GPR146
5390239	1.04586	0.009091845	KPNA1
1990270	1.04422	0.036459079	2610318C08RIK
3520221	1.04321	0.001117080	LXN
7400187	1.03812	0.037976417	9430034D17RIK
7610451	1.03411	0.017829353	BZRAP1
2480072	1.03410	0.007264106	GPX4
3130707	1.03285	0.003918310	PDGFB
7200259	1.03117	0.000743324	TMEM43

3190685	1.02718	0.002299262	LDH1
3370239	1.02537	0.009109680	E130118D18RIK
5900070	1.02383	0.004624219	GATA3
7380364	1.02236	0.001466715	CARHSP1
4830477	1.02209	0.013144245	2810410P22RIK
3420497	1.02032	0.047504226	DCTN4
2760750	1.01756	0.007296981	MREG
5810521	1.01711	0.018459336	ATP6AP2
2030358	1.01436	0.000706935	BTG1
6650750	1.01421	0.002309325	9130011J04RIK
2140433	1.01283	0.002665788	GI_6679936_REF_NM_008084.1__328
2320201	1.01200	0.001536253	TRIP10
2190239	1.01185	0.005548012	MORF4L2
1980373	1.00943	0.034997584	MYLC2B
5360685	1.00882	0.019586584	IGFBP7
6110037	1.00839	0.016682843	PLD3
290576	1.00829	0.014630024	DHRS1
2340358	1.00697	0.032840029	IMPA2
5260315	1.00373	0.007845959	A830080D01RIK
540398	1.00247	0.000706279	E130012A19RIK
3800390	1.00194	0.002970767	SCL00238693.1_37
1230040	1.00187	0.036235448	5730525O22RIK
6130138	1.00181	0.001710999	RAI12
5360707	-3.29580	0.000096206	SELL
4590136	-3.20661	0.000478357	ACTN1
6200719	-3.15013	0.000071099	ACAS2L
6400463	-2.98498	0.001319751	GALNT10
3400747	-2.86419	0.000701651	IGFBP4
6620458	-2.81187	0.001085583	PACSIN1
1580528	-2.68492	0.000454023	USP18
4260609	-2.60304	0.000703866	NME7
6650626	-2.45556	0.000453740	A130090K04RIK
770669	-2.44051	0.002678931	A130092J06RIK
7040195	-2.42926	0.001296483	GPR83
3520746	-2.38881	0.001156726	SLFN1
7040446	-2.38588	0.000010012	GFI1
3930370	-2.37942	0.000705321	A130065C13RIK
4070402	-2.37565	0.000348871	EG241041
670204	-2.32067	0.000342477	IAN3
4900719	-2.26282	0.000114283	A930008A22RIK
2570154	-2.25263	0.000489964	CARD4
6900465	-2.25142	0.000602405	PLCB2
2710341	-2.24769	0.001981929	NSG2
6450520	-2.24704	0.003947197	7530408C15RIK
60639	-2.24307	0.000804742	SBK
7330292	-2.21129	0.000602405	MGST2
4220139	-2.15019	0.000391771	BC006933
130215	-2.14607	0.000706279	ATP1B1
3440646	-2.14159	0.000176863	PRKCB
2370465	-2.13968	0.000044421	5330403D14RIK
1570133	-2.13895	0.006028698	CTSW
1090647	-2.13136	0.000945620	9830148G24RIK
5340369	-2.12911	0.002386970	LRMP
6860544	-2.12270	0.001218239	9330140K16RIK
2190632	-2.12175	0.001058920	1110028E10RIK
1030133	-2.11462	0.018211938	TUBB2B
6940187	-2.09454	0.002425623	NRP
5270167	-2.08148	0.000506832	6330442E10RIK
5130343	-2.07827	0.000120156	GTF2I
1430368	-2.07055	0.000021054	ST6GAL1
6650477	-2.06222	0.000303917	IAN6
7510452	-2.02937	0.001355808	ICAM2
1470605	-2.02096	0.005133740	D11ERTD759E
3060546	-2.01636	0.001032998	DPP4
5570358	-1.99590	0.001117080	BCL2
6100674	-1.99184	0.000114283	AI875142

3190722	-1.99054	0.008812744	5830496L11RIK
2600471	-1.98724	0.002581857	D630014A15RIK
4040435	-1.98358	0.011497165	NDG2
2810541	-1.93530	0.000324114	HCPH
4640463	-1.92945	0.001109140	EVL
6450687	-1.92776	0.002652854	ABI3
5720239	-1.91137	0.001058920	INPP5F
940102	-1.90759	0.002867770	PSCD3
1010138	-1.89041	0.005451348	IGH-6
5340278	-1.88099	0.005205966	IGH-6
5960746	-1.87240	0.001117080	FOLR4
830377	-1.86543	0.002079929	TSPAN32
5390440	-1.83612	0.003533045	LOC269401
2970528	-1.81067	0.005272979	FMNL3
6860022	-1.80338	0.000632640	DTX1
5550671	-1.80099	0.002299262	LY6C
4280402	-1.78318	0.003099525	EPHX1
1660541	-1.77253	0.000021973	2610009I02RIK
2370041	-1.77090	0.000703866	AU040320
2810040	-1.75146	0.000482653	D14ERTD668E
2900592	-1.74540	0.001536926	SFXN1
1990152	-1.73420	0.000871928	PRMT3
2900474	-1.73360	0.002726847	LTA
4010243	-1.72704	0.005177536	RAMP1
4120538	-1.72455	0.000099042	RASA3
4250681	-1.72144	0.001259260	GART
5670634	-1.71965	0.012362523	SYNPO
70221	-1.70393	0.014206043	MTAP7
4290133	-1.70276	0.002616467	0610025L06RIK
4560731	-1.69760	0.017154332	1110014O20RIK
70717	-1.69297	0.001117080	CD96
4540767	-1.69077	0.001032998	TSNAX
2600132	-1.68931	0.040853350	NOC2L
2260332	-1.67818	0.031369195	TNRC6C
870519	-1.67506	0.000787843	PPM1F
4050653	-1.67455	0.002499441	PITPNM2
2370484	-1.67403	0.026600306	9930033H14RIK
6980672	-1.67399	0.000851334	BTLA
730458	-1.66636	0.009030125	SEPT9
510687	-1.66248	0.000334940	6720425G15RIK
1340450	-1.66223	0.005822986	D6ERTD245E
4490224	-1.65991	0.000144248	LOC241041
7510008	-1.64388	0.012815754	0610039P13RIK
3450072	-1.64373	0.001570082	ZFP261
5690246	-1.64195	0.000217816	GBP1
2350300	-1.63691	0.003104600	HIVEP3
4760129	-1.62403	0.004101185	CAMTA2
7650240	-1.62398	0.004077143	6720458F09RIK
3140056	-1.61637	0.000701651	4732472I07RIK
6590187	-1.61063	0.008513196	DGKZ
7160474	-1.60915	0.005323707	ARHGAP4
4480468	-1.60001	0.009174152	ARHGEF3
1660039	-1.59048	0.003099525	SLC14A1
2690102	-1.58738	0.016163278	FNTB
4150196	-1.58398	0.007873483	COX10
2470753	-1.57453	0.002299262	AI415330
5490358	-1.56948	0.001418036	KLHL6
1990014	-1.56682	0.001021362	MAST3
2450064	-1.55856	0.001832155	PSMB9
130008	-1.55344	0.000009375	ARHGEF18
4060437	-1.54522	0.001251393	GNB1L
2750521	-1.53919	0.000804742	2510005D08RIK
2680402	-1.53403	0.003966788	2210408F11RIK
1740020	-1.52567	0.003370710	5730419I09RIK
160463	-1.52532	0.002826454	LGALS3BP
7550730	-1.52302	0.001599140	DGKD

6200630	-1.51837	0.002003822	ARMCX2
1340193	-1.51382	0.000911091	PHF11
1580170	-1.50955	0.001021362	PRKCQ
4490014	-1.50631	0.000662761	KLHL17
110554	-1.49479	0.000623898	OSBPL5
4060239	-1.48815	0.008036082	PLEKHG2
150433	-1.47915	0.024641864	GIMAP1
610491	-1.47831	0.016035902	D12ERTD553E
870156	-1.47407	0.005923921	B830021E24RIK
1230703	-1.47369	0.000554560	NUP210
5870470	-1.45839	0.001198205	ARHGAP9
6520192	-1.45000	0.000178800	EXOSC7
70392	-1.44345	0.001334514	NFATC1
3850039	-1.43847	0.003918310	ZFP512
2120086	-1.43846	0.010192847	PIP5K2B
5670156	-1.43417	0.000362087	LOC625360
6560703	-1.42356	0.028663078	H6PD
2260424	-1.42302	0.000859940	PRKD2
6770630	-1.42060	0.043263318	2210008I11RIK
2850670	-1.41585	0.002140748	C030002B11RIK
7330131	-1.41559	0.026629555	A630006E02RIK
1070709	-1.41074	0.001536253	NEDD9
20301	-1.40895	0.000426990	ELP3
4640239	-1.40322	0.003432125	RPL22
780524	-1.40196	0.018629896	STX1A
3830601	-1.40159	0.002793778	ENO3
6250672	-1.39791	0.009950680	PFKM
1980209	-1.39751	0.007882696	ACTG2
50091	-1.39713	0.000752629	BLR1
6960608	-1.39417	0.005291033	ARHGEF1
1110445	-1.39393	0.002216679	LOC380706
1990021	-1.39303	0.006074133	LOC545007
7400575	-1.39192	0.001040147	KCNAB2
2340349	-1.39049	0.002026988	ALDH2
7400092	-1.38814	0.023242529	A130070G01RIK
730039	-1.37984	0.005363012	CSK
6200543	-1.37781	0.004700230	2610528C06RIK
3140102	-1.37290	0.020109444	PAOX
620646	-1.37158	0.016490013	HVCN1
360437	-1.36912	0.046198777	MAGED2
1770239	-1.36850	0.001743380	RGS10
6940079	-1.36279	0.002779879	CNP1
6620446	-1.36105	0.000334940	IL27RA
2060719	-1.35303	0.000689378	PHGDHL1
2570754	-1.35254	0.002645806	SGPP1
4050138	-1.34810	0.008489044	C230075L19RIK
5090678	-1.34710	0.033334755	BC035291
3060600	-1.34463	0.029371082	RAB6B
4250270	-1.33760	0.004883249	PRKACB
5310600	-1.33637	0.006519166	PDCD4
1340373	-1.33330	0.014230433	TRB
6420021	-1.33142	0.002914180	C030026E19RIK
7400152	-1.32932	0.025624678	BRP16
610315	-1.32720	0.010125173	BC058638
2940441	-1.32626	0.007551121	D230007K08RIK
4540278	-1.32526	0.003031083	2700061N24RIK
3130433	-1.32165	0.000463340	2610511O17RIK
6020609	-1.31617	0.000536192	SESN1
4390682	-1.31592	0.024275784	C430002D13RIK
2320541	-1.31538	0.006692532	CAR12
5260204	-1.31356	0.007451221	PDLIM2
10402	-1.31002	0.006980964	TRIM25
4150008	-1.30540	0.001459791	IGF2R
2810288	-1.30260	0.002193463	MBP
1010528	-1.29779	0.013313989	DDEF1
450491	-1.29739	0.026348735	NFATC1

4640047	-1.29667	0.002119593	ADD1
7610092	-1.29574	0.004163048	UBTF
7050717	-1.29494	0.004811412	LOH11CR2A
2970332	-1.29212	0.043848937	KLF2
7050364	-1.28696	0.001846782	FTO
4780681	-1.28545	0.003412458	2700084L06RIK
5670440	-1.28433	0.014357784	LBH
2900445	-1.28425	0.001711311	RARSL
1410554	-1.27275	0.001782673	TYKI
6620767	-1.27130	0.032285254	ARID1A
5860131	-1.27114	0.007128860	2310047A01RIK
6940132	-1.27100	0.031976896	A230050P20RIK
7400328	-1.26930	0.002827379	C130099A20RIK
4070278	-1.26767	0.019390259	SLC12A6
6760025	-1.26618	0.001226266	A930040G15RIK
1570487	-1.26407	0.014246861	TLR7
2340519	-1.26204	0.023064687	SEPT6
380594	-1.25545	0.008573273	PLCL2
5420484	-1.25446	0.002074155	5730455O13RIK
5340180	-1.25070	0.016519917	WAS
870154	-1.24781	0.022505017	H2-DMA
3850112	-1.24744	0.001167585	DNAHC8
1580309	-1.24488	0.001278887	HAP1
3310278	-1.24273	0.004745827	2610318I18RIK
2900307	-1.24248	0.020158166	5830405N20RIK
3060162	-1.24096	0.000426990	PBX2
3610056	-1.23964	0.014091058	PPIF
5690192	-1.23655	0.009105953	A630077B13RIK
2760445	-1.23638	0.011227768	9830160G03RIK
540608	-1.23321	0.026591585	SUPT3H
1510014	-1.23081	0.000703866	HEATR1
620626	-1.23037	0.002826454	APEH
3310538	-1.22288	0.002311694	PCBD2
5130066	-1.21608	0.003483045	UBE1L
10392	-1.21437	0.003060076	ANKMY2
3290259	-1.21241	0.002826454	CDC23
3140735	-1.21235	0.006377802	ZDHHC3
20612	-1.21161	0.037141660	EGR3
670050	-1.21007	0.011531159	A430107D22RIK
1990204	-1.20962	0.019291555	RIN3
2600072	-1.20873	0.006812814	GNE
2230731	-1.20769	0.001981929	H2-T17
4670706	-1.20195	0.014401946	9330134C04RIK
6650364	-1.20129	0.006585779	DDX51
430551	-1.20010	0.000244609	D6WSU176E
3870608	-1.19968	0.002504925	CSRP2BP
6350343	-1.19822	0.011522230	PSMB10
4540736	-1.19651	0.003670848	CCS
780221	-1.19629	0.001273500	H2-T9
3310131	-1.19597	0.004426953	A630023P12RIK
3370201	-1.19556	0.019586584	PRG4
4180575	-1.18975	0.000342477	PPM1M
4920746	-1.18942	0.020058507	AA408296
1780037	-1.18933	0.027601632	BC030476
1190446	-1.18872	0.000426990	GRHPR
1340382	-1.18845	0.016317774	DGUOK
2600026	-1.18717	0.009760350	REC8L1
3190609	-1.18589	0.003099525	ZC3HDC5
4640168	-1.18369	0.017415054	3110001D03RIK
10730	-1.17933	0.000689378	5730406O18RIK
240189	-1.17804	0.002897957	2610024N01RIK
7610215	-1.17795	0.004935349	2810410A03RIK
1820148	-1.17544	0.001983180	1200008N06RIK
70243	-1.17290	0.024893600	9130221H12RIK
4050328	-1.17279	0.008351348	MTAP
1850437	-1.17150	0.001679907	ARMC3

160703	-1.16921	0.007873483	TIMELESS
1090605	-1.16804	0.005262927	TSPYL3
1340092	-1.16796	0.001117080	UNC13D
2320296	-1.16248	0.001981929	TIMM10
6100050	-1.16228	0.025118290	AI316807
1470519	-1.16093	0.014938991	LOC433224
830041	-1.15635	0.011203857	G22P1
5550187	-1.15434	0.000589784	GANC
2350274	-1.15277	0.007375123	IQCE
3130750	-1.15136	0.026625048	UNG
2850747	-1.14398	0.000212192	2810423O19RIK
2060431	-1.14195	0.034871447	USP36
2630543	-1.14120	0.002867770	NDRG2
5390019	-1.13429	0.007040999	PLA2G4B
2030524	-1.13120	0.005822986	5430437P03RIK
650609	-1.13030	0.004505410	TPCN1
7150349	-1.12763	0.022695425	2310079N02RIK
4640008	-1.12695	0.004021025	SLC38A2
1170022	-1.12464	0.020732261	RMND1
360348	-1.12374	0.012768305	GSTA4
7510020	-1.12292	0.021316544	IFIT3
4570309	-1.12232	0.008488634	MYO9B
4900632	-1.12101	0.030382779	DSCR1L2
6940224	-1.12010	0.008827782	5730578N08RIK
460220	-1.11965	0.004815142	SLC22A5
2360554	-1.11961	0.017087036	PSTPIP1
3310091	-1.11606	0.022605449	BC052040
2650204	-1.11602	0.000653465	ABCA3
3180068	-1.11404	0.026955972	AKR7A5
5310091	-1.11332	0.005518964	ADD3
4200224	-1.11229	0.004704403	HELB
6110242	-1.10965	0.027256748	MUM1
7610612	-1.10854	0.001048573	RFX1
2340403	-1.10818	0.032922771	ZFP41
4860598	-1.10656	0.007814274	MAP3K7IP1
2140215	-1.10291	0.004023203	2010004M13RIK
2970307	-1.10004	0.016500516	RHBDL2
2480474	-1.09662	0.000554560	LOC380763
2000128	-1.09588	0.005579017	DNAJA3
7610450	-1.09459	0.004691459	ITPR2
2970167	-1.09386	0.004687509	5830417I10RIK
5870725	-1.09126	0.001645954	CCDC58
4830703	-1.08953	0.005444675	SEC15L1
7100300	-1.08881	0.046733774	TMC6
150372	-1.08732	0.032935903	RASL11B
2120400	-1.08727	0.000689378	PDCD11
5270452	-1.08361	0.019586584	TIAM1
5900347	-1.08349	0.011908053	PIGO
1340671	-1.08032	0.002193463	RPA1
4610170	-1.07286	0.018154300	E030002F19RIK
1710332	-1.07189	0.001669104	6430706D22RIK
3440463	-1.07184	0.003092285	GUCY1A3
7050673	-1.07173	0.014669451	ZXDA
3120470	-1.07073	0.001679907	2010110K16RIK
4260400	-1.06895	0.007628112	1200013B08RIK
1510753	-1.06522	0.004260026	CENTD1
6290435	-1.06276	0.013261196	6530405K19
5870669	-1.05896	0.001334514	A830007P12RIK
3440112	-1.05879	0.009150319	NLK
3780471	-1.05844	0.000703866	TCF7
6350161	-1.05804	0.001977710	IFT140
70386	-1.05541	0.003964512	SATB1
1820470	-1.05400	0.004410674	KRBA1
6510544	-1.05351	0.006793870	HDAC10
4050400	-1.05269	0.023508071	ZYX
2810494	-1.05154	0.007882696	E2F2

4390458	-1.05017	0.002175333	5830482F20RIK
6480242	-1.04898	0.003049497	2700094F01RIK
4280255	-1.04741	0.020679827	STATIP1
6760167	-1.04733	0.006262031	H2-OB
7000475	-1.04702	0.041490908	GEMIN4
1240554	-1.04643	0.001325906	CALM3
4060288	-1.04584	0.005427358	TRIM8
1990546	-1.03760	0.014320834	1810037B05RIK
1030577	-1.03628	0.001117080	SNN
2690292	-1.03619	0.001058920	MAPK9
2340167	-1.03596	0.010918783	RAD52B
1260673	-1.03430	0.002936639	SCOTIN
4640528	-1.03385	0.004021025	MACF1
5690139	-1.03334	0.001326384	MANBA
5310079	-1.03019	0.015371873	PRF1
5560139	-1.03008	0.006377802	SRFBP1
6330592	-1.02897	0.001796055	D11LGP2E
5960341	-1.02810	0.002842643	MSRB2
3310725	-1.02796	0.009143224	TK2
1070451	-1.02776	0.002392428	PKN1
360524	-1.02773	0.004807566	2700087H15RIK
270711	-1.02729	0.036374206	GALGT1
6280414	-1.02628	0.010322616	TBC1D5
4210333	-1.02583	0.008877506	VAV2
6590053	-1.02502	0.030473783	E2F6
5870687	-1.02492	0.006908415	SLC29A1
5390082	-1.02461	0.001984824	HMG20A
3190021	-1.02450	0.022605449	KEAP1
430037	-1.02290	0.000394694	1700012B18RIK
4200543	-1.02129	0.045355612	VARS
6860253	-1.01872	0.044520153	H13
2030639	-1.01635	0.011250544	AI413582
5220639	-1.01384	0.014950743	9530090G24RIK
2570672	-1.01354	0.019586584	ATP2A3
2650326	-1.01211	0.035411041	PML
240259	-1.01125	0.012075098	LDH2
6940719	-1.00978	0.002386970	TLR1
2570131	-1.00833	0.004745827	DLG3
1230731	-1.00547	0.028162289	SRF
830598	-1.00501	0.012636929	CBX7
7210706	-1.00426	0.003010695	CASP9
4060647	-1.00250	0.019586584	2310038D14RIK
7150066	-1.00220	0.042038057	KLF7
1710524	-1.00038	0.028523528	9630009A08RIK

Supplementary Table 1
Genes differentially up- and down-regulated in skin resident Foxp3^{+} CD4 T cells

Data was normalized as described in Chapter 2. Genes listed have a p value of >0.05 and a log2 fold change of >1 or <-1.

Supplementary Table 2

GO Biological Process	Gene	Log2 fold change
response to molecule of bacterial origin	IL10	5.510848933
	TNFAIP3	2.310387466
	CXCL2	1.745142578
	BCL10	1.190850285
	CD14	0.915551506
	MALT1	0.681782785
negative regulation of inflammatory response	IL10	5.510848933
	IER3	4.592142983
	TNFAIP3	2.310387466
	IL2RA	1.965295352
	TNFRSF1B	1.735527323
	NDFIP1	1.63289078
	ZFP36	1.55451678
	APOE	1.108747631
	GATA3	0.958814405
	KLF4	0.850839899
	PRKCD	0.495460923
	GBA	0.45631388
response to lipopolysaccharide	IL10	5.510848933
	ICAM1	2.600533039
	LITAF	2.559818682
	JAK2	2.509710415
	CEBPB	2.174583663
	GCH1	2.145509267
	MAPKAPK2	1.922787967
	TNFRSF1B	1.735527323
	MAPKAPK3	1.463212309
	EDNRB	1.32629297
	FOS	1.30477231
	IRAK3	1.225360315
	IL1B	1.221194429
	SLC11A1	1.174948155
	NFKBIA	1.163865702
	LY96	1.123729507
	CD14	0.915551506
	DCN	0.865714576
	SOD2	0.84841798
	RPS6KA3	0.739192244
	MYD88	0.607711801
	F2R	0.558709632
response to organic cyclic compound	CDKN1A	3.957074717
	ICAM1	2.600533039
	CTGF	2.249487155
	STAT3	1.628749676
	JUNB	1.572843383
	EDNRB	1.32629297
	FOS	1.30477231
	CD83	1.301491587
	PDGFB	1.181095315
	ALDOC	1.157237232
	IL1RN	1.112170277
	TGFB1	1.109684414
	PPARG	1.069391269
	CTNNA1	0.99146353
	CDKN2B	0.736348963
	HMGCS1	0.690690148
	PRKCD	0.495460923
	MMP14	0.476078159
	ANXA1	0.407550727

inflammatory response	IL10	5.510848933
	CXCL1	3.973657028
	KLRG1	3.059304277
	MAP2K3	2.639735502
	CCRL2	2.377590894
	LYZ	2.332776918
	TNFAIP3	2.310387466
	CEBPB	2.174583663
	CALCA	2.164684112
	CCR5	1.993330253
	MAPKAPK2	1.922787967
	NFKBIZ	1.801552266
	KIT	1.797517567
	CXCL2	1.745142578
	TNFRSF1B	1.735527323
	SPHK1	1.692398676
	TNIP2	1.444616222
	FOS	1.30477231
	TNFRSF4	1.284423073
	IL1B	1.221194429
	CCL5	1.220827011
	IRAK2	1.216237563
	CXCR4	1.194343036
	SLC11A1	1.174948155
	LXN	1.157333577
	LY96	1.123729507
	TGFB1	1.109684414
	GPR68	0.922868665
	CD40	0.916588543
	CD14	0.915551506
	IL18RAP	0.799120371
	MYD88	0.607711801
	AXL	0.589872535
	RIPK2	0.567359772
	F2R	0.558709632
	CXCR6	0.551977166
	ANXA1	0.407550727
	ADAM8	0.402672025
	CYSLTR1	0.392248268
negative regulation of apoptotic process	IL10	5.510848933
	IER3	4.592142983
	HSPA1A	4.271202582
	CDKN1A	3.957074717
	CTSH	2.445150888
	TNFAIP3	2.310387466
	ASNS	2.205741648
	CEBPB	2.174583663
	CD44	2.051858082
	SOCS3	2.025198399
	BAG3	1.970503101
	HSPB1	1.935619495
	BCL3	1.921089542
	MUC1	1.827500268
	SQSTM1	1.75089083
	BIRC2	1.692796893
	SPHK1	1.692398676
	FAS	1.492096849
	FAIM	1.480572879
	TNFRSF18	1.43849473
	CIAPIN1	1.405237926
	BCL6	1.354469769
	POR	1.353316472
	EDNRB	1.32629297
	TNFAIP8	1.318220439
	IL1B	1.221194429

neg. regul, of apoptotic process (continued)	YBX3	1.168362889
	NFKBIA	1.163865702
	STAT5A	1.132292031
	SPHK2	1.11592519
	IL1RN	1.112170277
	APOE	1.108747631
	BNIP2	1.063031493
	CTNNA1	0.99146353
	PSEN2	0.932838745
	CCNG1	0.932593338
	PIM3	0.883137742
	AHI1	0.880463978
	IVNS1ABP	0.864173015
	SOD2	0.84841798
	IL6ST	0.827469528
	PDCD10	0.793268633
	RPS6KA3	0.739192244
	UBE2B	0.724947125
	GCLM	0.712683756
	SSBP3	0.682843805
	MALT1	0.681782785
	UBC	0.623408736
	CFL1	0.618178222
	PEA15	0.607873333
	MYD88	0.607711801
	BCL2L2	0.605811822
	MPO	0.600577169
	TAX1BP1	0.593159614
	AXL	0.589872535
	PLK3	0.584531077
	NUP62	0.574993022
	RIPK2	0.567359772
	IVNS1ABP	0.545180869
	ITGAV	0.530208399
	FHL2	0.521661273
	CITED2	0.51822894
	BECN1	0.501726639
	HSPA1B	0.49996549
	JTB	0.481804957
	BNIP3L	0.466589597
	YAP1	0.454233913
	SIAH2	0.440391945
	SH3GLB1	0.41359951
	TRAF6	0.411871949
	HSPD1	0.408050469
	ANXA1	0.407550727
	SOD1	0.402964135
	ANXA4	0.368683735
	BAG1	0.329535598
	HPN	0.308715108
	ARAF	0.062180391
	IVNS1ABP	0.060189123

Supplementary Table 2
Significantly enriched GO biological functions in skin Tregs (discussed in Chapter 3)

Data was normalized and analyzed as described in Chapter 2.

Supplementary Table 3

Probe ID	Log 2 fold change	adj..p value	gene
130608	2.2404	0.0013	LAG3
6940184	2.2091	0.0084	CCL4
670204	1.9579	0.0069	IAN3
5360707	1.9282	0.0129	SELL
6200719	1.7316	0.0129	ACAS2L
1990021	1.5335	0.0231	LOC545007
70386	1.4440	0.0069	SATB1
4540767	1.3840	0.0184	TSNAX
2030139	1.3620	0.0152	GPR15
6650626	1.3584	0.0449	IPCEF1
1980209	1.3477	0.0450	ACTG2
6650477	1.3211	0.0189	IAN6
6290053	1.3081	0.0422	TRERF1
3120091	1.2471	0.0198	NCK2
3440646	1.2469	0.0184	PRKCB
4920487	1.2305	0.0162	CKB
5820739	1.1821	0.0063	GP49A
1690719	1.1163	0.0159	LGMN
2940356	1.1015	0.0181	SCL0001709.1_980
4010402	1.0840	0.0365	GIMAP8
2680168	1.0738	0.0411	GATS
1820040	1.0655	0.0019	A430093F15RIK
50059	1.0655	0.0248	AI504432
3780403	1.0544	0.0022	TRERF1
1230703	1.0465	0.0198	NUP210
2710152	1.0303	0.0500	HTATIP2
3310189	1.0289	0.0248	CST7
4120538	1.0288	0.0126	RASA3
5260731	1.0269	0.0312	PKP3
630192	-2.3453	0.0039	MPP7
1580349	-1.9726	0.0003	CAMK2N1
6250193	-1.9044	0.0181	TXNIP
60239	-1.7556	0.0068	DUSP6
4120187	-1.6625	0.0063	SP6
1090438	-1.5257	0.0193	ATF3
4010082	-1.4697	0.0439	CTGF
3290747	-1.3676	0.0069	BEX2
7510020	-1.3476	0.0422	IFIT3
6420762	-1.3397	0.0198	A530026H04RIK
1300121	-1.2933	0.0365	MGAT4A
7150377	-1.2544	0.0068	CD83
6760546	-1.2511	0.0165	RBBP5
1580187	-1.2499	0.0003	MAT2A
1090093	-1.2294	0.0412	TTC3
2850010	-1.2281	0.0068	CD86
2600301	-1.2182	0.0181	TROVE2
1050092	-1.2043	0.0159	SERPINA3G
3370239	-1.1714	0.0283	E130118D18RIK
3850017	-1.1477	0.0422	TGFBR1
1710286	-1.1358	0.0310	ZFP420
3780500	-1.1314	0.0378	GTF2IRD2
6290133	-1.1313	0.0013	ENDOD1
940129	-1.1296	0.0133	4930486L24RIK
60056	-1.1103	0.0063	RNF185
5690167	-1.1082	0.0152	MRPL49
2850082	-1.0933	0.0353	ZFP869
3840324	-1.0792	0.0149	BLCAP
6200300	-1.0629	0.0410	ZFP874B

Supplementary Table 3

Genes differentially up- and down-regulated in skin resident $CD4^{+}Foxp3^{+}$ T cells from inflamed skin vs. homeostatic skin

Data was normalized as described in Chapter 2. Genes listed have a p value of >0.05 and a log2 fold change of >1 or <-1.

Supplementary Table 4

ID	log2 fold change	adj. p value	gene
10598	4.324011839	0.00000060689	CXCL9
1690768	4.167377267	0.00000000001	CCL5
1690079	4.075821647	0.00000000021	CD8B
6290037	3.696799824	0.00000000006	IGTP
4040035	3.656924455	0.00000000010	NKG7
6860600	3.376265704	0.00000000021	GBP2
2490653	3.199481506	0.00000000134	LOC240327
1050092	3.113847065	0.00000000021	SERPINA3G
3140209	3.109337027	0.00000000001	CXCL10
4260463	3.099905073	0.00000020362	LOC382896
7040170	3.083656817	0.00000000001	UBD
1570133	3.043019412	0.00000000168	CTSW
60553	3.025950496	0.00000000004	GBP4
2570095	2.882793281	0.00000015684	PSMB8
1090139	2.804948749	0.00000000168	IFI47
5820608	2.791930776	0.00000000001	IRGM
460221	2.790793772	0.00000004419	G1P2
2230386	2.75930512	0.00000000010	AI481100
1400220	2.670447515	0.00000000001	LOC215405
1110445	2.641810892	0.00000000041	LOC380706
1440681	2.537307452	0.00000007681	CD6
1820541	2.504454431	0.00000000148	LCK
4540082	2.482144936	0.00000007504	BC049975
6590215	2.391289936	0.00000002543	H2-T22
7510020	2.366374872	0.00000001276	IFIT3
4830010	2.365404978	0.00000000137	OASL2
450735	2.355606722	0.00000070218	GVIN1
4260528	2.323640836	0.00000000021	STAT1
4890279	2.318882601	0.00000015036	KLRD1
4810204	2.2544998	0.00000030688	CD27
5270398	2.249660798	0.00000000148	IFIT2
2450064	2.247076195	0.00000000363	PSMB9
2340044	2.202652121	0.00000000041	SLAMF8
5550671	2.14917456	0.00000047856	LY6C
3360138	2.144562951	0.00000003288	IRF1
6330692	2.143968978	0.00000000168	GBP6
520040	2.138688315	0.00000000554	AI451557
7200100	2.057000464	0.00000006043	H2-T23
610324	2.052508027	0.00151219939	CD3D
5690192	2.037388615	0.00000020420	A630077B13RIK
2970521	2.027883836	0.00000001998	PARP14
2510138	2.012181869	0.00001938490	TCRB-V8.2
1090647	2.007774108	0.00000000004	9830148G24RIK
870446	2.007299664	0.00000000001	H2-T10
1470605	1.993856521	0.00000000365	D11ERTD759E
5130066	1.989621587	0.00000006210	UBE1L
7400528	1.97986203	0.00000682656	IFI205
5900520	1.97593721	0.00000000137	GBP5
4490017	1.958115762	0.00000050890	TAP2
160463	1.957100217	0.00000057370	LGALS3BP
940747	1.932697662	0.00003829671	CD3G
4640348	1.928453963	0.00000017502	EG630499
6270682	1.917413938	0.04957533452	SLC15A2
1580528	1.899895657	0.00000005043	USP18
1170181	1.894466752	0.00182111118	CD52
3890328	1.891030929	0.00000010279	OAS1G
1740692	1.888521668	0.00000000248	TNFSF6
6590239	1.885890977	0.00000957972	CD3E
7650242	1.880134206	0.00000182052	IL18R1
6940386	1.877768776	0.00000002354	H2-Q7
5690246	1.871471392	0.00018981103	GBP1
380672	1.87005962	0.00007605876	1810062O14RIK
4760575	1.869389982	0.00001042221	SH2D2A

5870093	1.867864794	0.00000000018	TAP1
2230731	1.864802052	0.00000000012	H2-T17
3130292	1.843401697	0.00000299587	IDB2
3190577	1.836028783	0.00000030688	SAMHD1
4810575	1.830404694	0.00000029885	HK3
7160047	1.829446418	0.01910096151	AA467197
2750128	1.822943698	0.00000000804	H2-Q8
2850092	1.809797992	0.00000000007	IFNG
2810040	1.807185866	0.00000000021	D14ERTD668E
830632	1.799594195	0.00007095263	FCRL3
770669	1.798852489	0.00000345012	A130092J06RIK
270717	1.795543436	0.00000001829	BC023741
60221	1.794417531	0.00000006421	CD2
5670398	1.783051819	0.00000000021	TRIM21
540647	1.778658383	0.00020046863	CD69
3130240	1.773579162	0.00000003987	H2-Q5
780221	1.764155524	0.00000000015	H2-T9
150138	1.762673164	0.00011661525	H2-DMA
3060450	1.761207193	0.00000004227	OAS2
1240646	1.747915956	0.00000241597	CCR5
6180154	1.728439847	0.00000005043	ITK
5810576	1.724974071	0.00000330603	CXCR3
6220594	1.72490932	0.00000000343	STAT2
6860040	1.718865184	0.00021744818	KLHL6
5860243	1.709370326	0.00588698672	PLAC8
6280221	1.694273391	0.00000048501	SP100
3780736	1.68118055	0.00000002224	H2-K1
7160246	1.677100144	0.00000000015	4933430F08RIK
1440307	1.667401455	0.01005475091	H2-AB1
3520746	1.665978291	0.00022355843	SLFN1
3870561	1.664073284	0.00001042221	PDCD1LG1
1300673	1.653349892	0.00304511051	CLECSF12
1740609	1.651199814	0.00000134800	AU020206
5560474	1.632671981	0.00190029814	2510004L01RIK
5720048	1.631812375	0.00000186880	H2-Q2
3420451	1.624194341	0.00000004957	ESM1
4890092	1.619827573	0.00001542944	GPR114
5900324	1.618400107	0.00018400488	A330102K04RIK
1500246	1.607590716	0.00000000055	LOC626578
4490243	1.601778219	0.00014363238	RAC2
2480725	1.582594295	0.00223056637	CORO1A
1570564	1.579605081	0.00000005888	CD160
4490709	1.559100508	0.00005353383	GZMK
2650754	1.557350255	0.00000170789	UBE2L6
2940441	1.557216284	0.00000186447	D230007K08RIK
7560307	1.554754605	0.00393617623	IRG1
670050	1.55314409	0.00000109972	A430107D22RIK
940161	1.54327252	0.00000010759	CD28
2100139	1.532018521	0.00000017494	BST2
2760274	1.530345496	0.00000079885	2310046K10RIK
3460102	1.520938114	0.00000001675	9130022K13RIK
3060482	1.512101897	0.00000366963	ISGF3G
2190475	1.508199652	0.00044490634	MS4A6D
1340050	1.504131281	0.00000002375	ZC3HDC1
830543	1.500137667	0.00000885301	ITGB7
6450253	1.491674225	0.00000025201	5830484A20RIK
150433	1.483233862	0.00000345792	GIMAP1
4040095	1.481034697	0.00000000286	H2-Q6
6760762	1.471069201	0.00001256839	SDC3
1170521	1.461400514	0.00000779733	DUSP2
6900044	1.45705871	0.00002898431	LAT
1940338	1.453609156	0.00001456181	H2-M3
5870398	1.453085888	0.00000006508	PSMB10
6770195	1.450264859	0.00584908268	II
5820128	1.448912971	0.00000006612	0610037M15RIK
2850575	1.448659896	0.00293816949	VCAM1

4220603	1.424042315	0.00000236859	FCGR1
430167	1.423889729	0.00831854768	LY86
7040731	1.391992704	0.00089164551	H2-DMB2
20358	1.390383968	0.00000000828	TAPBP
1510497	1.384666228	0.00004762631	HCST
6040072	1.377975605	0.00028710987	E430021P16RIK
7040202	1.375519548	0.01634917088	BCL2A1D
110064	1.367584271	0.00191760443	SLA
3710170	1.360780157	0.00640702134	C1QG
4010221	1.35582198	0.00083598550	MPEG1
2340301	1.355354802	0.00001237900	HSD11B1
6480131	1.355148627	0.00000038295	TAPBPL
6370010	1.349474295	0.00529113518	CHI3L3
630025	1.344375942	0.00000008321	MLKL
2120491	1.341147374	0.00000124644	BC010462
3940561	1.340464031	0.01362195184	AIF1
3450167	1.340037218	0.00000952684	SNX10
3190722	1.339509371	0.00001115995	5830496L11RIK
4120243	1.33642823	0.02363874203	UPP1
6580379	1.3362445	0.00000188008	P2RY14
670491	1.335787524	0.00000143456	SCL0001132.1_96
6940398	1.333642922	0.00053910532	LOC270152
270176	1.319625117	0.00002981688	IL2RG
6290592	1.318823448	0.00021027037	LOC226691
2630463	1.318095591	0.00000768308	C2TA
2750543	1.317389579	0.00003369859	GPR18
4120687	1.316440271	0.00027989638	GLIPR2
6760735	1.316431449	0.00000026013	TCRB-V13
3940242	1.311501958	0.00000449053	AA175286
5390088	1.311233002	0.00073352220	LOC327957
10167	1.310823739	0.00000008821	LOC56628
4210470	1.307751005	0.00003441145	C2
1660504	1.305842049	0.00001155412	IL7R
1410554	1.304898981	0.00000428458	TYKI
130097	1.303274754	0.01573721186	BCL2A1B
2450239	1.302350307	0.00614305981	ICOS
6450682	1.294089965	0.00000280214	H2-L
4260400	1.293539781	0.00047634253	1200013B08RIK
2340463	1.282297251	0.00000004461	MS4A8A
670204	1.279191131	0.00000809392	IAN3
1690093	1.276077809	0.00000957972	LYT-2
3370221	1.272242839	0.01242434991	BC028528
2970544	1.269150476	0.00005017606	ZAP70
6270259	1.268530904	0.00001237900	T_CELL_RECEPTOR_BETA_VARIABLE_8_270
1660400	1.266814672	0.00000001960	4933412E12RIK
6280521	1.264585525	0.00000026013	A530060O05RIK
3390253	1.264524053	0.00786770993	IL1RA
5900593	1.263673703	0.00000351693	PTPN8
4780184	1.256604721	0.00000670078	LY6E
3830678	1.254816834	0.00486196769	FCGR3
7650048	1.25340331	0.00614305981	FPR-RS2
1940722	1.251352961	0.00040396100	CASP1
1030519	1.241240473	0.00001793868	ID2
270367	1.240000399	0.00030087321	H2-GS17
2680520	1.239613553	0.01861137750	MTDNA_ND4L
3870091	1.23023864	0.00000324333	0610007P22RIK
1340193	1.229561473	0.00000002631	PHF11
1230639	1.226906229	0.00398117046	F10
4640093	1.220624997	0.00000273330	TCRB-V8.3
580332	1.220186417	0.01209030153	C1QB
5290017	1.215274742	0.00190029814	CASP4
5720397	1.20697601	0.00000004012	D11LGP2E
5360707	1.204505711	0.01203553253	SELL
7200356	1.203248447	0.00014510655	MYO1G
4150414	1.197804343	0.00069670930	FYB
520072	1.186010912	0.01135790107	H2-EB1

1110326	1.182106162	0.00415392679	FCGR2B
2710128	1.180441007	0.00018702111	DOCK10
5560066	1.171829772	0.00003829671	STAT4
5700392	1.16901463	0.00001107456	T_CELL_RECEPTOR_BETA_VARIABLE_7_29
610184	1.164208018	0.00000006421	TRIM34
5090491	1.161989101	0.02753377687	SIRPB1
770273	1.161407778	0.00001619813	BC013712
7050433	1.159411598	0.00185386088	LPXN
5810048	1.154300064	0.00006845968	ZFPN1A1
6180082	1.153751853	0.00000022940	SH2D1A
2680475	1.153616181	0.00000000964	1600029O10RIK
770189	1.152473005	0.00023531515	1810044J04RIK
2370039	1.151307339	0.00080309604	GPR171
3360639	1.150770142	0.00001487200	T_CELL_RECEPTOR_BETA_VARIABLE_12-2_155
6590653	1.14930459	0.00001099832	IRF7
6220274	1.145157706	0.00138795782	LOC381276
5700528	1.142535163	0.00335507758	CD72
3520735	1.139156161	0.00022006059	BCL2A1C
4860719	1.13799944	0.00296225002	MYO1F
5130156	1.137869782	0.01307810138	CCRL2
7570204	1.134493661	0.00002593191	GSDMDC1
1070307	1.130777091	0.00764138536	SELPL
1820040	1.126024643	0.00003063799	A430093F15RIK
940367	1.123990552	0.00002724319	TCRB
6840594	1.122783372	0.00012268179	RGS1
5890328	1.118734834	0.00000461981	2810038K19RIK
6520349	1.115084699	0.00061544400	PIRA11
6560431	1.113674559	0.00000103828	B630009B09RIK
1190477	1.113672212	0.00058075280	A430084P05RIK
2480577	1.112353174	0.01095299470	ACTB
60603	1.111371647	0.00079934917	HAVCR2
4540564	1.109983318	0.00004508314	DOK2
1470711	1.109833055	0.00398117046	LCP1
3060040	1.109481128	0.04704899968	CXCL13
1230703	1.105907383	0.00016299201	NUP210
4640754	1.105583798	0.00000001927	F730045P10RIK
160408	1.104219287	0.00227961375	LTB
4760241	1.097138875	0.00002909859	CD40
3120037	1.094623714	0.00013134571	CENTB1
430132	1.091361495	0.00002119909	LGALS9
6770259	1.083748611	0.00000001960	LOC435565
2030358	1.079883949	0.00907438150	BTG1
60050	1.078832201	0.00000345792	INSL6
6760255	1.077955451	0.01556109911	EVI2A
830762	1.074534604	0.00002822348	PRKR
2510164	1.072371779	0.00171526688	TRAF1
2490553	1.069979558	0.03706960763	IL1A
2340242	1.067766272	0.00014443827	FGL2
2320181	1.061648703	0.00000007671	A330042I21RIK
1400132	1.059635384	0.00000382943	LOC547343
5310672	1.056505249	0.00559091075	FXYD5
4730246	1.055429999	0.00000015805	LOC226690
2650326	1.055416385	0.00008871567	PML
6060520	1.051582538	0.00584908268	CCL11
650707	1.049231571	0.00976856360	H2-AA
4010402	1.045248484	0.00011661525	GIMAP8
6110671	1.04195718	0.00000003514	LOC223672
3850324	1.041589183	0.00003684972	LOC381010
6020398	1.039653998	0.00003522189	ETS1
2680669	1.039118133	0.00022295019	36951
2350132	1.038920477	0.02218843629	C1QA
4830543	1.035769063	0.00190890372	2310061N23RIK
870156	1.035090706	0.00000092941	B830021E24RIK
2000373	1.034352027	0.00382534142	SERPING1
4810154	1.03108349	0.01245921738	CLEC4A3
3850497	1.030800414	0.00249115939	SLC11A1

2850133	1.02753307	0.00069779255	MSN
3390021	1.027185559	0.00564307490	SDCBP
3400097	1.023099694	0.00007095263	LOC434197
5700538	1.01794631	0.00002282213	AOAH
4120014	1.016490543	0.00000017494	IFI35
7100762	1.010979807	0.00000073360	SLC28A2
1260673	1.010022957	0.00000190231	SCOTIN
7000187	1.00787724	0.00154428705	TGM2
3120259	1.007794037	0.00017164335	ZFP313
3930370	1.006283976	0.00084383397	A130065C13RIK
4200192	1.005679099	0.03461468634	IRG1
2230039	1.002131038	0.00210604647	FCER1G
3780193	-1.000197679	0.00012501975	GSTA3
5340064	-1.007449399	0.01870968103	PVALB
70544	-1.028693821	0.02565586008	GSTA1
5310497	-1.057728222	0.00378496086	ODZ4
620167	-1.062348729	0.01382006614	AKR1C18
580364	-1.073078174	0.00289616111	IGFBP2
4250681	-1.074710334	0.00059967560	GART
2000414	-1.077455081	0.02908822080	IL17F
3850102	-1.253498737	0.00233253805	EPGN
940541	-1.331746733	0.02632001881	MSR2
360348	-1.343985976	0.02151740085	GSTA4
5090706	-1.553649174	0.00318943404	LRRC15
4640114	-2.409050864	0.00338874385	ACTB

Supplementary Table 4
Genes differentially up- and down-regulated at day 7 of imiquimod treatment in Treg depleted skin vs. day 7 of imiquimod treatment in Treg replete skin

Data was normalized as described in Chapter 2. Genes listed have a p value of >0.05 and a log2 fold change of >1 or <-1

Supplementary Table 5

GO Biological process	p value	fold change	FDR
immune response	0.00000000000000000001	4.63	0.00
regulation of immune response	0.00000000000000000001	7.34	0.00
type I interferon-mediated signalling pathway	0.00000000000000011462	8.08	0.00
defence response to virus	0.00000000000001026300	5.06	0.00
inflammatory response	0.00000000000009800500	3.22	0.00
innate immune response	0.00000000000041196000	2.5	0.00
positive regulation of T cell proliferation	0.00000000000066152000	6.98	0.00
T cell costimulation	0.00000000000072828000	6.24	0.00
cytokine-mediated signalling pathway	0.00000000000093784000	3.47	0.00
cell surface receptor signalling pathway	0.00000000001390800000	3.27	0.00
response to virus	0.00000000002674000000	4.27	0.00
interferon-gamma-mediated signalling pathway	0.00000000010507000000	5.91	0.00
chemotaxis	0.00000000326450000000	4.16	0.00
defence response	0.00000003645100000000	4.87	0.000005
T cell receptor signalling pathway	0.00000007357900000000	4.02	0.000009
T cell activation	0.00000008183800000000	4.93	0.000009
leukocyte migration	0.00000021108000000000	3.39	0.000022
cellular defence response	0.00000026196000000000	5.24	0.000026
leukocyte cell-cell adhesion	0.00000047971000000000	6.57	0.000046
defence response to Gram-positive bacterium	0.00000125120000000000	5.49	0.000109
natural killer cell activation	0.00000168270000000000	10.7	0.00014
negative thymic T cell selection	0.00000198020000000000	8.74	0.000158
positive regulation of interferon-gamma production	0.00000268990000000000	5.67	0.000206
positive regulation of cytokine secretion	0.00000321710000000000	6.24	0.000237
positive regulation of I-kappaB kinase/NF-kappaB cascade	0.00000399680000000000	2.89	0.000283
B cell activation	0.00000627150000000000	6.66	0.000414
cell-cell signalling	0.00000929520000000000	2.56	0.000593
T cell differentiation	0.00001089700000000000	4.99	0.000673
negative regulation of viral genome replication	0.00001166700000000000	6.24	0.000698
positive regulation of monocyte chemotaxis	0.00001818400000000000	10.4	0.001055
adaptive immune response	0.00002285000000000000	6.72	0.00125
response to interferon-gamma	0.00002285000000000000	6.72	0.00125
cellular response to lipopolysaccharide	0.00002393900000000000	3.5	0.001273
positive regulation of phagocytosis	0.00003432300000000000	5.55	0.001767
neutrophil chemotaxis	0.00003507300000000000	4.46	0.001767
positive regulation of T cell mediated cytotoxicity	0.00004089200000000000	7.49	0.002007
complement activation, classical pathway	0.00004255300000000000	6.24	0.002036
antigen processing and presentation of exogenous peptide antigen via MHC class I	0.00005341200000000000	3.12	0.002493
integrin-mediated signalling pathway	0.00006569400000000000	3.07	0.002924
apoptotic signalling pathway	0.00007949400000000000	2.79	0.003458
lymph node development	0.00008387900000000000	6.81	0.003483
positive regulation of interleukin-2 biosynthetic process	0.00008387900000000000	6.81	0.003483
JAK-STAT cascade	0.00008552300000000000	4.99	0.003483
induction of apoptosis	0.00017877000000000000	2.24	0.007129
regulation of small GTPase mediated signal transduction	0.00020797000000000000	2.38	0.007961
positive regulation of nitric oxide biosynthetic process	0.00026820000000000000	4.34	0.009972
chemokine-mediated signalling pathway	0.00027093000000000000	5.76	0.009972
T cell proliferation	0.00029688000000000000	4.86	0.010268

GO Biological process	p value	fold change	FDR
positive regulation of interferon-beta production	0.00029688000000000000	4.86	0.010268
positive regulation of interferon-alpha production	0.00031117000000000000	6.94	0.010268
immunoglobulin mediated immune response	0.00031117000000000000	6.94	0.010268
humoral immune response	0.00039459000000000000	3.75	0.012588
release of sequestered calcium ion into cytosol	0.00043788000000000000	4.6	0.013088
positive regulation of calcium ion transport	0.00043788000000000000	4.6	0.013088
negative regulation of interleukin-6 production	0.00044221000000000000	5.35	0.013088
activation of cysteine-type endopeptidase activity involved in apoptotic process	0.00044446000000000000	2.85	0.013088
defence response to bacterium	0.00075871000000000000	3.2	0.021226
positive regulation of cell migration	0.00076520000000000000	2.41	0.021226
defence response to protozoan	0.00099607000000000000	5.67	0.025763
induction of positive chemotaxis	0.00099607000000000000	5.67	0.025763
response to zinc ion	0.00099607000000000000	5.67	0.025763
negative regulation of growth of symbiont in host	0.00099607000000000000	5.67	0.025763
positive regulation of inflammatory response	0.00118790000000000000	3.57	0.029915
response to tumor necrosis factor	0.00147970000000000000	4.41	0.036187
antigen processing and presentation of exogenous peptide antigen via MHC class I, TAP-dependent	0.00154910000000000000	2.63	0.036362
positive regulation of interleukin-12 production	0.00159580000000000000	5.2	0.036362
regulation of type I interferon-mediated signalling pathway	0.00159580000000000000	5.2	0.036362
complement activation	0.00159580000000000000	5.2	0.036362
positive regulation of T cell activation	0.00207110000000000000	4.16	0.045564
positive regulation of defence response to virus by host	0.00219630000000000000	6.24	0.047233

Supplementary Table 5
Enriched biological processes (GO) upregulated at day 7 of imiquimod treatment in Treg depleted skin vs. day 7 of imiquimod treatment in Treg replete skin

Data was normalized and analysed as described in Chapter 2.